Using the Potent Pasteurella multocida toxin to Probe G-protein Signalling

Thompson, Cherrie Delos Santos

Awarding institution:
King's College London

Using the Potent *Pasteurella multocida* Toxin to Probe G-protein Signalling

Cherrie Delos Santos Thompson

A thesis submitted for the degree of Doctor of Philosophy
at King's College London

2016

Department of Salivary and Mucosal Department

London, UK

Declaration

No part of the work presented in this thesis has been submitted in support of another degree or qualification at this or any other academic institution.

All experimental data and analysis presented in this thesis were all done by myself.

Cherrie delos Santos Thompson

Acknowledgements

I would like to thank my supervisors, Professors Alistair Lax and Agi Grigoriadis who gave me the opportunity to work on such an interesting project while learning and mastering useful techniques in the process. Their guidance and support throughout my research are very much appreciated.

People who have embarked on a PhD lab-based research would agree with me that this journey is extremely stressful. For this, I would like to thank all the wonderful people who made my stay at King's College London an enjoyable one. Special thanks to Dr. James Kistler, Dr. Giuseppe Cama, and my late good friend, Aleksandra 'Ola' Adamowska who passed away during the final year of her PhD. Ola, your amazing energy, passion for science research and life were an inspiration to everyone you met. You are immensely missed!

I would like to thank the people from my department and other groups for letting me use some of their equipment and/or for their advice: Prof. Gordon Proctor, Dr. Julian Naglick, Dr. David Moyes, Dr. Frederic Festy, Dr. Nina Raulf, Dr. Bernadine Idowu, Dr. Borzo Gharibi, Steve Gilbert, Hassan Farah, Susmitha Rao, and the retired Senior Bioinformatics Officer, Phil Cunningham.

I would like to dedicate this research paper to the smartest and most mature little girl I know, my daughter Mikayla Leigh Thompson. I also would like to thank Sean and Nancy Marino for their love and support. To my family specially my wonderful parents, my mum and dad, who passed away decades ago, I miss and love you both very much!

Abstract

The heterotrimeric G-proteins are critically important intracellular signalling molecules that regulate fundamental processes in cellular homeostasis. A unique bacterial toxin, *Pasteurella multocida* toxin (PMT) modifies 3 of the 4 families of G-proteins (G_q, G_i, and G_{12}) by deamidation which leads to a plethora of downstream signalling. PMT induces drastic morphological changes such as loss of adherence to the matrix, foci and stress fibre formation in Swiss 3T3 and Vero cells. PMT is mitogenic for many cell types but not all, and the work reported in this thesis aims to compare two cell lines that respond differently to PMT.

Swiss 3T3 and Vero cells were treated with different concentrations of PMT to determine the effects on cell proliferation, cytoskeletal reorganisation and cell death. PMT induced prominent cytoskeletal changes, mitogenic and anti-cell death responses in Swiss 3T3 cells while delayed cytoskeletal changes with no evidence of mitogenicity and cell death were observed in Vero cells. PMT modified G-proteins at different times in Swiss 3T3 and Vero cells. The PMT-induced anti-cell death response in Swiss 3T3 cells was dose-dependent while the delayed cytoskeletal response in Vero cells was linked to the late PMT-mediated G_{12} activation. The amino acid sequence of $G\alpha_{12}$ differed in the two cell types – the $G\alpha_{12}$ subunit in Vero cells is missing N-terminal cysteine residue, which may have contributed to the differences. $G_{q/11}$ signalling is active and sustained in Swiss 3T3 cells, but not in Vero cells. $G\beta\gamma$ may have inhibited adenylyl cyclase activity so it is unknown whether G_i signalling is active and sustained over the 3-day period as the forskolin-stimulated cAMP level decreased in both serum-starved untreated and PMT-treated cell lines. In summary, I have identified changes in both the primary effect of PMT on the two cell types and also on downstream signalling that is likely to reflect the differential cell response.

Table of Contents

List of Figures

identifier after the name of species. The nucleotide sequences of $G\alpha_{12}$ of *M*. *musculus* obtained from Uniprot is designated with an asterisk (*).

Fig A7 The Aligned Nucleotide Sequences of $G\alpha$ subunits of *H*. *sapiens*, *C*. *sabaeus*, *M*. *musculus* and the Sample. A long segment of sequences with the fewest ambiguities was selected. Each $G\alpha$ subtype bears the CCDS identifier after the name of species.

Fig A8 The Aligned Amino Acid Sequences of $G\alpha_{12}$ subunit of different species. Each species bears the $G\alpha_{12}$ protein identifier after the name of species.

Fig A9 The Aligned Nucleotide Sequences of IP_3R1 of different species: human, mouse and rat. Each species bears the protein identifier.

Fig A10 The Complete Amino Acid Sequences of Different $G\alpha$ subunits of *H*. *sapiens*, *C*. *sabaeus*, and *M*. *musculus*. A segment of the conserved sequences containing the target amino acid of PMT, glutamine (Q) is highlighted with a black box. Each $G\alpha$ subtype bears the protein identifier after the name of species.

List of Tables

Abbreviations

7TM	Seven-transmembrane
AC	Adenylyl cyclase
BSA	Bovine Serum Albumin
Btk	Bruton's tyrosine kinase
CaM	Calmodulin / Calcium-modulated protein
cAMP	3'-5'-cyclic adenosine monophosphate
cGMP	3'-5'-cyclic guanosine monophosphate
CHO	Chinese hamster ovary
CNF1	Cytotoxic Necrotizing Factor type 1
CNF2	Cytotoxic Necrotizing Factor type 2
CT	Cholera toxin
CTGF	Connective tissue growth factor
DAG	Diacylglycerol
DSF	Dorsal stress fibre
DPBS	Dulbecco's Phosphate Buffer Saline
DRiP78	Dopamine receptor interacting protein 78
DTT	Dithiothreitol
EEA1	Early Endosome Antigen 1
ECL	Enhanced Chemiluminescence
EGF	Epidermal growth factor
EGFR	Epidermal growth factor receptor
ER	Endoplasmic reticulum
ERK	Extracellular signal-related kinase
ETEC	Enetrogenic *E. coli*
FBS	Foetal Bovine Serum
GAP	GTPase activating protein
GAIP	Gα-interacting protein
GDI	Guanine nucleotide dissociation inhibitor
GDP	Guanine nucleotide diphosphate

GEF	Guanine nucleotide exchange factor
GIRK	G protein-inwardly-rectifying K+ channel
GPCR	G-protein Coupled Receptor
GTP	Guanosine-5'-triphosphate
GTPγS	Guanosine 5′-*O*-(3-thiotriphosphate) or guanosine 5'-[γ-[35S]thiotriphosphate
GRK	G protein-coupled receptor kinase
HCl	Hydrochloric acid
IP_3	Inositol 1,4,5 triphosphate
JAK-STAT	Janus kinase, signal transducer and activator of Transcription
JNK	c-Jun N-terminal kinase
LARG	Leukaemia-associated RhoGEF
LPA	Lysophosphatic acid / Lysophosphatidate
LT	*E. coli* Heat-labile enterotoxin toxin
MAPK	Mitogen-activated protein kinase
MEF	Mouse embryonic fibroblast
MLC	Myosin light chain
MLCK	Myosin light chain kinase
mTORC1	Mammalian Target of Rapamycin Complex 1
NCS	Newborn Calf Serum
PACAP	Pituitary adenylylcyclase-activating polypeptide
PCNA	Proliferating cell nuclear antigen
PDGF	Platelet-derived growth factor
PI3K	Phosphoinositide-3-kinase
PIP_2	Phosphatidylinositol 4,5-bisphosphate
PIP_3	Phosphatidylinositol (3,4,5)-triphosphate
PLC	Phospholipase C
PLCβ	Phospholipase C beta
PIP_2	Phosphotidylinositol 4,5-biphosphate
PIP_3	Phosphotidylinositol 3,4,5-triphosphate

PI3K	Phosphoinositide-3-kinase
PKA	Protein kinase A
PKB	Protein Kinase B
PKC	Protein kinase C
PKD	Protein kinase D
PT	Pertussis toxin
PVDF	Polyvinylidene difluoride
Pyk2	Proline-rich tyrosine kinase-2
Ric-8	Resistance to inhibitors of cholinesterase 8
RGS	Regulators of G-protein signalling
RhoGEF	Rho guanine exchange nucleotide factor
ROCK	Rho-associated kinase
RTK	Receptor tyrosine kinase
RT-PCR	Real-Time Polymerase Chain Reaction Reverse Transcriptase Polymerase Chain Reaction
PMT	*Pasteurella multocida* toxin
RACK1	Receptors for Activated C-Kinase 1
rPMT	Recombinant *Pasteurella multocida* toxin
RGS	Regulatory of G-protein Signalling
SDS PAGE	Sodium Dodecyl Suphate Polyacrylamide Gel Electrophoresis
Shc	Src homology 2 domain containing (transforming protein)
SOCS-1	Supressor of cytokine signalling 1
SRF	Serum response factor
S6K1	Ribosomal S6 Kinase
TA	Transverse arc
TCF	T-cell factor
TBS-T	Tris buffered saline - Tween 20
VSF	Ventral stress fibre

1 INTRODUCTION

1.1 Signal Transduction

Cells use a large array of defined signalling pathways to regulate their activities. The cell membrane separates the soluble, organised and proteinaceous intracellular content of the cell from its extracellular environment. It permits passage of some extracellular non-charged and small polar molecules while other molecules are transported via vesicles, carrier or channel proteins (Cooper, 2000). Information from non-permeant molecules is transferred across its lipid bilayer via a specialised signal transduction system.

One of the hallmarks of multicellular organisms is their cells' ability to communicate with each other using signalling molecules. These cells, therefore, are constantly bombarded by extracellular signals generated locally or remotely. Coupling of extracellular molecules to specific membrane receptors may lead to activation of signalling pathways. Signals are then conveyed across the cell membrane by a variety of transducers and amplifiers thereby producing a cascade of events that lead to specific biochemical responses. These intracellular signalling molecules are controlled by regulatory molecules via enhancement of their activities, modulation of their active or inactive states in the form of covalent modifications, or switching and hydrolysis of bound nucleotides. The

complexity of such signalling system resulting in cellular altered gene expression, phenotype and biological function involves many key signalling players.

1.2 Cell Surface Receptors: Physical Conduits For Extracellular Message Transfer

In the late 1800s, the concept of the receptor was presented by German immunologist, Paul Ehrlich through his early work on blood cells and chemotherapy for infectious diseases, and British physiologist, John Langley who postulated that some molecules act and behave in cells as ‘receptive molecules’ (Klinge and Rao, 2008; Maehle, 2009; Lefkowitz, 2013). For decades, pharmacologists and endocrinologists further supported and developed the concept of receptors as membrane-associated molecules that specifically recognise and bind extracellular molecules. The initial direct evidence of the receptor-ligand binding concept came from the availability of highly purified peptide hormones and the ability to radio-label them without losing their biological activity (Lefkowitz et al., 1974; Williams et al., 1976; Hoffman and Lefkowitz, 1981; Klinge and Rao, 2008).

The advancement in receptor research has established cell surface receptors as the major gateways for the conversion of extracellular message to intracellular message. All cells maintain a diversity of receptors located on their extracellular surface. Receptors are physical conduits for the

transmission of extracellular signals across the cell membrane. The major classes of membrane receptors are divided into two: the enzymatically active tyrosine and serine/threonine kinases, and the non-enzymatically active G-protein coupled receptors (GPCRs), also known as seven transmembrane (7TM) receptors or heptahelical receptors (Little et al., 2012). GPCRs constitute the largest panoply of specialised integral membrane receptors for therapeutic drugs (Little et al., 2012).

1.2.1 The Promiscuous G-protein Coupled Receptors

G-protein coupled receptors are the most diverse and ubiquitously expressed transmembrane domain proteins in all cell types of mammalian organisms (Lodish et al., 2000; Lefkowitz, 2004). All GPCRs share similar topology with the N-terminal extracellular domain responsible for binding the extracellular signal molecules; the seven transmembrane spanning helices which contain the hydrophobic region embedded in the lipid bilayer and serve to anchor the receptor to the membrane; and the intracellular C-terminal domain, responsible for relaying the extracellular signals to the cytoplasm (Uings and Farrow, 2000). Following activation of GPCR by a ligand, attentuation and cessation of GPCR-mediated signalling is regulated by a class of serine/threonine kinases known as G-protein coupled receptor kinases (GRKs). Phosphorylation of GPCR by GRK prepares the receptor for β-arrestin binding (Lefkowitz and Shenoy, 2005). Recruitment of β-arrestin to GPCR promotes internalisation of receptor via clathrin coated pits

endocytosis, inhibits further G-protein mediated signalling, and diverts the existing signalling to non-G-protein signalling such as β-arrestin signalling (Luttrell and Lefkowitz, 2002).

There are about 950 predicted human GPCR members responsible for converting extracellular signals from chemical or physical stimuli such as neurotransmitters, hormones and sensory stimuli to intracellular signals (Maudsley et al., 2005). Most of these GPCRs are orphans as their physiological roles are still unknown (Deupi and Kobilka, 2007). Based on sequence identity of all predicted 7TMs, these GPCRs can be grouped into five families namely, rhodopsin, secretin, adhesion, glutamate, and frizzled/taste (Fredrikson et al., 2003).

GPCRs virtually control many essential biological functions including development, hormone secretion from endocrine and exocrine glands, neurotransmission, inflammatory responses, and cardiac functions (Reynolds et al., 1991). Many potent mitogens stimulate cell proliferation via GPCRs. Constitutively active mutant GPCRs can be oncogenic. Recent cancer sequencing studies in some of the most prevalent human malignancies revealed a high proportion of GPCR mutations (~5-30%) (O'Neill, 2012). Due to the importance of their role in intracellular signalling, they are common targets of over 30% of all approved pharmaceutical drugs (Hill, 2006; Brogi, et al., 2014).

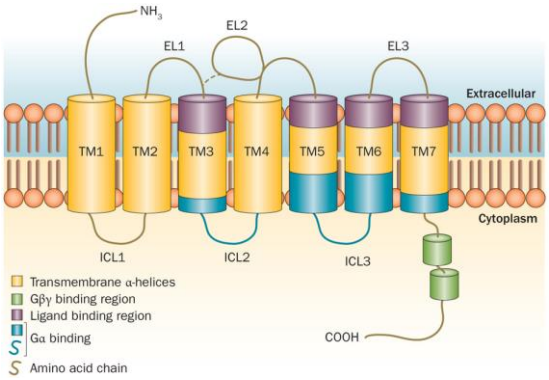

Fig 1.2 The G-protein Coupled Receptor. A schematic diagram of GPCR showing the 7 TM domains (TM1 - TM7) embedded in cell membrane, extracellular loops (EL1 – EL3), and intracellular loops (ICL1 – ICL3). Image adapted from Neumann et al. (2014).

Our understanding of the complexity of GPCR signalling mechanisms has increased since their discovery through major advances in GPCR research and pharmacology. Initially, it was thought that activation of GPCRs only stimulated the canonical linear signalling pathways involving signal amplification and propagation via these three secondary messengers: phospholipase C (PLC), adenylyl cyclase (AC), and phosphoinositide-3-kinase (PI3K) (Little et al., 2012) but different studies have provided mechanistic insights into the novel features of GPCR signalling leading to the generation of pleiotropic biochemical responses. Evidence suggest that different agonists could bind to the same receptor type coupled to different effector pathways and produce multiple biochemical responses (Kenakin, 1995a; Kenakin, 1995b; Leff et al., 1997; Little et al., 2012). These generated GPCR-mediated responses led to the understanding of the growing promiscuity of these versatile cell surface receptors, which depend on the strength of the extracellular signals, and the molecules involved in signal transduction (Kenakin, 1995b).

In the 1990s, a two-model conformation equilibrium state of GPCRs: the active (R*) and the inactive (R), was proposed to explain the efficacy of ligands (Lefkowitz et al., 1993; Leff, 1995). The efficacy of ligands reflects their ability to alter the intrinsic properties of the receptor. Agonists have high affinity to GPCRs in their active state and can stabilise the GPCRs' R* state or when bound to an inactive GPCR, can allosterically shift the receptor's R state in to R* state, while partial agonists can bind to both states but are less effective in shifting equilibrium of the receptor from the R to R* state. Inverse agonists, on the other hand, favour and stabilise GPCRs' R state while antagonists have no effect in shifting equilibrium in either direction but can inhibit the function of the previously mentioned agonists when bound to the receptor (Kenakin, 1995a; Deupi and Kobilka, 2007; Park et al., 2008, Park et al., 2012). However, the proposed two-model conformational state of receptors did not fit other evidence involving complex GPCR-mediated signalling. An extended ternary complex model which explains GPCR activation by cooperative interactions between receptor, G protein, and agonist was proposed (De Lean et al., 1980). Lefkowitz et al. (1993) reported that agonists have higher affinity to constitutively active mutant receptors than their counterpart wild-type receptors by which they assumed that the 'mutation increases all parameters of trimolecular interaction between the ligand, GPCR, and G-proteins (the key mediators of extracellular information transfer to intracellular signaling). More studies indicated that receptors undergo different active conformational substates depending on the agonists that promote the conformational change leading

to selective binding of specific G-protein subtypes (Spengler et al., 1993; Park et al., 2012). One example came from a study of type-1 pituitary adenylylcyclase-activating polypeptide (PACAP) receptor and two different agonists: PACAP-27 and -38 (Spengler et al., 1993). Spengler et al. (1993) showed that both PACAP-27 and -38 stimulate adenylyl cyclase via the GPCR-G_s complex while only PACAP-38 stimulates PLC with high potency via the GPCR-$G_{q/11}$ complex.

Two decades ago, scientists discovered that cognate GPCR-agonist activation could also result in the transactivation of enzymatically active receptors (Daub et al., 1996; Little et al., 2012). One example is the transactivation of Epidermal Growth Factor Receptor (EGFR), a Tyrosine Kinase Receptor (TKR), via GPCR using agonists such as thrombin, lysophosphatidic acid (LPA), and endothelin-1 in Rat-1 fibroblasts (Daub et al., 1996; Pyne and Pyne, 2011). Different studies revealed that occurrence of kinase receptor transactivation may be ligand dependent or independent, as in the case of EGFR activation via selective phosphorylation of its tyrosine residues by GPCR-activated Src kinase (Slomiany and Slomainy, 2005; Little et al., 2012).

Alderton et al. (2001) reported that two GPCRs tethered to platelet-derived growth factor β (PDGFβ) receptors lead to a significant increase in p42/44 MAPK activation. Activation of multiple signalling pathways could also emanate from a single GPCR-G-protein interaction via cross talk between

intracellular molecules, i.e. activation of bradykinin receptors caused a decrease in the level of 3'-5'-cyclic adenosine monophosphate, (cyclic AMP or cAMP) through a pathway involving phospholipase C in cultured rat mesangial cells (Bascands et al., 1993; Kenakin, 1995b).

Receptor density may also affect the type of G-proteins that the receptors interact with and activate. According to Eason et al. (1992), overexpression of α_2-adrenergic receptor in Chinese hamster ovary (CHO) cells resulted in coupling and activation of not just G_i, but also G_s, not an α_2-adrenergic receptors' target. In some cases, GPCRs activate multiple G-protein families, independent of receptor density, as in the case of the opioid agonist, D-Ala^2,D-Leu^5-enkephalin (DADLE) binding to δ-opioid receptors which results in the activation of multiple G-protein types in NG108-15 cells (Prather et al., 1994). Various studies also suggested that most receptors coupled to $G\alpha_{12/13}$ are also coupled to G_q (Riobo and Manning, 2005; Hermans, 2003; Zhang et al., 2006).

Lastly, there is evidence suggesting that 'active' GPCRs can activate signalling pathways in the absence of agonists, and that active GPCRs, and their cognate G-proteins may already be pre-coupled (Kenakin, 1995a; Nakashima et al., 2013). GPCRs can also activate signalling pathways independently of G-proteins, as in the case of G protein-independent β-arrestin-related signalling (Luttrell and Lefkowitz, 2002; Azzi et al., 2003;

Shenoy et al., 2006; Zheng et al., 2010). It is also well established that G-protein activation via GPCRs leads to activation of signalling pathways regulated by two functional subunits that comprise the heterotrimeric G-proteins: the Gα and the βγ subunits. This will be discussed in more detail in sections 1.3 and 1.6 of this chapter.

1.3 Transducers of GPCR Signalling

GPCRs have no catalytic domain, and therefore require specialised information-transducing proteins found in the inner leaflet of the cells. GPCR-mediated signals are transduced by a specific class of molecules called the heterotrimeric guanosine-5'-triphosphate (GTP)-binding proteins or G-proteins.

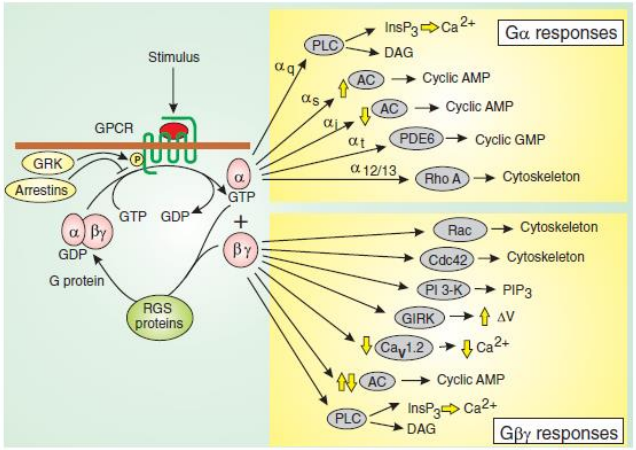

Fig 1.2.2 The heterotrimeric G-protein activation-deactivation cycle and early downstream signalling pathways. Image adapted from Berridge (2012).

1.3.1 Classes of G-proteins and the Ras-like GTPases

GTPases (or GTP-binding proteins) are important regulators of major cellular processes. They are divided into two large classes according to their sequence and structure similarity: the TRAFAC class (translation factor) and SIMIBI class (signal recognition particle, MinD, and BioD) (Verstraeten et al., 2011). Signal recognition-associated GTPases, the MinD-like GTPases, and proteins with kinase or phosphate transferase activity belong to the SIMIBI class while the TRAFAC class includes the elongation factor GTPases, related motor ATPases, SEPTIN GTPases, and the Ras-like superfamily of GTPases (Nelson, 2008). The latter includes two well-known families of GTPases: the monomeric G-proteins and heterotrimeric G-proteins. The heterotrimeric G-proteins play a major role in reception and numerous signal transduction involved in proliferation, motility, differentiation, transformation and cell death (Yanamadala et al., 2009). This will be discussed in great detail in section 1.3.2.

The monomeric G-proteins consist of five families: 1) Ras which regulates gene expression involved in cell differentiation and proliferation, 2) Rho which is responsible for the regulation of cytoskeletal reorganisation, and gene expression via actin and actin-binding proteins, 3) Rab and 4) Sar1/Arf which each regulate vesicle trafficking, and 5) Ran which is responsible for nucleocytoplasmic transport and microtubule organization (Takai et al., 2001; Rajakylä and Vartiainen, 2014). The most well studied and

characterised small G-proteins, which are involved in cytoskeletal reorganisation and adhesion, are the Rho, Rac, and cdc42 subfamilies from the Rho family (Wojciak-Stothard and Ridley, 2003; Holmes et al., 2012). The members of the Rho subfamily (RhoA, B, C) have very similar sequences and are all involved in contractility, stress fibre formation, and focal adhesion (Burridge and Wennerberg, 2004). RhoA and RhoC are involved in cell proliferation while RhoB negatively regulates this effect (Du et al., 1999; Chen et al., 2000). RhoA is also involved in many physiological and biochemical changes such as cell rounding, and serum response factor (SRF)-dependent gene expression (Mizuno and Itoh, 2009). Rac, on the other hand, is specifically responsible for the formation of lamellipoedia and membrane ruffling while cdc42 helps form filopodia (Nobes and Hall, 1995). Rac1 also has a role in stress fibre and focal adhesion complex formation. Genetic deletion of Rac1 in MEF abrogated stress fibre and focal contact formation (Guo et al., 2006). Both G-protein types are substrates of many bacterial toxins, which either inhibit their functions or render them in their locked activated state.

1.3.2 The Heterotrimeric G-proteins: The Molecular Switch for GPCR Signalling

The discovery of the GTP-binding proteins started from the observation that glucagon-induced adenylyl cyclase activity in hepatocytes specifically required guanine nucleotides for hormonal function and thus, the term GTP-

binding protein (G-protein or heterotrimeric G-protein) was adopted (Rodbell et al., 1971).

The guanine nucleotide binding proteins (G-proteins) are made up of three polypeptides: α, β and γ subunits. In humans, there are twenty one α, five β and twelve γ subunits (Yanamadala et al., 2009). Human heterotrimeric G-proteins, based on subsequent cloning by homology, are derived from 35 genes of which 16 genes encode α subunits, 5 for β subunits, and 14 for γ subunits (Milligan and Kostenis, 2006). These G-proteins, unlike the G-protein coupled receptors (GPCRs), are loosely attached to the cytoplasmic leaflet of the plasma membrane through covalently attached lipids on the Gα subunit and Gγ subunit. Gβ is tightly attached to the Gγ subunit. G-proteins are closely associated to the C-terminal intracellular domain of GPCRs (McCudden et al., 2005).

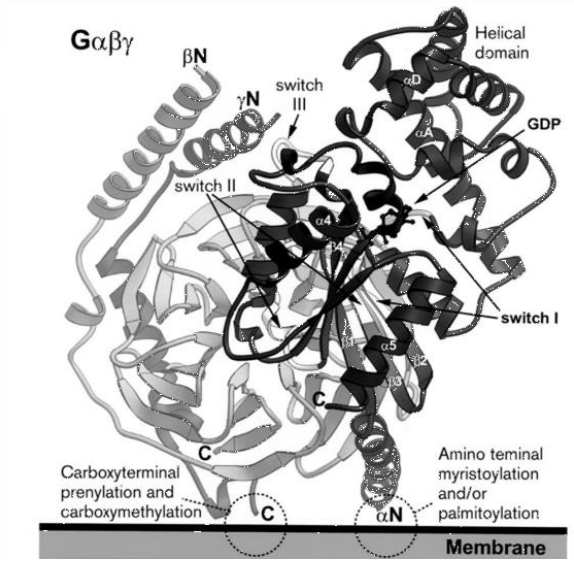

Fig 1.3.2. The heterotrimeric G-protein structure. The subunits are indicated as α, β, and γ with the amino acid terminus indicated as N and the carboxyl terminus as C Image adapted from Bohm et al. (1997).

G-proteins act as molecular switches (Kleuss et al., 1994). In the inactive state, the guanosine diphosphate (GDP)-bound Gα subunit is bound to the βγ complex. In the classical GPCR-G-protein signalling paradigm, upon agonist-dependent receptor activation, the GPCR functions as a guanine nucleotide exchange factor (GEF) triggering release of GDP and promoting binding of GTP in the guanine nucleotide-binding cleft of the linked Gα subunit (Sprang, 1997b; McCudden et al., 2005; Maudsley et al., 2005). Nucleotide release is negatively regulated by guanine nucleotide dissociation inhibitors (GDIs). The binding of GTP to the Gα subunit leads to a conformational change in the GTPase domain of the switch II region of the Gα subunit which reduces its affinity to the receptor, and the βγ heterodimer resulting in their dissociation (Neer, 1995; Hamm, 2001; McCudden et al., 2005; Kleuss et al., 1994). However, some evidence suggests that the GTP-mediated conformational change does not always lead to subunit dissociation and that tethered heterotrimers are still functional (Levitzki and Klein 2002; Klein et al., 2000).

Both the Gα and βγ subunits have a set of effector partners and independently trigger specific signalling pathways (Diel et al., 2006; Smrcka, 2008; Dupre et al., 2009). The activity of both signalling molecules terminates upon hydrolysis of the GTP in the Gα subunit thereby reverting the G-protein into its GDP-bound inactive state, reinstating its heterotrimeric form, and completing G-protein cycle (McCudden et al., 2005).

1.3.2.1 The Gα Subunit

The Gα subunit is the largest of the three subunits with molecular masses ranging from 33 to 55 kDa (Malbon, 2005). The Gα subunits can be divided into four major groups based on their sequence similarity: $G\alpha_{(s,\ olf)}$, $G\alpha_{(i\text{-}1,\ i\text{-}2,\ i\text{-}3,\ o,\ t\text{-}rod,\ t\text{-}cone,\ gust,\ z)}$, $G\alpha_{(q,\ 11,\ 14,\ 15/16)}$, and $G\alpha_{(12,\ 13)}$ (McCudden et al., 2005; Moreira, 2014). Sixteen of them are direct gene products while others are alternatively spliced isoforms (Kaziro et al., 1991; Simon et al., 1991; Sandhya and Vemuri, 1997). Sequence identity amongst the Gα subunits is ~45-80% (Simon et al., 1991). The Gα subunit consists of two domains: the GTP-binding domain, and the helical domain; the two held together by two highly conserved linker regions (Heydorn et al., 2004). The GTP-binding domain comprises about ~200 amino acid residues made up of six-stranded β sheets surrounded by α helices. It provides the binding surfaces for the βγ complex, receptors and effectors, and has three flexible loops: switch regions I, II, and III, while the function of the helical domain is still unclear (Mizuno and Itoh, 2009).

The Gα subunits are synthesised on free ribosomes in the cytoplasm and require the chaperone protein known as resistance to inhibitors of cholinesterase 8 (Ric-8) for proper folding and the initial association of the heterotrimeric G-protein to the plasma membrane (Gabay et al., 2011; Chan et al., 2013). The Gα subunit interacts with different regions of the βγ

complex: 1) the N-terminal α helix of the Gα subunit interacts with blade 1 on the side of the Gβ propeller (discussed in more detail in section 1.3.2.2), 2) the Gα switch II region interacts with the top of the Gβ propeller (Smrcka, 2008). Several studies indicate that association of the βγ complex with the Gα subunit makes the heterotrimer stable and a better substrate for Gα subunit palmitoylation, a lipid modification essential for plasma membrane localisation and anchorage, than the Gα subunit alone (Fishburn et al., 1999; Bhattacharyya and Wedegaertner, 2000).

The activated Gα subunits interact with their immediate effectors to amplify extracellular signals via production of secondary signals. Signal modulators such as GPCR kinases, and regulators of G-protein signalling (RGS) proteins enhance the performance of G-proteins as molecular switches of signal transduction. The GTP hydrolysis of many G-proteins can be slow and requires the intervention of G-protein activating proteins (GAPs) to facilitate the intrinsic GTPase activity (Sprang, 1997b). Some findings suggest that apart from the regulatory G-protein signalling molecules; target effectors can also enhance and influence the duration of the GTPase activity of the Gα subunit (Mberu et al., 1995; Sprang, 1997b; Wettschureck and Offermanns, 2005).

1.3.2.2 The βγ Heterodimer

The tightly complexed βγ subunits function as a monomer. The Gβ subunit has two distinct regions: the N-terminus is made up of a 25-amino acid α helix and a loop (residues 26-45) that connects the helix to the WD-repeats, a 40 amino acid motif, which comprises the C-terminus (Dupre et al., 2009). The WD-repeats contain seven distinct anti-parallel β strands arranged like blades on a propeller-like structure (see Fig 1.3.2.2). The regions of Gβ that bind Gγ are found in blade 5 and the adjacent small α helix. Observations on the structure of the βγ subunit showed that there is no significant difference in the overall structure whether it is linked or unlinked to the Gα subunit or any effector proteins except in the case of βγ linked to phosducin, which shows movement in blades 6 and 7 forming a cavity between these two blades (Smrcka, 2008). It is unknown whether this movement has significance in G-protein function.

The $G\beta_{1-4}$ subunits share ~80% amino acid sequence identity while $G\beta_5$ is structurally distinct from other $G\beta_5$ subunits with only ~51-53% sequence identity and has an additional 13 amino acid residues (Schwindinger and Robishaw, 2001). The $G\beta_5$ subunits, which appears to be an outlier of all Gβ polypeptides, can form a stable complex with RGS7, an RGS protein. The function of the Gβ/RGS7 complex, its physiological role and regulation remain unclear (Smrcka, 2008). The nascent Gβ subunits undergo proper

folding by a chaperone protein called chaperonin containing tailless-complex polypeptide 1 (CCT), which also prevents aggregation of unfolded Gβ subunits, and a co-chaperon protein called phosducin-like protein (PhPL1) (Kubota et al., 2006; Marrari et al., 2007).

The Gγ subunit, on the other hand, is more structurally diverse than the Gβ subunits with 27-76% sequence homology (Dupre et al., 2009). $G\gamma_1$, $G\gamma_{11}$, and $G\gamma_{13}$ subunits share 62-73% homology (Schwindinger and Robishaw, 2001). The ~70 amino acid Gγ subunit, however, consists of two helices, and is folded by a chaperon protein called dopamine receptor interacting protein 78 (DRiP78), an ER resident protein (Dupre et al., 2007). In cultured cells, the Gβ and Gγ subunits interact to form the βγ heterodimer within 2.5 minutes after synthesis (Rehm and Ploegh, 1997; Marrari et al., 2007). It is not clear whether the Gβ and Gγ subunits assemble in the ER, but according to reports, Gβ can compete with DRiP78 in binding Gγ and DRiP78 interacts with phosducin-like protein (PhLP) suggesting a role for both proteins in Gβ and Gγ subunit assembly (Dupre et al., 2007; Marrari et al., 2007). Although Gβ can bind to lipid-modified or unmodified Gγ, it preferentially binds to unmodified Gγ (Higgins and Casey, 1996). Most Gβ and Gγ subunits can irreversibly form a complex (Marrari et al., 2007). Some exceptions have also been reported; for example the $G\beta_1$ subunit can pair with all Gγ subunits, while $G\beta_2$ can form a functional dimer with $G\gamma_2$ but not $G\gamma_1$, which is restricted to retinal rod cells (Iniguez-Lluhi et al., 1992; Schmidt et al., 1992;

Dupre et al., 2009). In comparison to other GPCRs, the rhodopsin receptor has high affinity for the $\beta\gamma_1$ complex (Pronin and Gautam, 1992).

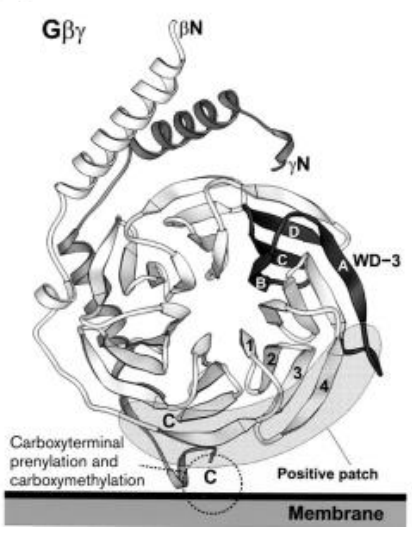

Fig 1.3.2.2 The βγ structure. The subunits are indicated as Gβ and Gγ with the amino acid terminus indicated as N and carboxyl terminus as C. Image adapted from Bohm et al. (1997). (Bohm, Gaudet and Sigler, 1997)

Initially, the βγ heterodimer was thought to be a negative regulator of Gα signalling and was responsible for slowing the rate of GDP release in the Gα subunits (Dupre et al., 2009). In 1987, purified βγ dimers from bovine brain were shown to activate a cardiac potassium channel (Logothetis et al., 1987). Devoid of a catalytic site, the active lifetime of βγ complex signalling depends on the rate of GTP hydrolysis in the Gα subunits (Neer, 1995).

The Gβ and Gγ subunits are both essential for the regulation of their effectors. A fully functional C-terminal extremity of the $G\gamma_2$ subunit is required for the activation of Kir3 channels (Peng et al., 2003), while a point mutation (S67K, T128F, S98T) in the $G\beta_1$ subunit alters the regulation of the Kir3 channel without affecting other functions such as PLCβ2 activation (Mirshahi

et al., 2002). Recombinant $G\beta_{1\text{-}3}\gamma_2$ has been shown to stimulate PI3K, while $G\beta_5\gamma_2$ could not. Reports also show that the combinations $G\beta_5\gamma_2$ and $G\beta_1\gamma_2$ could activate PLCβ1 and PLCβ2 while only $G\beta_1\gamma_2$ could activate PLCβ3 (Khan et al., 2013).

Other studies showed that the βγ heterodimer interacts with GPCRs, and receptors on the ER, and modulates some downstream effectors that are also regulated by Gα subunits (Robishaw and Berlot, 2004; Dupre et al., 2009). It has been suggested that the region where the Gγ subunit defines its specificity to form a complex with the Gβ subunit is localised to 14 amino acid residues near the middle of the molecule (Spring and Neer, 1994). Different combinations of these subunits suggest that there is a selectivity, with generation of a wide range of signals transmitted via different G-protein combinations.

1.4 Specificity Determinant of G-proteins

Despite being fewer in number and less diverse than the GPCRs, G-protein signalling leads to diverse biological responses. Different contact sites in the α subunits are thought to contribute to coupling specificity to GPCRs and their target effectors (Baltoumas et al., 2013). A chimeric Gα subunit consisting of the N-terminus of $G\alpha_q$ fused to the C-terminus of the GTPase domain of $G\alpha_s$ via G_s-coupled receptor lead to the activation of adenylyl

cyclase, a $G\alpha_s$ effector (Orth et al., 2013). In a similar study with a different result, chimeric $G\alpha$ subunits consisting of $G\alpha_q$ with a $G\alpha_i$ C-terminus via G_i-coupled receptor resulted in the stimulation of phospholipase C, a $G\alpha_q$ effector (Conklin et al., 1993).

Diversity in the heterotrimeric G-proteins due to the potential combination of different subunits (also discussed in section 1.3.2.2) has been a major challenge to understanding their function in cell regulation. GPCRs such as somatastin and muscarinic cholinergic receptors use different G-protein combinations in controlling a calcium channel in pituitary cells (Kleuss et al., 1993), while adrenergic and prostaglandin receptors use different G-protein combinations to stimulate adenylyl cyclase activity (Wang et al., 1997b). Schwindinger et al. (2003) demonstrated the first conclusive evidence for a receptor recognising a specific heterotrimeric G-protein combination in an organism using a gene-targeting approach. According to them, the γ_7 subunit is required for the D1 dopamine receptor to stimulate adenylyl cyclase activity in striatum. Reports on the different combinations of G-protein subunits provide strong evidence for functional selectivity and generation of different signals.

1.5 Modifications of α and γ subunits

The activity of G-protein subunits is regulated by a number of covalent modifications, such as phosphorylation, dephosphorylation, palmitoylation, depalmitoylation, myristoylation, prenylation and carboxymethylation (Chen and Manning, 2001). These modifications are involved in plasma membrane localisation, anchorage of G-protein subunits and protein-protein interaction.

Gα subunits are considered non-functional without undergoing essential covalent modifications linked to their function. Most Gα subunits except α_t and α_{gust} are palmitoylated by palmitoyl acyltransferase on a cysteine(s) within the first 20 amino acids in the N-terminal region with the exception of $G\alpha_s$ which can also be palmitoylated at N-terminal Gly^2 residue (Sprang, 1997a; Chen and Manning, 2001; Vogler et al., 2008). Membrane association of most $G\alpha_i$ subunits follow a two-membrane trapping model: irreversible myristoylation and reversible palmitoylation (Chen and Manning 2001). The polypeptides α_o, α_i, α_z, and α_t (belonging to the G_i family) are additionally N-myristoylated by N-myristoyltransferase (NMT) on Gly^2 which requires specifically Ser^6 or Thr^6 as well and a removal of a methionine residue prior to lipidation (Sprang, 1997a). The covalent attachment of a myristate moiety in $G\alpha_i$ is critical for docking of the subunit to the plasma membrane and a pre-requisite process prior to palmitoylation, although over-expression of βγ subunits appears to replace myristate group function as a requirement for palmitoylation and initial membrane interaction (Jones et al.,

1990; Mumby et al., 1994; Hallak et al., 1994; Galbiati et al., 1994; Chen and Manning 2001). It is believed that the geranylgeranyl group in the $\beta\gamma$ complex is a functional equivalent of the myristate moiety, as a membrane-targeting signal (Morales et al., 1998; Chen and Manning, 2001). The reversible palmitoylation of the Gα subunits appears to be an important process in recycling the subunits between the membrane and cytosolic compartments, but other studies have shown that depalmitoylation of Gα subunits by thioesterase did not lead to translocation of Gα subunits from the plasma membrane to the cytosol (Wedegaertner and Bourne, 1994; Mumby et al., 1994; Huang et al., 1999; Chen and Manning, 2001).

Some studies also show that myristoylation and palmitoylation of Gα subunits have significant roles in signal transduction. Gallego et al. (1992) reported that myristoylation of constitutively active mutant Gα_{i2}, also known as gip2 oncoproteins, is essential in cell transformation. Myristoylated mutant Gα_{i-2} negatively regulated adenylyl cyclase activity and stimulated activation of p42 mitogen-activated protein kinase (MAPK) while the non-myristoylated active mutant Gα_{i-2} was unable to do so. A similar study showed that a constitutively active mutant Gα_{12} devoid of palmitoylation in NIH3T3 cells was incapable of causing cell transformation (Jones and Gutkind, 1998). Bhattacharyya and Wedegaertner (2000) reported that Gα_{13} required palmitoylation for its plasma membrane localisation in transfected cells. They also reported palmitoylation of Gα_{13} is essential for activation of

the Rho-dependent serum response factor-mediated transcription, p115-RhoGEF translocation, and actin stress fibre formation.

Palmitoylation also negatively regulates the intrinsic GTPase activity of Gα subunits via RGS, while depalmitoylation promotes interaction between Gα subunits and RGS (Tu et al., 1997; Chen and Manning, 2001). Palmitoylated $G\alpha_z$ decreased the maximal rate of GTP hydrolysis and had reduced affinity to $G\alpha_z$ GTPase-accelerating protein (GAP) while palmitoylation of $G\alpha_z$ and $G\alpha_i$ inhibited their response to Gα-interacting protein (GAIP), and RGS4 respectively (Tu et al., 1997).

The Gγ subunits undergo several post-translational modifications, including the irreversible isoprenylation of a cysteine residue in a CAAX motif at the carboxyl terminal of the protein (Schafer and Rine, 1992). Isoprenylation involves covalent attachment of either a farnesyl or a geranylgeranyl moiety to the Gγ subunit. If the X in the CAAX motif is a leucine, then a geranylgeranyl group via a thioester bond is covalently attached to the preceding cysteine, but in some Gγ subunits such as Gγ1, $G\gamma_9$, $G\gamma_{11}$, the X is a serine or methionine which permits attachment of a farnesyl group (Balcueva et al., 2000; Ong et al, 1995; Wedegaertner et al., 1995; Vogler et al., 2008). Isoprenylation of this cysteine in Gγ is followed by removal of three amino acids at the C-terminus and reversible carboxymethylation catalysed by isoprenylcysteine carboxyl methyltransferase. The latter

modification augments hydrophobicity of the subunit especially in the case of farnesylated G**γ,** thereby enhancing its membrane anchorage properties (Vogler et al., 2008). These modifications are essential for membrane anchorage of the βγ complex.

G-proteins also undergo reversible phosphorylation at tyrosine, serine, or threonine residues, which may affect the specificity of their interactions with other proteins and their function in a positive or negative fashion (Sandhya and Vemuri, 1997; Sprang, 1997). In yeast, phosphorylation of Gβ in the free βγ dimer is essential for mediating signal amplification, communication between receptor and the chemotropic complex which are all important for chemotrophic growth (DeFlorio et al., 2013).

Kozasa and Gilman (1996) reported that PKC equally phosphorylated $G\alpha_{12}$ and $G\alpha_z$ on a serine residue in their GDP- or GTP-bound forms. Such modification reduced the affinity of both functional Gα and βγ subunits and did not alter the guanine nucleotide binding properties and function of the subunits. Other studies indicated that PKC preferentially phosphorylates a monomeric form of $G\alpha_z$, as the βγ heterodimer negatively regulates such process by blocking the N-terminus of the Gα polypeptide, which is the apparent site for phosphorylation (Fields and Casey, 1995; Wang et al., 1999a). Phosphorylation of Gα inhibits binding of the βγ complex and various RGS proteins such as RGSZ1, RET-RGS1, and GAIP, which may result in

prolonging the activity of G-proteins (Fields and Casey, 1995; Glick et al., 1998; Wang et al., 1998).

In an early *in vitro* experiment, Krupinski et al. (1988) showed that $G\alpha_i$ and $G\alpha_o$ were phosphorylated on tyrosine residue by the insulin receptor. The GDP-bound $G\alpha$ subunits were the preferred substrates for phosphorylation as guanosine 5'-[γ-[35S]thiotriphosphate ($GTP\gamma S$) prevented the $G\alpha$ subunit from being phosphorylated. The presence of these phosphorylated $G\alpha$ subunit also resulted in an enhanced insulin-stimulated receptor autophosphorylation and incorporation of insulin receptors to phospholipid vesicles. However, they did not report any functional consequences of such phosphorylation events and speculated that phosphorylation may help in keeping a $G\alpha$ subunit in its inactive GDP-bound state and thus, serves as an 'off switch' for signalling pathways, or in facilitating $G\alpha$ activation, or stimulate the activity of the effector proteins. In a study involving a different kinase protein, Hausdorff et al. (1992) reported that $pp60^{c\text{-}src}$ preferentially phosphorylates a tyrosine residue of inactive GDP-bound $G\alpha s$ and transducin, which resulted in a modestly increased rate of $GTP\gamma S$ binding and GTP hydrolysis, and that coupling of $\beta\gamma$ subunits inhibited such processes. Although they did not specifically identified the tyrosine residue site for phosphorylation, initial speculation pointed to near the amino terminal region due to the anti-phosphorylation properties of the $\beta\gamma$ complex. However, none of the conserved tyrosine residues is located in the said

terminus and the investigators proposed two conserved residues as possible phosphorylation sites: Tyr^{170} and Tyr^{312}.

Phosphorylation may also result in positive or negative regulation of signal transduction. Phosphorylation of $G\alpha_{13}$ at Thr^{203} by protein kinase A (PKA) led to stabilised coupling of receptor and $G\alpha$ subunit, destabilised coupling of $G\alpha$ and $\beta\gamma$ subunits, and inhibition of Rho activation (Manganello et al., 2003). Stimulation of tyrosine phosphorylation of $G\alpha_{i2}$ by PDGFβ receptors coupled to GPCRs in human embryonic kidney (HEK) 293 cells led to an increase in p42/p44 MAPK activation (Alderton et al., 2001) while epidermal growth factor (EGF)-induced tyrosine phosphorylation of $G\alpha_s$ decreased bradykinin-induced activation of cAMP signalling pathway in A431 cells (Liebmann et al., 1996).

Another question that needs addressing is whether phosphorylation is required for activation of G-proteins or not. Umemori et al. (1997) reported that activation of $G_{q/11}$ essentially requires phosphorylation of $G\alpha$ subunits at $tyrosine^{356}$ residue. Baldwin et al. (2003), on the other hand, reported that *Pasteurella multocida* toxin (PMT), and non-toxic mutant PMT^{C1165A} stimulated phosphorylation of $G\alpha_q$ at $tyrosine^{349}$ but such phosphorylation event did not in itself lead to $G\alpha_q$ activation as only the wild-type (WT) PMT was able to activate G_q. However, they showed that both active and mutant toxin allosterically enhanced the ability of other agonists to enable G_q to

activate PLCβ (Baldwin et al., 2003; Lax et al., 2004). It is not clear whether activation depends on the tyrosine site, cell type (although both experiments were carried out mostly in fibroblasts: Swiss 3T3, mouse embryonic fibroblast (MEF), $G_{q/11}$ -/- double deficient fibroblasts, with the exception of CHO cells which, however, generated similar results), the origin of Gα subunit, or the type of agonists used. It appears that in most cases, phosphorylation of Gα blocks association of Gβγ, may upregulate or downregulate downstream biochemical signals, and enhances effector protein activities.

Several bacterial toxins specifically attack certain Gα subunits, as the main substrates of their catalytic activity. Pertussis toxin (PT), an AB enterotoxin produced by the bacterium *Bordetella pertussis*, modifies all members of the $G\alpha_i$ family, except $G\alpha_z$, by a process called ADP-ribosylation. The addition of an ADP-ribose moiety to the cysteine residue located at the C-terminus of Gα subunits inhibits the polypeptides from interacting with the receptors and abolishes their GTPase activity (Locht, 1999; Carbonetti, 2010; Locht et al., 2011). Cholera toxin (CT), produced by the bacterium *Vibrio cholerae*, and *E. coli* heat-labile enterotoxin toxin (LT) each catalyse ADP-ribosylation of $G\alpha_s$ to promote GDP release, GTP binding, and inhibition of GTP hydrolysis thereby locking the G-proteins in their constitutive active state (Lee et al., 2001; Moss and Vaughan, 1991; Lemichez and Barbieri, 2013). *Pasteurella multocida* toxin (PMT) targets some members of three of the four families of

heterotrimeric G-proteins and catalyses deamidation of their glutamine residue to convert it into glutamic acid rendering the G-proteins in their constant active state. Bacterial toxins and toxin-catalysed modifications will be discussed in more detail in section 1.8 of this chapter.

1.6 The Heterotrimeric G-proteins: 4 Distinct Classes

The heterotrimeric G-proteins are classified according to the specific class of the α subunit, having amino acid homology of 50% or more, namely $G\alpha_q$, $G\alpha_{12}$, $G\alpha_s$, and $G\alpha_i$ (Simon et al., 1991; Goldsmith and Dhanasekaran, 2007).

Each G-protein has been linked to a specific (canonical) signalling pathway. However, there is now an increasing evidence of non-canonical functions of G-proteins independent of GPCRs. In this chapter, signalling pathways via canonical and non-canonical functions of G-proteins will be discussed here.

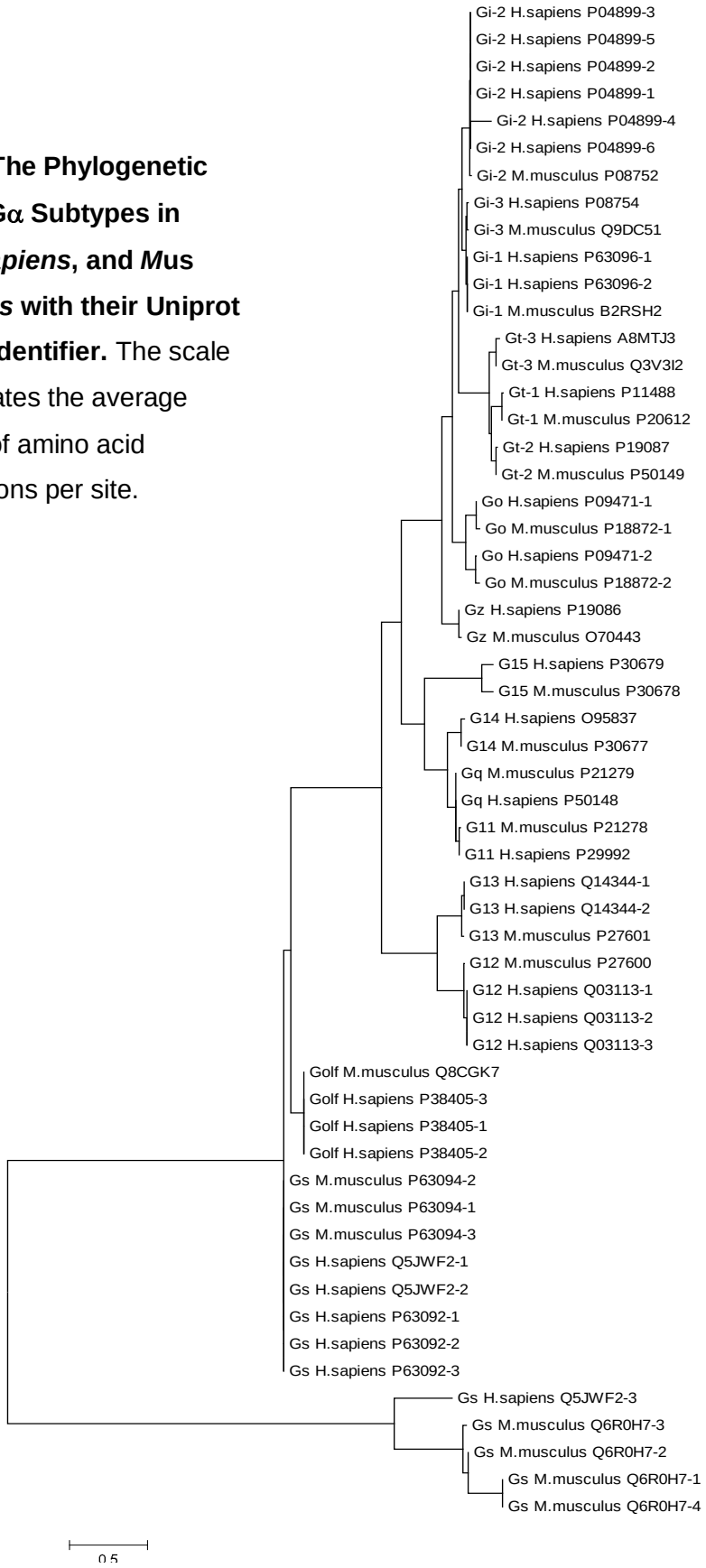

Fig 1.6 The Phylogenetic Tree of Gα Subtypes in *H*omo *sapiens*, and *M*us *musculus* with their Uniprot Protein Identifier. The scale bar indicates the average number of amino acid substitutions per site.

1.6.1 The G_q Family

The G_q family has five members: $G_{q,}$ G_{11}, G_{14}, and G_{15} (mouse orthologue) G_{16} (human orthologue) with overall 57% amino acid sequence identity (Hubbard and Hepler, 2006; Mizuno and Itoh, 2009). $G\alpha_q$ and $G\alpha_{11}$ are the most ubiquitously expressed members of this family with 88.5% amino acid sequence identity (Astesano et al., 1999), whereas the expression of G_{14} is more restricted and normally seen in specialised cells. $G_{15/16}$, on the other hand, is limited to a subset of haematopoietic cells (Amatruda et al., 1991; Wilkie et al., 1991; Davignon et al., 1996; Mizuno and Itoh, 2009).

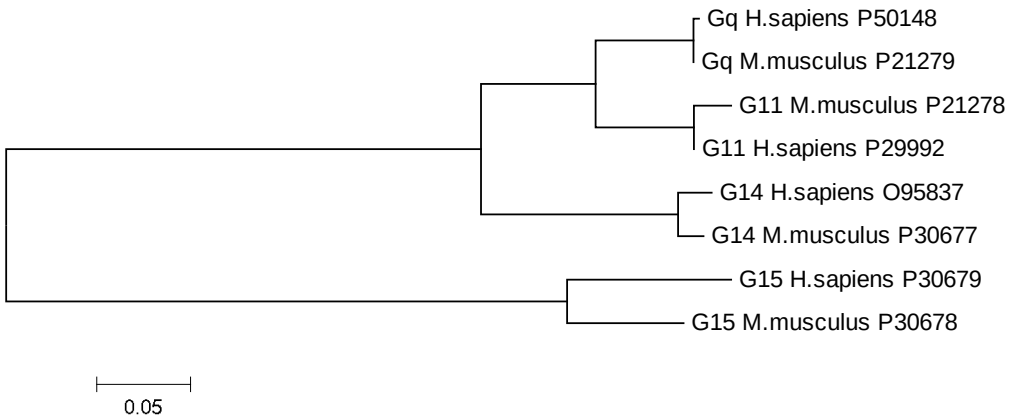

Fig 1.6.1 The Phylogenetic Tree of $G\alpha_q$ Family Members Protein Sequences of *H. sapiens*, and *M. musculus* with their Protein Identifier. The scale bar indicates the average number of amino acid substitutions per site. A supplement figure (Fig A1) of the aligned amino acid sequence of the above proteins can be found in the appendix section.

Activation of these G-proteins stimulates activation of their canonical downstream targets: different beta isoforms of phospholipase C (PLCβ)

(PLCβ1-4). PLCβ1 and PLCβ3 are ubiquitously expressed in most cell types while PLCβ2 is restricted to haematopoietic cells, and PLCβ4 is largely expressed in retina (Mizuno and Itoh, 2009; Kozasa et al., 1993). $G_{q,}$ G_{11}, and G_{14} activate PLCβ1-4 *in vitro* with PLCβ2 being poorly activated while $G_{15/16}$ activates PLCβ1-3 *in vitro*, which in the case of PLCβ2, could be cell type specific as both $G_{15/16}$ and PLCβ2 expression are restricted to haematopoietic cells and thus, could be functionally linked. PLCβ activation leads to hydrolysis of phosphatidylinositol 4,5-bisphosphate (PIP_2), and generation of second messengers: inositol-1,4,5-triphosphate (IP_3) and diacylglycerol (DAG). The free IP_3 binds to IP_3-specific receptors, which lead to intracellular Ca^{2+} mobilisation while the membrane bound DAG activates PKC. These events lead to a profound biochemical and physiological alteration of the cells and are involved in mitogenesis, muscle contraction, chemotaxis, opioid sensitivity, survival and others (Lyon and Tesmer, 2013). PLCβ, apart from being a target effector of the $G_{q/11}$, also serves as GAP by increasing the intrinsic GTPase activity of the Gα subunit (Paulssen et al., 1996; Chidiac and Ross, 1999). G_q-mediated intracellular Ca^{2+} mobilisation resulted in downregulation of β-catenin signalling by promoting nuclear export and calpain-mediated degradation of β-catenin (Li and Iyengar, 2002). G_q-PLC activates the extracellular-signal-regulated kinase (ERK)-proliferative pathway via a novel pathway involving proline-rich tyrosine kinase-2 (Pyk2), Ras and Raf (Dhanasekaran et al., 1998).

Recently, the p63RhoGEF, Trio, and Duet were identified as target effectors of $G\alpha_q$, which activates RhoA (Rojas et al., 2007, Williams et al., 2007). A crystal structure of the $G\alpha_q$-p63RhoGEF-RhoA complex confirms involvement of G_q in RhoA signalling (Lutz et al., 2007). p63RhoGEF binds to $G\alpha_q$ to increase GTP exchange on RhoA, RhoB, and RhoC. In another study, activation of $G_{q/11}$ was shown to inhibit osteoblast differentiation via the RhoA-p63RhoGEF activation (Siegert et al., 2013).

Various reports show the involvement of $G_{q/11}$ in promoting apoptosis or cell survival in different cell types. In HeLa cells, Ueda et al. (2001 and 2004) reported that $G_{q/11}$ induced apoptosis via proteolytic activation of Rho-associated kinase I (ROCK-I) by caspase, activation of RhoA and reduced phosphorylation of Akt by insulin-stimulated tyrosine phosphatase. A similar observation in HEK293 cells was reported but according to investigators, RhoA activation did not involve stimulation of PKC and calcium signalling, and inhibition of Akt phosphorylation did not involve PLC activation (Ueda et al., 2001; Chikumi et al, 2002). In another study using HEK293 cells, constitutively active $G\alpha_{11}$, $G\alpha_{14}$, and $G\alpha_{16}$ supressed basal and EGF-induced Akt phosphorylation and such inhibitory effect in pro-survival signalling was PLC-independent and dependent on mobilisation of intracellular calcium (Wu et al., 2006). In CHO and COS-7 cells, G_q-mediated apoptosis is PKC dependent while G_{11}-mediated apoptosis is independent of PLC (Althoefer et al., 1997).

In contrast, constitutively active mutant G_{11} did not induce apoptosis and promoted Akt phosphorylation in NIH3T3 cells (Ueda et al., 2001). Two papers reported contradicting observations on the effect of G_q on Akt activation in COS-7 cells. Murga et al. (1998) reported G_q-mediated activation of Akt while Bommakanti et al. (2000) reported G_q-mediated inhibition of Akt stimulation. Thus, it appears that $G_{q/11}$-mediated apoptosis is cell-specific and in the case of similar cell type e.g. COS-7, variability among different COS-7 cell lines or the origin of the cell line.

Ric-8A, a cytosolic resident protein, possesses a GEF activity to G_q, G_{i-1}, G_o and G_{12} but not G_s. Ric-8A appears to enhance G_q-mediated ERK activation in intact cells (Nishimura et al., 2006). Ric-8B, another homologue of Ric-8, associates with $G\alpha_q$, $G\alpha_s$ but not $G\alpha_i$, and $G\alpha_{12}$ (Tall et al., 2003). Ric-8B and G_{olf} are both predominantly expressed in mature olfactory sensory neurons and appear to be functional partners in G-protein-mediated odorant signal transduction. To understand the biochemical role of Ric-8B and regulation of G_{olf}, Von Dannecker et al. (2005) showed that Ric-8B potentiated the G_{olf}-dependent cAMP level in HEK293 cells.

The scaffolding protein, Caveolin-1 and the lipid raft resident proteins, flotillins interact with $G\alpha_q$ and appear to serve as scaffolding proteins of G_q signalling (Oh and Schnitzer, 2001; Sugawara et al., 2007). Caveolin-1 scaffolding of G_q appears to be essential in GPCR-mediated signalling as

siRNA knockdown of caveolin-1 impaired GPCR signalling which suggests that caveolin-1 may have a role in receptor coupling (Gonzalez et al., 2004; Bhatnagar et al., 2004). A knockdown of flotillins-2, on the other hand, attenuated the UTP (a P2Y GPCR agonist)-induced p38 MAPK activation via Src kinases in lipid rafts (Sugawara et al., 2007; Nagao et al., 1998). Src kinase inhibitors can disrupt p38 MAPK activation by UTP and lipid rafts (Sugawara et al., 2007). G_q-GPCR-mediated p38 MAPK activation has been previously reported to be dependent on Src kinases.

1.6.2 The G_{12} Family

The G_{12} family consists of two ubiquitously expressed 43 kDa proteins: $G\alpha_{12}$ and $G\alpha_{13}$ with over 67% identity in amino acid sequences (Strathmann and Simon, 1991). The GPCR-mediated activation of $G\alpha_{12/13}$ has a slow rate of nucleotide exchange and GTP hydrolysis (Suzuki et al., 2009). Both members activate the small GTPases Rho that leads to the downstream activation of c-Jun N-terminal kinase (JNK) and PLD amongst other effects (Juneja et al., 2011).

The downstream effectors of $G_{12/13}$ are Rho, Rac, and Cdc42, which belong to the Rho GTPases family from the Ras superfamily of small GTP-binding proteins. These small G-proteins are regulated by two groups of proteins: GEF which catalyses the exchange of GDP to GTP, and GAP which regulates the hydrolysis of GTP. $G_{12/13}$-mediated RhoA signal transduction

via RhoGEFs is the best described of the signalling pathways regulated by $G_{12/13}$. These G-proteins interact with RhoGEFs, which contain the N-terminal homology RGS (known as RH-RGS or rgRGS) domain, such as PDZ-RhoGEF/GTRAP48, leukaemia-associated RhoGEF (LARG) and lymphoid blast crisis-like-2 (Lsc), also known as p115-RhoGEF (Hart et al., 1996; Kozasa et al, 1998; Fukuhara et al., 2001). Apart from acting as effector proteins, these RhoGEFs also function as RGS, i.e. LARG and p115-RhoGEF were shown to enhance the GTPase activity of $G_{12/13}$ *in vitro* by acting as GAPs (Kozasa et al., 1998; Suzuki et al., 2003).

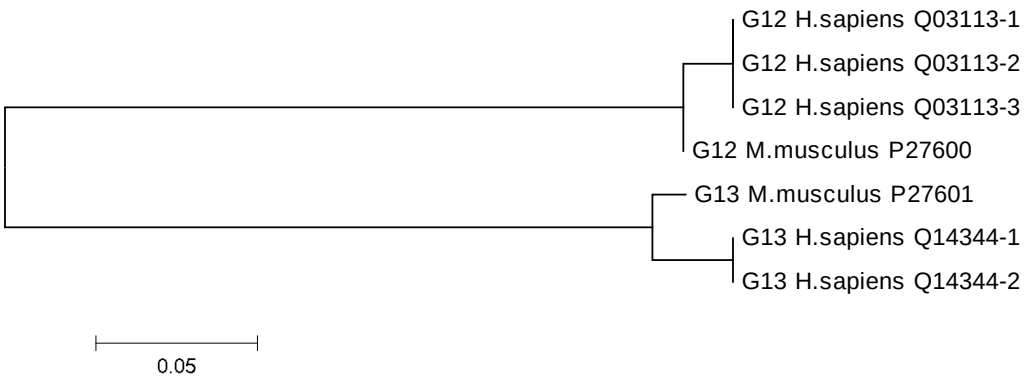

Fig 1.6.2 The Phylogenetic Tree of $G\alpha_{12}$ Family Members Protein Sequences of *H. sapiens*, and *M. musculus* with their Protein Identifier. The scale bar indicates the average number of amino acid substitutions per site. A supplement figure (Fig A2) of the aligned amino acid sequence of the above proteins can be found in the appendix section.

Wu et al. (2006) reported that constitutively active $G_{12/13}$ inhibits the pro-survival Akt signalling via activated RhoA in HEK293 cells while a dominant negative mutant RhoA blocked that effect. Similar to the effect of $G\alpha_{11/14/16}$,

the constitutively active $G\alpha_{12/13}$ also attenuated basal and EGF-induced Akt phosphorylation (Wu et al., 2006).

As mentioned in section 1.6.1, G_{12} (also G_q, G_{i1}, G_o) binds to Ric-8A, which contributes in the enhancement of ERK activation (Nishimura et al., 2006). $G_{12/13}$ also binds to Bruton's tyrosine kinase (Btk), a non-receptor tyrosine kinase belonging to the Tec family, which is involved in B-cell maturation, differentiation and signalling. However, the functional importance of such interaction remains unclear (Jiang et al., 1998). Btk contains a pleckstrin homology (PH) domain and binds to phosphatidylinositol (3,4,5)-triphosphate (PIP_3) which then phosphorylates PLC leading to hydrolysis of PIP_2 and generation of two second messengers: IP_3 and DAG (Mohamed, 2009).

Activated G_{12} also directly interacts with E-cadherin, a cell-cell adhesion molecule, leading to the release of the pro-mitogenic factor β-catenin, a key component of the canonical Wnt pathway (Meigs et al., 2001). $G_{12/13}$ is also involved in platelet shape change via regulation of Rho-Rho kinase-dependent phosphorylation of myosin light chain (MLC) which also includes tyrosine phosphorylation of $pp72^{syk}$ and stimulation of $pp60^{c\text{-}src}$.

1.6.3 The G_i Family

The G_i family is the most diverse of all G-protein classes. It has six members: $G_{i\text{-}1}$, $G_{i\text{-}2}$, $G_{i\text{-}3}$, G_o (a predominantly neural α subunit), $G_{t\text{-}r}$, $G_{t\text{-}c}$, G_g,

and G_z. $G\alpha_{i-1}$, $G\alpha_{i-2}$, and $G\alpha_{i-3}$ share 85-95% amino acid sequence identity (Plummer at al., 2012). The G_i: rod transducin G_{t-r}, cone transducin G_{t-c}, and gusducin G_g are involved in the signal transduction related to vision and taste.

With the exception of G_z, the pertussis toxin targets the $G\alpha$ subunits of this family by ADP-ribosylation which results to the paralysis of their normal signalling function in receptor coupling and their own activation (Casey et al., 1990; Fong et al., 1988). G_i and G_z regulate G_s activity by inhibiting the activity of adenylyl cyclase and the production of cAMP. However, prolonged activation of $G_{i/o}$-coupled receptors-$G\alpha_{i/o}$ may also result in sensitisation or superactivation of AC thereby enhancing AC activity (Brust et al., 2015).

The sensory $G\alpha_g$ activates PLCβ resulting in an increase in intracellular Ca^{2+}. Activation of the cyclic cGMP-dependent phosphodiesterase (PDE) 8 by G_{t-r} and G_{t-c} causes a decrease in intracellular cGMP and hyperpolarisation of photocells via cGMP-gated ion channels (Meoli, 2010). Reduction in $G\alpha_{i-2}$ led to differentiation of F9 cells into a primitive endoderm (Dhanasekaran et al., 1998). Similar to G_q and G_{12} (as discussed in sections 1.6.1 and 1.6.2), G_{i1} and G_o also bind to Ric-8A, which contribute in the enhancement of the G_q-mediated ERK activation (Nishimura et al., 2006).

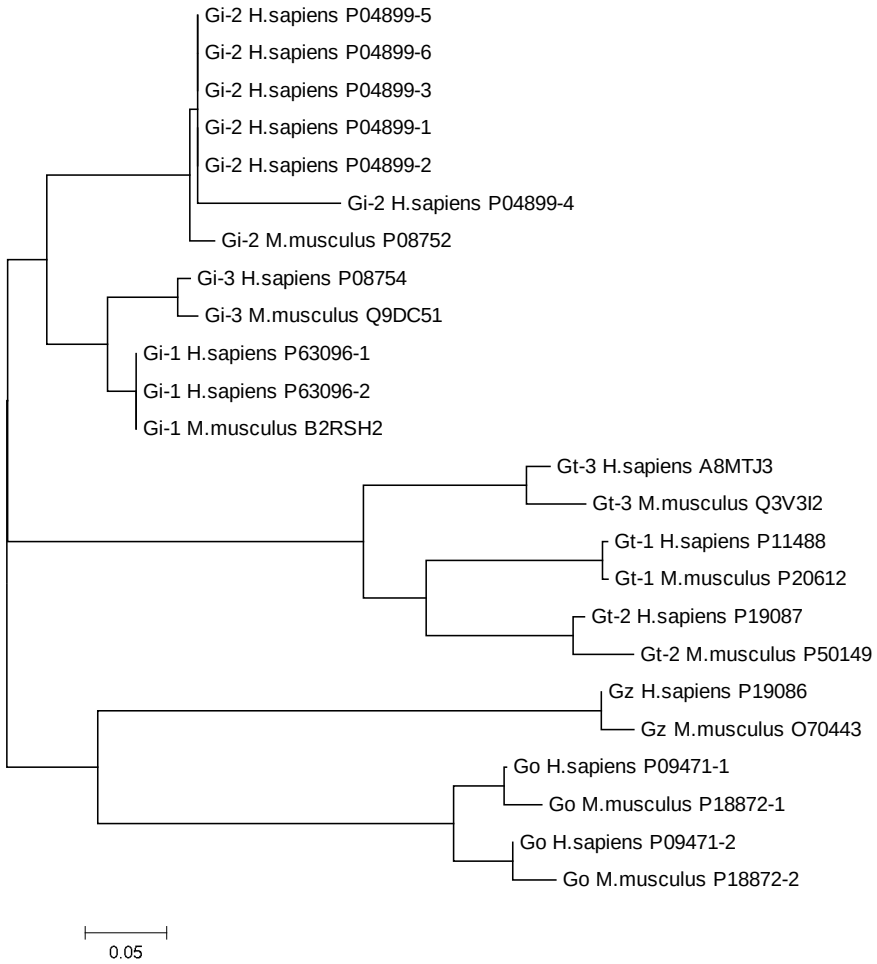

Fig 1.6.3 The Phylogenetic Tree of $G\alpha_{i/o}$ Family Members Protein Sequences of *H. sapiens*, and *M. musculus* with their Protein Identifier. The scale bar indicates the average number of amino acid substitutions per site. A supplement figure (Fig A3) of the aligned amino acid sequence of the above proteins can be found in the appendix section.

1.6.4 The G_s family

The G_s family has two members: the ubiquitous $G\alpha_s$ and the olfactory $G\alpha_{olf}$ with over 88% identity in amino acid sequences (Jones and Reed, 1989). Cholera toxin targets this family of G-proteins by constitutively activating the $G\alpha$ subunits by ADP-ribosylation (Cassel and Pfeuffer, 1978; Gill and Meren, 1978).

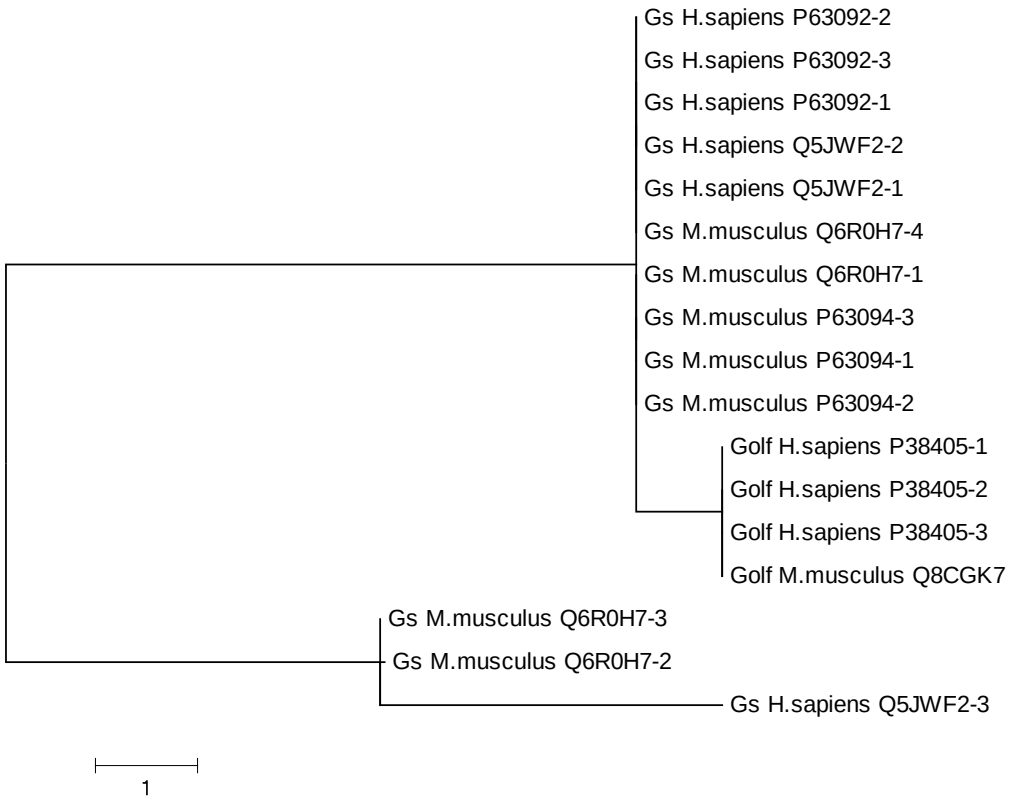

Fig 1.6.4 The Phylogenetic Tree of Gα_s Family Members Protein Sequences of *H. sapiens*, and *M. musculus* with their Protein Identifier. The scale bar indicates the average number of amino acid substitutions per site. A supplement figure (Fig A4) of the aligned amino acid sequence of the above proteins can be found in the appendix section.

The $G_{s/olf}$ family is known to activate adenylyl cyclase, which leads to an increase in intracellular cAMP and activation of Protein Kinase A (PKA). cAMP-mediated signalling pathways activated by growth hormone releasing hormone (GHRH) and thyroid stimulating hormone (TSH) via G_s-GPCR results in cell proliferation (Dhanasekaran *et al*., 1998). Phosphorylation of PKA, on the other hand, attenuates β_2-adrenoceptor-G_s uncoupling and promotes β_2-adrenoceptor-G_i coupling, which results in the activation of MAPK pathway (Hill and Baker, 2003). However, other data showed that

MAPK activation is independent of G_i but instead works via G_s/PKA-dependent activation of Rap1, a small G-protein and the serine/threonine kinase B-Raf (Schmitt and Stork, 2000; Friedman et al., 2002). According to Lefkowitz et al. (2002), such conflicting data were all derive from the use of different HEK293 cell lines, which may display differences in the role of G_s/G_i switching.

Beas et al. (2012) reported that inactive $G\alpha_s$-G226A (GA) binds to GIV (also known as Girdin, a signal transducing protein), which then negatively regulates the EGF-induced proliferative signalling via early endosome antigen 1 (EEA1) endosomes (Beas et al., 2012). $G\alpha_s$ and GIV promote maturation of EEA1 endosomes by facilitating dissociation of EEA1 in endosomal membranes. Depletion of $G\alpha_s$ and/or GIV resulted in increased level of EEA1 in membranes, prolonged residence of activated EGFR and EGF in EEA1 endosomes, activation of ERK1/2, increased EGFR autophosphorylation, src homology 2 (SH2) adaptor recruitment and cell proliferation.

G_s can also activate L-type voltage gated calcium channels in skeletal muscle cells, and cardiac myocytes via the cAMP/PKA pathway. G_s can also inhibit cardiac sodium channels via coupling of β-adrenergic receptors and sodium channels and lead to enhanced membrane depolarisation (Wickman and Clapham, 1995a; Wickman and Clapham, 1995b; Schubert et al., 1989;

Kamp and Hell, 2000). Constitutive activation of G_s also plays a role in the regulation of osteoblast function, which results in increased trabecular bone formation (Hsiao et al., 2010).

Ric-8B, a homologue of Ric-8, associates with $G\alpha_q$, $G\alpha_s$ but not $G\alpha_i$ and $G\alpha_{12}$ (Tall et al., 2003). Ric-8B and G_{olf} are both predominantly expressed in mature olfactory sensory neurons and appear to be functional partners in G-protein-mediated odorant signal transduction (Von Dannecker et al., 2005).

1.6.5 The Gβγ Signalling

The βγ heterodimer is a membrane associated signalling partner of the Gα subunit. The βγ heterodimers are known to regulate PLCβ, AC isoforms, phosphoinositide 3-kinase (PI3K), G protein-coupled receptor kinase 2 (GRK2), and G protein-inwardly-rectifying K+ channels (GIRKs), also known as Kir3 channels (Lin and Smrcka, 2011). Gβγ also binds to a protein involved in regulating the visual signalling system called phosducin.

The GIRK or Kir3 channel is the first discovered direct effector protein of Gβγ (Khan et al., 2013). Binding of Gβγ to GIRK strengthens the interaction of PIP_2 and the channel, and also alters the conformation of the conductance pore of the channel, which increases its activity (Jin et al., 2002; Mirshahi et al, 2003). Gβγ with the help of PIP_2 recruits and binds to the C-terminus of

GRK2, which then phosphorylates and desensitises the activated agonist-GPCR complex (Pitcher et al., 1996; Daaka et al., 1997). Gβ also has an odd biochemical function in a non-canonical system involving the protein GRK2. Zha et al. (2015) reported that Gβ2 binds to DDB1 of the DDB1-CUL4A-ROC1 ubiquitin ligase independently of Gγ, which then targets GRK2 for ubiquitylation and degradation by the 26S proteasome thereby keeping a steady-state level of the protein.

The ubiquitin-proteasome pathway is a complex regulatory system responsible for intracellular protein degradation (Lecker et al, 2006). Proteins bound for degradation are tagged with ubiquitin, which are then recognised by 26S proteosome. The covalent attachment of mono or poly-ubiquitins in the lysine residues of proteins is carried out by E1 (Ub-activating), E2 (Ub-conjugating) and E3 (Ub-ligating) enzymes. The main internal lysine sites for ubiquitin tagging are lysine 48 and lysine 63, yielding K48- and K63-linked polyubiquitin chains (Sun, 2008). The K48 linkages having a closed conformation serve as a signal for target protein degradation by the 26S proteasome, while the K63 linkages with an extended linear conformation serve as non-proteasome addressing dock sites for a variety of functions such as DNA repair, endosomal trafficking, signal transduction, transcription, and multivesicular body sorting for lysosomal decay (Marx et al., 2010). Protein ubiquitylation can be reversed by deubiquitinating enzymes (DUBS), which maintain a pool of free ubiquitins in the cytoplasm (Turcu et al, 2009).

Specific amino acid residues (E574-K583) and a PH homology domain were identitfied as binding regions on PLCβ2 (Sankaran et al., 1998). It was proposed that such interactions may contribute to the reorientation of PLCβ for efficient binding of effector proteins (Drin and Scarlata, 2007; Drin et al., 2006). Gβγ also regulates voltage dependent Ca^{2+} channels, which facilitate calcium ion flux across the plasma membrane. Binding of Gβγ to these channels inhibits the activity of the channel, a phenomenon known as voltage-dependent inhibition (Khan et al., 2013). In macrophages, the activated $G\alpha_{i-}$ and $G\alpha_q$-coupled GPCRs require βγ subunits for the synergistic increase in intracellular Ca^{2+} via PLCβ3 and with a minor contribution from PLCβ2, while PLCβ4 antagonises such synergy (Brothers et al., 2011).

Certain isoforms of AC are canonical cascade effectors of Gβγ, which may either promote production or reduction of cAMP. All AC isoforms have two catalytic domains: C1 and C2. Gβγ interacts with two motifs in AC: the QEHA motif found in C2 which is less important and the PFAHL motif (only found in AC2, AC4 and AC7) in the C1 domain, which proves to be an important binding site for Gβγ. Gβγ released from $G\alpha_s$-coupled receptors but not $G\alpha_i$-couple receptors inhibits AC1, AC5 and AC6 (Nielsen et al., 1996); such inhibition depends on particular combinations of Gβ and Gγ (Bayewitch et al., 1998a and b). Gβγ is also involved in heterologous sensitisation of AC2 via dopamine D2 receptors in HEK cells while chronic activation of the μ-

opioid receptor inhibits AC2 in COS-7 cells (Conley and Watts, 2013; Schallmach et al., 2006).

The Gβγ-activated PI3K phosphorylates phosphotidylinositols. PIP_3, a primary product is a downstream cascade effector of the survival signalling pathway, and also an activator of protein kinase B (PKB). Gβγ activates and binds to multiple sites of two class I PI3Ks namely PI3Kβ and PI3Kγ (Khan et al., 2013) which contain P110γ catalytic subunit and P101 regulatory subunit responsible for increased specificity to PIP_2 (Stephens et al., 1997; Maier et al., 1999). Although Gβγ heterodimer stimulates the PI3K/Akt survival signalling, the inhibitory effects of $G\alpha_q$ on this pathway is greater than Gβγ as Gβγ signalling pathways typically require 10-100 folds concentration of Gβγ than the Gα (Lee et al., 1993).

Gβγ is also involved in the activation of MAPKs by three different mechanisms (Khan et al., 2013). The first one is through PI3K. Touhara et al. (1995) reported that Gβγ is involved in G_i-GPCR-mediated activation of MAPK and $p21^{ras}$. They reported that Gβγ mediates early phosphorylation of p52, an Shc protein, which is an early event prior to $p21^{ras}$ activation. Inhibition of Gβγ-mediated PI3K activation abolished p52 phosphorylation. The second mechanism is via recruitment of different proteins that serve as scaffolds for MAPK activation. Gβγ can recruit kinase suppressor of Ras-1 (KSR-1), a regulator of Ras-mediated signalling; and GRKs to phosphorylate

GPCRs, which then result in the recruitment and binding of β-arrestins. The latter protein may serve as an adaptor protein for Src (Luttrell et al., 1999). The last mechanism is via transactivation of RTKs, which is the major activator of the classic MAPK signalling pathways (Della Rocca et al., 1999).

1.7 G-protein Signalling in Diseases and Development

G-proteins are known to regulate many different cell functions, which involve a complex networking of various signalling pathways.

The role of G-proteins in the regulation of cell growth and differentiation became apparent when several hormones were shown to promote cell proliferation and differentiation via the cAMP-dependent pathway, suggesting that G_s or G_i might be involved (Radhika and Dhanasekaran, 2001). This observation was followed by studies involving a number of endocrine tumours which showed mutations in $G\alpha_s$ and $G\alpha_i$.

A number of pituitary and thyroid tumours show constitutively active $G\alpha_s$. Point mutation in either arginine 201 (R201) or glutamine 227 (Q227) in $G\alpha_s$ was found in pituitary GH secreting tumours and thyroid hyperfunctioning adenomas. Mutated and constitutively active G_s later became known as the *gsp* oncogene (Radhika and Dhanasekaran, 2001).

The involvement of $G\alpha_i$ in cell transformation is the result of mutations in R179 or Q205 which lead to its constitutive activation. These $G\alpha_{i2}$ mutant forms are referred to as *gip2* oncogenes. Although the mechanism linking this oncogene in cell growth is not clear, its negative effect on the levels of cAMP leads to constitutive activation of the Ras-independent MERK-ERK signalling, and transactivation of T-cell factors (TCFs) in the nucleus may be responsible.

Investigation of $G\alpha_q$ bearing the mutation in $G\alpha_q$Q209L confirms its role in the transformation of different cell lines in tumour formation. Expression of $G\alpha_q$Q209L in NIH3T3 cells leads to transformation and foci formation, albeit cytotoxicity was more prominent than its transforming effect (De Vivo and Iyengar, 1994; Kalinec et al., 1992). Based on the findings from the NIH3T3 studies, it has been proposed that low levels of expression of the mutant $G\alpha_q$ leads to transformation of fibroblasts, while a high concentration leads to cell death. The mechanisms by which transformation occurs involve a number of $G\alpha_q$ interacting partners and downstream effectors. Microinjection of PLC resulted in mitogenic transformation of NIH3T3 cells (Smith et al., 1989). Expression of different PLC-coupled GPCRs such as m1, m2, m5 muscarinic-, α1b adrenergic- or $5HT_{1c}$-receptors also caused oncogenic transformation of NIH3T3 cells suggesting that transformation occurs via the PLC pathway. Activation of PLC generates two products, DAG and IP_3 via cleavage of phosphatidylinositols. DAG activates PKC which then stimulates

ERK through Raf. Depending on the cell type, the ERK-mediated mitogenic effect involves two pathways; one is PKC-dependent but Ras-independent; the other involves a Pyk2 and Ras via IP_3. IP_3 leads to Ca^{2+} flux which then stimulates Pyk2 activity to activate Shc through tyrosine phosphorylation. This results in the formation of Shc-GRB2-SOS complexes which then stimulate Ras leading to the activation of ERK. Both pathways lead to the activation of TCFs or TRE-specific transcription factors. A recent report about a highly conserved GEF, Trio, showed its essential role in the activation of JNK and p38 via Rho- and Rac-regulated signalling pathways from G_q (Vaque et al., 2013).

$G\alpha_{12}$ was first identified as the transforming oncogene in some soft-tissue osteosarcomas and was classified as part of the *gep* family of oncogenes (Chan et al., 1993; Radhika and Dhanasekaran, 2001). However, the transforming ability of $G\alpha_{12}$ is dependent on the presence of serum, as serum starvation caused a loss of its potent mitogenic effect (Chan et al., 1993). On the other hand, expression of the GTPase-deficient $G\alpha_{12}$Q229L led to transformation even in a serum-starved environment or in the absence of agonists. As expected, the transforming effects of $G\alpha_{12}$Q229L and $G\alpha_{13}$Q226L did not involve generation of cAMP, Ca^{2+} or IP_3 but resulted in Ras-, Rac- and CDC42-mediated activation of JNK without an apoptotic effect. Other growth-promoting signals include Ras/Rac-dependent transient activation of ERK, and Rho-dependent activation of the focal adhesion

complex formation. Ras-dependent ERK and Ras/Rac-dependent JNK activities are essential for G1 to S phase cell cycle progression in NIH3T3 cells. The synergistic cooperation of $G\alpha_{12}$, Raf1, and Rac1 are also important in the $G\alpha_{12}$-mediated transformation of NIH3T3 cells. $G\alpha_{12}$ is involved in the phosphorylation and activation of tyrosine kinases such as FAK and Tec/Bmx kinases. $G\alpha_{12}$ activation of other signalling pathways involves activation of small GTPases such as Ras, Rac, CDC42 and Rho. These signalling pathways are a result of Ras/Rho dependent stimulation via PC-PLC or PLD, and Rac, Rho-dependent activation of phosphotidylinositide 4-kinase (PI4K), and phosphotidylinositide 4-phosphate and 5-kinase (PIP5K). In other cell types, PKC-dependent signalling pathways can also be activated by $G\alpha_{12}$. $G\alpha_{12}$QL has been shown to activate SRF via the Rho-dependent signalling pathway while $G\alpha_{13}$QL activates the transcription of egr-1 which is considered to be a primary response for cell proliferation and differentiation (Prasad et al., 1994). Both members can also activate transcription of the pro-oncogene cyclooxygenase-2 (COX-2) (Radhika and Dhanasekaran, 2001).

Various studies showed that $G\alpha_{12}$ and $G\alpha_{13}$ can also activate small GTPases by stimulating specific GEFs, competing with GDIs, or inhibiting specific GAPs. There have been suggestions that $G\alpha_{12}$ can activate Ras and Rac via Shc and Tiam-1, an exchange factor for Rac through a PKC-dependent pathway in some cell lines. Direct interaction of $G\alpha_{12}$ with RasGAP and Btk

may play a role in cell proliferation and oncogenic transformation but this still needs to be defined (Jiang et al., 1998).

Reports show that $G_{12/13}$ plays an important role in organism development. Mice deficient in G_{13} died during at the early embryonic stage due to a malfunction in angiogenesis while deficiency in G_{12} with fully functional G_{13} appeared to be normal (Offermanns et al., 1997). G_{12}-deficient mice with only one intact G_{13} allele, on the other hand, also lead to death *in utero*. The role of $G\alpha_{12/13}$ in cell proliferation appears to be mediated by the small GTPases Rac, Ras, and Rho. These molecules and cdc42 play an important role in cell cycle progression from G1 to S phase. Rac appears to be essential for cell cycle progression from G2 to M phase. Rho also has a role in the regulation of cytoskeletal rearrangements, which is associated with cell division and proliferation. It also activates specific SRFs by an unknown mechanism, which may contribute to a mitogenic effect in some cell types (Hill et al., 1995).

Free $G\beta\gamma$ has been shown to enhance β-catenin/TCF signalling (Jernigan et al., 2010). The $\beta\gamma$ complex, together with Dsh activates GSK3 which then phosphorylates LRP6. The phosphorylated LRP6 inhibits the degradation of β-catenin leading to its stability. The β-catenin then translocates to the nucleus to mediate transcription.

An abnormally high level of GRK2, a Gβγ effector protein, has been linked to many human diseases such as heart attack/failure, portal hypertension, insulin resistance, and Alzheimer's disease (Zha, et al. 2015). Previously, the regulation of the steady-state level of GRK2 via the Gβ2-E3 ligase complex-dependent ubiquitylation and degradation was mentioned in section 1.6.5 of this chapter.

1.8 Bacterial Toxins and Modification of GTP-binding Proteins

Bacterial toxins are powerful tools for understanding the molecular mechanisms behind cellular signal transduction exploited by pathogens. Such toxins helped in the discovery and characterisation of G-proteins in mammalian cells, which up to present remain essential in the studies of many G-proteins (Milligan and Kostenis, 2006; Denis et al., 2012).

Some strains of bacteria produce toxins as a mechanism to increase their chance of survival. Many of these toxins modify cellular signalling pathways by acting on their host proteins. Bacterial toxins can be classified as endotoxins or exotoxins. Endotoxins are cell-associated toxins and integral part of the cell wall of the gram-negative bacteria i.e. lipopolysaccharide, which is released upon lysis or death while exotoxins are proteins synthesised and released by bacteria during their exponential growth or upon lysis (Rajendram et al., 2003).

Bacterial exotoxins are grouped according to their structure and functions: the A-B toxins, superantigens (SAgs which also include the superantigen-like toxins (SSL)) and the pore forming toxins. SAgs do not enter the cell but binds to cell surface molecules (e.g. SAgs bind to major histocompatibility complex II and T-cell receptor while SSL binds to sialyllactosamine, C5 or IgA) and activate the immune system (Henkel et al., 2010). SAgs such as Streptococcal pyrogenic exotoxin (Spe), Toxic shock syndrome toxin (TSST), and Staphylococcal enterotoxin are responsible for toxic shock-like syndrome and scarlet fever, toxic shock syndrome, and food poisoning respectively.

The pore-forming toxins (PFTs) make up 25 - 30% of cytotoxic bacterial proteins produced by many pathogenic bacteria such as *Staphylococcus aureus*, *Streptococcus pneumoniae*, *Escherichia coli*, and *Mycobacterium tuberculosis* (Woodford and Livermore, 2009; Los et al., 2013). The main function of this bacterial protein is to perforate the membranes (plasma or intracellular organelle membranes) of the host cells (Iacovache et al., 2010). These toxins are produced to kill other bacterial species, escape the immune system by killing the immune cells, enter the host system and escape a phagosome. PFTs are divided into two groups: α-PFTs and β-PFTs based on the structure of their spanning elements: α-helix or β-sheets (Henkel et al., 2010; Del Peraro and Van Der Goot, 2016). These toxins bind to specific membrane receptors thereby increasing their concentration in the area

which leads to oligomerisation, an essential process for pore formation. Colicin produced by *E. coli*, haemolysin E by *Salmonella enterica*, *Shigella flexneri* and some strains of *E. Coli*, and cry toxins from *Bacillus thuringiensis* are examples of α-PFT while V. cholerae cytolysin (VCC) from *V. cholerae*, and necrotic enteritis toxin B (NetB) from *C. perfringens* are examples of β-PFT.

Almost all A-B toxins have two domains. The A domain harbours a catalytic activity while the B domain is responsible for cellular receptor binding and translocation of the toxin inside the cell (Henkel et al., 2010). Many of these bacterial toxins target GTP-binding proteins, which lead to deregulation of their specific signalling pathways via different covalent modification: deamidation (Schmidt et al., 1997; Schmidt et al., 1998; Flatau et al., 1997; Orth et al., 2009), ADP-ribosylation (Sehr, et al., 1998, Aktories et al., 1987), glucosylation (Just et al., 1995; Sehr, et al., 1998), adenylylation (Worby et al., 2009), transglutamination (Schmidt et al., 1998; Schmidt et al., 1999), and proteolysis (Shau et al., 2003).

The cytotoxic necrotizing factor types 1 and 2 (CNF1/2) from necrotizing *E. coli* are responsible for gastrointestinal diseases, urinary tract infections and septicemia in humans and animals (Kadhum et al., 2008). Both share 99% amino acid sequence similarity and target Rho proteins (Oswald et al., 1994; Aktories, 1997; Schmitt et al., 1999).

The N-terminal of CNF1 and CNF2 contains the cellular binding domain which has 24% and 27% amino acid sequence identity respectively to PMT, while the C-terminus contains the catalytic domain which has amino acid sequence similarity with the Bordetella dermonecrotic toxin (Lemichez et al., 1997; Busch et al., 2001) (PMT will be discussed in more detail in section 1.8.1). CNF toxins activate Rho via deamidation of glutamine 63 (Gln63) of Rho or glutamine 61 (Gln61) of Rac or Cdc42 resulting in the inhibition of GTP hydrolysis and their constitutive activation (Flatau et al., 1997; Lerm et al., 1999; Schmidt et al., 1997). Phenotypic effects dependent on the inherent deamidation activity of the toxins include multinucleation, actin stress fibre formation, apoptosis, appearance of lamellipodia and filopodia in different cell lines (Mills et al., 2000).

Dermonecrotic toxin (DNT) is produced by bacteria from the genus *Bordetella*. It possesses a transglutaminase activity that catalyses deamidation of Gln63 of RhoA and Gln61 of Rac and Cdc42 thereby keeping them in their constitutive active state (Fukui and Horiguchi, 2004; Matsuzawa et al., 2004). DNT causes splenoatrophy in mice (Fukui and Horiguchi, 2004), and moderate turbinate atrophy and lobular pneumonia in pigs (Brockmeier et al., 2002). At a cellular level, DNT causes reorganisation of actin cytoskeleton, focal adhesion and stress fibres, DNA synthesis, inhibition of osteoblast differentiation, and multinucleation (Fukui and Horiguchi, 2004).

Clostridia, *Bacilli*, and *Staphylococci* produce the toxin exoenzyme C3 (Just et al., 1992; Wilde et al., 2001; Wilde et al., 2003). Devoid of binding and translocation domains, its apparent mode of entry is via vimentin-dependent endocytosis (Rohrbeck et al., 2014). It is an ADP-ribosylating transferase which catalyses the hydrolysis of nicotinamide adenine dinucleotide (NAD) to ADP-ribose and nicotinamide, and transfers the ADP-ribose moiety to asparagine-41 of Rho isoforms A, B, C thereby inactivating their Rho GTPase activity (Aktories et al., 1987; Sekine et al., 1989; Wilde et al., 2000). ADP-ribosylated Rho results in reduced level of RhoA-GTP, inhibition of cell cycle progression, and protection of serum-starved HT22 cells from programmed cell death (Rohrbeck et al., 2012).

Heat-labile (LT) toxin from enterotoxigenic *E. coli* causes diarrhoea by inducing water and electrolyte loss from the intestines of humans and animals (Nataro and Kaper, 1998). LT is a heterohexameric A-B toxin with similar structure and function to cholera toxin (CT) (Spangler, 1992). Cholera toxin (CT) is the main virulence factor of *Vibrio cholera* that causes extreme diarrhoea, cramps, and vomiting which may result in death. The A domains of LT and CT possesses an ADP-ribosylation activity that modifies the $G\alpha_s$ subunits thereby locking them in their constitutive active state. Activation of $G\alpha_s$ then leads to AC activation, increased cAMP level, and PKA activation (Johnson et al., 2009). The activated PKA phosphorylates the R domain of cystic fibrosis transmembrane conductance regulator (CFTR) leading to

efflux of ions and water in the infected enterocytes causing the diarrhoeal disease. Apart from its role in causing diarrhoea, LT promotes adhesion of ETEC to intestinal epithelial cells through its ADP-ribosylation activity (Johnson et al., 2009) and LT-induced p38 MAPK activity (Wang et al., 2012). It has also been implied that vesicle-bound LT can bind to cellular GM1 and bacterial LPS at the same time, which appear to contribute to the pro-adherence phenotype (Horstman and Kuehn, 2002).

Pertussis toxin (PT) from the bacterium *Bordetella pertussis* is linked to the pathogenesis of whooping cough or pertussis (also discussed in section 1.5). PT catalyses ADP-ribosylation of $G\alpha_i$, thereby locking the subunit in their GDP-bound inactive state and thus, inhibit it from interacting with the receptor, unable to inhibit AC activity leading to increased cAMP levels (Locht, 1999; Carbonetti, 2010; Locht et al., 2011).

The bacterium *Clostridium difficile* causes nosocomial diarrhea in mammals. The toxigenic strains of *C. difficile* encode two toxins: A (308 kDa) and B (269 kDa), which are essential virulence factors in the pathogenesis of the disease (Kuehne et al., 2010). The central part of the C-terminus of the toxin harbours a cysteine protease activity responsible for cleaving and releasing the N-terminus, which contains the glucosyltransferase domain, into the cytosol (Hofmann et al., 1997; Pfeifer et al., 2003; Egerer et al., 2007; Reineke et al., 2007). This domain catalyses monoglucosylation of the Rho family members: RhoA, -B, -C, Rac, and Cdc42 (Just et al., 1995; Just and

Gerhard, 2004). Such modification inhibits Rho GTPase functions, which leads to physiological changes in the cell such as cell rounding, actin cytoskeletal reorganisation, and apoptosis (Just et al., 1995).

1.8.1 *Pasteurella multocida* Toxin (PMT)

Pasteurella multocida, a gram negative coccobacillus, is a pathogenic bacterium that causes a wide variety of diseases in mammals and birds (Weber et al., 1984; Lloret et al., 2013). They are normally found in oral flora of various animals such as cats and dogs. They can cause respiratory tract infection, and are found in infected wounds. They have also been linked to conditions such as spinal empyema and meningo encephalomyelitis (Lloret et al., 2013). Some strains of the organism with a lysogenic bacteriophage produce a protein toxin [*Pasteurella multocida* toxin (PMT)] (Pullinger et al., 2004). PMT, a 146kDa dermonecrotic toxin is the virulence factor of *P. multocida* associated with atrophic rhinitis in swine, characterised by twisting and shortening of the snout, and atrophy of the nasal turbinate bones. At less than 1μgkg^{-1} body weight, PMT is lethal. Experimental injection of PMT leads to liver and kidney damage, proliferation of bladder and ureter epithelial cells (Hoskins et al., 1997; Lax and Chanter, 1990).

PMT is an intracellularly acting toxin which activates multiple signalling pathways downstream of the heterotrimeric G-proteins. PMT activates three of the four families of heterotrimeric G-proteins, G_i, G_q and G_{12}, which lead to

a strong mitogenic response in many cell types (Orth and Aktories, 2009; Rozengurt et al., 1990).

1.8.1.1 Structure and Catalytic Domain of PMT

The N-terminus of PMT harbours the membrane receptor binding and translocation domains responsible for its entry and delivery of the catalytic domain of the C-terminal in to the cytosol (Baldwin et al., 2004; Pullinger et al., 2001). PMT binds to membrane phospholipids such as sphingophospholipid sphingomyelin or phosphatidylcholine with other lipid components (Brothers et al., 2011) and is then trafficked to a low-pH compartment where it is proteolytically activated between pH 5 – 5.5 (Baldwin et al., 2004; Smyth et al., 1995).

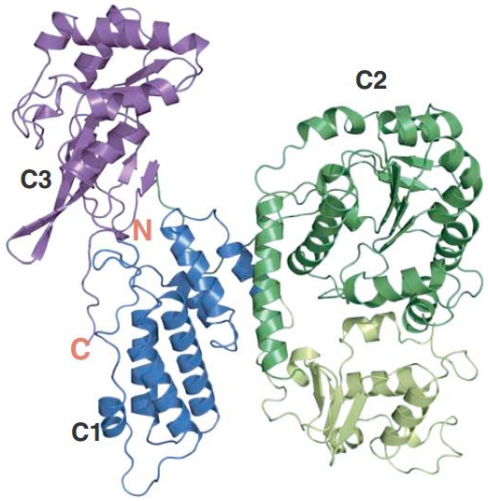

Fig 1.6.1.1. Ribbon diagram of C-PMT. The secondary structure of PMT shows a Trojan-horse like shape which composed of three domains designated as C1 (blue), C2 (green) and C3 (magenta) (Kitakodoro et al., 2007). The helices and β-strands are drawn as coils and arrows respectively.

The C-terminus contains the active domain (Pullinger et al., 2001; Orth and Aktories, 2009). The Trojan horse-like structure of the C-terminus of PMT

has 3 regions, C1, C2 and C3. The C1 subdomain (residues 575-719), which is essential for cytoxicity contains a lipid membrane localisation motif (Kitadokoro et al., 2007). The C2 subdomain (residues 720-1104) has 2 subdomains, α and β. Its function is still unknown but according to homology searches with DALI, it is similar to folypolyglutamate synthetase and cdc14bs phosphatase, which can interact with the phosphate groups of their substrates and co-substrates. It has been suggested that this domain may have a role in the stabilisation of the entire structure of C-PMT (Kitadokoro et al., 2007). Lastly, the C3 subdomain (residues 1105-1285) contains the latent cysteine-protease-like catalytic triad, Cys1165-His1205-Asp1220 (Kitakodoro et al., 2007; Pullinger and Lax, 2007; Ward et al., 1998) which functions as a glutamine-specific protein deamidase (Orth and Aktories, 2010).

1.8.1.2 Covalent Modification of the Gα subunits by PMT

PMT changes the conserved glutamine amino acid in the switch II region of the α subunit into glutamic acid, which inhibits hydrolysis of bound GTP into GDP, thereby locking the G-protein in its constitutive active state. This glutamine is responsible for positioning the attacking water molecule during the GTP hydrolysis process.

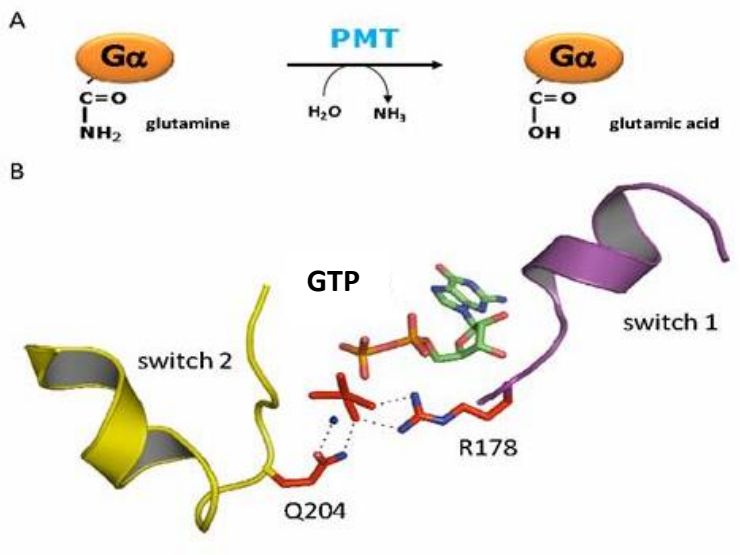

Fig 1.8.1.2-A Deamidation of Gα subunit catalysed by PMT. PMT converts the conserved residue, glutamine in glutamic acid thereby inhibiting GTP hydrolysis. **–B Gα subunit in action.** Hydrolysis of GTP with water molecule in placed (blue dot) Image adapted from Orth and Aktories (2010).

Orth et al. (2009 and 2013) and Babb et al. (2012) confirmed that PMT covalently modifies members of the G_i family ($G\alpha_{i-1}$, $G\alpha_{i-2}$ and $G\alpha_{i-3}$), G_q family ($G\alpha_q$ and $G\alpha_{11}$) and G_{12} family ($G\alpha_{12}$, $G\alpha_{13}$) but not G_s. Babb et al. (2012) also reported that prolong treatment of Swiss 3T3 cells with PMT led to a loss of membrane associated $G\alpha_i$.

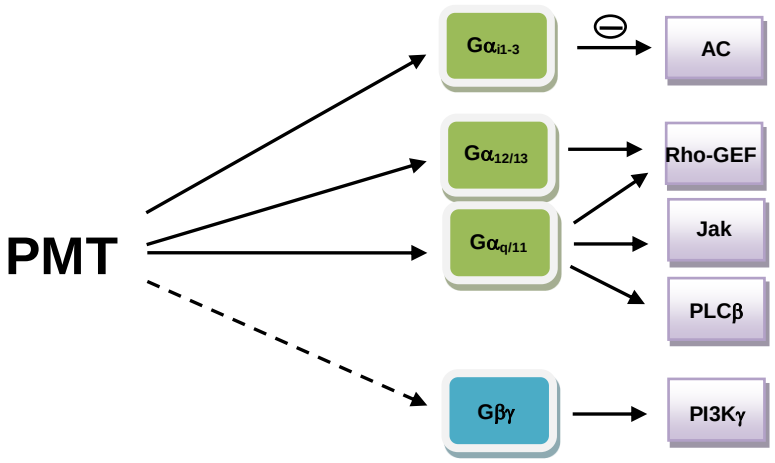

Fig 1.8.1.2-B A schematic representation of PMT-induced activation of different Gα subunits and their immediate downstream effector proteins. The active Gβγ dimer, although indirectly activated by PMT, also shows their regulated downstream effector proteins.

1.8.1.3 PMT, the Antagonist of Cellular Homeostasis

Various studies showed that PMT caused morphological havoc in different cell types via deregulation of some of the major signalling pathways.

PMT is a potent mitogen in confluent, quiescent fibroblastic cells causing pleiotropic effects such as increased levels of inositol phosphates, activation of PKC, intracellular Ca^{2+} mobilisation, activation of small GTPases, stimulation of β-catenin signalling, and depression of cyclic AMP (Orth et al, 2008; Aminova and Wilson, 2007; Lax and Grigoriadis, 2001; Wilson et al., 1997; Lacerda et al., 1996; Rozengurt et al., 1990; Murphy and Rozengurt,

1992; Staddon et al., 1990). Enhanced DNA synthesis, anchorage-independent growth, development of foci, cytoskeletal rearrangements with prominent stress fibres and later on decreased adherence were observed in cultured fibroblasts (Higgins et al, 1992; Rozengurt et al, 1990; Wilson et al, 2000). According to Rozengurt et al. (1990), PMT stimulated-DNA synthesis was comparable to the mitogenic effect induced by 10% serum. However, in other cell lines such as Vero (kidney epithelial cells derived from African Green Monkey), PMT caused a cytotoxic or cytopathic effect, cytoskeletal rearrangements without prominent stress fibres and no apparent cellular growth or proliferation (Pennings and Storm, 1984; Sunder and Kumar, 2000; Wilson et al., 2000).

Numerous studies showed that PMT activates MAPK signalling pathways via $G_{q/11}$ which lead to cell proliferation. In HEK293 cells, PMT activates the ERK1/2 pathway via G_q-dependent transactivation of the EGFR (Seo et al., 2000). In cardiomyocytes however, stimulation of the ERK/MAPK pathway via G_q occurs in an EGFR-independent manner (Sabri et al., 2002). PMT activates PLCβ via the $G_{q/11}$ α-subunits which then leads to the production of IP_3 and DAG via PIP_2 cleavage. The release of these secondary messengers stimulates Ca^{2+} mobilisation, activates PKC-dependent phosphorylation and calcineurin-dependent Nuclear factor of activated T cells. The released Ca^{2+} binds and activates calmodulin (CaM) and other effector proteins. Notch1 has also been linked to PMT-induced activation of G-protein signalling in adipocyte differentiation. The role of Notch1 is still

unclear but activation of the Ca^{2+}/calmodulin-dependent serine/threonine phosphatase calcineurin downstream of G_q blocks adipocyte differentiation (Wilson and Ho, 2011).

PMT also induced the expression of serine/threonine kinase Pim-1 via phosphorylation of Akt which effectively disrupts the activity of suppressor of cytokine signalling 1 (SOCS-1). The phosphorylated SOCS-1 enhances the JAK-STAT (Janus kinase, signal transducer and activator of transcription) activity (Hildebrand et al., 2010). These actions lead to stimulation of survival pathways and inhibition of apoptotic pathways. Activation of STAT1, 3, and 5 alters gene expression, e.g. upregulation of cancer-associated cyclooxygenase (COX)-2 expression (Orth et al., 2007). Activation of G_q and $G_{12/13}$ also leads to the activation of c-*jun*, a critical step for transformation via the MAPK pathway (Marinissen et al., 2003).

The mammalian target of rapamycin complex 1 (mTORC1) protein activated via the $G_{q/11}$/PLC/PKC pathway has been shown to be partially involved in the mitogenic response induced by PMT (Oubrahim et al., 2013). PMT induces upregulation of the connective tissue growth factor (CTGF) which then leads to the phosphorylation of ribosomal S6 kinase (S6K1) at Thr^{389} residue by mTOR (Koch et al., 1991). S6K1 then phosphorylates its substrate, ribosomal S6 protein (rpS6) at Serine residues. All of these actions lead to protein and ATP synthesis which are involved in cell growth, cell division and migration.

Cytoskeletal signalling is an early event mediating cell growth and differentiation. PMT via G_q and $G_{12/13}$ families activates RhoA via RhoGEFs leading to proliferation and cytoskeletal rearrangements (Orth et al., 2005). The formation of actin stress fibre and focal adhesion assembly in Swiss 3T3 cells are the result of activation of focal adhesion kinase and Src proto-oncogene, phosphorylation of $p125^{FAK}$ and adaptor protein paxillin via Rho (Lacerda et al., 1996).

PMT affects bone formation by inhibiting osteoblast differentiation via the Rho/ROK pathway (Harmey et al., 2004). PMT acts on osteoblast precursors to promote proliferation of the primary osteogenic cells via activation of the Ras-dependent Erk/MAPK pathway. This activation inhibits expression of growth factors such as bone morphogenetic protein (BMP) 2 and 4 and expression of osteoblast differentiation markers such as Cbfa1, as well as osteocalcin and alkaline phosphatase. PMT also inhibits osteoblast differentiation by transactivation of MAPK via activation of $G_{q/11}$, p63RhoGEF and RhoA (Siegert et al., 2013).

Wilson et al. (2000) analysed the effects of PMT on the expression of cell cycle markers such as MAPKs, cyclins D and E, p21, PCNA, c-Myc, and Rb proteins. They reported that in Swiss 3T3 cells, recombinant PMT (rPMT) stimulated phosphorylation of Rb/p130 and upregulated the expression of cyclins D and E which are required for cell cycle progression in particular from G_0 - G_1 and then to S-phase. In Vero cells, on the other hand, cyclins

D1 and 2 were detected on the first day. Cyclins D3 and E were almost not detectable.

PMT induces an anti-apoptotic effect in HEK293 cells. PMT was able to block stauroporine-induced apoptosis (Preuss et al., 2010). Staurosporine is a protein kinase inhibitor and a pro-apoptotic chemical, which works via caspase-dependent and caspase-independent mechanisms.

1.9 Aims

PMT inhibits the intrinsic GTPase activity of some members of G_i, G_q and G_{12} families. In many cell types (e.g. Swiss 3T3 cells), stimulation of signalling by PMT leads to a mitogenic response and cytoskeletal rearrangements while in others (e.g. Vero cells), PMT induces a cytotoxic phenotype with no evidence of mitogenicity (Wilson et al., 2000). The primary aim of this research is to investigate the cause of this notable difference as a tool to understand how G-protein activation leads to different responses in different cell types and the downstream interactions of these signalling molecules in controlling cellular function. Swiss 3T3 cells are mouse-derived fibroblast cells that are a standard model for cell proliferation assay while Vero cells are kidney epithelial cells derived from African Green Monkey. The specific aims are outlined below to help understand the primary aim.

- To quantify G-protein content and compare at the subtype level
- To determine which G-protein subtypes are modified by PMT
- To obtain preliminary evidence of downstream signalling events
- To investigate whether PMT causes differential loss of specific Gα-subunits

2 MATERIALS AND METHODS

2.1 General Solutions

The water used in all stock solutions was autoclaved at 123 °C for 28 min in Prioclave bench top autoclave. All recipes listed are for solutions made up to a volume of 1 L.

10x TBS-T	200mM Tris(hydroxymethyl)aminomethane (Sigma-Aldrich 252859), 1.5M NaCl (Sigma-Aldrich S3014), 1% (v/v) Tween-20 (Sigma-Aldrich P2287), distilled water
10x Running Buffer (~pH 8.3)	30.3g Tris(hydroxymethyl)aminomethane, 144 g glycine (Santa Cruz Technology SC-29096C), 10g sodium dodecyl sulfate (SDS) (Sigma-Aldrich L3771), distilled water (if properly weighed, pH is approximately 8.3)
10x Transfer Buffer (~pH 8.3)	30.3g Tris(hydroxymethyl)aminomethane, 144 g glycine, distilled water (if properly weighed, pH is approximately 8.3)

10x TBE	108g Tris(hydroxymethyl)aminomethane, 55g Boric Acid (Sigma-Aldrich B6768), 40ml of 0.5M Ethylenediaminetetraacetic acid (EDTA) (Sigma-Aldrich E9884) (pH 8.0), distilled water
1x TAE	20ml of 50x Tris-acetate-EDTA (TAE) (Thermo-Scientific B-49), distilled water

2.2 Reagents

NCS and Foetal Bovine Serum (FBS) were obtained from Invitrogen Ltd. (Paisley, UK). DMEM, Dulbecco's Phosphate Buffer Saline (DPBS), Trypsin/EDTA solution 0.05%, 10,000 unit/ml:10 mg/ml PS, 200 mM L-glutamine solution were purchased from Sigma-Aldrich Co. Ltd. (Dorset, UK). Cell culture dishes were purchased from Helena Biosciences Ltd. (Sunderland, UK). Cell culture flasks were purchased from Triple Red Ltd. (Buckinghamshire, UK). Pipette tips were purchased from Greiner Bio-One Ltd. (Stonehouse, UK).

Phalloidin Tetramethylrhodamine B isothiocyanate (TRITC) and Hoescht 33258 were purchased from Sigma-Aldrich. Western stripping buffer and ECL Western Blotting^{TM} detection reagent were purchased from Santa Cruz

Biotechnology (Wembley, UK) and GE Healthcare Ltd. (Buckinghamshire, UK) respectively.

2.3 Cell Culture

Swiss 3T3 cells were a kind gift of Dr. Rob Brookes from the School of Biomedical Sciences of King's College London. Vero cells were obtained from Dr Gill Pullinger of Pirbright Institute (UK). Swiss 3T3 cells were grown in Dulbecco's modified Eagle's medium (DMEM) supplemented with 1% 200 mM L-glutamine, 1% penicillin streptomycin (PS), and 10% newborn calf serum (NCS), in 10% CO_2 at 37°C. Vero cells were grown in DMEM supplemented with 1% 200 mM L-glutamine, 1% PS, and 10% NCS in 5% CO_2 at 37°C.

2.3.1 Preparation of Cell Culture Stock

Ampoules of Swiss 3T3 and Vero cells stock culture (2-4 X 10^6 cells/ampoule) containing 10% dimethyl sulfoxide (DMSO) and 90% DMEM-NCS medium were frozen slowly at -70°C in a Nalgene Cryo 1°C freezing container and later stored in liquid nitrogen.

2.4 Antibodies

The anti-$G\alpha_q$ (SC-393), anti-$G\alpha_{11}$ (SC-394), anti-$G\alpha_{12}$ (SC-409), anti-$G\alpha_{13}$ (SC-410), anti-$G\alpha_{i-2}$ (SC-7276), anti-$G\alpha_{i-3}$ (SC-262), and anti-Vinculin (SC-

5573) were purchased from Santa Cruz Biotechnology (Wembley, UK) and the anti-$G\alpha_{i-1}$ was purchased from Merck Chemicals Ltd - Calbiochem (Nottingham, UK). The anti-$G\alpha_{i-1}$ for immunoprecipitation was purchased from Abcam (Cambridge, UK). The anti-Na^+/K^+ ATPase α-1 was purchased from Merck Millipore (Hertfordshire, UK). The anti-RhoA (Part No. 240302), anti-Rac1 (Part No. 240106), and anti-Cdc42 (Part No. 240201) used in the pull-down assay were part of the RhoA/Rac1/Cdc42 Activation Assay Combo Kit from Cell Biolabs (Cambridge, UK). The anti-rabbit and anti-rat IgG, HRP-linked were purchased from Santa Cruz Biotechnology while the anti-mouse IgG, HRP-linked was purchased from Cell Signaling Technology Inc.

The anti-QE-producing Hybridoma cells were a kind gift of Dr. Yasuhiko Horiguchi from the Research Institute for Microbial Diseases, Osaka University, Japan. The anti-QE antibody, which recognises only the deamidated form of $G\alpha$ polypeptides, from the Hybridoma cells was prepared by Arshiya Banu, a PhD student of this institute.

The anti-PMT monoclonal antibody was a kind gift of Dr. Gill Pullinger from the Pirbright Institute.

2.5 Bacterial Toxin

The recombinant *Pasteurella multocida* toxin (rPMT) and mutant toxin rPMT^{C1165S} had been previously prepared by Dr. Rebecca Babbs of this institute, according to published protocols (Ward et al., 1998). PMT^{C1165S} is the mutant form of PMT where the 8th cysteine (C1165) is replaced with alanine in the catalytic core, abrogating its catalytic activity on the Gα subunits (Ward et al., 1998). The recombinant toxins were kept at –20ºC freezer.

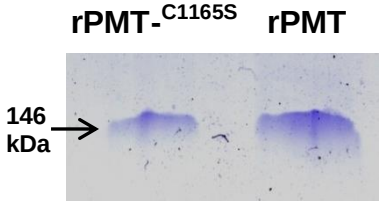

Fig 2.5 The purified recombinant PMT and PMT^{C1165S}. The stock solution of rPMT and rPMT^{C1165S} (3 µg) were resolved by SDS-PAGE and protein bands were visualised using CCBB stain (see section 2.13).

2.6 Cell Proliferation Assay Using Haemocytometer

2.6.1 Confluent Swiss 3T3 and Vero Cells

Swiss 3T3 and Vero cells were plated in 24-well plates at 2 x 10^4 cells and 4 x 10^4 cells per well respectively and cultured in media (DMEM containing 1% PS, and 1% L-glutamine) supplemented with 10% FBS and 10% NCS for 5 days until cells were confluent and quiescent. Swiss 3T3 and Vero cells were incubated at 37°C in 10% and 5% CO_2 respectively. Cells were washed three times with DPBS to remove any residue of serum from the

previous cell culture medium, and serum-starved using media only for 40-48 h. Subsequently, cells were washed three times with DPBS and treated with 200 ng/ml of recombinant PMT (rPMT) or PMT-^{C1165S} (rPMT-^{C1165A}) in media with 1% FBS for Swiss 3T3, and media with 1% NCS for Vero cells. Cells were washed twice with DPBS, trypsinised, neutralised with media with 10% FBS or NCS and counted at different time points: 0, 24, 48, 72, 96, 120, 144, 168, 192 h using a haemocytometer. Morphological changes were captured using a phase-contrast microscope (see section 2.8).

2.6.2 Subconfluent Swiss 3T3 and Vero Cells

For the 3- and 10-day proliferation assays, Swiss 3T3 and Vero cells were cultured in 24-well plates at 2 x 10^4 cells and 4 x 10^4 cells per well respectively in media with 10% NCS for 3-4 days until cells were ~50 - 60% confluent. Cells were washed with DPBS, serum-starved and subsequently washed with DPBS (as described in section 2.6.1) prior to treatment with or without 15 ng/ml of rPMT or PMT-^{C1165S} in media with or without 10% NCS. For the 10-day treatment, Swiss 3T3 and Vero cells were either left untreated or treated with 15 ng/ml of rPMT maintained in media with or without 1% NCS. Cells were washed twice with DPBS, trypsinised, neutralised with media supplemented with 10% NCS, and counted at different time points: 0, 24, 48, 72, 96, 120, 144, 168, 192 h for the 10-day proliferation assay, and 0, 24, 48, 72 h for the 3-day proliferation assay using a haemocytometer.

2.7 Phalloidin Staining of Actin Filaments

Swiss 3T3 and Vero cells were cultured on 22 x 22 mm Corning coverslips (Thermo-Scientific, UK) in 6-well plates at 4 x 10^4 cells and 8 x 10^4 cells per well respectively in media with 10% NCS for 4 days until cells were confluent and quiescent. Cells were washed with DPBS, serum-starved and subsequently, washed with DPBS (as described in section 2.6.1) prior to treatment with or without 200 ng/ml of rPMT in media with 1% NCS.

Cells were fixed at different time points with 4% paraformaldehyde (Santa Cruz Biotechnology) and left overnight at 4ºC. Cell membranes were permeabilised with 0.1% Triton X-100 in DPBS for 15 min at 4ºC, then non-specific sites were blocked with a blocking buffer (1% BSA in DPBS). Fixed cells were stained with Phalloidin TRITC and left for 1 h at 37ºC. Cells were washed three times with wash buffer (DPBS with 0.5% Tween-20) at 5 min intervals. Stained cells were washed three times with a wash buffer and fixed with Mowoil 4-88 (Sigma-Aldrich) anti-fade mounting medium (4.8% (w/v) Mowoil 4-88, 12% (w/v) glycerol, 24% (v/v) 0.2M Tris-HCl buffer (pH8.5), 64.8% (v/v) distilled water, sodium azide (NaN_3) on a microscope slide (Thermo-Scientific). Cells were visualised using a fluorescence microscope (section 2.8).

2.8 Microscopy/Photography

Phase-contrast and fluorescence imaging were done using an Olympus IX5I Fluorescence microscope and captured by CellSens version 1.12 software. Image J (National Institutes of Health, Maryland, USA) was used to merge fluorescent images. A two-photon excitation fluorescence Nikon Eclipse Ti microscope was also used in fluorescence imaging (used in section 3.2.2.2 of chapter 3).

2.9 Cytotoxicity Assay

2.9.1 LDH Assay

The Cytotox® 96 Non-Radioactive Cytotoxicity Assay Kit (Promega, UK) was used to assess the cytotoxicity of rPMT in Swiss 3T3 and Vero cells. Swiss 3T3 and Vero cells were cultured in 96-well plates at 8×10^4 cells and 1.6×10^5 cells per well respectively in media with 10% NCS for 2 days until cells were confluent and quiescent. Cells were washed with DPBS, serum-starved and subsequently washed with DPBS (as described in section 2.6.1). Cells were either left untreated or treated with 0.01, 0.1, 1, or 10 ng/ml rPMT or $rPMT^{C1165S}$ in media without or with 10% NCS.

A standard curve was generated using lactate dehydrogenase from porcine heart (Sigma-Aldrich) to determine the concentration of LDH in the samples. Cells were processed after 48 h using the Cytotox® 96 Non-Radioactive

Cytotoxicity Assay Kit. Supernatant (50 µl) from each well was transferred to a new 96-well plate including supernatant from wells without cells. Cytotox® 96 reagent (12 ml of assay buffer, 1 bottle of Cytotox® substrate mix) (50 µl) was added to each well. Samples were incubated at 37°C for 30 min. Cytotox® stop reaction solution (50 µl) was added to each well. Plates containing the standard curve and samples were immediately read using Microplate Reader Labtech LT-4000 (Labtech, Vienna, Austria) at 495 nm and data were acquired using Labtech Manta software.

2.10 Calcium Assay

The Fluo-4 NW Calcium Assay Kit was used to determine $G\alpha_q$ activity by measuring the calcium influx in the cytosol from the Ca^{2+} stores.

Swiss 3T3 and Vero cells were cultured in 96-well plates at 8 x 10^4 cells and 1.6 x 10^5 cells per well respectively in media with 10% NCS until cells were confluent. Cells were washed with DPBS, serum-starved and subsequently washed with DPBS (as described in section 2.6.1) prior to treatment with or without 15 ng/ml of rPMT in media only.

After 24, 48, or 72 h, growth medium was removed from the plates and 100 µl of the dye-loading solution (10 ml of assay buffer and 100 µl of probenecid stock solution [1 vial of probenecid and 1 ml of assay buffer]) was added to all wells. Plates were incubated for 30 min at 37°C and another 30 min at

room temperature. Fluorescence was measured in Flouraskan Ascent/FL (Thermo Scientific) with wavelengths: Excitation 485; Emission 510 nm.

2.11 Activation of Rho GTPases

The RhoA/Rac1/Cdc42 Activation Assay Combo Kit (Cell Biolabs, Cambridge, UK), which includes Rhotekin RBD and PAK PBD agarose beads, antibodies for RhoA, Rac1, and Cdc42, was used to determine the activity of Rho GTPase family members. Swiss 3T3 and Vero cells were cultured in 150 mm plates at 8 x 10^4 cells and 1.6 x 10^5 cells per well respectively in media with 10% NCS until cells were subconfluent (approximately 80 - 90% confluent as per manufacturer's protocol). Cells were washed with DPBS, serum-starved and subsequently washed with DPBS (as described in section 2.6.1) prior to treatment with or without 15 ng/ml of rPMT in media only.

After 24, 48, or 72 h, culture media were removed and washed twice with ice-cold PBS. Ice-cold 1x Assay Lysis buffer (1.5 ml) was added to the cells and incubated for 15 min on ice. Cells were detached using a cell scraper and lysates were transferred to a 2 ml microtube and kept on ice. Lysates were centrifuged at 14,000 x g for 4°C for 10 min. The protein concentration of the samples was determined using the BCA assay. The supernatant (1 ml) with a protein content of >0.5 mg was aliquoted to a new centrifuge tube (if supernatant was less than 1 ml, it was adjusted to this volume using

Assay Lysis Buffer). Rhotekin RBD (for RhoA) or PAK PBD beads (for Rac1 or Cdc42) (40 µl) was added to each tube and incubated at 4°C for 1 h with gentle agitation. The beads were pelleted at 14,000 x g for 10 s. The supernatant was aspirated and the pellet was washed three times with 0.5 ml Assay Lysis Buffer with centrifugation after each wash. The bead pellet was resuspended with 2x SDS-PAGE sample buffer and heated at 95°C for 5 min. Proteins were separated by conventional SDS-PAGE, transferred to PVDF membrane and subjected to Western blotting analysis.

2.12 Suppression of cyclic AMP (cAMP)

The cAMP Glo® Assay (Promega) was used to determine the activity of $G\alpha_i$ via suppression of the cAMP level. A standard curve was generated using a cAMP standard (Promega) to determine the concentration of cAMP in the samples. Swiss 3T3 and Vero cells were cultured in 96-well plates at 8 x 10^4 cells and 1.6 x 10^5 cells per well respectively in media with 10% NCS for 3 days until cells were confluent and quiescent. Cells were washed with DPBS, serum-starved and subsequently washed with DPBS (as described in section 2.6.1) prior to treatment with or without 15 ng/ml of rPMT in media only.

Samples were processed at different time points: 0, 24, 48, or 72 h. Forskolin (Sigma-Aldrich) or DPBS (20 µl) was added to each well of the untreated or rPMT-treated samples, and incubated for 15 min at 37°C. The

cAMP-Glo™ Lysis Buffer (20µl) was added to each well. Plates were incubated with gentle shaking at room temperature for 15 min. cAMP-GloTM Detection Solution (2.5µl of Protein Kinase A per 1.0ml of cAMP-Glo™ Reaction Buffer) (40µl) was added to each well with 30-60 s shaking before incubation at room temperature for 20 min. Kinase Glo Reagent (80µl) was added to each well with 30-60 s shaking before incubation at room temperature for 10 min. Luminescence was measured in Flouraskan Ascent/FL (Thermo Scientific).

2.13 Molecular and Cell Biology

2.13.1 Preparation of membrane and cytoplasmic fractions from Swiss 3T3 cells and extraction of G-proteins from membrane fractions

Quiescent cultures of Swiss 3T3 and Vero cells were grown in 150 mm dishes and rinsed twice with ice cold DPBS and scraped into 2 ml of DPBS containing proteinase inhibitors (Complete™, Roche Diagnostics). Cells from 20 dishes were transferred to 12 ml falcon tubes and pelleted by centrifugation (200×g, 10 min, 4°C), DPBS was aspirated and the cell pellet was frozen at –70°C until required. The frozen cell pellets were thawed on ice and suspended in 5 ml of membrane buffer (10 mM Tris-HCl, 10 mM $MgCl_2$, 0.1 mM EDTA, pH 7.4, containing proteinase inhibitors). The cells were ruptured by passing through a 23-gauge needle/syringe. The

homogenate was centrifuged at 800×g for 10 min to remove intact cells and nuclei. The resulting supernatant was centrifuged at 50,000×g using a Beckman Coulter™ Avanti-J-20 XPI Expanded-Performance Centrifuge unit (Kendro Laboratory Products Ltd.) for 30 min at 4°C. The membrane pellet was resuspended in membrane buffer to a protein concentration of 1 mg/ml and centrifuged at 50,000×g for 30 min to remove contaminating cytosolic proteins. The membrane pellet was resuspended in 1ml of membrane buffer and protein concentration was determined using the BCA assay. The membrane proteins (1.5 mg/ml) from Swiss 3T3 cells or (2.5 mg/ml) Vero cells were mixed with 2x sample buffer and boiled at 95°C for 5 min. Proteins were separated by conventional SDS-PAGE, transferred to PVDF membrane and subjected to Western blotting analysis.

2.13.2 Sodium-Dodecyl-Sulphate Polyacrylamide Gel Electrophoresis (SDS-PAGE)

SDS-PAGE was based on the method provided by Laemmli (1970) and BioRad (Hempstead, UK) SDS-PAGE Laemmli Buffer System. Resolving gels were prepared using 10 – 14 % acrylamide/bis (30 %, 37.5:1), and 4 % stacking gel acrylamide/bis (30 %, 37.5:1). Samples were denatured by the addition of an equivalent volume of 2x SDS PAGE buffer (240mM Tris/HCL, pH 6.8, 8 % (w/v) SDS, 40 % (v/v) glycerol, 7 % (v/v) 2-mercapthoethanol, 0.05 % (w/v) bromophenol blue) and boiling for 2 min. Gels were run on the

mini-Protean system (Bio-Rad) using SDS-electrophoresis at 200V for ~45 min or until the dye had reached the end of the gel.

2.13.3 Colloidal Coomassie Blue Staining

Colloidal Coomassie Blue Staining (CCBB) staining was used to visualise the protein bands on the gels. Following electrophoresis, gels were rinsed three times for 5 min in a large volume of ultra-pure water and stained with Coomassie Brilliant Blue R-250 solution (50 % methanol, 10 % acetic acid, and 0.05 % Brilliant Blue R-250) for 1 h, and destained with Coomasie destain solution (40 % methanol, 50 % distilled water, and 10 % acetic acid) for 1 - 2 h.

2.13.4 Protein Transfer and Western Blotting

Proteins separated by SDS PAGE were transferred to PVDF membranes by a method adapted from Towbin et al. (1979). A gel ‘sandwich’ (fibre pad (BioRad), thick filter paper membrane (BioRad), SDS gel, nitrocellulose or methanol-pre-wetted PVDF membrane (BioRad), thick filter paper membrane and fibre pad) in a gel cassette holder was assembled and placed in a Mini TransBlot cell (Bio-Rad) filled with pre-chilled transfer buffer (25 mM Tris base, 192 mM glycine, 10 % methanol). Transfer was performed at 90 mA and 30V overnight.

Following protein transfer the membrane was soaked briefly in methanol and allowed to air dry to fix the proteins before being rewetted in methanol and washed three times in distilled water. Membranes could then be stained with Ponceau S (0.1 % (w/v) Ponceau S in 5 % (v/v) acetic acid) if visualisation of transferred proteins was required. Membranes were incubated in blocking buffer (5 % non-fat dried milk and Tris buffered saline (TBS, 137 mM Sodium Chloride, 20 mM Tris, 0.1 % Tween-20 at pH 7.6) solution for 1h at room temperature on an orbital shaker. The blocking buffer was removed and membrane was washed three times for 10 min each with wash buffer (0.1 % Tween 20 in TBS). The membrane was probed with primary antibody (1:1000) in 5 % non-fat dried milk and 0.1 % Tween-20 in TBS overnight at 4ºC on an orbital shaker. Following the primary antibody incubation period the membrane was washed three times for 10 min each with wash buffer, followed by incubation with horseradish peroxidase-coupled secondary antibody at a dilution of 1:10000 for 1 h at room temperature. The membrane was washed three times for 10 min each with wash buffer. Membrane was incubated with ECL™ chemiluminescent substrate (GE HealthCare) and signals were detected using the BioRad ChemiDoc™ MP Imaging System and BioRad Image Lab™ software.

2.13.5 Determination of Protein Concentration Using Bicinchoninic Acid (BCA) Assay

The Pierce™ BCA protein assay kit was purchased from Life Technologies (Paisley, UK). The Bovine Serum Albumin (BSA) used as the protein standard to generate the standard curve was purchased from Sigma-Aldrich. BSA standard (25 µl) (BSA in DPBS or lysis buffer) with concentrations: 0, 62.5, 125, 250, 375, 500, 750, and 1000 µg/ml and samples (25 µl) with unknown protein concentration were transferred in triplicates to a 96-well plate. 200µl of BCA working reagent (50:1 Reagents A and B) was added to each well. The 96-well plate was then incubated at 37°C for 30 min and cooled to room temperature for 5 min prior to OD measurement (540 nm). The linear regression equation from the standard curve was used to determine the unknown protein concentration of each sample.

2.13.6 Detection of Unmodified and Deamidated Gα subunits by Immunoprecipitation

Unmodified and deamidated endogenous G-proteins alpha subunits of Swiss 3T3 and Vero cells were resolved by immunoprecipitation. Quiescent cultures of Swiss 3T3 and Vero cells were grown in 150 mm dishes, serum starved, left untreated or treated with rPMT (as per section 2.7.2), collected and processed (as per section 2.13.1). Frozen pelleted samples kept in -70ºC were resuspended in CHAPS lysis buffer (50 mM Tris, pH 7.4, 250 mM

NaCl, 5 mM EDTA, 50 mM NaF, 1 mM Na_3VO_4, 1 % CHAP, 0.02 % NaN_3) supplemented with 1x protease inhibitor cocktail solution and kept on ice for 30 min, vortexing at 10-min intervals and subjecting to brief sonication. Samples were centrifuged at 17,000 x g for 10 min at 4ºC. Clear lysates were transferred to clean microtubes. Protein concentration was determined by the BCA assay. Proteins from Swiss 3T3 (500 µg) or Vero cells (700 µg) was aliquoted in each tube and stored at -70ºC until required.

Samples ready for immunoprecipitation, 1 µg of antibody specific to Gα subunit was added to each tube and left to conjugate overnight at 4ºC on an orbital shaker. Magnetic Dynabeads® (Life Technologies Ltd) (50 µl) were added to each tube and left to cross-link for 10-15 min at room temperature on an orbital shaker. The cross-linked Dynabeads® (antibody-antigen) were washed three times with 100 µl wash buffer (0.1%Tween-20 in DPBS). 4x sample buffer (1 part) and nuclease free water (3 parts) were added to the cross-linked Dynabeads® and boiled at 95ºC for 5 min. Proteins were separated by conventional SDS-PAGE, transferred to PVDF membrane and subjected to Western blotting analysis.

2.13.7 RNA Extraction from Swiss 3T3 and Vero Cells

RNA molecules from Swiss 3T3 and Vero cells were extracted using the QIAGEN RNeasy® Plus Mini Kit.

Buffer RLT Plus (600 µl) (containing 0.1 % of β-mercaptoethanol) was added to each microcentrifuge tube containing ~1 x 10^7 Swiss 3T3 or Vero cells. Tubes were then vortexed for 10s to homogenise. The homogenised lysate was transferred to the gDNA eliminator spin column placed in a 2ml collection tube and centrifuge for 30 s at ≥8000 x g. The column was discarded and 1 volume of 70 % ethanol was mixed with the flow-through. Part (700 µl) of this mixture was transferred to a RNeasy spin column placed in a 2ml collection tube which was then centrifuged for 15 s at ≥8000 x g. The flow-through was discarded and 700 µl of Buffer RW1 was added to the RNeasy spin column in a 2 ml collection tube and centrifuged for 15 s at ≥8000 x g. Flow-through was discarded and 500 µl of Buffer RPE (containing 80 % (v/v) of 94 - 100 % ethanol) was added to the RNeasy spin column and centrifuged for 15 s at ≥8000 x g. The last step was repeated and centrifuged for 2 min instead of 5 s. To elute the RNA molecules from the RNeasy spin column which was placed in a new 1.5 collection tube, 30 µl of nuclease free water (BioRad) was added to it and centrifuged for 60 s at ≥8000 x g. RNA elution was repeated using the same RNA eluate.

2.13.8 Integrity and Purity of the Extracted Cellular RNA

One of the most common methods to assess integrity of total RNA samples is by visualising 28s and 18s ribosomal RNAs (rRNAs) on a denaturing agarose gel stained with gel red or ethium bromide (EtBr) (Fleige and Pfaffl, 2006). The secondary structure of RNAs alters their migration properties and

therefore would not migrate according to their size. Samples with intact total RNAs will have a clear ~2:1 ratio intensity of 28s and 18s rRNA bands.

Extracted RNAs in samples were electrophoresed on 1 % (w/v) agarose gel, which were composed of molecular grade agarose (Sigma-Aldrich) dissolved in 1x TAE (Thermo-Scientific) containing 1 % household bleach (Clorox®, CA, USA), by heating the solution in a microwave oven. RNA samples were mixed with approximately 1/6 volume of loading dye (Thermo-Scientific) prior to loading. A commercially prepared 100bp DNA ladder (New England Biolabs, UK) was used to determine that electrophoresis was successful. Electrophoresis was carried out in horizontal electrophoresis unit in trays at approximately 6V/cm of gel (constant voltage) for ~1 - 1.5 h. Gels were then stained using GelRed (Biotum, UK) for 30 min then visualised on UV transilluminator (AlphaImager; λ= 302) to allow the UV detection of the stained DNA bands.

2.13.9 Generation of cDNA from extracted RNA by PCR

For the generation of cDNA template from mRNA, *Precision nanoScript™ 2* Reverse Transcription kit (Primerdesign, UK) containing dNTPs, reaction buffer, enzymes, DTT, oligodT primer, nuclease-free water. For a 10µl reaction (designated as tube A), 2ng-2µg of mRNA template, 1 µl of primer, nuclease-free water were mixed and heated to 65°C to denature any double stranded RNAs for 5 mins. The mixed sample was then immediately

transferred to ice. In another tube (designated as tube B), 2 µl of buffer, dNTPs, 2 µl of 100 mM DTT, 1 µl of enzymes, and 4 µl of nuclease-free water were mixed. Tube A and B were mixed to make a 20 µl reaction and briefly vortexed followed by a pulse spin and incubation at 55°C for 20 min. cDNA was stored at -20°C until use.

High-Capacity cDNA Reverse Transcription Kit (Life Technologies) was also used to generate cDNA. The 2x RT master mix was prepared on ice by mixing 2 µl of 10x RT buffer, 0.8 µl of 25x dNTP mix (100 mM), 2 µl of 10x RT random primers, 1 µl of Multiscribe™ reverse transcriptase, 1 µl of RNAse inhibitor, and 3.2 µl of nuclease-free water. cDNA reverse transcription reaction was then prepared by mixing 10 µl of RT master mix and 10 µl of RNA sample and was briefly centrifuge to eliminate any air bubbles. Individual tubes containing the mix were placed in a thermal cycler with different temperatures. Samples were then stored at -70°C until required.

2.13.10 Amplification of cDNA by Real-Time Polymerase Chain Reaction (RT-PCR)

Primers for sequencing the complete CDS (coding sequence) of G-proteins in Vero cells were designed using primer3 software (http://primer3plus.com/) and the National Center for Biotechnology Information (NCBI) primer blast (http://www.ncbi.nlm.nih.gov/tools/primer-blast/) based on the complete

mRNA of *Homo sapiens*, and the predicted mRNA of *Chlorocebus sabaeus* of $G\alpha_q$, $G\alpha_{11}$, $G\alpha_{12}$, $G\alpha_{13}$, $G\alpha_{i\text{-}1}$, $G\alpha_{i\text{-}2}$ and $G\alpha_{i\text{-}3}$. A comparative analysis of the gene sequences of the G-proteins alpha subunits from primates such as *Chlorocebus aethiops*, *Chlorocebus cynosuros*, *Chlorocebus pygerythrus*, *Chlorocebus sabaeus*, and *Chlorocebus tantalus* using Exonorate was also consulted (by our senior bioinformatics office, Phil Cunningham).

For the amplification of cDNA, GoTaq® Hot Start Colourless Master Mix (Promega, UK), a premixed ready-to-use solution containing Taq Polymerase, dNTPs, $MgCl_2$ and reaction buffers for real-time Polymerase Chain Reaction (rt-PCR) was used. For a 25 µl reaction volume, the PCR mixture consisted of 1x GoTaq® Hot Start Colourless Master Mix, 1 µM each of the forward and reverse primers, 1 µM each of the forward and reverse primers, <250 ng of the DNA template, and nuclease free water. The reaction was carried out in a PCR machine programmed to carry out 40 cycles at different annealing temperatures.

Table 2.13.10 Primer Sequences Used in PCR for Genotyping

Gα	Forward	Reverse	Expected Product Size (bp)
$G\alpha_q$	GGAGGCACTTTGGAAGAATGAC	AACTCTGTGGACACGCTCAC	1,239
$G\alpha_{11}$	GATGACTCTGGAGTCCATGATG	TGCGGAGGGAGAGATGTACA	1,284
$G\alpha_{12}$ (A)	CGGCAAGTCCACGTTCCTTA	TCCTGCAGGAGACGACAAAC	974
$G\alpha_{12}$ (B)	CAGTCTCAGCGTTCCCTTCA	CGAGGACCACACAGACAACA	1,123
$G\alpha_{13}$	GTCAGTTCGCTGGTTCCCTC	CACTCAACAGCTTTCAGCCAC	1,463
$G\alpha_{i-1}$	GCCCGCTGGGAGAGAGAAAG	CACACTGCAGGACCATCTGTC	1,375
$G\alpha_{i-2}$	CTGAACTGCCGACCCGATAG	CCTCCCCTACATCTGGAGCT	1,375
$G\alpha_{i-3}$	CGCTTTCGGTCTCAACTCCT	GTAGCTGCCCCGTAAGACAG	1,371

2.13.11 DNA Agarose Gel Electrophoresis

PCR (cDNA) products were electrophoresed on 1 – 2 % (w/v) agarose gels, which were composed of molecular grade agarose (Sigma-Aldrich) dissolved in 0.5x TBE (Tris-Borate EDTA) buffer or 1x TAE (Tris-acetate-EDTA) buffer (Thermo-Scientific), by heating the solution in a microwave oven. DNA samples were mixed with approximately 1/6 volume of loading dye (Thermo-Scientific) prior to loading. A commercially prepared 100 bp DNA ladder (New England Biolabs, UK) or 1 kb DNA ladder (New England Biolabs, UK) were used as molecular markers. Electrophoresis was carried out in horizontal electrophoresis unit in trays at approximately 3-6V/cm of gel (constant voltage) for 1 - 2 h. Gels were then stained using Gel Red (Biotum, UK) for 30 min then visualised on a UV transilluminator (AlphaImager; λ= 302) to allow the UV detection of the stained DNA bands.

2.13.12 DNA Extraction and Sequencing

For samples with more than one band on the gel, each band was cut using a scalpel, weighed and placed in an eppendorf tube. DNA fragments were extracted using the QIAquick Gel Extraction Kit (QIAGEN). Buffer GQ (6 volumes) was mixed with 1 volume of 2 % agarose gel containing the DNA fragments (100 mg ~ 100 µl). Samples were then incubated at 50°C for 10 min, vortexing the tube every 2 - 3 min. One volume of isopropanol was added to the sample mix. Sample mix was then transferred to a QIAquick spin column in a 2 ml collection tube and centrifuge for 1 min at 17,900 x g. The flow-through was discarded and 500 µl of Buffer GQ was added to the QIAquick spin column and centrifuge for 1 min at 17,900 x g. The flow-through was discarded and the QIAquick spin column containing the DNA was washed with 750 µl Buffer PE mixed with ethanol. QIAquick spin column was centrifuged twice for 1 min at 17,900 x g before placing it into a clean 1.5 ml microcentrifuge tube. The DNA from the QIAquick spin column was eluted by incubating with 30 µl nuclease-free water for 4 min prior to centrifugation for 1 min at 17,900 x g. Samples were then sent to Eurofins Genomics (Germany) for sequencing.

2.13.13 Quantification of mRNA Level by RT-qPCR (Real-Time Quantitative Polymerase Chain Reaction)

For the quantification of mRNA level, Precision™ 2X qPCR SYBRgreen Mastermix (Primer Design, Southampton, UK), a premixed ready-to-use solution containing 2x reaction buffer, 0.025 U/µl Taq Polymerase, 5 mM $MgCl_2$, dNTP Mix (200 µM each dNTP) was used. For a 10 µl real-time PCR volume, the PCR mixture consisted of 5 µl of Precision™ 2X qPCR Mastermix, 25 ng of cDNA template, 6 pmols of primer mix (forward and reverse), and nuclease free water. The reaction was carried out in a Corbett Rotor-Gene 6000 qPCR machine programmed to carry out 40 cycles at different temperatures. The primers for the qPCR for Swiss 3T3 cells were obtained from Origene Technologies (MD, USA).

Table 2.13.13 The RT-qPCR Primer Sequences for Gα subunits of Swiss 3T3 Cells

Gα	Forward	Reverse	Expected Product Size (bp)
$G\alpha_q$	AGCGATGGACACGCTCAAGATC	CAGACACCTTCTCCACATCAACC	92
$G\alpha_{11}$	GTTCTTGGTGGCACTAAGCGAG	GACAGACGAGTTCTGGAACCAG	127
$G\alpha_{12}$	TCCACCTTCCTCAAGCAGATGC	AGCGTCCACAAGAACCCTCGAA	123
$G\alpha_{13}$	TCCACCTTCCTGAAGCAGATGC	AGCTTCTCTCGGGCATCTACCA	134
$G\alpha_{i-1}$	CTCGGAAGAGGAGTGTAAGCAG	GCAAGCACGAAAAGTTGGCGAG	150
$G\alpha_{i-2}$	TGACTTGGTGCTGGCTGAGGAT	GATGGAGGTGTCTGTGAACCAC	103
$G\alpha_{i-3}$	GACTACAGGCATTGTGGAGACC	GGTCGTAATCACTGAGAGCCAC	155
Actin-β	CAGCAGTTGGTTGGAGCAAA	GTGGCTTTTGGGAGGGTGAG	167

2.14 Statistical Analysis

All values in the graphs are expressed as mean ± SD. The statistical significance of differences between rPMT-, $rPMT^{C1165S}$-treated, and untreated cells in two cell lines was evaluated by Two-way ANOVA while the statistical significance of differences between rPMT-treated and untreated cells in each cell was evaluated by an F-test two sample variances. $P < 0.05$ was considered statistically significant. All experiments were performed in triplicate ($n = 3$).

3 THE EFFECTS OF PMT ON SWISS 3T3 AND VERO CELLS: CELL PROLIFERATION, CYTOSKELETAL REORGANISATION, CELL DEATH

PMT is a potent intracellular-acting mitogen to various cell lines (Rozengurt et al., 1990; Higgins et al., 1992; Lacerda et al., 1996; Mullan and Lax, 1996; Ward et al., 1998; Wilson et al., 2000) but not to others such as Vero cells (Wilson et al., 2000). The action of PMT includes constitutive activation of $G_{q/11}$, $G_{11/13,}$ and $G_{i\text{-}1\text{-}3}$ leading to numerous sequelae as detailed in chapter 1.

3.1 The Growth Kinetics of Swiss 3T3 and Vero Cells

Swiss 3T3 cells are contact inhibited mouse-derived fibroblasts from *Mus musculus* while Vero cells are kidney epithelial cells derived from African Green Monkey. To compare the effect of PMT on the growth kinetics of Swiss 3T3 and Vero cells, confluent Swiss 3T3 and Vero cells were subjected to serum deprivation for 2 days to quiesce them before treatment with a final concentration of 200 ng/ml of rPMT or $rPMT^{C1165S}$, or left untreated and maintained in media with 1 % serum (see section 2.6.1) throughout the 7-day period as opposed to Wilson et al. (2000) experimental condition in which the media with 1 % serum were changed every day. Cell

numbers were directly counted from the plate in triplicate at different time points.

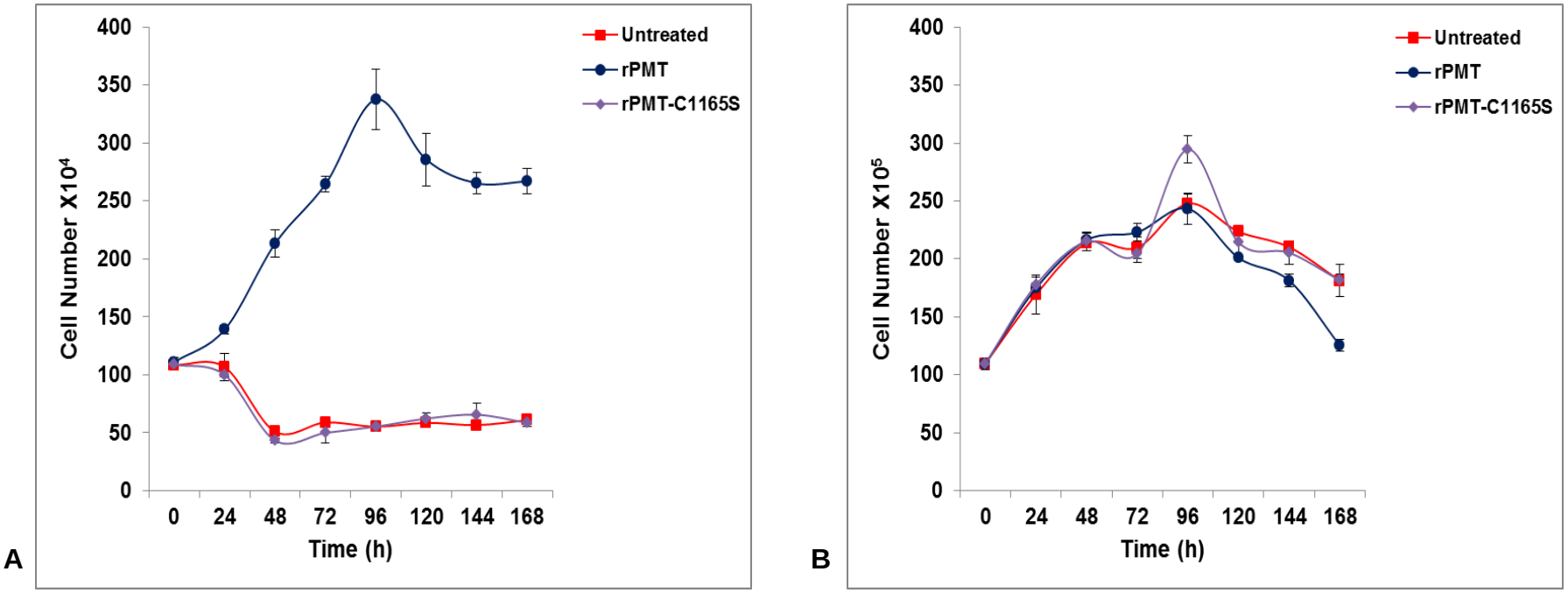

Fig 3.1.1 Effects of rPMT on the growth kinetics of confluent Swiss 3T3 (A) and Vero (B) cells. Shown above are time courses of cell number for confluent (A) Swiss 3T3 (P = 0.00003) B) Vero (P = 0.16) cells that were either left untreated or treated with 200 ng/ml of rPMT- or rPMT^{C1165S}-treated and maintained in media supplemented with 1% serum. Red (Untreated), Blue (rPMT-treated), and Purple (rPMT^{C1165S}-treated). Each value is the mean and ± SEM (n = 3).

rPMT-treated confluent Swiss 3T3 cells in the presence of 1 % serum proliferated and reached a maximum of a 2.3-fold increase in cell number at 96 h post rPMT exposure with an exponential increase of ~0.5 – 0.7 fold in cell number from 1 – 4 days compared to the untreated and rPMT^{C1165S}-treated cells which had approximately similar cell number with a ~0.5 fold decrease in cell number from 2 days (Fig 3.1.1 A). The confluent Vero cells, on the other hand, had a ~1.5-fold increase in cell number over the 4 days but there was no significant change in cell numbers between untreated, rPMT-, and rPMT^{C1165S}-treated cells (Fig 3.1.1 B). Cell debris in both rPMT-treated cell lines was observed during counting, but this observation was more prominent in Vero cells as they appeared to be very fragile especially during trypsination and pipetting of cells to break up the clumps.

Wilson et al. (2000) treated subconfluent Swiss 3T3 and Vero cells with a final concentration of 200 ng/ml of rPMT in media with 15% NCS and 10% FBS respectively and showed a similar mitogenic effect in rPMT-treated confluent Swiss 3T3 maintained in media with 1% serum, but not in Vero cells. A very high concentration of rPMT (200 ng/ml) appeared to be detrimental to the morphological stability of confluent Swiss 3T3 and Vero cells. Also, Rozengurt et al. (1990) reported that rPMT (at a concentration of 1.25 ng/ml) and 10% FBS each stimulated DNA synthesis in a strikingly similar fashion in the absence of other factors in Swiss 3T3 cells.

To determine if subconfluent Swiss 3T3 or Vero cells would behave differently when exposed to PMT at a lower concentration, Swiss 3T3 and Vero cells were cultured until they reached 50% confluence before subjecting them to serum starvation for 40 h (see section 2.6.2). The subconfluent quiescent cells were then treated with 15 ng/ml of rPMT or left untreated in media with 1% NCS. Cell numbers were counted in triplicate using a haemocytometer at the following time points: 0, 2, 4, 6, 8, and 10 days.

The rPMT-treated Swiss 3T3 cells underwent proliferation, reaching a ~0.8-fold increase by day 4 which is also the onset of the plateau growth phase compared to its untreated counterpart (Fig 3.1.2 B). The untreated and rPMT-treated Vero cells, on the other hand, each demonstrated a ~0.8-fold increase in cell numbers (Fig 3.1.2 B). Many untreated and rPMT-treated Vero cells detached, and cell growth ceased by day 4.

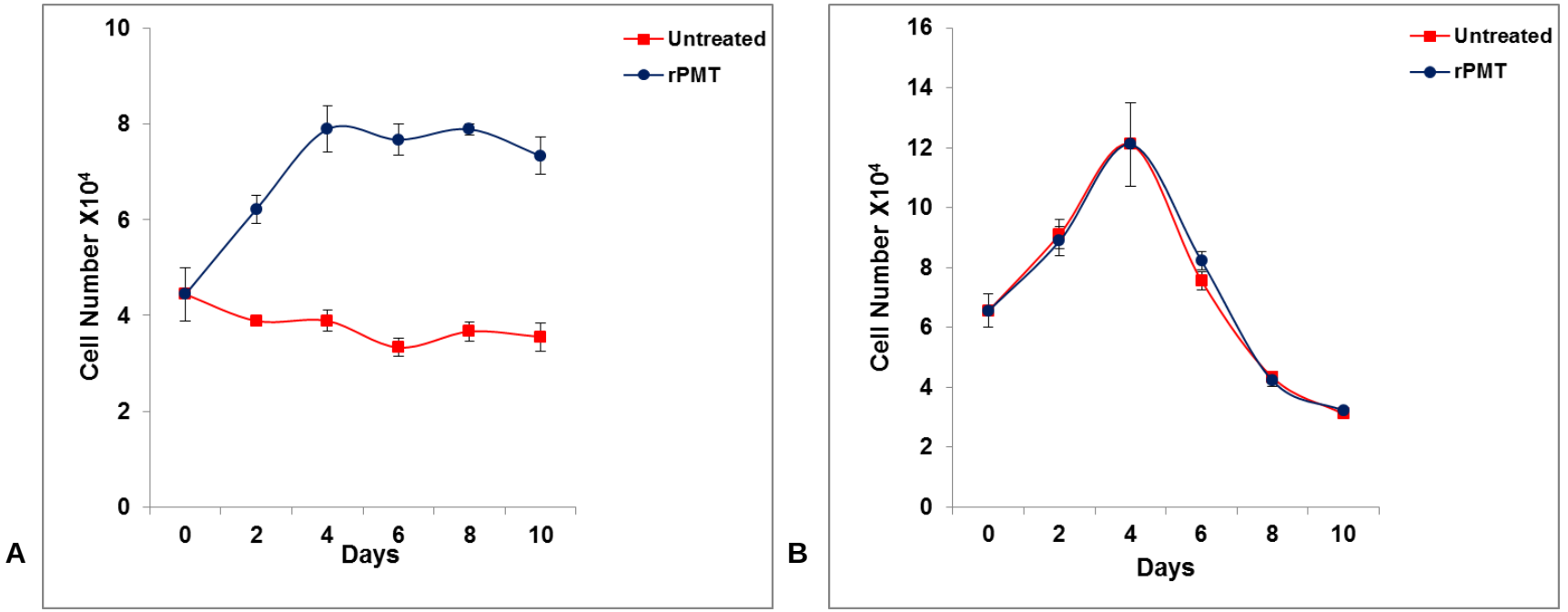

Fig 3.1.2 Effects of rPMT on the growth kinetics of subconfluent Swiss 3T3 (A) and Vero (B) cells. Shown above are time courses of cell number of (A) Swiss 3T3 (*P* = 0.006) and (B) Vero (*P* = 0.58) cells that were either untreated or treated with 15 ng/ml of rPMT-treated and maintained in media supplemented with 1% NCS. Red (Untreated) and Blue (rPMT-treated). Each value is the mean and ± SEM (*n* = 3).

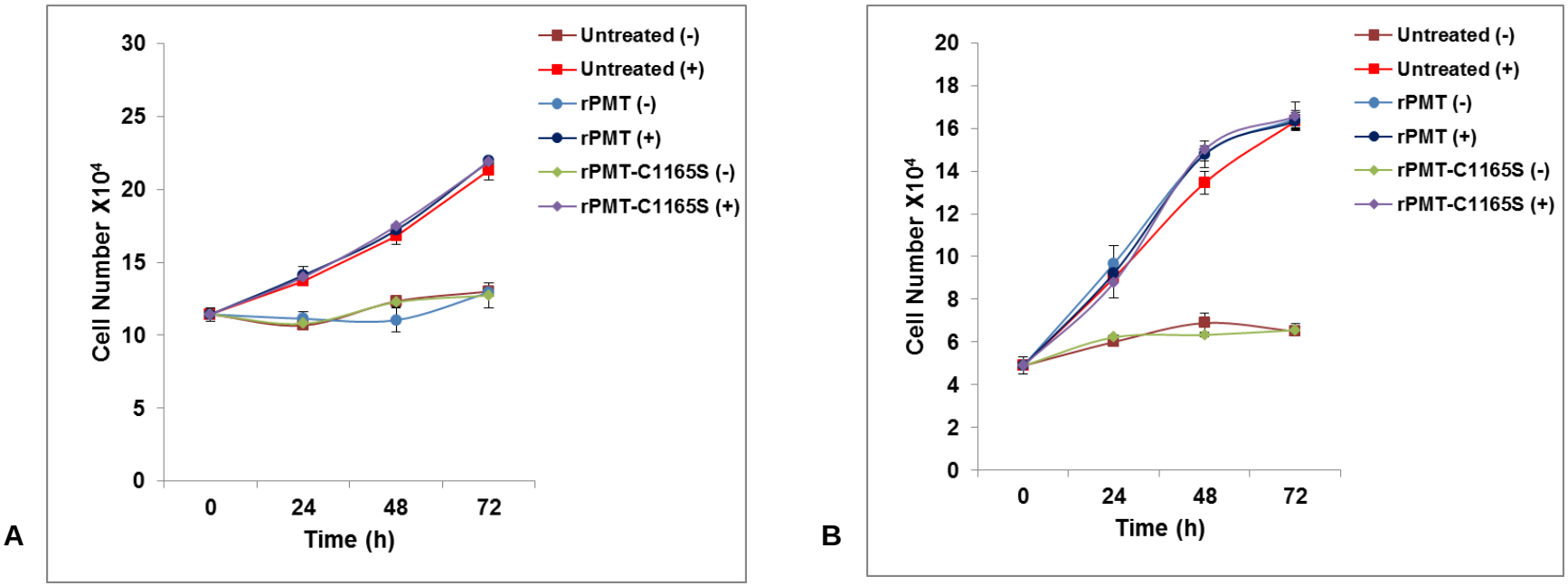

Fig 3.1.3 Effects of rPMT on the growth kinetics of serum-starved subconfluent Swiss 3T3 (A) and Vero (B) cells. Shown above are time courses of cell number for subconfluent Swiss 3T3 and Vero cells that were either left untreated or treated with 15 ng/ml of rPMT or rPMT^{C1165S} maintained in media with (+) or without (-) 10% serum. rPMT- or rPMT^{C1165S}-treated and untreated A) Swiss 3T3 cells (P = 0.005); B) Vero cells (P = 0.005) maintained with or without serum. rPMT- or rPMT^{C1165S}-treated and untreated A) Swiss 3T3 cells (P = 0.04); B) Vero cells (P = 0.76) maintained without serum. Brown (Untreated -), Red (Untreated +), Light Blue (rPMT-treated -), Blue (rPMT-treated +), Light Green (rPMT^{C1165S}-treated -), Purple (rPMT^{C1165S}-treated +). Each value is the mean and ± SEM (n = 3).

To date, the growth kinetics of rPMT-treated Swiss 3T3 and Vero cells in the absence and presence of serum have not been comparatively examined. In order to understand the full mitogenic effects of rPMT in the absence of serum in Swiss 3T3 and Vero cells and compare it to the growth kinetics of untreated cells maintained in 10% serum over a 3-day period, cells were cultured until they reached 50 - 60% confluence before subjecting them to serum starvation for 40 h then either left untreated or treated with 15 ng/ml of rPMT or rPMT^{C1165S} in media with or without 10% NCS.

The untreated, rPMT^{C1165S}- and rPMT-treated subconfluent Swiss 3T3 cells maintained in media with 10% serum had an approximately ~2.1-fold increase in cell number by day 3 compared to the untreated and rPMT^{C1165S}-treated Swiss 3T3 cells maintained in media without serum (Fig 3.1.3 A). rPMT-treated Swiss 3T3 cells maintained without serum, on the other hand, underwent marked proliferation and had the same increase in cell number as those maintained in media with 10% serum with or without rPMT-treatment.

The increase in cell number of the untreated, rPMT^{C1165S}- and rPMT-treated subconfluent Vero cells maintained in media with 10% NCS, on the other hand, was ~2.2-fold while those maintained without serum, either untreated, rPMT^{C1165S}- or rPMT-treated had a ~0.2-fold increase in cell numbers (Fig 3.1.3 B).

3.2 Morphological Changes in Swiss 3T3 and Vero Cells

3.2.1 Effects of PMT on Confluent Swiss 3T3 and Vero Cells

Growth arrest in cells can be the result of contact inhibition, loss of nutrients and/or growth factors, senescence or when cells are in their 'terminal stage' (Modiano et al., 1999; Nelson and Daniel, 2002; Blagosklonny, 2011). With nutrients and in the absence of serum, I have confirmed that PMT acts as a growth factor promoting proliferation in Swiss 3T3 cells but not in Vero cells (Fig 3.1.3). Various reports showed that PMT induces morphological changes such as actin stress fibre formation, and cell rounding in Swiss 3T3 cells (Lacerda et al., 1996; Dudet et al., 1996; Wilson et al., 2000). Wilson et al. (2000) showed a difference in actin stress fibres formation in Swiss 3T3 and Vero cells at 2 h post rPMT-treatment.

Continuous remodelling of the cytoskeleton is essential to cell adhesion, embryonic development, tissue regeneration, and immune responses (Hotulainen and Lappalainen, 2006). Deregulation of cytoskeleton dynamics is associated with pathological disorders such as cancer (Pollard and Cooper, 2009). Stress fibres, a type of cytoskeletal remodelling arising from polarisation of actin and assembly of focal adhesions, are responsible for adhesion, motility, and morphogenesis. Animal cells contain at least three different classes of stress fibres: ventral (VSF), transverse arc (TA) and

dorsal (DSF) (Naumanen et al., 2008; Pellegrin and Mellor, 2007; Hotulainen and Lappalainen, 2006). VSFs, positioned at the base of the cell, are actin bundles usually associated with focal adhesions at both their ends while DSFs are also associated with one of its ends to focal adhesions. TA stress fibres, on the other hand, are curved actomyosin filaments unattached to focal adhesions (Naumanen et al., 2008; Pellegrin and Mellor, 2007).

To re-examine the morphological changes in rPMT-treated Swiss 3T3 and Vero cells, Swiss 3T3 and Vero cells were cultured for 3 days by which time cells were confluent. Cells were quiesced by serum deprivation for 40 h before treatment with a final concentration of 200 ng/ml of rPMT, or left untreated in media with 1% serum (see section 2.6.1).

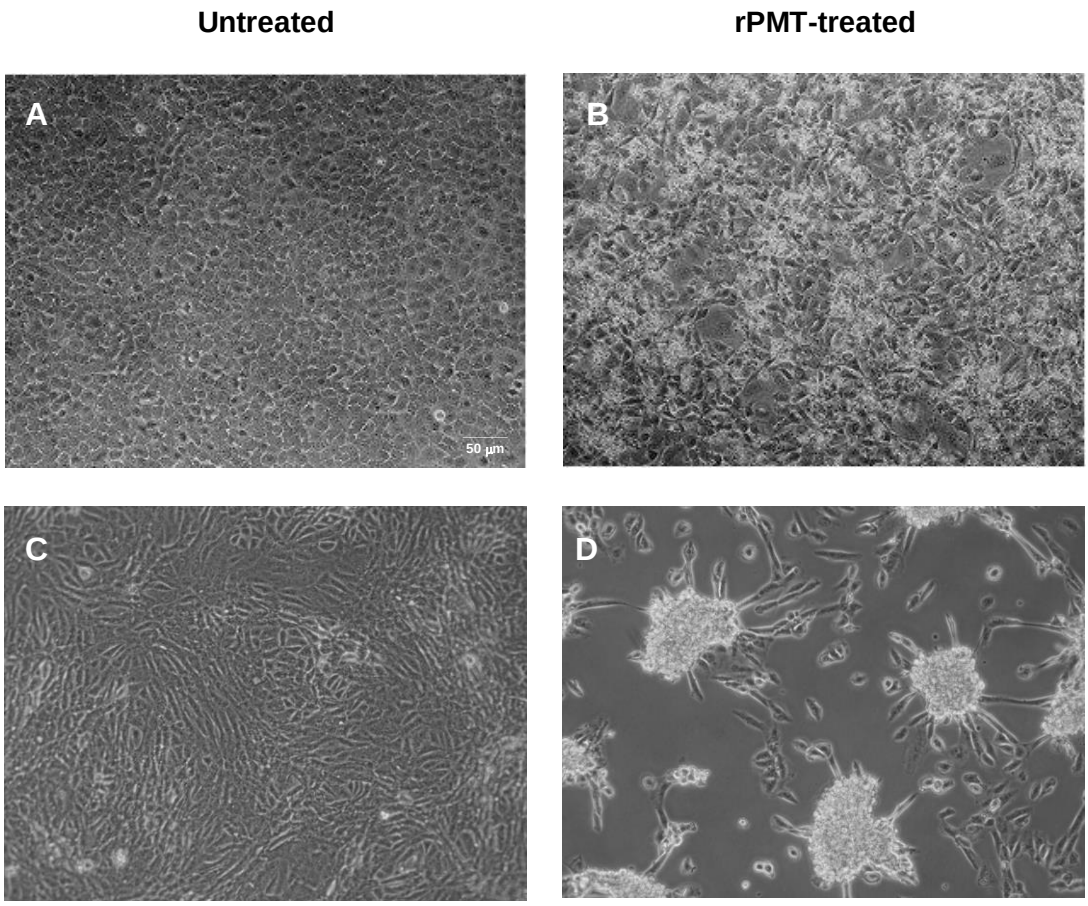

Fig 3.2.1.1 The effect of rPMT on serum-starved confluent (A-B) Swiss 3T3 and (C-D) Vero cells. Shown above are representative phase contrast micrographs of untreated (A) Swiss 3T3 and (C) Vero cells, and rPMT-treated (200 ng/ml) (B) Swiss 3T3 and (D) Vero cells maintained in media with 1% serum for 6 days.

Swiss 3T3 and Vero cells appeared rounded 24 h post rPMT exposure. rPMT-treated confluent Swiss 3T3 cells eventually formed a dense monolayer and developed dense cell clusters while Vero cells developed more pronounced foci (Fig 3.2.1.1). In agreement with Wilson et al. (2000), both rPMT-treated cell lines lost adherence to the matrix, with Vero cells detaching in sheets (Fig 3.2.1.1-B-D). In addition to these findings, both cell types became very fragile, and debris was present but the latter was more

apparent in the rPMT-treated Vero cells. Both confluent cell types also showed a fibroblastic phenotype compared to those that were left untreated.

To check whether different PMT concentrations would give different effects compared to the high concentration of rPMT (~200 ng/ml) used in previous assays, serum-starved semi-confluent Swiss 3T3 and Vero cells were either left untreated or treated with different concentrations of rPMT: 0.01, 0.1, 1, or 10 ng/ml maintained in media without serum for 3 days.

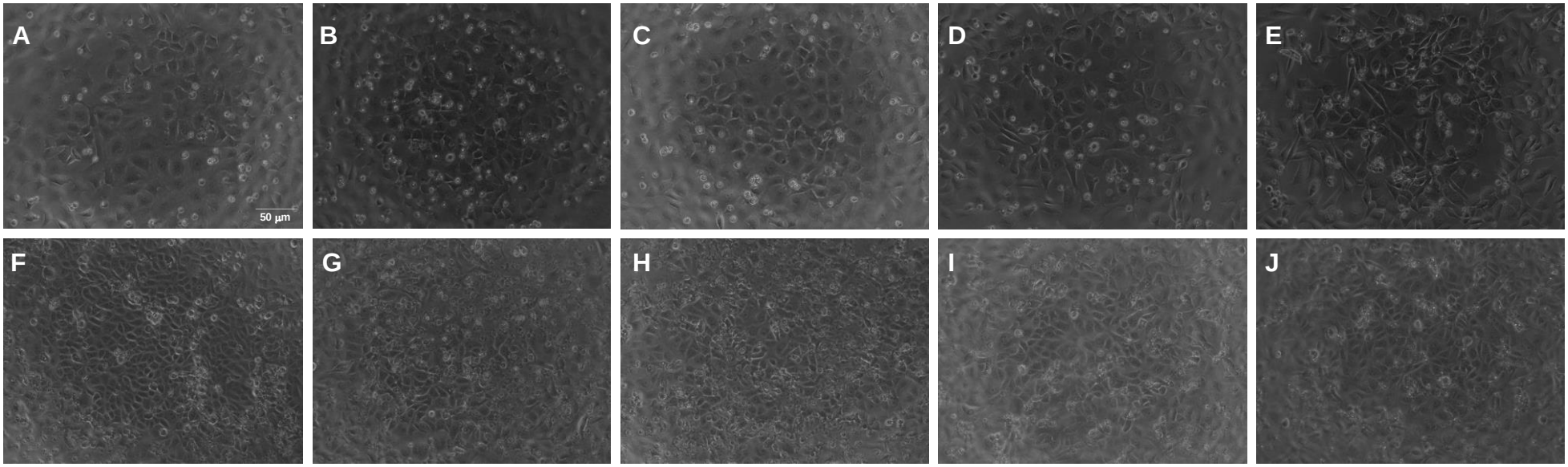

Fig 3.2.1.2 The Effect of rPMT on serum-starved semi-confluent (A-E) Swiss 3T3, and (F-J) Vero cells. Shown above are representative phase contrast micrographs of (A) untreated; and (B-E) rPMT-treated with a final concentration of (B) 0.01, (C) 0.1, (D) 1, (E) 10 ng/ml Swiss 3T3, and (F) untreated (G-J) rPMT-treated Vero cells with a final concentration of (G) 0.01, (H) 0.1, (I) 1, (J) 10 ng/ml maintained in media without serum for 3 days.

rPMT-treated Swiss 3T3 and Vero cells at concentrations of 1 and 10 ng/ml each appeared more rounded than the untreated cells or those with PMT at lower concentrations (Fig 3.2.1.2). Swiss 3T3 cells appeared more fibroblastic in character than Vero cells (Fig 3.2.1.2). Swiss 3T3 cells treated with 1 and 10 ng/ml of rPMT appeared to form cell clusters at day 3.

Wilson et al. (2000) reported a decrease adherence and formation of foci or dense cell clusters in Swiss 3T3 and Vero cells even after changing the media with 1% serum everyday. In the previous experiment (Fig 3.1.1) where rPMT-treated confluent Swiss 3T3 and Vero cells kept in the same media with 1% serum throughout a 7-day time course, significant decrease in adherence and formation of foci or dense cell clusters were observed at later stage. To check the longer term effects of PMT and whether changing of media with minimal amount of serum could attenuate the drastic morphological changes brought by PMT, Swiss 3T3 and Vero cells were subjected to a 40-hour serum deprivation prior to treatment with 15 ng/ml of rPMT in media without serum. Media containing rPMT were removed after 3 days; cells were gently washed twice with DPBS and replaced with media with 1% NCS added twice a week for 3 weeks.

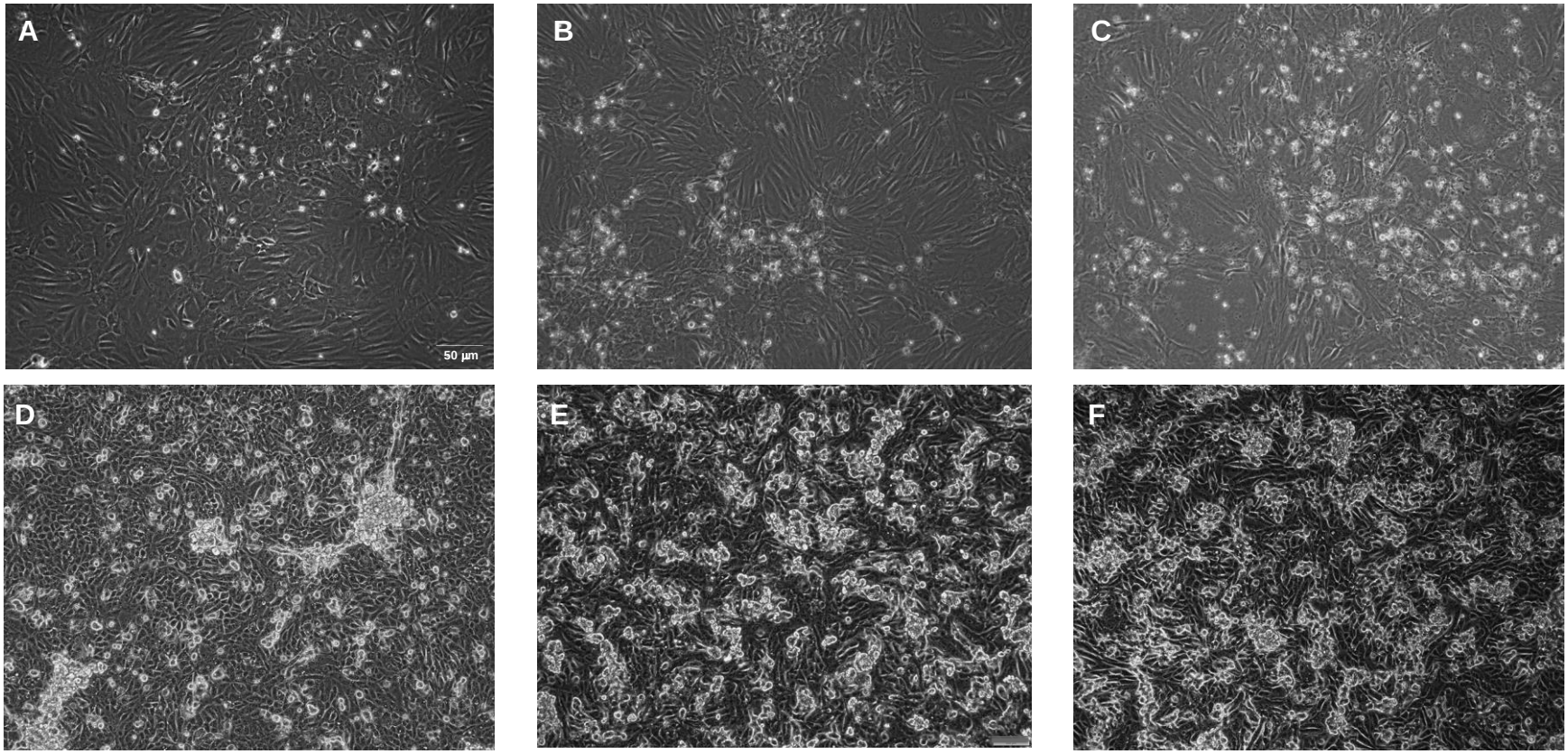

Fig 3.2.1.3 The long term effect of rPMT on confluent Swiss 3T3 and Vero cells. Shown are representative phase contrast micrographs of rPMT-treated (A-C) Swiss 3T3 and (D-F) Vero cells. Swiss 3T3 and Vero cells were treated with 15 ng/ml of rPMT for (A, D) 1, (B, E), 2, and (C, F) 3 weeks. Media with 1% serum were changed twice a week up to a period of 3 weeks.

A minimal loss of adherence and detachment of both cell lines were rarely observed during the gentle changing of media. As with earlier observations, Swiss 3T3 and Vero cells developed dense cell clusters or foci but this development was gradual and more prominent in Vero cells (Fig 3.2.1.3). Looking at the development of foci in Vero cells from weeks 1 - 3, it appears that the cells underwent proliferation.

3.2.2 Effects of PMT on Cytoskeletal Organisation

Stress fibres are composed of bundles of actin filament and myosin IIa held together by actin crosslinking proteins, which ensure structural and mechanical integrity by generating tension forces on focal adhesions that are anchored to the extracellular matrix surrounding the cells (Naumanen et al., 2007). They are involved in adhesion, motility and morphogenesis.

It has been well documented that PMT promotes cytoskeletal rearrangement in Swiss 3T3 cells via Rho activation (Lacerda et al., 1996, Wilson et al., 2000). According to Wilson et al. (2000), Vero cells treated with 200 ng/ml of rPMT did not show prominent stress fibres as observed in rPMT-treated Swiss 3T3 cells, but these workers reported cytoskeletal disruption in rPMT-treated Vero cells after 2 h.

To determine the effects of PMT in the cytoskeleton of Swiss 3T3 and Vero cells in greater detail, confluent quiescent cells were subjected to a 40-hour serum starvation prior to treatment of 200 ng/ml (Figs 3.2.2.1 and 3.2.2.2) of rPMT maintained in media with 1% NCS. Cells were then fixed with 4% paraformaldehyde in DPBS and stained with Phalloidin-TRITC.

The majority of rPMT-treated Swiss 3T3 cells produced a robust stress fibre response from day 1, compared to Vero cells (Fig 3.2.2.1). Long and thick stress fibres are scarcely present in rPMT-treated Vero cells on day 1 (Fig 3.2.2.1-E) but became more heavily visible on day 2 (Fig 3.2.2.1-F). This effect was also observed in Swiss 3T3 and Vero cells treated with low concentration of rPMT (final concentration of 15 ng/ml) (data not shown).

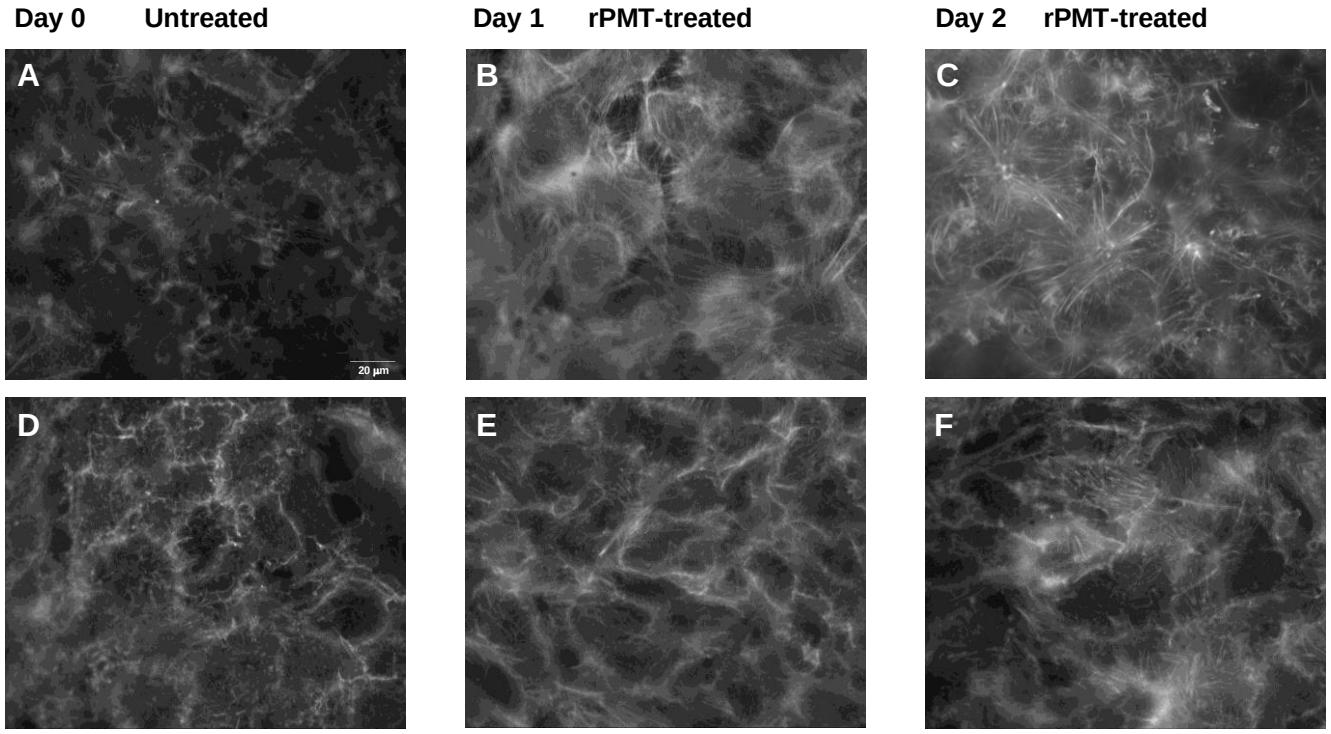

Fig 3.2.2.1 The effect of rPMT in actin cytoskeletal organisation of (A-C) Swiss 3T3 and (D-F) Vero cells. Shown above are representative TRITC-conjugated-phalloidin-stained fluorescence micrographs of confluent Swiss 3T3 and Vero cells either untreated or treated with 200 ng/ml of rPMT as described in section 2.7. (A-C) Swiss 3T3 cells, (D-F) Vero cells; (A) Untreated Swiss 3T3 and (D) Vero cells; (B-C) Swiss 3T3 and (E-F) Vero cells treated with rPMT for 1 and 2 days.

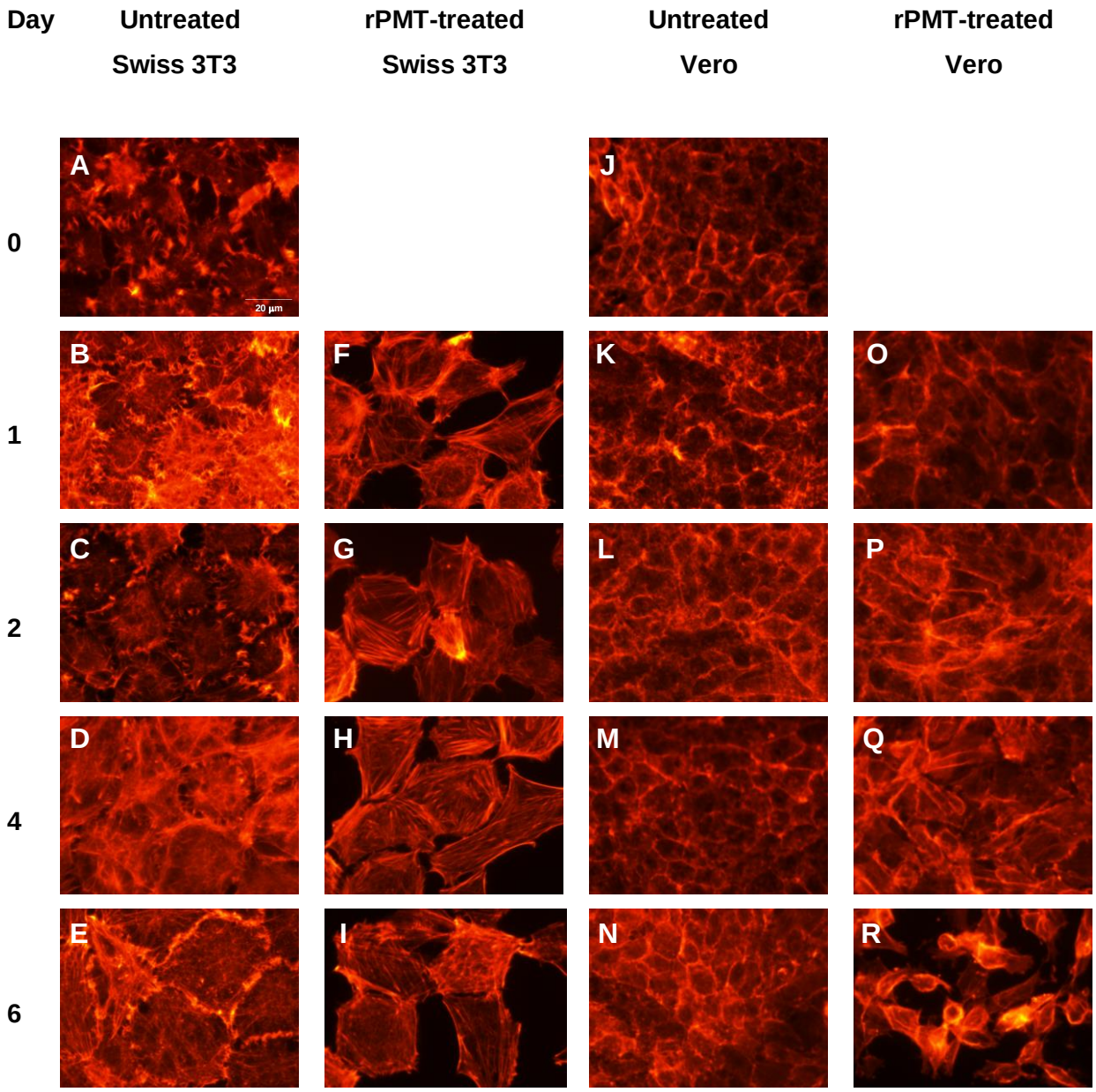

Fig 3.2.2.2 The effect of rPMT in actin cytoskeletal organisation of (A-I) Swiss 3T3 and (J-R) Vero cells. Shown above are representative TRITC-conjugated-phalloidin-stained fluorescence micrographs of confluent Swiss 3T3 and Vero cells treated with 200 ng/ml of rPMT. (A-I) Swiss 3T3 cells; (J-R) Vero cells; (A-E) Untreated Swiss 3T3 and (J-N) untreated Vero cells; (F-I) rPMT-treated Swiss 3T3 and (M-R) rPMT-treated Vero cells.

Actin stress fibre formation accompanies the stretch-induced cell orientation of rPMT-treated Swiss 3T3 and Vero cells. Consistent with the previous highly magnified TRITC-conjugated-phalloidin-stained fluorescence micrographs (Fig 3.2.2.2), this PMT effect can already be seen in Swiss 3T3 on day 1 (Fig 3.2.2.2-F) unlike the elongated feature in Vero cells, which became more apparent from day 2 (Fig 3.2.2.2-P).

3.2.3 The Cytotoxic Effects of PMT in Swiss 3T3 and Vero Cells

Preuss et al. (2010) reported that PMT treatment in HEK293 cells inhibited staurosporine-mediated apoptosis via PI3K-dependent Akt phosphorylation, and Pim-1 expression. On the other hand, PMT has been reported to cause apoptosis (Pennings and Storm, 1986) in Vero cells, and in cardiomyocytes via inhibition of Akt phosphorylation (Sabri et al., 2002). Wilson et al. (2000) reported that the detached Vero cells appear to be viable by tryphan blue exclusion assay and that such phenomena were consistent with the results obtained by Pennings and Storm (1986), but no data were shown. Pennings and Storm (1986) used diluted supernatant from a *Pasteurella multocida* culture containing PMT in media without serum. They reported that the cytopathic effect in Vero cells could be detected after 48 h. Sunder and Kumar (2000) observed a cytopathic effect (CPE) of PMT on Vero cells after 7 days. They reported that a minimum cytopathic dose of 5.8 μg of crude PMT exhibited such an effect.

To determine and confirm whether confluent quiescent Swiss 3T3 and Vero cells would behave differently to different concentrations of rPMT, and also if PMT would prevent or promote cell death in the two representative cell lines, confluent quiescent cells were subjected to 40-h serum deprivation before treating them with 0.01, 0.1, 1, or 10 ng/ml rPMT or rPMT^{C1165S}.

Cell death can be measured using the lactodehydrogenase (LDH) released in cell culture (Burd and Usategui-Gomez, 1973). LDH assay measures cytoplasmic LDH or the membrane integrity of cells. LDH is a stable cytoplasmic enzyme released upon cell lysis which converts tetrazolium salt (INT) into formazan product in LDH assay. A spectrophotometer was used to measure the colorimetric product (see section 2.9).

Similar to the report of Preuss et al. (2010) about the anti-apoptotic effect of PMT in HEK293 cells, rPMT also protected Swiss 3T3 cells from cell death, which was detected after 2 days post rPMT treatment (Fig 3.2.3-A). In this experiment, concentrations of 1 and 10 ng/ml of rPMT in media without serum showed a ~1 – 1.5 fold protection from cell death in Swiss 3T3 cells compared to untreated and rPMT^{C1165S}-treated ones (Fig 3.2.3-A). Swiss 3T3 cells treated with 0.1 ng/ml of rPMT in media without serum, on the other hand, showed minimal protection (approximately ~0.5 - 0.9 fold) from cell death compared to the untreated and rPMT^{C1165S}-treated Swiss 3T3 cells. Swiss 3T3 cells either untreated, rPMT- or rPMT^{C1165S}-treated maintained in media with 10% NCS showed higher protection from cell

death. After 4 days treatment, the protective effect of rPMT was completely abolished (Fig 3.2.3-C).

rPMT treatment of Vero cells, on the other hand, did not show any effect or protection against cell death. Cell death appeared to be linked to the absence of serum regardless of the presence of rPMT after 2 and 4 days treatment (Fig 3.2.3-B and -D).

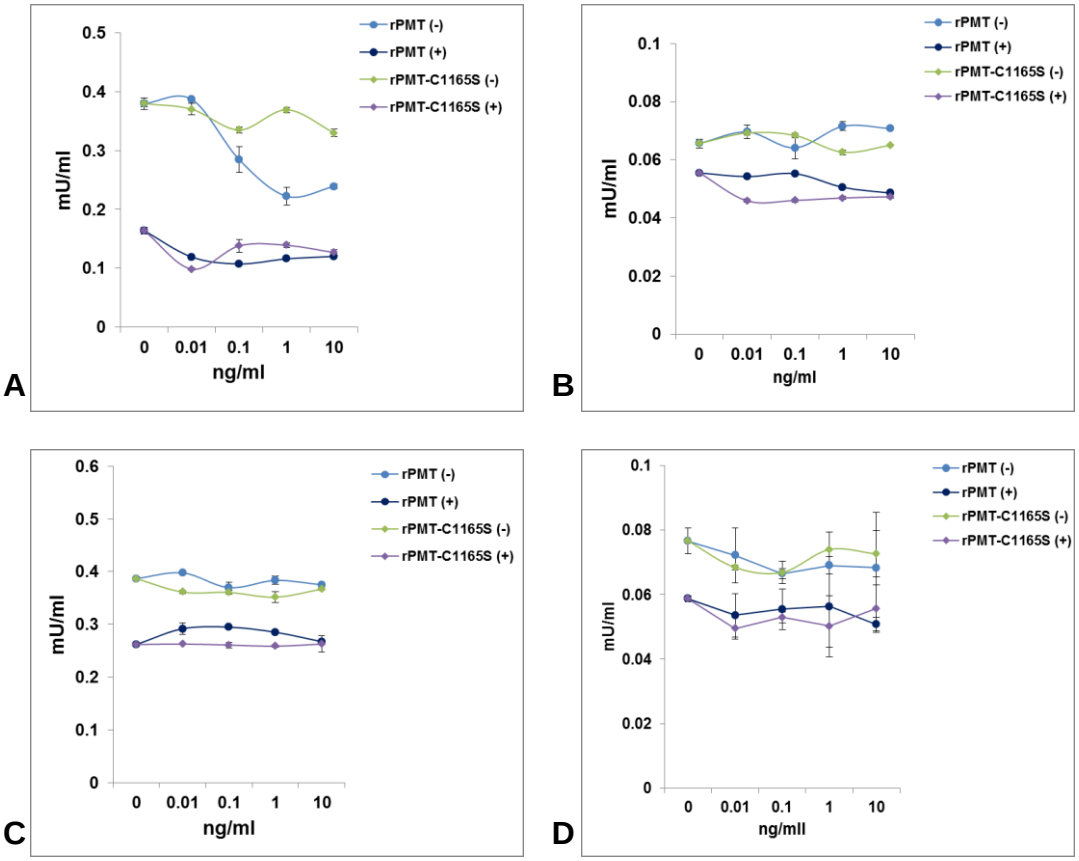

Fig 3.2.3 The cytotoxic effect of rPMT on (A and C) Swiss 3T3 and (B and D) Vero cells. Confluent (A and C) Swiss 3T3 and (B and D) Vero cells were either left untreated or treated with different concentrations (0.01, 0.1, 1 and 10 ng/ml) of rPMT or rPMT^{C1165S} maintained with or without serum for 2 (A, P = 0.0000006 and B, P = 0.000002) and 4 (C, P = 0.000000005 and D, P = 0.0000001) days. (A and C) Swiss 3T3 and (B and D) Vero cells were either left untreated or treated with different concentrations (0.01, 0.1, 1 and 10 ng/ml) of rPMT or rPMT^{C1165S} maintained without serum for 2 (A, P = 0.02 and B, P = 0.36) and 4 (C, P = 0.46 and D, P = 0.49) days. Samples were processed using LDH assay (section 2.9.1). No serum [-], with 10 % serum [+], Brown (Untreated -), Red (Untreated +), Light Blue (rPMT-treated -), Blue (rPMT-treated +), Light Green (rPMT^{C1165S}-treated -), Purple (rPMT^{C1165S}-treated +). Each value is the mean and ± SEM (n = 3).

3.3 DISCUSSION

3.3.1 Growth Kinetics of Swiss 3T3 and Vero Cells

PMT is a potent mitogen in vivo (Hoskins et al, 1997) and to most cultured cells (Rozengurt et al., 1990; Higgins, et al., 1992; Mullan and Lax, 1996; Dudet et al., 1996; Wilson et al., 2000, Lax and Grigoriadis, 2001; Lax et al., 2004).

To re-examine whether PMT is a mitogen to Swiss 3T3 and not to Vero cells, each cell line was either left untreated or treated with a final concentration of 200 ng/ml of rPMT or rPMT^{C1165S} in media with 1 % serum over a 7-day period, the same rPMT concentration used by Wilson et al. (2000). The rPMT-treated confluent Swiss 3T3 cells (Fig 3.1.1A) underwent marked proliferation by day 4 which was also the onset of the plateau growth phase, compared to the untreated or rPMT^{C1165S}-treated Swiss 3T3 cells. The untreated, rPMT- or rPMT^{C1165S}-treated confluent Vero cells (Fig 3.1.1B), on the other hand, maintained in media with 1 % serum showed no significant difference in cell density.

Wilson et al. (2000) reported a ~2-3-fold increase in cell density of rPMT-treated Swiss 3T3 cells over the 7-day period, but without any evidence of a plateau growth phase. Their experimental condition involved changing of the media containing 1 % serum without the toxin everyday as opposed to the

condition set in this research, keeping the same media with 1 % serum and toxin throughout the 7-day period. I attempted to repeat exactly the conditions set out in the paper by Wilson et al. (2000), namely changing the medium everyday, but found that this gave variable results due to loss of cells (data not shown). This occurred even with gentle washing of the cell sheet and aspiration of media. It is well known that Vero cells tend to lift even with gentle treatment (Dr David Moyes, personal communication).

rPMT-treated Swiss 3T3 and Vero cells each lost adherence after a few days and this observation was also reported by Wilson et al. (2000). In order to prevent loss of cells, the untreated, rPMT^{C1165S}- and rPMT-treated Swiss 3T3 and Vero cells were kept in the same medium with or without serum over the specified time period for each growth kinetics proliferation assay. This might have led to nutrients being depleted, which would inhibit cell proliferation. However, the loss of cells during washing and replacement of media with fresh nutrients and 1 % serum may be the cause of continuous gradual increase in cell numbers of Swiss 3T3 as seen by Wilson and et al. (2000).

Wilson et al. (2000) examined if a final concentration of 200 ng/ml of PMT in media with full serum (10 % FBS for Vero, and 15 % calf serum (CS) for Swiss 3T3) would influence the rate of proliferation of subconfluent Swiss 3T3 and Vero cells. They reported approximately 45% increase in cell numbers in rPMT-treated Swiss 3T3 cells by day 4 compared to the

untreated, heat-inactivated rPMT-treated cells which was also the onset of the ‘plateau growth phase’. The untreated, heat-inactivated rPMT- and rPMT-treated Vero cells, on the other hand, showed similar exponential increase in cell numbers, reaching their maximum cell numbers by day 4 which also appeared to be the onset of the ‘plateau growth phase’.

Most studies with PMT have used much lower concentration of toxin. In the original paper on the subject, Rozengurt et al. (1990) showed that the maximum stimulation of DNA synthesis in Swiss 3T3 cells, over a 40-hour period, was achieved at around 1.2 ng/ml. Subsequent papers have used higher concentrations for longer term experiments, but seldom as high as 200 ng/ml. Work reported later in this thesis shows that PMT activity can be detected several days after toxin removal (chapter 5).

To determine whether a lower concentration of PMT would also influence the relative cell growth kinetics of the two cell types cultured subconfluently (Fig 3.2.2), cells were either left untreated or treated with a final concentration of 15 ng/ml of rPMT in media with 1 % serum and kept in the same media over a 10-day period. Each cell type reached its maximum cell number by day 4, which is also the onset of the ‘plateau growth phase’ of Swiss 3T3 (Fig 3.1.2C). The rPMT-treated subconfluent Swiss 3T3 cells had a significant increase in cell number compared to the untreated Swiss 3T3 cells (Fig 3.1.2C). No significant change in cell number between untreated and rPMT-treated subconfluent Vero cells (Fig 3.1.2D) was observed but both

displayed a cell number increase which ceased by day 4. As before, cell debris was more apparent in Vero cells than in Swiss 3T3 cells. The termination of cell proliferation by day 4 in both cell lines could be due to the loss of nutrients and/or serum in the media compared to the data published by Wilson et al. (2000) where they changed the media with 1% serum everyday so that growth was still detectable in confluent rPMT-treated Swiss 3T3 cells throughout the 7-day period but not in confluent Vero cells. The rPMT-dependent growth of Swiss 3T3 appears to require continuous supplement of nutrients required to keep the cell proliferating. The continuous cell number increment in their confluent rPMT-treated Swiss 3T3 cells may be due to the lost cells being replaced with a fresh supply of media supplemented with nutrients and minimal growth factors in the serum. In their subconfluent proliferation experiments, it was unclear whether Wilson et al. (2000) changed the media with or without full serum but they mentioned that they cultured the cells in media with 10% FBS for Vero cells, and 15% CS for Swiss 3T3 cells. Both subconfluent cell types showed the plateau growth phase after day 4, which is consistent with the results in this thesis.

Rozengurt et al. (1990), on the other hand, found that the onset of plateau growth phase in subconfluent Swiss 3T3 cells maintained in media with 10% FBS occurred after 6 days post treatment with 10 ng/ml of rPMT while subconfluent MEF treated with 10 ng/ml of rPMT maintained in media with 0.5% FBS had an onset of plateau growth phase after 8 - 9 days.

The different experimental conditions used in three independent proliferation assays led to proliferation in subconfluent rPMT-treated Swiss 3T3 cells. However, a delay in the onset of the growth phase in Rozengurt et al. (1990) may be due to a high concentration of serum and low concentration of rPMT and/or the origin of batch of Swiss 3T3 cells used. Wilson et al. (2000) used a high concentration of serum and rPMT and showed a similar onset of the plateau growth phase and general growth pattern to the results in this thesis which used different experimental conditions: a low concentration of both serum and rPMT. It appears that the high concentration of serum (in the case of the Rozengurt et al. (1990) experiment) may play a role in the integrity of cells by providing anti-apoptotic protection thereby prolonging the cells viability and the effect of rPMT. However, the effect of the high concentration of serum used by Wilson et al. (2000) may interact with cellular effects induced by a high concentration of rPMT, which led to constitutive activation of the majority of the G-protein molecules in Swiss 3T3 cells resulting in the earlier onset of plateau growth phase compared to that noted by Rozengurt et al. (1990). The use of a lower concentration of serum in my experiments may have affected the viability of cells and the effect of rPMT. The loss of cells during gentle washing and trypsinisation prior to counting of cells may also affect the relative cell number of rPMT-treated Swiss 3T3 cells after 4 - 6 days.

In this research, the growth kinetics of subconfluent Swiss 3T3 and Vero cells treated with rPMT^{C1165S} or rPMT in the absence and presence of serum

have been scrutinised (Fig 3.1.3E). rPMT-treated subconfluent Swiss 3T3 cells underwent proliferation in the absence of serum with the same cell number increment per day as the Swiss 3T3 cells maintained in 10% serum with or without 15 ng/ml of rPMT-treatment. The untreated or rPMT^{C1165S}-treated Swiss 3T3 cells maintained in media with 10% serum, and rPMT-treated Swiss 3T3 cells maintained in media without serum had over ~2-fold increase compared to the untreated and rPMT^{C1165S}-treated Swiss 3T3 cells maintained in media without serum. The untreated, rPMT- and rPMT^{C1165S}-treated Vero cells maintained in media with 10% serum, on the other hand, proliferated reaching ~2–3-fold increase in cell numbers compared to the untreated, rPMT- and rPMT^{C1165S}-treated Vero cells maintained in media without serum. The above data confirms that the mitogenic effect of either the serum or rPMT masks the proliferative effect of the other in Swiss 3T3 cells during the 3-day treatment. PMT in media without serum, on the other hand, shows the same proliferative effect as the 10% serum in Swiss 3T3 cells. I have therefore confirmed that PMT is mitogenic to Swiss 3T3 cells but not to Vero cells. Rozengurt et al. (1990) reported that DNA synthesis elicited by rPMT at a concentration of 1.25 ng/ml had similar effect to that induced by 10% FBS in the absence of other factors, and that lower concentration (~0.16 - 0.32 ng/ml) resulted only in half-maximal stimulation of DNA synthesis.

3.3.2 The Morphological Changes in Swiss 3T3 and Vero Cells

I have confirmed that treatment with 200 ng/ml of rPMT results in the development of dense clusters and/or foci, loss of adherence and detachment in both Swiss 3T3 and Vero cells (Fig 3.2.1-A) (Wilson et al, 2000). Although both cell lines showed detachment of cells, Vero cells rolled up, which suggests weakened cell-cell adhesion. The loss of adherence in rPMT-treated Vero cells was observed after 6 - 10 days growth, where the decrease in cell number was due to poor adherence of Vero cells to the well (Figs 3.1.1, 3.1.2 and 3.2.1.1). Wilson et al. (2000) reported that detached Vero cells remained viable by trypan blue exclusion assay. Detached Vero cells were difficult to count due to their size, and most appeared to be cell debris. The end results of the morphological effects induced by PMT treatment in Swiss 3T3 or Vero cells were the same regardless of whether cells were treated with high or low PMT concentration, but the progression of these effects was concentration-dependent. It appears that the concentration of PMT and the rate of cellular response are directly proportional to each other, meaning the higher the concentration of PMT, the faster the appearance of these effects. Changing of the media, however, containing 1% NCS twice a week for the course of 3 weeks appeared to lead to both rPMT-treated cells being more adherent (Fig 3.2.1.3) than the cells left in the same media (Fig 3.2.1.1), but both rPMT-treated cell types still remained fragile. It appears that Vero cells underwent proliferation due to the gradual

development of foci. This phenomenon was made possible due to the presence of 1 % NCS which appeared to help the integrity of cell-cell adhesion and possibly cell growth (Fig 3.2.1.3).

The previous observation stating that rPMT-treated Vero cells did not form prominent stress fibres as rPMT-treated Swiss 3T3 after 2 h post rPMT treatment (Wilson et al., 2000) suggested different mechanisms of stress fibre formation in each cell line. Stress fibre formation and actomyosin contractility is regulated by activated Rho-associated kinases via RhoA GTPases activation (Ridley and Hall, 1992; Pellegrin and Mellor, 2007). Rho-associated kinases promote stress fibre assembly via inhibition of actin filaments depolymerisation. According to Hotulainen and Lappalainen (2006), association and dissociation of actin filament cross-linking may be important in the formation and contractility of stress fibres. The role of actin filaments in many cellular processes such as migration and cellular development is to produce force, which can be achieved via coordinated polymerisation of actin filaments against the cell membrane, and formation of contractile structure (Tojkander et al., 2012). The orientation of proteins, in particular actin filaments and myosin II, which makes up the structure of actin filament networks appear to define the polarity of actin filaments and the cell's contractile properties (Pellegrin and Mellor, 2006).

There are many key players involved in the development of stress fibres. Rho-associated kinases, activated by RhoA, directly phosphorylate myosin

light chain (MLC), and also CPI-17, ZIPK and S19P which are involved in the activation of kinases and/or inhibition of phosphatases responsible for increased myosin phosphorylation leading to stress fibre assembly and contractility (Leung et al., 1996; Pellegrin and Mellor, 2006). Mammalia Dia1 (mDia1), a Rho GTPases effector protein, is also essential for the formation of stress fibres (Watanabe et al., 1997; Pellegrin and Mellor, 2006), formation of DSFs *in vivo* (Hotulainen and Lappalainen, 2006), and production of actin filaments via nucleation and polymerization (Narumiya et al., 2009). Stress fibre assembly can be blocked by overexpression of small GTPases RhoE, which inhibits ROCK (Riento et al., 2003), and Gem and Rad (Ward et al., 2002).

There are three types of stress fibres namely, DSF, TA, and VSF (Pellegrin and Mellor, 2007; Naunamen et al., 2007). DSFs are short actin bundles attached to focal adhesions at their distal end while TAs are curved actomyosin bundles that extend to both ends without association to focal adhesions and often terminate to DSFs. VSF are made of actin filament bundles associated with focal adhesions and considered the major contractile machinery of the cell (Tojkander et al., 2012). Hotulainen and Lappalainen (2006) showed that DSFs and TAs in motile cells (U2OS cells) underwent continuous formation and assembly. Contraction promotes elongation and association of these stress fibres with each other, which often lead to their conversion in to VSFs. They proposed that elongation of DSFs, which then anneals to each other, could lead to VSFs formation.

However, it is still unclear how each stress fibre type contracts specifically those with uniform polarity (i.e. DSFs) and unattached to the membrane (i.e. TAs) which raise questions about their contractile nature (Pellegrin and Mellor, 2007). DSFs do not contain myosin II, therefore do not have the ability to contract (Tojkander et al., 2011). TAs, on the other hand, have periodic α-actin-myosin contractile pattern and when attached to DSFs could convey contractile force (Tojkander et al., 2012). In U2OS cells, VSFs can be assembled in 27 minutes through reorganisation of the DSFs and TAs (Hotulainen and Lappalainen, 2006). Although stress fibres assembly in non-motile cells (i.e. Swiss 3T3 and Vero cells) remains unclear, according to Deguchi and Sato (2009), based on the similarity of structures of VSFs in motile cells such as U2OS, the mechanisms of its assembly appear to be the same.

The rPMT-treated Vero cells had less stress fibres than rPMT-treated Swiss 3T3 cells (Fig 3.2.2.1). Stress fibre formation in rPMT-treated Vero cells appeared to be generated at a very slow pace compared to rPMT-treated Swiss 3T3 cells. The majority of these stress fibres appeared to be short, and were found close to the cell membrane, which indicates that they may be DSFs. DSFs do not contain myosin II, therefore, do not have the ability to contract. Contraction is essential in the elongation and association of stress fibres to generate VSFs. This may be the case why stress fibres in Vero cells were not as prominent as the ones in Swiss 3T3 cells, even though both cell lines were treated with a high concentration (200 ng/ml) of rPMT,

as reported by Wilson et al. (2000). I have shown that both low (15 ng/ml) and high concentrations (200 ng/ml) of rPMT resulted in a slower development of stress fibres in Vero cells compared to Swiss 3T3 cells, which showed prominent cytoskeletal reorganisation by day 1 post rPMT treatment. The development of fibroblastic feature or the stretch-induced orientation of both rPMT-treated cell lines appears to be associated with the presence of advanced formed (i.e. VSFs) or all types of stress fibres.

Contractility, which is essential in stress fibre assembly, is regulated by phosphorylated MLC (Somlyo and Somlyo, 2000), which promotes assembly of myosin II filaments and increases the myosin motor domain ATPase activity (Vincente-Manzanares et al., 2009). The two important pathways that regulate this event are G_{q}-, $Ca^{2+/}$calmodulin-dependent and $G_{12/13}$-, Rho-dependent (Katoh et al., 2001a and 2001b; Klages et al., 1999; Walsh et al., 2011; Tojkander et al., 2012), which each lead to phosphorylation of MLC. The $Ca^{2+/}$calmodulin-dependent pathway leads to a rapid response whereas the Rho-dependent pathway results in a more sustained response (Tojkander et al., 2012).

It is possible that the slow stress fibre response of Vero cells to PMT is due to discrimination in activating proteins involved in either pathway, or there may be a delay in the activation of one of the pathways. It is impossible to speculate that only one of the two pathways was activated by PMT as more prominent stress fibres (long and short ones) appeared in rPMT-treated Vero

cells from day 2. Such a delay in activation of the one of the two pathways involved in stress fibre formation in rPMT-treated Vero cells could also indicate specialised mechanisms in which PMT activates G-proteins, which will be discussed in great detail in chapter 5.

3.3.3 The Cytotoxic Effects of PMT in Swiss 3T3 and Vero Cells

According to the reports of Pennings and Storm (1986), and Sunder and Kumar (2000), PMT is cytotoxic to Vero cells while Preuss et al. (2010) showed the anti-apoptotic effect of PMT in HEK293 cells via PI3K-dependent Akt phosphorylation, and Pim-1 expression. According to Pennings and Storm (1986), the cytotoxicity of PMT can be detected from 48 h. Wilson et al. (2000), on the other hand, reported that they did not find any evidence of cell death under their experimental condition and that the detached cells remained viable by trypan blue dye exclusion assay. I have shown here that two days post treatment, Swiss 3T3 cells with 1 or 10 ng/ml of rPMT showed a marked decrease in cell death while those 0.1 ng/ml rPMT showed minimal protection against cell death (Fig 3.2.3-A). However, after 4 days, the protective effect of PMT in Swiss 3T3 cells was completely abolished (Fig 3.2.3-C). I have shown that PMT exhibited protective behavior in Swiss 3T3 cells up to 48 h only, compared to the longer time noted by Preuss et al. (2010).

In contrast to reports of Pennings and Storm (1986), and Sunder and Kumar (2000), there was no significant decrease or increase in the number of dead cells in rPMT-treated Vero cells maintained in media without serum compared to those untreated and treated with $rPMT^{C1165S}$ maintained in media without serum (Fig 3.2.3-B and -D). Untreated, $rPMT^{C1165S}$- and rPMT-treated Vero cells maintained in media with 10% serum showed a decrease in the number of dead cells compared to those untreated, $rPMT^{C1165S}$- and rPMT-treated Vero cells maintained in media without serum.

This research confirms that rPMT is not cytotoxic to either cell line and exhibits a protective effect against cell death in Swiss 3T3 cells up to 48 h only but not to Vero cells. Cytotoxicity appears to be linked to the absence of serum or loss of serum/nutrients in both cell lines as observed 4 days post rPMT treatment (Fig 3.2.3-C-D).

Wilson et al. (2000) reported that rPMT-treated Swiss 3T3 and Vero cells became insensitive to further treatment with rPMT 2 – 3 days after initial treatment, and that most of them were found in the G_0/G_1 phase of the cell cycle after 3 – 4 days. The loss of an anti-apoptotic effect of rPMT detected after 4 days post treatment appears to coincide with the loss of proliferative effect of rPMT in Swiss 3T3 cells. Assuming that Akt and Pim-1 are also involved in the anti-apoptotic effect of PMT in Swiss 3T3 cells similar to that shown for HEK293 cells, it is possible that these proteins are involved in regulating PMT-induced cell proliferation. The Akt and Pim oncogenes

stimulate cell survival, growth and transformation via phosphorylation of different apoptotic proteins and stimulation of mTOR signalling in haemopoetic cells (Hammerman et al., 2005). In Swiss 3T3 cells, the PMT-mediated activation of mTORC1 has a partial role in cell growth, migration and proliferation (Oubrahim et al., 2013). However, this mTOR signalling is $G_{q/11}$/PLCβ/PKC-dependent. It is unknown if the mTOR pathway via Akt is also activated in Swiss 3T3 cells. In HEK293 cells, Akt and Pim-1 were activated by PMT via Gβγ/PI3K which played a role in cell survival and proliferation (Preuss et al., 2010).

4 THE PRESENCE AND ABUNDANCE OF G-PROTEINS IN SWISS 3T3 AND VERO CELLS

The G-protein coupled receptors (GPCRs) and several types of the heterotrimeric G-proteins are ubiquitously expressed in all cell types of mammalian organisms (Offermanns, 2001). The heterotrimeric G-proteins are important internal mediators of the extracellular signals that bind to GPCRs, which lead to the generation of a specific biochemical response.

4.1 The Presence of G-proteins

Babb et al. (2012) reported the presence of all G-proteins in Swiss 3T3 cells while reports from Kamitani et al. (2011), Babb et al. (2012), and Orth et al. (2013) confirmed that PMT activates $G\alpha_{i1\text{-}3}$, $G\alpha_{q/11}$, and $G\alpha_{12/13}$ but not G_s.

In spite of the reported differential response of Vero cells to PMT compared to other cell lines, the presence of different G-protein subtypes in Vero cells has not been investigated. Prior to starting this research, our group predicted that the presence and differences in G-protein abundance might have functional differences in Swiss 3T3 and Vero cells.

To determine whether all the G-protein α subtypes that PMT modifies are present in untreated Swiss 3T3 and Vero cells, membrane proteins were extracted and the Gα subunits in the samples were analysed using SDS-PAGE and Western Blotting using antibodies specific to Gα subtypes. These antibodies are listed as interacting to both human and mouse G-proteins, and from the information available about green monkey G-proteins (see section 4.3) were predicted to interact with both cell types.

This result indicated that all Gα subtypes that PMT modifies are present in both Swiss 3T3 and Vero cells (Fig 4.1.1). This result also confirms the report of Babb et al. (2012) that there appears to be less $G\alpha_{i\text{-}1}$ in Swiss 3T3 cells compared to the other Gα subtypes. It is impossible to measure and compare the amount of all Gα subtypes in both cell lines as different antibodies were used; however, it appears that there is a difference in the amount of each Gα subtype between two cell lines. Prior to SDS-PAGE, Vero cell lysate contained ~0.7 fold more proteins than Swiss 3T3 cell lysate. It appears that there are more Gα subunits in Swiss 3T3 cells with the exception of $G\alpha_{i\text{-}1}$ than Vero cells. Although the βγ complex is not directly activated by PMT, it participates in PMT-linked signalling, so it was of interest to also look for the presence of the β subunit of G-protein (Fig 4.1.1). Due to the thickness of the band, the Gβ subunit in both cell lines appears to have similar amount.

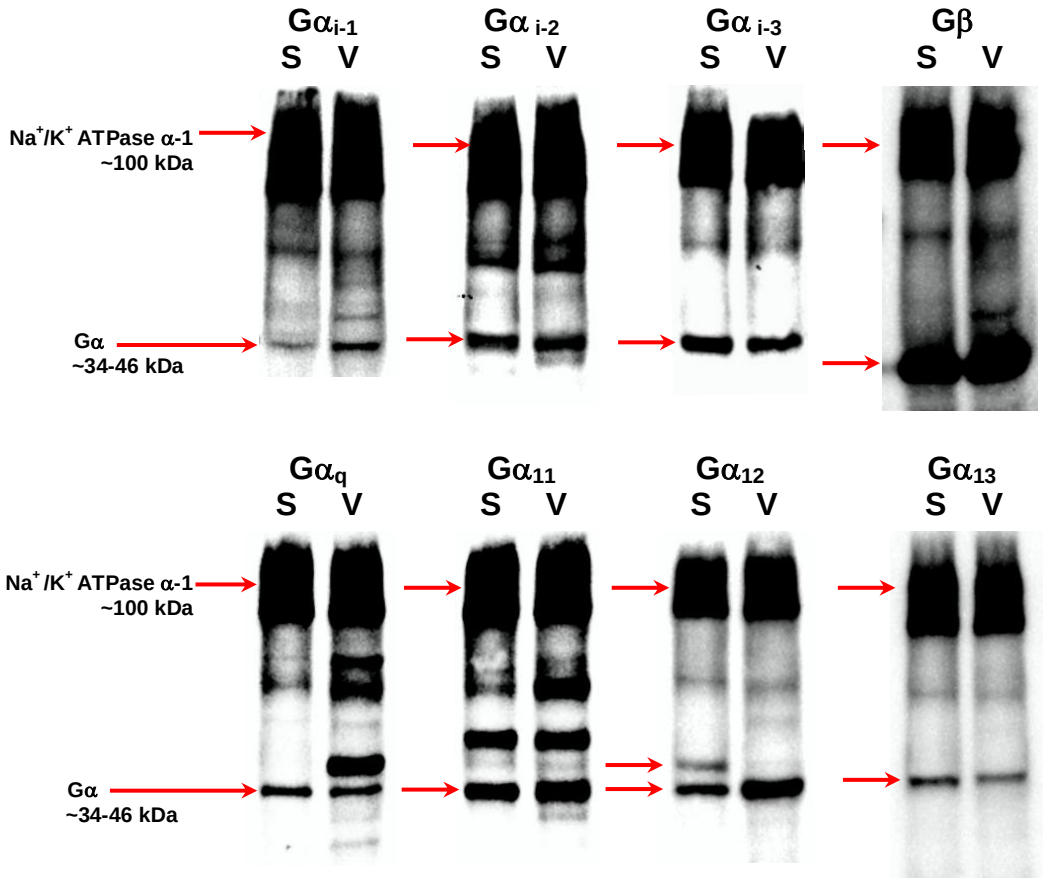

Fig 4.1.1 The presence of different Gα subtypes in Swiss 3T3 and Vero cells. All Gα subtypes that are modified by PMT are present in both Swiss 3T3 and Vero cells. The Gβ subunit is also shown here. Cell lysates were immunoblotted with antibodies against $G\alpha_q$, $G\alpha_{11}$, $G\alpha_{12}$, $G\alpha_{13}$, $G\alpha_{i-1}$, $G\alpha_{i-2}$, $G\alpha_{i-3}$, Gβ and Na^+/K^+ ATPase α-1 subunit. Legend: S = Swiss 3T3 and V = Vero cells.

The molecular weight of different Gα subtypes is shown in appendix, Table A3 (obtained from the Uniprot and National Center for Biotechnology Information (NCBI) database). Swiss 3T3 cells appear to have two isoforms of $G\alpha_{12}$, which according to Uniprot and NCBI database have a molecular weight of 34 (computer annotated, UniProt/TrEMBL) and 42 kDa (reviewed,

UniProt/Swiss-Prot). The $G\alpha_{12}$ of Vero cells appeared to have a molecular weight of 36 kDa which compared closely to the predicted $G\alpha_{12}$ of *C. sabaeus*, which has a molecular weight of 36 kDa (protein predicted, Uniprot/TrEMBL) (see table A3 in appendix section). The aligned amino acid sequences show that the $G\alpha_{12}$ subunit of *C. sabaeus* is 20% shorter than the 42 kDa $G\alpha_{12}$ isoform in mouse (Fig 4.1.2). Humans (*H. sapiens*), on the other hand, have three $G\alpha_{12}$ isoforms: 1 unspliced form (44 kDa) and 2 spliced variants (34 kDa and 38 kDa) (NCBI and UniProt). The extra bands seen with $G\alpha_q$ and $G\alpha_{11}$ antibodies are likely to be a result of cross reaction, as there are no isoforms in the protein or nucleotide databases (Fig 4.1.1).

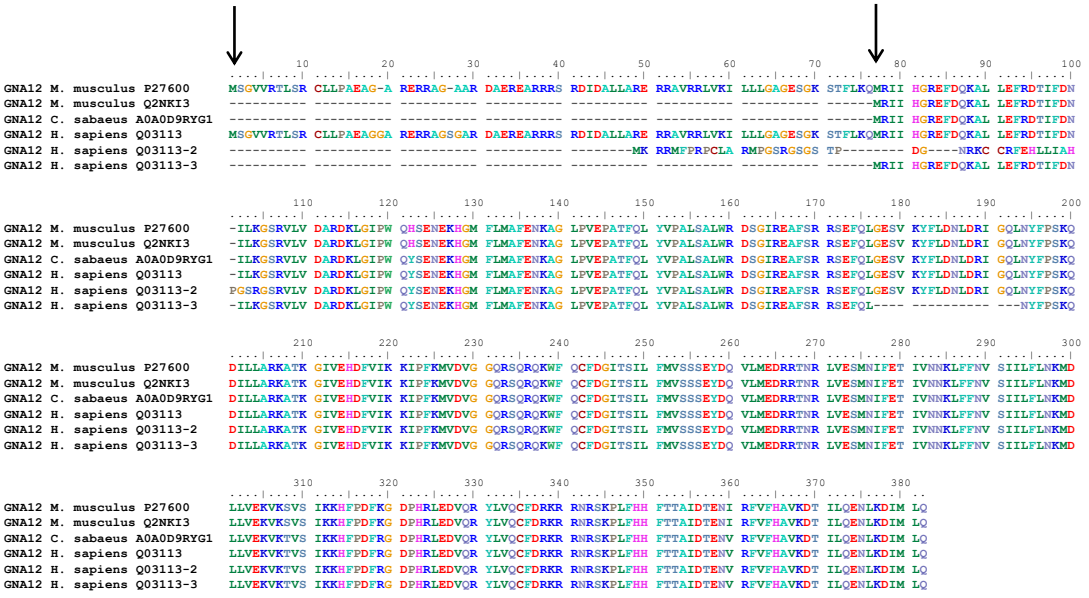

Fig 4.1.2 The Aligned Complete Amino Acid Sequences of $G\alpha_{12}$ subunits of *H. sapiens*, *C. sabaeus*, and *M. musculus*. The start codon of each $G\alpha_{12}$ was highlighted with an arrow which also shows the difference in the length of the protein. Each $G\alpha$ subtype of species bears the protein identifier. The amino acid sequences of $G\alpha_{12}$ of *M. musculus* obtained from Uniprot is designated with an asterisk (*).

4.2 The Abundance of G-proteins

Little is known about the differences in Gα subtypes in different cells. Krumins and Gilman (2006) catalogued the presence and abundance of different G-proteins in HeLa cells.

Fig 4.1.1 shows that the amounts of G-protein α subtypes that PMT modifies differ between the two cell lines. However, it is not possible to measure the amounts of G-proteins present using different antibodies. I, therefore, decided to attempt to quantify the expression levels of these Gα subunits. Real-time qPCR (RT-qPCR) would confirm the mRNA level of the Gα subtypes in Swiss 3T3 and Vero cells.

4.3 Sequencing of the Collaborative Consensus Coding Sequences (CCDS) of Different Gα subunits in Vero Cells

The CCDS of each G-protein α subtype is represented by the complete mRNA sequences, composed of exons, that translate into protein while the reference mRNA (or RNA) sequence includes untranslated regions (Mignone et al., 2002; Pruitt et al, 2009).

Vero cells are kidney epithelial cells derived from African Green Monkey, previously classified as *Cercopithecus aethiops* which has now been placed

within the genus *Chlorocebus* (Haus et al., 2013). Researchers are still disputing about this taxonomy and consider *Chlorocebus aethiops* as one species with 4 monotypic and 2 polytypic species with subspecies. According to Groves (2001), the 4 monotypic species are C. aethiops (Grivet Monkey, also known as African Green Monkey and Savannah Monkey) (Kingdon, 1997; Kingdon and Butynski, 2008), *C. sabaeus* (Green Monkey, also known as Sabaeus Monkey or Callithrix Monkey) (Groves, 2005), *C djamdjamensis* (Bale Monkey or Blue Mountain Vervet), and *C. cynosauros* (Malbrouck Monkey). According to Yamasura and Kawakita (1963), Vero cells were derived from the African Green Monkey (*C. aethiops*) but according to genome analysis, Vero cell lineage came from a female *C. sabaeus* (Osada et al., 2014).

As there was confusion regarding where Vero cells derived from, the importance of the sequences to determine the amount of different G-protein α subtypes in Vero cells, I did a nucleotide comparative analysis of G-protein α subtypes in *C. aethiops* and *C. sabaeus*. Also, since the CCDS of all G-protein G-protein α subtypes of *Homo sapiens* (human) and *Mus musculus* (mouse – origin of Swiss 3T3 cells) are available in the NCBI database they were used to search for refseq RNA, CCDS or any nucleotide sequences of each G-protein α subtype in *C. aethiops*. The NCBI blast tool, however, did not resolve any refseq RNA, CCDS or nucleotide sequences with high degree of identity to any of the G-protein α subtype in *C. sabaeus*, *H.*

sapiens or *M*. *musculus*. After multiple blast runs, it was concluded that the nucleotide sequences of *C. aethiops* in the NCBI database were incomplete and had not been annotated. King's senior bioinformatics officer, Phil Cunningham was also consulted, and did independent multiple comparative analyses, and came to a similar conclusion (data not shown).

Due to limited sequence information available for *C. aethiops*, and also in order to carry out comparative nucleotide analysis of G-protein α subtypes to *C. sabaeus*, I have attempted to sequence the different G-protein α subtypes in Vero cells. In order to design a primer for each of the Gα subunits of *C*. *aethiops,* comparative nucleotide and amino acid sequence analyses were carried out. The sequences from the NCBI database were used since the database contains all the RefSeq RNA, CCDS and the corresponding protein sequences of each Gα subtype of the different species. The CCDS of each of Gα subtype of *H*. *sapiens* was compared to *M. musculus* and the predicted refseq RNA from *C. sabaeus* stored in the NCBI database (Table 4.3-A).

The nucleotide sequences of *Chlorocebus sabaeus* appeared to have been annotated, albeit mostly were predicted sequences. The CCDS (taken from the predicted refseq RNA) of different Gα subunits of *C. sabaeus* generated a very high degree of identity, 98 - 99% to *H*. *sapiens*. The CCDS of *H. sapiens* and *M. musculus*, on the other hand, showed between 89 - 95%

identity. The CCDS of different Gα subtypes between *M. musculus* and *C. sabaeus*, on the other hand, were only 84 – 94% identical. It appears that the predicted CCDS of $G\alpha_{12}$ of *C. sabaeus* is different to its mouse and human counterparts, covering only 93 – 94 % of the full CCDS coverage query, which may indicate a difference in the size of $G\alpha_{12}$ in *C. sabaeus* compared to these other species. The coverage query is the percent of the query length (i.e. the CCDS) that was included in the comparative blast runs (see appendix Figs A5 and A6).

Next, the CCDS of all Gα subunits in the three species were obtained from the NCBI database and aligned by ClustalW in the Bioedit Sequence Alignment Editor (Hall, 1999) and the MEGA6.0 (Tamura et al., 2013) programs. A phylogenetic tree was constructed using MEGA6.0 program to show common homology and identity in nucleotide sequences (i.e. CCDS) between Gα subtypes in different species (Fig 4.3-A).

Table 4.3-A A Comparative Analysis of CCDS of Different Gα subunits of *H. sapiens*, *M. musculus* and *C. sabaeus*

Gα subunits	*H. sapiens*$^{++}$				*M. musculus*$^{++}$	
	M. musculus^{+}		*C. sabaeus*$^{+}$		*C. sabaeus*$^{+}$	
	% Query Coverage*	% Identity**	% Query Coverage*	% Identity**	% Query Coverage*	% Identity**
$G\alpha_q$	100	95	100	99	100	94
$G\alpha_{11}$	100	90	100	98	100	89
$G\alpha_{12}$	100	92	93	98	94	91
$G\alpha_{13}$	100	91	100	98	100	90
$G\alpha_{i-1}$	100	89	100	99	100	89
$G\alpha_{i-2}$	100	92	100	99	100	92
$G\alpha_{i-3}$	100	94	100	99	100	94

* The percentage of CCDS covering the CCDS of two species$^{+ \text{ and } ++}$.
** The percentage of sequence identity in the coverage query between two species$^{+ \text{ and } ++}$.
The identifier/accession number of CCDS of each Gα subunit are in Fig 4.3-A.

The phylogenetic tree summarises the common homology and identity in nucleotide sequences of Gα subtypes between three species (Fig 4.3-A). It shows that $G\alpha_q$ and $G\alpha_{11}$, $G\alpha_{12}$ and $G\alpha_{13}$, $G\alpha_{i-1,2,3}$ are grouped together according to their homology and sequence identity, with $G\alpha_{i-1}$ and $G\alpha_{i-3}$ sharing higher identity than $G\alpha_{i-2}$. All the Gα subtypes of *H. sapiens* have a higher identity to the nucleotide sequences of *C. sabaeus* than *M. musculus*, as might be expected. All the aligned nucleotide and amino acid sequences are shown in the appendix section, Figs A5 and A6.

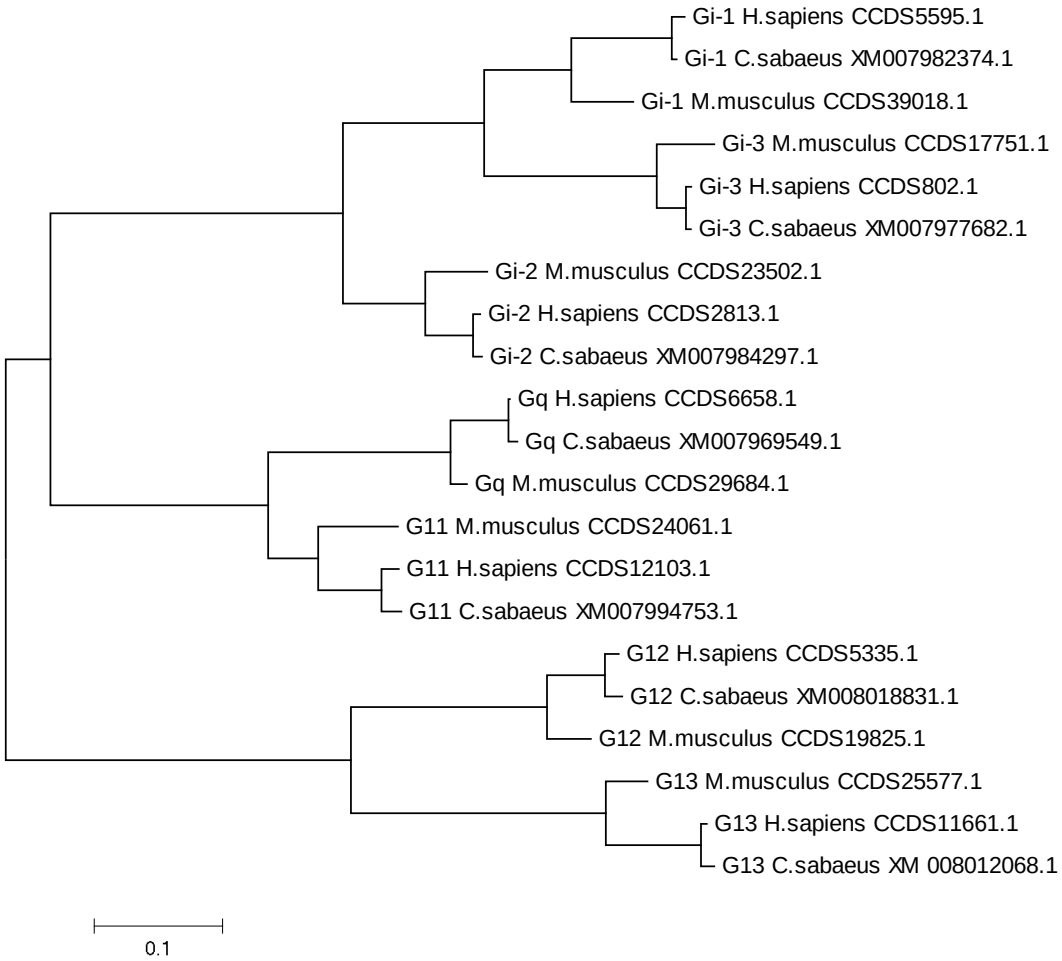

Fig 4.3-A The Phylogenetic Tree of Different CCDS of Gα Subtypes in *H. sapiens*, *M. musculus*, and *C. sabaeus* with their Identifier obtained from the NCBI Database. The scale bar indicates the average number of nucleotide substitutions per site.

A comparative analysis of the amino acid sequences of different Gα subunits of *H. sapiens*, and *M. musculus* and *C. sabaeus*, was also carried out (Table 4.3-B). All protein sequences were obtained from the NCBI database and aligned by ClustalW in the Bioedit Sequence Alignment Editor (Hall, 1999) and the MEGA6.0 (Tamura et al., 2013) programs. A phylogenetic tree was constructed using MEGA6.0 program to show common homology and

identity in amino acid sequences between Gα subtypes in different species (Fig 4.3-B).

Table 4.3-B A Comparative Analysis of Amino Acid Sequences of Different Gα subunits of *H. sapiens*, *M. Musculus* and *C. sabaeus*

Gα subunits	***H. sapiens*** $^{++}$				***M. musculus*** $^{++}$	
	M. musculus $^{+}$		*C. sabaeus* $^{+}$		*C. sabaeus* $^{+}$	
	% Query Coverage*	% Identity**	% Query Coverage*	% Identity**	% Query Coverage*	% Identity**
$G\alpha_q$	100	99	100	100	100	100
$G\alpha_{11}$	100	98	100	98	100	97
$G\alpha_{12}$	100	98	80	100	80	99
$G\alpha_{13}$	100	97	100	100	100	97
$G\alpha_{i-1}$	100	100	100	100	100	100
$G\alpha_{i-2}$	100	98	100	100	100	98
$G\alpha_{i-3}$	100	98	100	99	100	98

* The percentage of CCDS covering the CCDS of two species$^{+ \text{ and } ++}$.
** The percentage of sequence identity in the coverage query between two species$^{+ \text{ and } ++}$. The identifier/Accession number of amino acid sequences of each Gα subunit are in Fig 4.3-B.

The G-proteins, $G\alpha_{q/11}$, $G\alpha_{13}$, and $G\alpha_{i\text{-}1,2,3}$ show 97 – 100% amino acid sequence identity with 100% coverage query in *H. sapiens*, *M. musculus*, and *C. sabaeus*. $G\alpha_{12}$, on the other hand, has 99 – 100% identity and covering only 80% of the whole sequence query, which indicates a difference in the size of $G\alpha_{12}$ (both CCDS and protein sequences) of *C. sabaeus* compared to $G\alpha_{12}$ of *H. sapiens* and *M. musculus*.

The amino acid sequences of $G\alpha_{i\text{-}1}$ in the three species appear to be identical (see also Fig A5 in the appendix section). The amino acid sequences of all Gα subtypes in the three species were obtained from the

NCBI database and aligned by ClustalW in Bioedit Sequence Alignment Editor and MEGA6.0 programs.

A phylogenetic tree was constructed using the MEGA6.0 program to show common homology and identity in amino acid sequences between Gα subtypes in different species (Fig 4.3-B). The phylogenetic tree summarises the common homology and identity in amino acid sequences of Gα subtypes amongst the three species (Fig 4.3-B). Similar to the nucleotide sequences, it shows that $G\alpha_{q\ and}$ $G\alpha_{11}$, $G\alpha_{12}$ and $G\alpha_{13}$, $G\alpha_{i\text{-}1,2,3}$ are grouped together according to the homology and identity of their amino acid sequences. The amino acid sequence of $G\alpha_{i\text{-}1}$ is conserved across the three species. Similarly, all Gα subtypes of *H*. *sapiens* have a higher identity with the amino acid sequences of *C*. *sabaeus* than *M*. *musculus*.

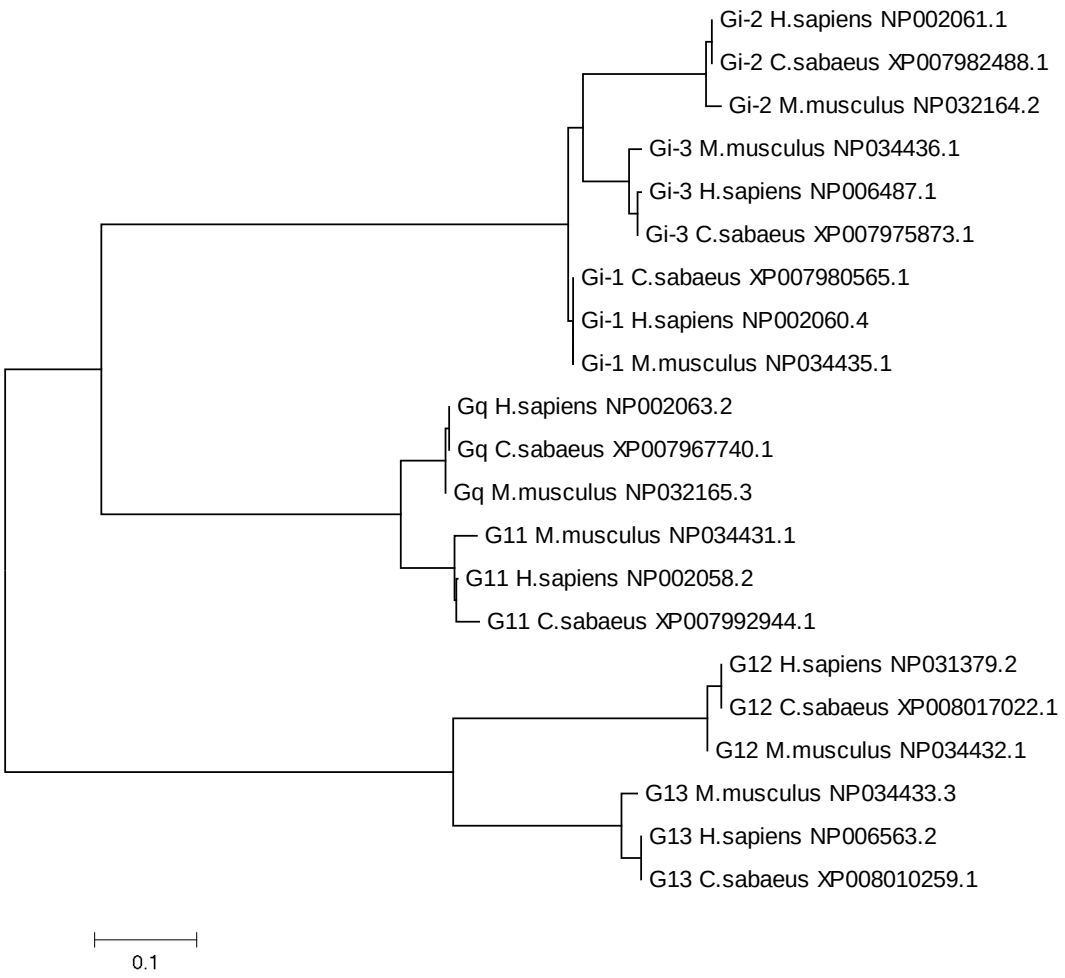

Fig 4.3-B The Phylogenetic Tree of Different Gα Subtypes Protein Sequences of *H. sapiens*, *M. musculus*, and *C. sabeus* with their Protein Sequence Identifier based on each CCDS obtained from the NCBI Database. The scale represents the average number of amino acid substitutions per site.

The nucleotide and protein sequences of $G\alpha_{12}$ of Swiss 3T3 cells from Uniprot which were not available in the NCBI database were also obtained to determine their similarity with $G\alpha_{12}$ from Vero cells (see Fig A5 in the appendix section). This particular CCDS gave a 100% coverage query to $G\alpha_{12}$ of Vero cells.

Since the nucleotide sequences of *C. aethiops* in the NCBI database were incomplete and had not been annotated, in order to measure the expression levels of all Gα subunits, it is essential to sequence the CCDS of all Gα subunits of Vero cells. PCR will amplify the cDNA prior to sequencing and genotyping. The generated sequences will be used for primer design for RT-qPCR.

4.4 Designing of Primers

The Primer3 program was used to design the primers based on the mRNA sequences of each Gα subunit of *C. sabaeus* and *H*. *sapiens* in order to sequence the CCDS of each of the Gα subunit of Vero cells. The primers for the RT-qPCR for Swiss 3T3 cells were obtained from Origene Technologies. The untranslated regions of the mRNA were included in order to get the full CCDS.

In order to quantify the mRNA levels of each G-protein α subtype, a Real-Time PCR requires forward and reverse primers with high degree of specificity for each G-protein α subtype. The NCBI primer design tool was used to design the RT-qPCR primers for the Gα subunits of Vero cells after sequencing and genotyping. The generated primers for sequencing (Table 4.4-A) and RT-qPCR (Table 4.4-B) were run on NCBI primer blast tool to check for related sequences in other genes to avoid amplification of products

other than the target product. The primers were synthesised by Eurofins MWG Operon (https://ecom.mwgdna.com).

The two main sets of primers for $G\alpha_{12}$ were $G\alpha_{12}$ (A) or $G\alpha_{12}$ (AA) (for forward and reverse), and $G\alpha_{12}$ (B) or $G\alpha_{12}$ (BB) (Table 4.4-A). They were also used interchangeably which also generated 2 more sets, e.g. forward primer of set A was paired with the reverse primer of set B which was denoted as $G\alpha_{12}$ (AB), and vice versa ($G\alpha_{12}$ (BA)). The latter 2 sets of primers were also run on the NCBI primer tool to confirm their specificity to the target cDNA template, determine the product size, and avoid amplification of other products.

Table 4.4-A The RT-PCR Primers for Sequencing of Gα subunits of Vero Cells

Gα	Forward	Reverse	Expected Product Size (bp)
$G\alpha_q$	GGAGGCACTTTGGAAGAATGAC	AACTCTGTGGACACGCTCAC	1,239
$G\alpha_{11}$	GATGACTCTGGAGTCCATGATG	TGCGGAGGGAGAGATGTACA	1,284
$G\alpha_{12}$ (A)	CGGCAAGTCCACGTTCCTTA	TCCTGCAGGAGACGACAAAC	974
$G\alpha_{12}$ (B)	CAGTCTCAGCGTTCCCTTCA	CGAGGACCACACAGACAACA	1,123
$G\alpha_{13}$	GTCAGTTCGCTGGTTCCCTC	CACTCAACAGCTTTCAGCCAC	1,463
$G\alpha_{i-1}$	GCCCGCTGGGAGAGAGAAAG	CACACTGCAGGACCATCTGTC	1,375
$G\alpha_{i-2}$	CTGAACTGCCGACCCGATAG	CCTCCCCTACATCTGGAGCT	1,375
$G\alpha_{i-3}$	CGCTTTCGGTCTCAACTCCT	GTAGCTGCCCCGTAAGACAG	1,371

Table 4.4-B The RT-qPCR Primer Sequences for Gα subunits of Swiss 3T3 Cells

Gα	Forward	Reverse	Expected Product Size (bp)
$G\alpha_q$	AGCGATGGACACGCTCAAGATC	CAGACACCTTCTCCACATCAACC	92
$G\alpha_{11}$	GTTCTTGGTGGCACTAAGCGAG	GACAGACGAGTTCTGGAACCAG	127
$G\alpha_{12}$	TCCACCTTCCTCAAGCAGATGC	AGCGTCCACAAGAACCCTCGAA	123
$G\alpha_{13}$	TCCACCTTCCTGAAGCAGATGC	AGCTTCTCTCGGGCATCTACCA	134
$G\alpha_{i-1}$	CTCGGAAGAGGAGTGTAAGCAG	GCAAGCACGAAAAGTTGGCGAG	150
$G\alpha_{i-2}$	TGACTTGGTGCTGGCTGAGGAT	GATGGAGGTGTCTGTGAACCAC	103
$G\alpha_{i-3}$	GACTACAGGCATTGTGGAGACC	GGTCGTAATCACTGAGAGCCAC	155
Actin-β	CAGCAGTTGGTTGGAGCAAA	GTGGCTTTTGGGAGGGTGAG	167

4.5 Extraction of mRNA

Construction of a cDNA library that can be translated to mRNA requires cellular RNA of high quality. Extraction of the RNA pool from Swiss 3T3 and Vero cells was carried out using the RNeasy Plus Mini Kit (QIAGEN). The RNA content and quality were determined using a NanoDrop 1000 Spectrophotometer (Thermo Scientific) (Table 4.5). The RNA samples from Swiss 3T3 and Vero cells both had A260/280 ratio of >2.0 which is considered high quality.

Table 4.5 Analysis of the Swiss 3T3 and Vero cells RNA Samples.

	Swiss 3T3	Vero
ng/µl	671.90	1079.10
λ Abs	8.35	14.53
A-260 10mm path	16.80	26.98
A-280 10mm path	7.98	12.73
260/280	2.10	2.12
260/230	2.01	1.86

Another common method to assess integrity of total RNA samples is by visualising 28s and 18s ribosomal RNAs (rRNAs) on a denaturing agarose gel stained with gel red or ethium bromide (EtBr) (Fleige and Pfaffl, 2006; Wieczorek et al., 2012). RNAs are usually not visible on denaturing agarose gel as their secondary structure alters their migration properties and therefore would not migrate according to their size.

The extracted RNAs was electrophoresed on a 1% denaturing agarose gel dissolved in 1x TAE, which contains 1% household bleach (Clorox) (Aranda et al., 2012) and later on stained with gel red. A DNA ladder was used only to show that the gel and samples were run properly. Intact total RNA in the samples should give a sharp intensity of the 28s and 16s rRNA bands when run on agarose gel. A clear 2:1 ratio of 28s and 16s rRNA is an indicative of good quality RNA (Wieczorek et al., 2012). The 28s and 16s rRNA bands

were visualised on UV transilluminator (AlphaImager; λ= 302) to allow the UV detection of the stained RNA bands.

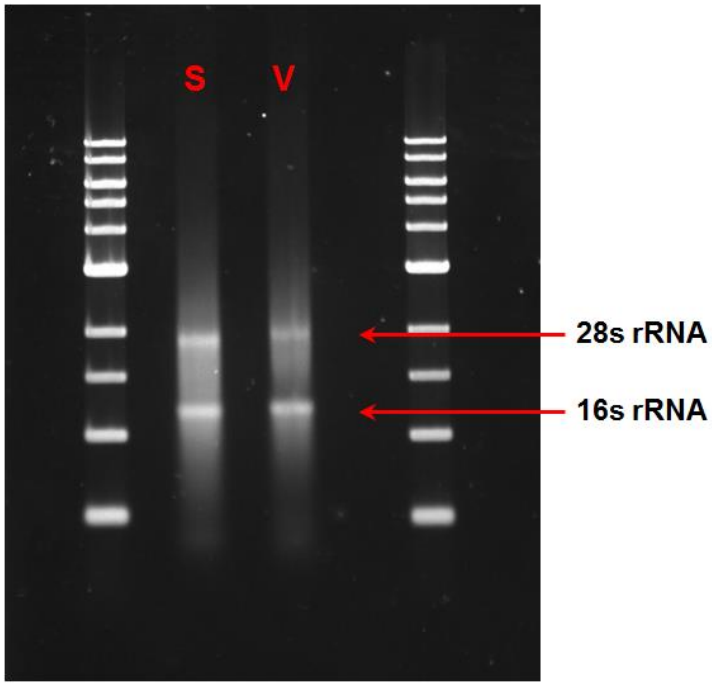

Fig 4.5 The 28s and 16s rRNA in Swiss 3T3 and Vero cells. 5μl of each RNA sample mixed with 1μl dye and DNA marker were run on 1% agarose gel in TAE with 1% household bleach, and visualised as described in the text. Legend: S = Swiss 3T3 and V = Vero cells.

The RNA samples from Swiss 3T3 and Vero cells produced visible clear 28s and 16s rRNA bands with light smearing but did not give a clear 2:1 ratio (Fig 4.5). However, these samples were used for the construction of cDNA library of different Gα subunits of Vero cells. The 2:1 ratio of 28s and 16s rRNA was not achieved, however, Fleige and Pfaffl (2006) reported that 28s rRNA rapidly disappears under UV light. According to Imbeaud et al. (2005), the low rRNA ratio in electrophoresis is not an indicative of poor quality of total RNA.

4.6 Generation of cDNA template

In order to generate cDNA templates for qPCR, a reverse transcription polymerase chain reaction was carried out using the mRNA from the extracted RNA samples, and the Precision nanoScript™ 2 Reverse Transcription Kit (PrimerDesign) or High-Capacity cDNA Reverse Transcription Kit (Life Technologies) (see section 2.13.9 in chapter 2). After reverse transcription, the cDNA content and quality were determined using a NanoDrop 1000 Spectrophotometer (Table 4.6). The cDNA samples from Swiss 3T3 and Vero cells both had A260/280 ratio of almost 1.8 which is considered good quality.

Table 4.6 Analysis of the cDNA Templates from mRNA in Swiss 3T3 and Vero cells.

	Swiss 3T3	Vero
ng/µl	3185.90	3072.70
λ Abs	28.19	27.06
A-260 10mm path	63.72	61.46
A-280 10mm path	35.87	34.49
260/280	1.78	1.78
260/230	2.26	2.27

4.7 Amplification of CCDS of Different Gα Subunits by Real-Time Polymerase Chain Reaction (RT-PCR)

In order to design the forward and reverse primers for each of the Gα subunit in Vero cells for RT-qPCR, it was essential to sequence the CCDS of each Gα subunit. The CCDS of different Gα subunits in Vero cells were amplified using GoTaq® Hot Start Colourless Master Mix (Promega, UK), cDNA templates, and Primer3-generated forward and reverse primers (Table 4.4-A). The amplified CCDS of each Gα subunit were electrophoresed in 1 - 2% denaturing agarose gel in either 1x TBE or TAE. The prospective bands (cDNA) with molecular size from 974 – 1463 (denoted by the red box) in the gel were cut and stored at -20°C (Fig 4.7).

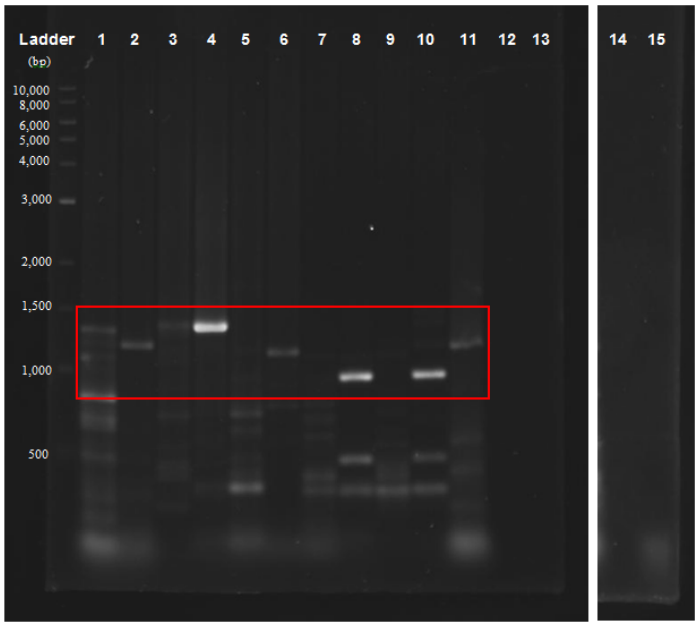

Gα	Product Size (bp)	
	Expected	Calculated
$G\alpha_q$	1,239	1,253
$G\alpha_{11}$	1,284	1,134
$G\alpha_{12}$ (BB)	1,123	863
$G\alpha_{12}$ (BA)	1,007	863
$G\alpha_{13}$	1,463	1,162
$G\alpha_{i-1}$	1,375	1,162
$G\alpha_{i-2}$	1,375	1,284
$G\alpha_{i-3}$	1,371	1,053

Fig 4.7 The Amplified cDNA of Different Gα Subunits of Vero cells Using the Primers for Sequencing. The generated cDNA of different Gα subunits (left, denoted by the red box) on agarorse gel. The expected and calculated molecular weights of Gα subunits according to their NCBI sequences their relative migration distance (Rf) (right). Lanes 1: $G\alpha_q$, 2: $G\alpha_{11}$, 3: $G\alpha_{13}$, 4: $G\alpha_{i-1}$, 5: $G\alpha_{i-2}$, 6: $G\alpha_{i-3}$, 7: $G\alpha_{12}$ (AA), 8: $G\alpha_{12}$ (BB), 9: $G\alpha_{12}$ (AB), 10: $G\alpha_{12}$ (BA), 11: GADPH, 12: H_2O, 13: Master Mix (MM), 14: MM+H_2O+Template, 15: MM+H_2O+Primer

4.8 Sequencing of Gα subtypes

The DNA bands in the denaturing agarose gel were extracted using QIAquick Gel Extraction Kit (QIAGEN). The extracted DNA was mixed with either the forward or reverse primer and the pre-mixed samples were sequenced by Eurofins. These sequences were aligned and compared to CCDS of H. sapiens, C. sabaeus, and M. musculus using ClustalW in the Bioedit Sequence Alignment and MEGA6.0 programs (Table 4.8-A and Fig 4.8-C).

After successful sequencing of some of the Gα subunits of Vero cells, these sequences were aligned and compared to the CCDS of *H. sapiens*, *C. sabaeus*, and *M. musculus* by ClustalW in Bioedit Sequence Alignment and MEGA6.0 programs (Table 4.8-A, and Fig A7 in the appendix section). The whole sequence of each Gα subunit was used to design the primers for RT-qPCR. The NCBI primer design tool was used to design the RT-qPCR primers for Gα subunits of Vero cells (Table 4.8-B). The generated primers were run on the NCBI primer blast tool to check for identical sequences in closely related genes and thus to avoid amplification of other products (Table 4.4-B).

Table 4.8-A A Comparative Analysis of the Nucleotide Sequences of Different Gα subunits of *H. sapiens*, *C. sabaeus*, *M. musculus* and the Sample

Gα subunits	Sample (Vero cells/*Chlorocebus aethiops*)					
	Homo sapiens+		*Chlorocebus sabaeus*+		*Mus musculus*+	
	% Query Coverage*	% Identity**	% Query Coverage*	% Identity**	% Query Coverage*	% Identity**
$G\alpha_q$	82	92	82	97	82	96
$G\alpha_{11}$	---	---	---	---	---	---
$G\alpha_{12}$	69	86	69	88	68	81
$G\alpha_{13}$	---	---	---	---	---	---
$G\alpha_{i-1}$	88	84	92	95	92	94
$G\alpha_{i-2}$	---	---	---	---	---	---
$G\alpha_{i-3}$	28	84	43	82	43	82

* The % of nucleotide sequence covering the sequence of the sample and species+.
** The % of nucleotide sequence identity in the query coverage between sequence of the sample and species+.
Identifier/Accession number of amino acid sequences of each Gα subunit are in Fig 4.3-A.

Table 4.8-B The Generated RT-qPCR Primer Sequences for Gα subunits of Vero Cells

Gα	Forward	Reverse	Expected Product Size (bp)
$G\alpha_q$	TCAACGACGAGATCGAGCG	CAGCTTGGTGAAGCCCCTTT	173
$G\alpha_{12}$	---	---	---
$G\alpha_{i-1}$	AGATGATCGACCGCAACCTC	AGATTCACCAGCACCAAGCA	83
$G\alpha_{i-3}$	---	---	---

4.9 The Quantification of mRNA Levels of Different Gα Subtypes

It was predicted that the presence and differences in G-protein abundance may have functional differences in both cell types and therefore, it was the aim of this research to quantify the mRNA level of each Gα subunit.

Prior to quantification of mRNA level of all Gα subunits of Swiss 3T3 cells, using the generated cDNA templates all primers were tested by amplifying the target products by RT-PCR. Amplicons were electrophoresed in 2% agarose gel and visualised on UV transilluminator (AlphaImager; λ= 302) to allow the UV detection of the stained DNA bands.

The amplicons of each Gα subunit appeared to be the correct size with the exception of $G\alpha_{i-1}$, which was not detected (Fig 4.9). The cDNA templates from Swiss 3T3 cells were used for the quantification of mRNA levels of

each Gα subunit using RT-qPCR technique. A 10-µl real-time PCR reaction was prepared using 5 µl Precision™ 2X qPCR SYBRgreen Mastermix, 25 ng of cDNA template, 6 pMol of primer mix, and nuclease-free water.

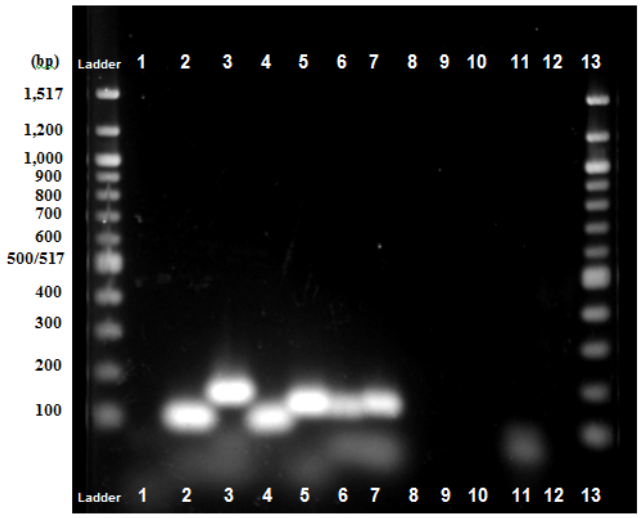

Gα	Product Size (bp)	
	Expected	Calculated
$G\alpha_q$	92	95
$G\alpha_{11}$	127	129
$G\alpha_{12}$	123	125
$G\alpha_{13}$	134	129
$G\alpha_{i-1}$	150	---
$G\alpha_{i-2}$	103	100
$G\alpha_{i-3}$	155	138

Fig 4.9 The Amplified cDNA (Amplicons) of Different Gα Subunits of Swiss 3T3 Cells Using the RT-qPCR Primers (left) on Agarose Gel. The expected and calculated molecular weights of Gα subunits according to their NCBI sequences their relative migration distance (Rf). Lanes 1: $G\alpha_{i-1}$, 2: $G\alpha_{i-2}$, 3: $G\alpha_{i-3}$, 4: $G\alpha_q$, 5: $G\alpha_{11}$, 6: $G\alpha_{12}$, 7: $G\alpha_{13}$, 8: H_2O, 9: Master Mix (MM), 10: MM+H_2O+Template, 11: MM+H_2O+ Primers

After many alterations in the amount of cDNA templates, primers, and temperature (data not shown), no result was generated. In addition, the difficulties in obtaining accurate sequence for Vero cell G-proteins made this whole approach very difficult and it was decided to discontinue this line of research and concentrate on other areas of interest.

4.10 Discussion

I have confirmed that the Gα subunits that PMT modifies are present in both Swiss 3T3 and Vero cells. However, the relative amount of each Gα subunit differs between two cell lines (Fig 4.1.1). While it is not possible to compare relative amounts of different G-proteins using different antibodies, it is possible to compare between two cell lines. In particular, the amount of $G\alpha_{i-1}$ in Swiss 3T3 cells was less than in Vero cells, confirming the observation made by Babb et al. (2012). $G\alpha_{i-1}$ is known to bind to microtubules and activates the tubulin GTPase activity which results in microtubule dynamic instability (Roychowdhury et al., 1999; Parekh et al., 2006). Although this subunit has been implicated to have a role in cytokinesis or the completion of mitosis, Swiss 3T3 cells has less $G\alpha_{i-1}$ than Vero cells. $G\alpha_{i-1}$ may have other roles such as depression of cAMP level.

In general, it appears that there are more G-proteins in Swiss 3T3 than in Vero cells considering that prior to SDS-PAGE, Vero cell lysate contained ~0.7 fold more proteins than Swiss 3T3 cell lysate. The differences in the amount of Gα subtypes might have a role in the differential responsiveness of Swiss 3T3 and Vero cells to PMT. As different antibodies each with different avidities can not be used to quantify different proteins, it was hoped to determine the amount of each Gα subunit in both cell lines by quantifying their protein expression level. The results from this experiment would have

validated the Western Blot results regarding the amounts of the different Gα subunits. The absence of reliable sequence information for *C*. *aethiops* (Yamasura and Kawakita, 1963), or *C. sabaeus* (Osada et al., 2014), from which Vero cells were derived, made this task extremely difficult and time-consuming and it was eventually decided not to pursue it further.

Relative protein abundance can not be assessed directly by measuring mRNA levels. Others have had variable success in correlating these two properties (Gry et al., 2009; Pascal et al., 2008; Schedel et al., 2004; Greenbaum et al, 2003). Discrepancies in the correlation of mRNA level and protein expression may be due to protein turnover, complicated post-transcriptional mechanisms involved in gene expression and other factors (Greenbaum et al, 2003). Different cell types within the same animal, although containing the same DNA sequence may have variable protein composition which may affect different cellular processes including gene transcription, and any changes in the cell may also change the protein expression and content. Foley et al. (2010) reported that T-cell differentiation changes the repertoire of expressed chemokine receptors (a subgroup of GPCRs) and Gα subunits, in particular, $G\alpha_{i/o}$. PMT is involved in CD4-positive T helper (Th) cell differentiation (Hildebrand et al., 2015) and inhibition of osteoblast differentiation (Lax et al., 2004). It would be interesting to see if PMT also affects the repertoire of expressed Gα subunits in these two cell lines or in other cell types.

In order to quantify the mRNA levels of different Gα subunits of Vero cells, specific primers for each Gα subunit are essential; however, although it was not possible to carry out quantification of different mRNA levels as intended, interesting information about the information of databases for the genus, *Chlorocebus* were obtained. It appeared that the sequences of *C*. *aethiops* in the NCBI databank and other databases were incomplete and most had not been annotated while the sequences of *C. sabaeus* were predicted. This initial work was carried out in collaboration with Phil Cunningham (Senior Bioinformatics Officer at King's). Comparative nucleotide and amino acid analyses of each Gα subunit of *H*. *sapiens*, *C*. *sabaeus* and *M*. *musculus* were used to design primers for the sequencing of Gα subunits of Vero cells (Tables 4.3-A-B; Figs 4.3-A-B). The results showed that the predicted nucleotide and amino acid sequences of Gα subunits of *C*. *sabaeus* are highly identical to *H*. *sapiens* than *M*. *musculus*, therefore, the refseq RNA of both *H*. *sapiens*, and *C*. *sabaeus* were used to design primers. During the comparative analyses of the protein and nucleotide sequences, the coverage query of 80 – 94% for $G\alpha_{12}$ indicated its length which appeared to be shorter than all Gα subtypes in three species. All CCDS and amino acid sequences of Gα subunits were obtained from NCBI database and aligned with other sequences which confirmed their length/size (Tables 4.3-A-B, and Figs A5 and A6 in the appendix section). Another nucleotide and protein sequences of $G\alpha_{12}$ of Swiss 3T3 cells were found only in Uniprot database, which were compared to the ones obtained from the NCBI database. This

particular $G\alpha_{12}$ has 100% coverage query to $G\alpha_{12}$ of Vero cells (see Figs A5 and A6 in the appendix section). It is impossible not to speculate that the missing 20% in protein sequences of $G\alpha_{12}$ might have a role in protein recognition, protein-protein interaction or other functions. A comparative analysis of $G\alpha_{12}$ protein sequences from different species reveals that the mouse, cattle and many primates including humans have similar $G\alpha_{12}$ isoform (see Fig A8 in the appendix section).

The varying amounts of different G-proteins between cell types may be linked to different response to PMT. There are two main questions that need to be addressed: First, does PMT recognise and deamidate the $G\alpha$ subunits of Vero cells? Secondly, does the complex signalling system involving these differential responses indicate roles of participating molecules that regulate different pathways? These questions will be addressed in chapters 5 and 6.

5 THE MODIFICATION OF Gα SUBUNITS IN SWISS 3T3 AND VERO CELLS

Activation of G-proteins by PMT involves deamidation of the conserved glutamine residue in the switch II of the Gα subunits to glutamic acid. The glutamine residue positions the attacking water molecule during hydrolysis of ATP. Deamidation of this amino acid residue renders the G-proteins in their constitutive active state leading to activities of the signalling pathways that each activated G-protein regulates.

5.1 Detection of Modified G-proteins in Swiss 3T3 and Vero Cells by PMT

Kamitani et al. (2011), Babb et al. (2012), and Orth, et al. (2013) confirm that PMT modifies $G\alpha_{i1\text{-}3}$, $G\alpha_{q/11}$, and $G\alpha_{12/13}$ but not G_s in different cell lines.

In order to understand the differential response of Swiss 3T3 and Vero cells to PMT, it was essential to determine if PMT modified all Gα subunits in each cell line. An immunoprecipitation experiment using magnetic Dynabeads® was carried out to collect both endogenous unmodified and deamidated Gα subunits from the cell lysates of the untreated and rPMT-treated cell lines (see section 2.13.6). The separated Gα subunits were analysed using SDS-PAGE and Western Blotting. PVDF membranes were

reacted with antibodies specific to Gα subtypes or the deamidated form of Gα subunits (a rat monoclonal anti-QE).

I have shown that the Gα subunits examined were present in different amounts in both cell types (Fig 4.1). The amount of each Gα subunit in Vero cells appears to be less when compared to their Gα subunit counterpart in Swiss 3T3 cells with the exception of $G\alpha_{i-1}$.

The Western Blot results show that all rPMT-modified Gα subunits in Swiss 3T3 and Vero cells were present up to a period of 3 days (Fig 5.1.1). As shown before by others (Kamitani et al., 2011 and Orth, et al., 2013), PMT leads to deamidation of its target Gα subunits starting at around 4 h. $G\alpha_{i-1}$ deamidation is greater after 72 h, which may reflect the relatively low abundance of this subunit in Swiss 3T3 cells. In Vero cells, on the other hand, the modification of Gα subunits were first detected at 16 h post rPMT treatment with the exception of $G\alpha_{i-2}$ and $G\alpha_{11}$ which appeared to be the first targets of rPMT. Interestingly, $G\alpha_{12}$ first begins to be modified by rPMT at around 48 h. The modification of $G\alpha_{13}$ was first detected at 16 h but this had increased substantially by 48 h. The unmodified Gα subunits, except for $G\alpha_{i-1}$, in the untreated and rPMT-treated Swiss 3T3 cells were all present up to a period of 3 days. It is difficult to detect the unmodified $G\alpha_{i-1}$ in Swiss 3T3 cells in small quantity using the polyclonal anti-$G\alpha_{i-1}$ antibody. (Fig 5.1.1, and Dr. Babb, personal communication). However, the monoclonal anti-QE

antibody was able to detect the modified Gα subunits in rPMT-treated Swiss 3T3 and Vero cells, which suggests its avidity to the deamidated form of Gα subunits.

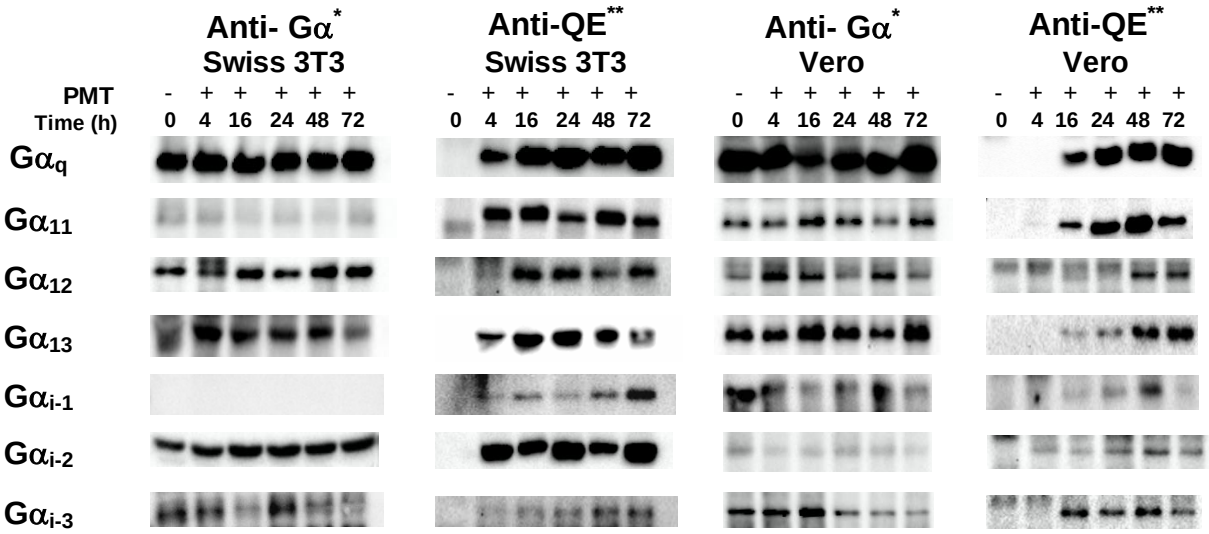

* Gα subunits of Swiss 3T3 and Vero cells probed with specific Gα antibody
** Gα subunits of Swiss 3T3 and Vero cells probed with anti-QE antibody

Fig 5.1.1 The immunoprecipitated unmodified and deamidated Gα subtypes in Swiss 3T3 and Vero cells. Both cell lines were either left untreated (-) or treated (+) with 15 ng/ml of rPMT and processed at different time points: 0, 4, 16, 24, 48, 72 h. Gα subunits were immunoprecipitated using specific Gα antibody and magnetic beads overnight at 4ºC in cell lysates containing a protein concentration of 500 µg (Swiss 3T3 cells) and 700 µg (Vero cells) and analysed by SDS-PAGE and Western Blotting as described in section 2.14.6.

As immunoprecipitation is more difficult to quantify, total amount of modified Gα subunits in cell lysates were analysed using the SDS-PAGE and Western Blotting.

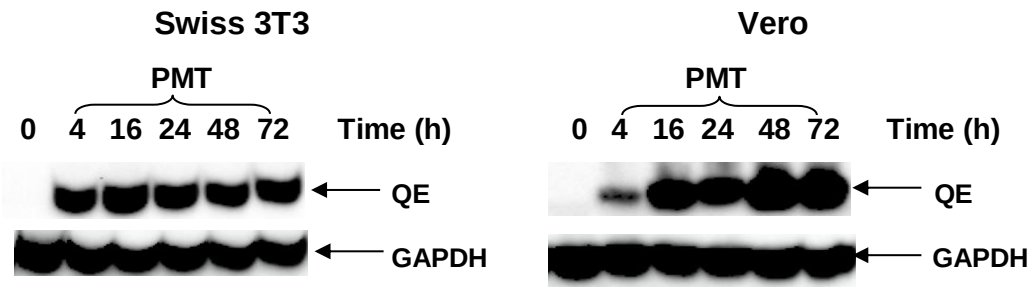

Fig 5.1.2 Deamidation of Gα subunits by PMT occurs later in Vero cells compared to Swiss 3T3 cells. Both cell lines were either left untreated or treated with 15 ng/ml of rPMT and collected at different time points: 0, 4, 16, 24, 48, 72 h. Cell lysates containing a protein concentration of 1000 µg/ml (Swiss 3T3 cells) and 1400 µg/ml (Vero cells) were analysed by SDS-PAGE and Western Blotting. Anti-QE antibody was used to detect the total modified Gα subunits.

The Western Blot results show that the Gα subunits of Swiss 3T3 cells were deamidated as early as 4 h while Vero cells show a low level of deamidated Gα subunits at 4 h (Fig 5.1.2). However, the amount of these modified Gα subunits in Vero cells increased at 16h reaching the maximum amount at 48 h. These modified Gα subunits were all present until day 3. The level of modified Gα subunits in Swiss 3T3 cells, on the other hand, remained the same from 4 h until 72 h.

The difference in the amount of deamidated Gα subunits at 4 h between the two cell lines raised a few more questions: 1) When did PMT start modifying

Gα subunits in Swiss 3T3 and Vero cells? 2) Would there be an increase in the level of modified Gα subunits in Vero cells after 4 h?

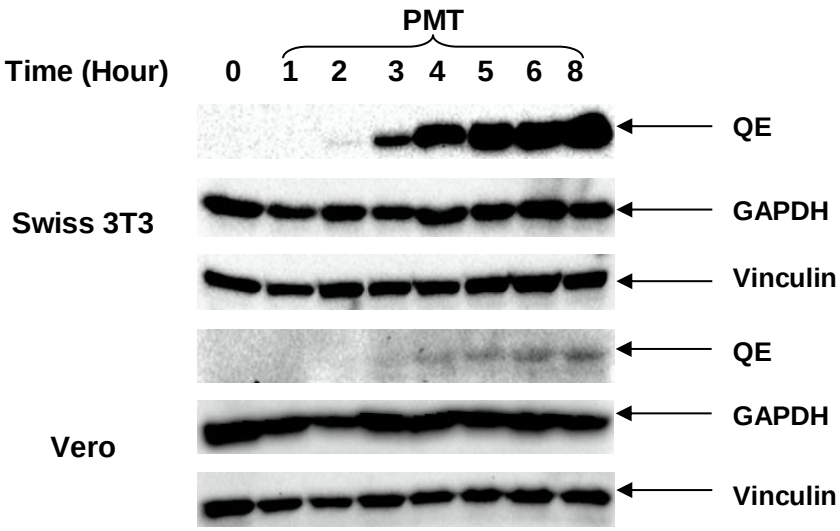

Fig 5.1.3 PMT modification of Gα subunits is faster in Swiss 3T3 cells compared to Vero cells. Both cell lines were either left untreated or treated with 15 ng/ml of rPMT and collected at different time points: 0, 1, 2, 3, 4, 5, 6 and 8 h. Cell lysates containing a protein concentration of 500 µg/ml were analysed by SDS-PAGE and Western Blotting. Anti-QE antibody was used to detect the total modified Gα subunits.

The Western Blot results show that the modified Gα subunits in Swiss 3T3 and Vero cells can be detected from 2 h post rPMT treatment (Fig 5.1.3). The rPMT-treated Swiss 3T3 cells show an increment in the level of modified Gα subunits from 2 h reaching a clear thick band at 4 h. In Vero cells, on the other hand, a visible faint band of modified Gα subunits is present at 2 h post rPMT-treatment but there was no noticeable huge increment in the level of modified Gα subunits after 4 h compared to rPMT-treated Swiss 3T3 cells. Taken with the results shown in Fig 5.1.2, this shows that modification of Gα

subunits in Vero cells appears to start at the same time, but takes a much longer time to reach a maximum.

All modified Gα subunits were present and their amount remained stable up to a period of 3 days. To determine whether these modified Gα subunits are still present for a longer period of time or undergo degradation by the ubiquitin proteasome degradation system and/or lysosomes, Swiss 3T3 and Vero cells were cultured and treated with rPMT (15 ng/ml) in DMEM without serum for 3 days and media were replaced with DMEM with 1% serum twice a week up to a period of 3 weeks.

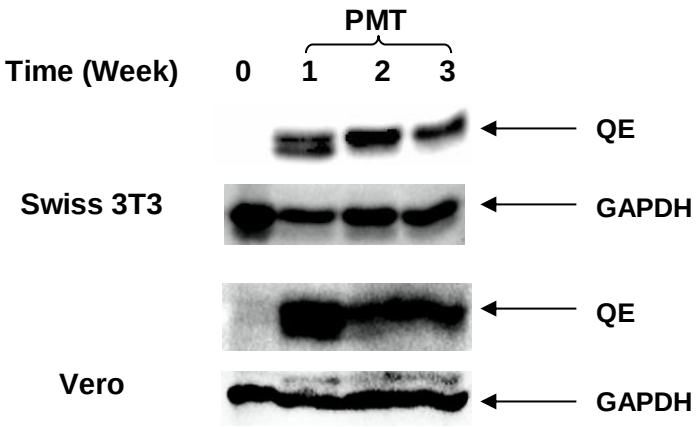

Fig 5.1.4 The stability of the modified Gα subunits in Swiss 3T3 and Vero cells. Both cell lines were either left untreated or treated with 15 ng/ml of rPMT and collected at different time points: 0, 1, 2, and 3 weeks. Cell lysates containing a protein concentration of 600 µg/ml (Swiss 3T3) and 1000 µg/ml (Vero cells) were analysed by SDS-PAGE and Western Blotting. Anti-QE antibody was used to detect the total modified Gα subunits.

The rPMT-modified Gα subunits in Swiss 3T3 and Vero cells were present in different amounts for up to a period of 3 weeks (Fig 5.1.4). In Swiss 3T3 cells, two bands of rPMT-modified Gα subunits were detected on week 1 and the lower band disappeared in weeks 2 and 3. In Vero cells, only a single thick band was detected on week 1 which was then reduced by approximately half in weeks 2 and 3.

In the 3 day experiment (Fig 5.1.2), only a single band of modified Gα subunits was detected from rPMT-treated Swiss 3T3 and Vero cells. Double bands of modified Gα subunits in Swiss 3T3 cells only appeared in week 1 and then disappeared in weeks 2 and 3 (Fig 5.1.4). In rPMT-treated Vero cells, on the other hand, only a single band was detected in the 3-day (Fig 5.1.2) and 3-week experiments but showed a decrease in the level of modified Gα subunits in weeks 2 and 3 (Fig 5.1.4). To determine the time that these double bands start to appear and/or if they disappear and reappear, Swiss 3T3 cells were treated with rPMT in DMEM without serum for 1 week.

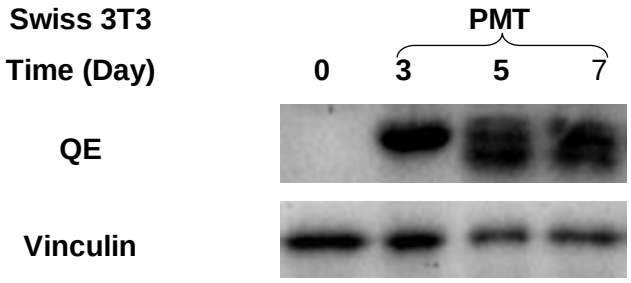

Fig 5.1.5 Detection of double bands from modified Gα subunits in Swiss 3T3 cells. Swiss 3T3 cells were either left untreated or treated with 15 ng/ml of rPMT and collected at different time points: 0, 3, 5, and 7 days. Cell lysates containing a protein concentration of 600 µg/ml were analysed by SDS-PAGE and Western Blotting. Anti-QE antibody was used to detect the total modified Gα subunits.

The Western Blot result shows that double or multiple bands from modified Gα subunits appeared at day 5, and were still present on day 7 (Fig 5.1.5) which is consistent with the long term exposure of Swiss 3T3 cells to rPMT (Fig 5.2.4). A single band was detected in day 3 which also confirms the previous results (Fig 5.2.2).

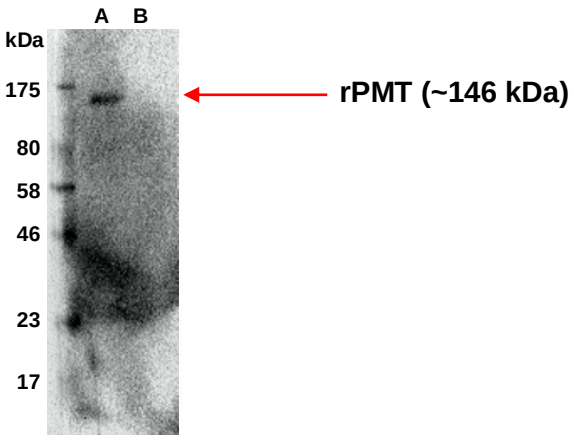

Fig 5.1.6 Attempt to detect PMT using a goat monoclonal anti-PMT antibody. A) 3 µg rPMT B) Swiss 3T3 cell lysate treated with 200 ng/ml of rPMT after day 1.

Since the modified Gα subunits appear to be stable or have a long half-life, I have attempted to detect them in cell lysates but our monoclonal antibody could only show a clear band from 3 µg of rPMT. It is not plausible to treat the cells with very high amount of rPMT as this could leave drastic effects to the cells and possibly may not survive a few days of rPMT treatment as they easily detach to the matrix. A concentration of 200 ng/ml of rPMT which was initially used in the first few experiments already showed severe morphological effects in Swiss 3T3 and Vero cells.

5.2 DISCUSSION

I have confirmed that PMT modifies $G\alpha_{i1\text{-}3}$, $G\alpha_{q/11}$, and $G\alpha_{12/13}$ in both rPMT-treated Swiss 3T3 and Vero cells up to a period of 3 days. However, the modification of most $G\alpha$ subunits in Vero cells was much delayed compared to Swiss 3T3 cells where all modified $G\alpha$ subunits were detected as early as 4 h. The modified $G\alpha_{i\text{-}2}$ and $G\alpha_{11}$ appear to be the first target of PMT in Vero cells which were detected at 4 h while the modified $G\alpha_{12}$ was detected at 48 h and the rest of $G\alpha$ subunits at 16 h.

The cell lysates also confirm the observed differences in the amount of modified $G\alpha$ subunits between the two cell lines (Fig 5.1.2). In particular, the Western Blot result shows a small amount of modified $G\alpha$ subunits at 4 h which possibly were the first target of PMT, $G\alpha_{i\text{-}2}$ and $G\alpha_{11}$ in Vero cells. The increase in the amount of modified $G\alpha$ subunits at 16 h and 48 h coincided with the observed modification of the rest of $G\alpha$ subunits. Swiss 3T3 cells, on the other hand, showed a similar amount of modified $G\alpha$ subunits from 4 h which confirms that all $G\alpha$ subunits were modified at 4 h.

It was initially thought that there might be a delay in the internalisation or translocation of PMT via endosomes in Vero cells due to a delay in the modification of $G\alpha$ subunits. To further understand this phenomenon, it is essential to determine when PMT starts modifying the $G\alpha$ subunits in both

cell lines and the increase in the amount of modified Gα subunits in Vero cells. The Western Blot result shows that the Gα subunits in both cell lines were modified by PMT as early as 2 h but the increase in the amount of modified Gα subunits in Vero cells was gradual compared to Swiss 3T3 cells which shows a huge increment in the amount of modified Gα subunits within 2 – 4 h. Lacerda et al. (1996) reported a lag period of 1 h between PMT treatment and phosphorylation of $p125^{FAK}$ and paxillin, both associated with focal adhesion, which indicates that PMT enters the cell and undergoes processing via an endosomal/lysosomal pathway. It is possible that PMT uses the same entry pathway in Vero cells. However, the low amount of modified Gα subunits detected at early time points in Vero cells may depend on the following factors: 1) the mechanism involved in trafficking, translocating, and activating PMT via endosomal pathway inside the cells, 2) recognition of Gα subunits by PMT (e.g. amino acid sequence of $G\alpha_{12}$), or 3) the presence or amount of cellular proteins that might be involved in the translocation and activation of PMT or modification of Gα subunits.

PMT binds to sphingophospholipid sphingomyelin or phosphatidylcholine with other lipid components (Brothers et al., 2011) and is then trafficked to late endosomes where it is proteolytically activated between pH 5 – 5.5 (Baldwin et al., 2004; Smyth et al., 1995). The required pH (5 – 5.5) for PMT activation was carried out in Swiss 3T3 cells. In viral research, various studies showed that the kinetics of viral release in different cell lines is

dependent on the timing of pH changes in different endosomes (Holtzman, 1976). Rybak and Murphy (1998) reported that the mouse kidney epithelial cells have higher endosomal pH than the mouse fibroblast and cardiac muscle cells, while Murakami et al. (2012) showed that Vero cells have higher endosomal pH than Madin-Darby canine kidney cells. Rybak and Murphy (1998) also mentioned that extended culture of different cell lines may result in the differences in endosomal pH. During PMT transport, the essential recruitment and binding of small GTPase Arf6 to vacuolar ATPases suggests the role of these proteins in intra-endosomal acidification (Repella et al., 2011). Actin and microtubules are also required in trafficking PMT as disruption of these cytoskeletal proteins inhibits the translocation and cytotoxicity of PMT (Repella et al., 2011).

Suzuki et al. (2009) reported that $G\alpha_{12}$ and $G\alpha_{13}$ have a slow rate of nucleotide exchange and GTP hydrolysis. In terms of their GTP-binding kinetics, Zhang et al. (2006) demonstrated that the fusion protein, thromboxane A_2 receptor-$G\alpha_{12}$ responded to agonists slower than the fused thromboxane A_2 receptor-$G\alpha_{13}$ in Spodoptera frugiperda (Sf9) cells. In contrast, purified $G\alpha_{12}$ and $G\alpha_{13}$ did not show any differences in their GTP-binding property *in vitro*. PMT directly activates G-proteins and does not require GPCR. However, the PMT-mediated activation of $G\alpha_{12}$ appears to be slower than $G\alpha_{13}$ in both Swiss 3T3 and Vero cells (Fig 5.1.1), which was similar to the behaviour of fusion proteins, and opposite to the results

generated from the purified $G\alpha_{12}$ and $G\alpha_{13}$. Ligand-GPCR coupling and PMT appears to have the same coupling efficiency to $G\alpha_{12}$ and $G\alpha_{13}$. Such delay in modification may also be due to the missing 20% N-terminal amino acid sequence in $G\alpha_{12}$ which may have a role in protein recognition, protein-protein interaction or other functions as discussed in chapter 4.

In line with the report of Wilson et al. (2000), stress fibre formation in rPMT-treated Vero cells was less prominent than rPMT-treated Swiss 3T3 cells a few hours post PMT treatment (Fig 3.2.2.1). Taken together with the results from the comparative analysis of the amino acid sequences of $G\alpha_{12}$ subunit (Table 4.3-B, and Table A2, Fig A5 in the appendix section), the $G\alpha_{12}$ subunit in green monkey (genus *Chlorocebus*) is 20% shorter than the other $G\alpha_{12}$ isoform in human and mouse (Table A2 in the appendix section). The 20% amino acid sequences missing in $G\alpha_{12}$ subunit situated in the N-terminus in the green monkey may have a role in protein recognition by PMT. It appears that humans, crab-eating macacaque (*Macaca fascicularis*), olive baboon (*Papio Anubis*), and domestic cow (*Bos tauraus*) have $G\alpha_{12}$ isoform similar to the $G\alpha_{12}$ subunit of Green Monkey (Table A2 and Fig A8 in the appendix section). The $G_{q/11}$- and $G_{12/13}$-Rho pathways regulate stress fibre formation in cells. The early cytoskeletal disruption in Vero cells was possibly due to the PMT-induced activation of $G\alpha_{q/11}$ and $G\alpha_{13}$ and later on, actin stress fibre formation became prominent upon modification of $G\alpha_{12}$. The G_{11} subunits in Vero cells were modified in very small quantities at 4 h

while G_q was modified at 16 h. G_{12}, on the other hand, was modified at 48 h. G_{13}, on the other hand, was modified in small quantities at 16 h. However, G_{12} appears to be required in stress fibre formation. It appears that activation of $G_{q/11}$ and $G_{12/13}$ is required for the synergistic effect in full development of stress fibres. Another important event in stress fibre assembly is the activation of Rho kinase and MLCK which leads to phosphorylation of two residues of MLC and actomyosin contractility. The G_q/Ca^{2+}-CaM-dependent MLCK and $G_{12/13}$-Ca^{2+}-independent Rho kinase systems phosphorylate MLC in Ser19 and Thr18 residues where the latter is essential in concert with Ser19 for full contractility (Totsukawa et al., 2000; Pellegrin and Mellor, 2007; Getz et al., 2010; Katoh et al., 2011). According to Tosukawa et al. (2000), MCLK and Rho kinase have distinct roles in stress fibre formation. Rho kinase is involved in stress fibers and focal adhesions while MLCK is involved in microfilament assembly in the cell periphery.

Post-translational modifications of proteins play a major role in cell signalling (as discussed in section 1.5). Palmitoylation and acylation of $G\alpha_{12}$ (Cys^{11}), palmitoylation of $G\alpha_{13}$ (Cys^{14} or Cys^{18}), and acylation of $G\alpha_{13}$ (Cys^{37}) have been implicated to be involved in cell transformation, protein interaction, membrane localisation and stress fibre formation (Ponimaskin et al., 2000; Jones and Gutkind, 1998; Suzuki et al., 2009; Waheed and Jones, 2002). Jones and Gutkind (1998) reported that a nonpalmitoylated constitutively active mutant $G\alpha_{12}$ did not form foci in NIH-3T3 cells. Myristoylation of a constitutively active $G\alpha_{12}$ (Q229L) mutant (due to substitutions: S2G and

R6S), on the other hand, restored its transforming capability with high efficiency. There is no cysteine residue in the N-terminus of the $G\alpha_{12}$ subunit in green monkey while one of the $G\alpha_{12}$ isoforms (~44 kDa) in mouse possesses all the residues for palmitoylation and acylation (Fig A5 in the appendix section). The $G\alpha_{13}$ subunit in both mouse and green monkey, on the other hand, has Cys^{14}, Cys^{18}, and Cys^{37} which are the sites for palmitoylation and acylation (Fig A5 in the appendix section). In the studies involving constitutively active $G\alpha_q$ and $G\alpha_s$ mutants, palmitoylation appears to be required for membrane anchorage in both $G\alpha$ subunits while acylation or the cysteine residues in $G\alpha_q$ are essential for effector interactions. These post-translational modifications appear to be essential for the $G\alpha$ subunits to carry out their normal signalling functions (Wedegaertner et al., 1993; Hepler et al., 1996). The $G\alpha_q$ subunit in mouse and green monkey contains two cysteine residues in the N-terminus, Cys^9 and Cys^{10} (Fig A5 in the appendix section). The lack of cysteine residue or palmitoylation and acylation site in $G\alpha_{12}$ subunit in Vero cells may have contributed to the loss of mitogenic effect of PMT. PMT-induced cell proliferation might require multiple G-protein families (e.g. G_q and $G_{12/13}$) or $G\alpha_{12}$ may antagonise the proliferative effect of PMT-activated $G\alpha_q$ signalling in Vero cells.

The rPMT-modified $G\alpha$ subunits were present up to 3 days. A longer time course experiments up to a period of 1 and 3 weeks were carried out to determine if these modified $G\alpha$ subunits were stable or would undergo

degradation. Results showed that the modified Gα subunits in both cell lines were present up to 3 weeks. However, multiple lower molecular weight bands appeared at days 5 and 7, and disappeared at weeks 2 and 3 in Swiss 3T3 cells. Vero cells, on the other hand, had a thick band in week 1 indicating a high amount of modified Gα subunits, which then decreases in weeks 2 and 3. It was difficult to resolve whether this band consisted of double or multiple bands due to its thickness. Also, it could not be determined if these Gα subunits were stable from the time they were modified or PMT was still stable and actively modifying the Gα subunits up to 3 weeks. The monoclonal anti-PMT antibody could detect ~2 - 3 µg of PMT, a 10 - 15-fold higher than the initial concentration (200 ng/ml) used in this research which caused detrimental effects to both cell lines.

Multiple lower molecular weight bands in the blot are an indicative of protein degradation. Protein degradation may also arise from poor handling; however, all samples were kept on ice while being processed at the same time in lysis buffer containing the same amount of protease inhibitor. This protein degradation most likely happened during the course of 3 weeks in particular 3 days post rPMT treatment in Swiss 3T3 cells. The monoclonal anti-QE antibody is very specific and has strong avidity to the deamidated form of Gα subunits which when used in cell lysate samples did not show any non-specific binding. The disappearance of multiple bands in weeks 2 and 3 may indicate that the proteins involved in the degradation pathway may had been inhibited while the single band on the first 3 days may

indicate that the degradation pathway was inactive possibly due to the activation of the survival pathway. Consistent with the results in the LDH assay, I have shown that PMT protected Swiss 3T3 cells but not Vero cells from cell death, and this anti-apoptotic property was completely abolished at day 4. It would be interesting to determine if the anti-apoptotic property of PMT was activated as the multiple bands disappeared after week 1. Another possible reason for the disappearance of these bands could be due to increased efficiency in degrading proteins with quick turnover (which may also be the case in Vero cells after week 1) or the degradation pathway was shut down due to the detrimental effect of PMT in both cell lines. Wu et al. (2006) reported that the constitutively active $G_{q/11}$ and $G_{12/13}$ inhibit the pro-survival Akt signalling. $G\beta\gamma$ heterodimer is known to stimulate the PI3K/Akt survival signalling. However, $G\alpha_q$ strongly inhibits this pathway with greater efficiency (Lee et al., 1993). In order to counteract such inhibition, $G\beta\gamma$ signalling pathways typically require 10-100 folds of its own concentration than the $G\alpha_q$.

Lastly, both cell lines in the long term (3-week) experiment would have resulted in cell death without the replacement of media containing miminal serum as shown in early experiments (Figs 3.1.1, 3.1.2 and 3.2.1.1). Deregulation of multiple pathways leading to abberant signalling by rPMT-modified $G\alpha$ subunits from 3 of the 4 G-protein families would be detrimental to cell homeostasis.

6 THE ACTIVATION OF G-PROTEIN SIGNALLING PATHWAYS BY PMT

I have shown that all the Gα subtypes that are modified by PMT in Swiss 3T3 and Vero cells are present in differing amounts. Furthermore, the timing of G-protein modification is not the same in the two cell types. The Gα subunits in Swiss 3T3 cells were modified by PMT as early as 4 hours while only the $G\alpha_{i-2}$ and $G\alpha_{11}$ were the first target of PMT and with the $G\alpha_{12}$ being the last. These modified Gα subtypes persisted up to 3 weeks.

These results may have contributed to the differential response of Swiss 3T3 and Vero cells to PMT. I have discussed in previous chapters the possible causes in the delay in stress fibre formation and cell proliferation. The PMT-induced cell proliferation in Swiss 3T3 cells which ceased by day 4, which was also the onset of the plateau growth phase appears to be related to the loss of nutrients and/or growth factors. Although re-treatment with PMT was not carried out in this research, Wilson et al. (2000) reported that the further addition of PMT to PMT-treated Swiss 3T3 cells did not re-initiate the cell cycle. In this chapter, I have investigated whether signalling pathways associated with PMT effects and activation of specific G-proteins related to mitogenesis are active and sustained over a same time period.

6.1 $G_{q/11}$ and Calcium Signalling

$G\alpha_q$ and $G\alpha_{11}$ play a major role in PMT-induced cell proliferation in various cell lines such as Swiss 3T3 cells. Although $G\alpha_q$ and $G\alpha_{11}$ of Vero cells were also modified by PMT, no significant cell proliferation was detected.

Activation of $G\alpha_{q/11}$ by PMT leads stimulation of calcium signalling pathways. $G\alpha_q$ and $G\alpha_{11}$ also activate RhoA, I therefore decided to determine if calcium signalling was also activated and sustained. Cells were either left untreated or treated with 15 ng/ml of PMT, and intracellular calcium level was measured over 3 days.

There was an increase in the intracellular calcium level of rPMT-treated Swiss 3T3 cells over the 3-day period compared to the untreated cells (~3-fold increase from day 0 compared to day 3) while there was no overall significant difference in intracellular calcium level in both untreated and rPMT-treated Vero cells (Fig 6.1).

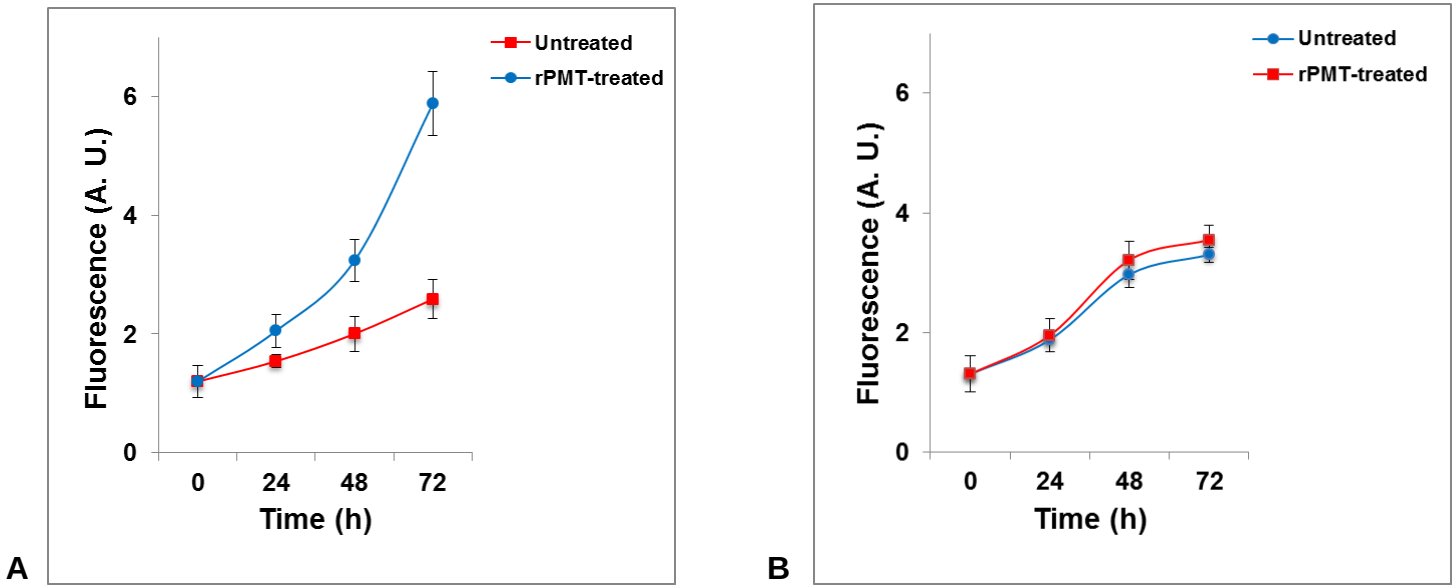

Fig 6.1 $G_{q/11}$ and Calcium Signalling. The PMT-induced activation of $G_{q/11}$-mediated calcium signalling is active and sustained in (A) Swiss 3T3 (*P* = 0.04), but not in (B) Vero cells (*P* = 0.42). Cells were prepared as described in section 2.11. Red (Untreated) and Blue (rPMT-treated, 15 ng/ml). Shown are mean ± SD of a representative calcium level carried out in triplicate.

6.2 G_{i1-3} and cAMP Signalling

The $G\alpha_i$ family is a negative regulator of the G_s family. G_i proteins play a role in the depression of AC activity which results in a decrease of cAMP levels. AC is an important intracellular signalling molecule that mediates cell proliferation via G_s. PMT, however, does not activate G_s. Reports also shows that the G_i family is involved in DNA synthesis and cell proliferation (Van Corven et al., 1989; LaMorte et al., 1999).

Since G_{i1-3} was modified by PMT in both cell lines, it was important that to determine if G_{i1-3} signalling was also activated and sustained. Cells were either left untreated or treated with 15 ng/ml of PMT, and the cAMP level in the cytosol was measured over 3 days. Since PMT does not activate G_s, forskolin was used to activate AC.

There was a decrease in the cAMP level in both PMT-treated cell lines, with a greater decrease in Swiss 3T3 cells in day 1 than Vero cells (Fig 6.2). It appears that forskolin did not sustain activation of G_s with a small decrease in cAMP levels on day 2, and no increase or decrease in cAMP levels at day 3.

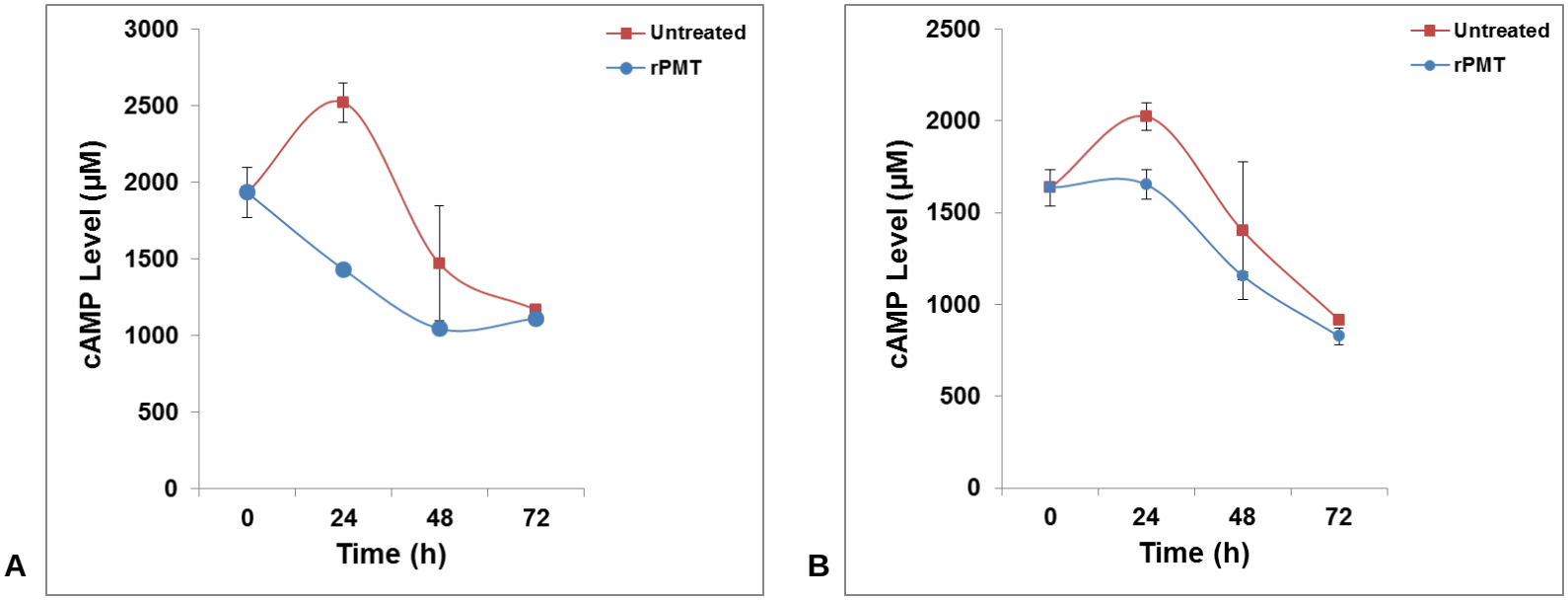

Fig 6.2 $G_{i1\text{-}3}$ and cAMP Signalling. The PMT-induced activation of $G_{i1\text{-}3}$ and depression of AC-cAMP signalling in A) Swiss 3T3 and B) Vero cells. Shown above are the time courses on the effect of rPMT in forskolin stimulated cAMP level in (A) Swiss 3T3 (P = 0.28) and (B) Vero (P = 0.41) cells, prepared as described in section 2.12. Red (Untreated) and Blue (rPMT-treated, 15 ng/ml). Shown are mean ± SD of a representative cAMP level carried out in triplicate.

6.3 $G_{12/13}$ and the Small GTPases: RhoA, Rac1, Cdc42

The 18 members of the mammalian Rho Small GTPases family have around ~50 – 90% sequence similarity (Karnoub and Der, 2000). RhoA, Rac1 and Cdc42 are the most well studied and the best described Rho GTPase members (Karnoub and Der, 2000).

The PMT-activated $G\alpha_{q/11}$ and $G\alpha_{12/13}$ subunits stimulate the Rho-ROCK signalling pathway, which leads to cytoskeletal reorganisation in various cell lines (Wilson and Ho, 2011; Orth et al., 2005; Harmey et al., 2004; Wilson et al., 2000; Dudet et al., 1996; Lacerda et al., 1996). Many reports also showed that these heterotrimeric G-proteins are involved in the induction of apoptosis in various cell lines via RhoA-induced reduction or inhibition of Akt phosphorylation (Wu et al., 2006; Ueda et al, 2004; Chikumi et al, 2002; Ueda et al., 2001; Althoefer et al., 1997), while Rac and Cdc42 are involved in cell polarisation, cell-cell and cell-substratum adhesion and regulation of cytoskeleton.

It was important to determine whether RhoA, Cdc42 and Rac1 were similarly activated in both PMT-treated cell lines. Cells were either left untreated or treated with 15 ng/ml of PMT, and the GTP-bound RhoA, Cdc42 and Rac1 were pulled down using Rhotekin RBD or PAK PBD agarose bead slurry (as

described in section 2.11 of chapter 2) and were analysed by SDS-PAGE and Western Blotting.

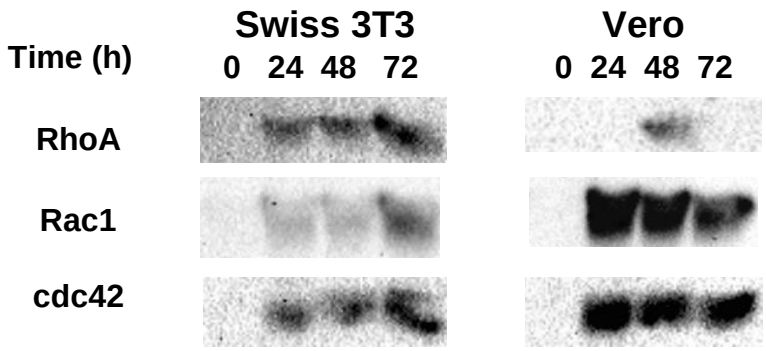

Fig 6.3 The PMT-induced activation of RhoA, Rac1, and Cdc42 in Swiss 3T3 and Vero cells. Both cell lines were either left untreated or treated with 15 ng/ml of rPMT and collected at different time points: 0, 24, 48, and 72 h. Shown are representative Western blot of GTP-bound RhoA, Rac1 and Cdc42 from rPMT-treated confluent Swiss 3T3 (left panels) and Vero (right panels) cells, prepared as described in section 2.11 of chapter 2. The mouse monoclonal anti-RhoA, anti-Rac1, and anti-Cdc42 were used to detect the pulled-down GTP-bound RhoGTPases.

PMT activated RhoA, Rac1, and Cdc42 in both PMT-treated cell lines, while the untreated cells did not show any detectable GTP-bound RhoA, Rac1 and Cdc42 (Fig 6.3). In terms of protein content, there was more activated RhoA in Swiss 3T3 cells than Vero cells. The amount of the GTP-bound RhoA also appeared to increase over time. The amount of GTP-bound RhoA could not be detected at either 24- or 72-hr PMT-treated Vero cells. Although careful handling and processing of the samples were carried out (e.g. keeping the samples on ice), it is known that GTP is quickly hydrolysed to GDP on small

GTPases. Vero cells contained more GTP-bound Cdc42 and Rac1 than Swiss 3T3 cells, while Swiss 3T3 cells showed more GTP-bound RhoA than Vero cells. The amount of both GTP-bound Rac1 and Cdc42 in Swiss 3T3 cells increased over time, while in Vero cells, the amount of GTP-bound Rac1 decreased. The GTP-bound Cdc42 in Vero cells, on the other hand, remained almost similar over the 3-day experimental period.

In general, morphological effects were the same regardless of the concentration of PMT (=/>1 ng/ml) used in treating the cells. However, the progression of these effects in particular the detachment of cells appears to be concentration-dependent but the addition of 1% serum attenuated this effect.

6.4 DISCUSSION

I have shown that PMT modifies $G\alpha_{q/11}$, $G\alpha_{12/13}$, and $G\alpha_{i1\text{-}3}$ at different times in the two cell types (section 5.1 in chapter 5). Although PMT modified the same set of G-proteins in both cell types, no significant increase in cell number was detected in Vero cells. It was therefore important to examine whether the signalling pathways downstream of the activated G-proteins was activated similarly in two cell types, over a 3-day period which could explain the different response of the cells to PMT.

The G_q-mediated calcium mobilisation in rPMT-treated Swiss 3T3 cells appeared to be active and sustained over a 3-day period, while no significant difference in intracellular calcium level was observed in Vero cells. There are several possible reasons why activated G_q in Vero cells fails to mobilise calcium. RGS2 and RGS4 are known to inhibit G_q signalling by attenuating a response or accelerating GTP hydrolysis to terminate the signal (Heximer et al., 1999). IP_3 receptors (IP_3R) possess the IP3 binding core, and suppressor domains in the N-terminus with the latter domain harbouring seven conserved amino acid residues in IP_3R1 (Leu^{30}, Leu^{32}, Val^{33}, Asp^{34}, Arg^{36}, Arg^{54}, and Lys^{127}) responsible for the suppression of IP_3 binding (Bosanac et al. 2005) while a deletion of this domain results in an enhanced IP_3 binding (Yoshikawa et al., 1996; 1999). These conserved amino acid residues are all present in the 8 isoforms of IP_3R1 found in human and mouse (see Fig A9 in the appendix section). It is possible that the

suppressor domain is the dominant domain which could inhibit intracellular Ca^{2+} mobilisation in Vero cells.

RACK1 (Receptors for Activated C-Kinase-1), a substrate of src, acts as a scaffold protein and binds to phosphorylated PKC and IP_3R to enhance its binding affinity to IP_3 (Patterson et al., 2004; Birikh et al., 2003). It has ~50% amino acid homology with Gβ subunit and seven WD40 repeats which present multiple protein-binding sites. RACK1 inhibits src tyrosine kinase activity, cell proliferation of NIH-3T3 and anchorage-independent growth of v-Src transformed cells (Chang et al., 2002; Mamidipudi et al., 2004). PKC and src are known to be stimulated by PMT via $G_{q/11}$. It is possible that RACK1 also inhibits proliferation in rPMT-treated Vero cells although there is no evidence yet that RACK plays a role in any PMT-treated cell lines.

G_q is known to either promote apoptosis or activate the PI3K/Akt survival signalling pathway in different cell lines (as discussed in section 1.6.1), and this may be relevant to the different responses elicited by PMT treatment in the two cell types. I have shown that PMT protected Swiss 3T3 cells from cell death, which was detected on day 2, but this phenomenon was not observed in Vero cells. It would be interesting to see if G_q signalling is still active and sustained in Swiss 3T3 cells after day 3, as the anti-cell death property of PMT was abolished by day 4. The failure to detect signalling downstream of G_q in rPMT-treated Vero cells, on the other hand, confirms that PMT is not cytotoxic in this cell line.

Ca^{2+}-CaM is important for the activation of MLCK and phosphorylation of Ser^{19} of MLC, while activation of Rho kinase leads to MLC phosphorylation of Thr^{18} (Getz et al., 2010). MLC can also be phosphorylated on Ser^{19} by Rho kinase (Amano et al., 1996). MLC phosphorylation and actomyosin contractility were possibly dependent on the $G_{12/13}$ Rho kinase pathway alone in Vero cells as the cytosolic free Ca^{2+} was not elevated and modification of G_{12} was delayed in rPMT-treated Vero cells compared to Swiss 3T3 cells. This could possibly contribute to the delay in stress fibre formation in Vero cells.

Some members of the G_i family are involved in mitogenesis e.g. $G\alpha_{i-2}$ subunit inhibited the serum-stimulated DNA synthesis in mouse Balb/c3T3 fibroblasts (LaMorte et al., 1999), while G_i inhibited the LPA-induced mitogenic activity (Van Corven et al., 1989). The forskolin-stimulated cAMP level decreased over time. It could not be determined if $G\alpha_i$ was active up to 3 days as the forskolin-stimulated cAMP level decreased and could not be detected in both either untreated or rPMT-treated cell lines on day 3. It is possible that other cellular proteins may inhibit AC activity due to the activation of multiple G-proteins or the G-protein-mediated deregulation of different signalling pathways.

According to Taussig et al. (1994), $G\alpha_s$- and forskolin-stimulated AC1, but not CaM-stimulated AC1 is weakly inhibited or not inhibited at all by $G\alpha_{i1-3}$, $G\alpha_z$, or $G\alpha_o$. $G\alpha_{i1-3}$ and $G\alpha_z$ effectively inhibit AC 5 and 6 while other AC isoforms are insensitive to the G_i family (Chen-Goodspeed et al., 2005;

Sadana and Dessaeur, 2009). The Gβγ heterodimer, on the other hand, can either stimulate or inhibit different AC isoforms (Sadana and Dessaeur, 2009). It inhibits AC isoforms 1, 3 and 8 (Tang and Gilman, 1991; Steiner et al., 2006). Inhibition of AC1 by Gβγ is more potent than the inhibitory effect of the $G\alpha_i$ subunit, while Gβγ negates the stimulatory effect of G_s in AC1 and AC8 in HEK293 cells (Nielsen et al., 1996). The G_s stimulatory effect is in synergy with Ca^{2+}/CAM in AC1 only, but not in AC8. Since forskolin was used to directly activate AC in this research, it is possible that the Gβγ heterodimer upon dissociation from Gα subunits inhibited AC activity which resulted in a low cAMP level over a period of 2 days and the non-detectable cAMP level in serum-starved untreated or rPMT-treated Vero cells in day 3. G-proteins may have activated the survival pathway in the serum-starved untreated cells. The G_i pathway is predicted to regulate the PI3K/Akt survival pathway (Huang et al., 2004) and it is likely that the synergistic effect of both Gi and Gβγ is enough to suppress the AC activity/cAMP level.

The small GTP-binding proteins: RhoA, Rac1, and Cdc42 regulate cell shape changes via remodelling of the cytoskeleton and the effects on cell adhesion (Wojciak-Stothard and Ridley, 2003). RhoA is a well-studied protein that PMT activates via $G_{q/11}$ and $G_{12/13}$ (Orth et al., 2005). RhoA mediates stress fibre formation, which is one of the many effects of PMT in different cell lines. Swiss 3T3 cells contained more GTP-bound RhoA than Vero cells. It appears that the active RhoA was present from days 1 – 3 in

rPMT-treated Swiss 3T3 cells, while in Vero cells, it was detected at day 2 and disappeared by day 3. Extreme care was applied during experiment (as per manufacturer's instruction, e.g. keeping the samples on ice); however, it is known that GTP is quickly hydrolysed to GDP (Cell Biolabs, 2015). It may be that the active RhoA was degraded and/or quickly hydrolysed by day 3 or the small amount of protein could not be detected by the anti-RhoA antibody. Members of the Rho subfamily are all involved in stress fibre formation, contractility and focal adhesions. However, only RhoA and RhoC are known to be involved in cell proliferation, while RhoB negatively regulates this effect (Berenjeno et al., 2007; Howe and Addison, 2012; Tseliou et al., 2016). Degradation of RhoA could also possibly delay stress fibre formation and attenuate the proliferative effect of PMT in Vero cells. The role of this protein and other members of the Rho subfamily e.g. RhoB needs to be explored in greater detail.

Vero cells contained more GTP-bound Cdc42 and Rac1 than Swiss 3T3 cells. The amount of GTP-bound Rac1 and GTP-bound Cdc42 in Swiss 3T3 cells appeared to increase over time while in Vero cells; the amount of GTP-bound Rac1 decreased and GTP-bound Cdc42 remained almost similar over the 3-day period. Activation of Rac1 and Cdc42 by PMT has not been investigated in detail before. Recently, PMT was shown to stimulate Rac1 and RhoA in neonatal rat cardiac fibroblasts which led to an increased secretion and expression of CTGF and pathologic remodelling of the cells (Weise et al., 2015). In endothelial cells, cell elongation is dependent on

Cdc42 and Rac1 (Wojciak-Stothard and Ridley, 2003). I have shown that the assembly of stress fibres accompanied the development of stretch-induced orientation or elongated phenotype of both rPMT-treated cell lines. Such phenomenon may be dependent on the activation of Cdc42 and Rac1. Various reports showed that Cdc42 and Rac1 can be activated via G_q, $G_{12/13,}$ G_i and the $G\alpha_i$-released $\beta\gamma$ complex (Tolkacheva et al., 1997; Ueda et al., 2000; Gratacap et al., 2001; Zeng at al., 2002a-b; Gonzales et al., 2003, Niu et al., 2003; Sabbatini et al., 2010).

I found an increased cell-cell detachment with the formation of foci or clumping of cells in rPMT-treated Swiss 3T3 and Vero cells, but this phenomenon was more prominent in the latter cell line at a very late stage of PMT treatment (see section 3.3.2). Cell-cell contacts are mediated by different adhesion molecules and their interacting partners which are regulated by the Rho GTPase family (Kaibuchi et al., 1999). Rho, Rac and Cdc42 play important roles in regulating cell-cell adhesions such as the tight and adherens junctions. Various studies have shown that Rho, Rac and Cdc42 are required in the association of α-/β-catenin, cadherin, and actin filaments in cadherin-mediated cell-cell adhesion (Kuroda et al., 1997; Braga et al., 1997; Takaishi et al., 1997). PMT is known to downregulate Wnt/β-catenin signalling and Notch1 level leading to inhibition of adipogenesis, but with a high level of β-catenin (Aminova and Wilson, 2007). Assuming that all the important adhesion molecules are present in both cell lines, however, cadherins require calcium for their cell adhesive activity or cell–cell adhesion

function (Vania et al., 1997). As discussed previously, calcium signalling was not observed in Vero cells, hence, prominent cell detachment was observed. The loss of adhesion in Swiss 3T3 cells, on the other hand, was not as prominent as Vero cells. This may be due to the synergistic effect of both $G_{q/11}$-Ca^{2+} and $G_{12/13}$ pathways which regulate GTPases activity. The prominent loss of cell adhesion in Vero cells at a later stage may have resulted in the decreasing level of Rac1 and Cdc42. Also, it s uknown if these GTPases and $G_{q/11}$-Ca^{2+} signalling are sustained and active after 3 days of rPMT treatment in both cell lines.

7 GENERAL DISCUSSION and FUTURE WORK

7.1 GENERAL DISCUSSION

PMT is a known potent mitogen in various cell lines, which causes havoc in cell homeostasis via deregulation of multiple signalling pathways. PMT targets the Gα subunits of 3 of the 4 families of G-proteins: G_q, G_{12}, and G_i via a process called deamidation which leads to their constitutively active state. G-proteins are important intracellular molecular switches that convert messages from extracellular stimuli to intracellular signalling, leading to multiple biochemical responses. G-proteins are involved in the regulation of almost every aspect of cell metabolism and homeostasis.

According to various reports, treatment of various cell lines with PMT leads to a plethora of downstream signalling, such as activation of protein kinase C, calcium signalling, activation of Rho GTPases, stimulation of β-catenin signalling and depression of cyclic AMP levels. In many cell types such as Swiss 3T3 cells, stimulation of signalling by PMT leads to a mitogenic response and cytoskeletal rearrangements while in others such as Vero cells, PMT induces a cytotoxic phenotype with no evidence of mitogenicity.

In this research, I have found new effects of PMT in both Swiss 3T3 and Vero cells which had not been reported previously. I have confirmed that

PMT treatment resulted in cytoskeletal reorganisation and cell proliferation in Swiss 3T3 cells while in Vero cells, cytoskeletal reorganisation was observed with no sign of significant change in cell number when compared to their untreated and PMT^{C1165S}-treated counterpart. Most of the experimental condition set in proliferation assays in various research involved maintaining the untreated and rPMT-treated cells in media with serum. In this research, I determined the effects of PMT in both cell lines in the absence of serum. PMT (15 ng/ml) and 10% NCS stimulated cell proliferation in a strikingly similar fashion in Swiss 3T3 cells but no proliferative effect was observed in Vero cells. I observed that the loss of nutrients and/or serum over an extended period of time compromised the ability of PMT to induce its mitogenic effect in Swiss 3T3 cells. The PMT-induced activation of G_q is known to activate different pathways such as ERK1/2, JNK, mTORC1, and JAK-STAT leading to mitogenesis. The absence of a calcium signalling, which is a secondary messenger via G_q, in rPMT-treated Vero cells can partly explain the non-proliferative effect of PMT.

Regardless of the concentration (low or high) of PMT used in treating both cell lines, both cell types showed signs of loss of adherence, formation of foci or dense cell clusters and became fragile at a later stage of the treatment but this phenomenon was more prominent in Vero cells than in Swiss 3T3 cells. The loss of adherence appeared to be circumvented by a fresh supply of nutrients and/or a minimal amount of serum, while foci

formation was not entirely avoided. The nutrients and/or serum possibly helped in maintaining the integrity of the cell and led to cell proliferation as the cells rolled up and developed foci. However, the presence of nutrients/serum and PMT appeared to mask the proliferative effect of the other in Swiss 3T3 cells.

The Rho subfamily members, RhoA, Rac1, and Cdc42 were all activated by PMT via $G_{12/13}$ and possibly $G_{q/11}$, G_i or $G\beta\gamma$ in both cell types (Tolkacheva et al., 1997; Ueda et al., 2000; Gratacap et al., 2001; Zeng at al., 2002a-b; Gonzalez et al., 2003, Niu et al., 2003; Sabbatini et al., 2010). The RhoA/Rac1/Cdc42-mediated cell adhesion is known to be regulated by two pathways - $G_{q/11}$ and $G_{12/13}$ in both cell types. Cell adhesion in Vero cells possibly depended solely on $G_{12/13}$ signalling pathway since this cell line is devoid of calcium signalling. Cadherin, which is an important cell adhesion molecule, requires intracellular calcium via $G_{q/11}$ in its cell adhesive function (Vania et al., 1997). The synergistic adhesive effect via $G_{q/11}$ and $G_{12/13}$ in Swiss 3T3 cells, on the other hand, may have circumvented the full loss of adhesion as RhoA, Rac1 and Cdc42 and calcium signalling are present. A milder loss of cell adhesion at later stage may have resulted due to the decrease in the level of Rac1 and Cdc42. Also, it is unknown if the $G_{q/11}$-Ca^{2+} signalling, RhoA, Rac1 and Cdc42 are present after 3 days post rPMT treatment since detachment was observed after this period in both cell lines. The amount of G-proteins in each cell line varies. It appears that Swiss 3T3 cells have more G-proteins than Vero cells with the exception of G_{i-1}, which

appears to be at reduced level compared to other G_i proteins (this work and Babb et al., 2012). PMT modified the different Gα subunits in Swiss 3T3 and Vero cells at different times and these modified G-proteins were present up to a period of 3 weeks after initial PMT exposure. However, the modification of most Gα subunits by PMT in Vero cells was much delayed compared to Swiss 3T3 cells. $G\alpha_{i\text{-}2}$ and $G\alpha_{11}$ subunits were the first target of PMT in Vero cells which were detected at 4 h. The modified $G\alpha_{12}$ was detected at 48 h, while the rest of Gα subunits were detected at 16 h post rPMT-treatment. The modified Gα subunits in Swiss 3T3 cells, on the other hand, were detected as early as 4 h. Analysis of cell lysates prepared from these cells confirmed the observed differences in the amount of modified Gα subunits between the two cell lines, i.e. Vero cells have lower amount of modified Gα subunits than Swiss 3T3 cells at 4 h post rPMT treatment.

Both rPMT-treated Swiss 3T3 and Vero cells formed stress fibres. However, I have shown that Vero cells developed stress fibre at slower pace than Swiss 3T3 cells. The appearance of the advanced form of stress fibres accompanied the development of the stretch-induced orientation or fibroblastic feature of both rPMT-treated cell lines. $G_{q/11}$- and $G_{12/13}$-Rho pathways regulate stress fibre formation. The two important events leading to stress fibre formation downstream of the $G_{q/11}$- and $G_{12/13}$-Rho pathways are the phosphorylation of MLC and actomyosin contractility. G_q/Ca^{2+}-CaM-dependent MLCK and $G_{12/13}$-Ca^{2+}-independent Rho kinase systems lead to

MLC phosphorylation of Ser^{19} and Thr^{18} (Totsukawa et al., 2000; Pellegrin and Mellor, 2007; Getz et al., 2010; Katoh et al., 2011). The absence of intracellular free Ca^{2+} via $G_{q/11}$ in rPMT-treated Vero cells may have contributed to the delay in stress fibre formation as MLC phosphorylation was dependent solely on the $G_{12/13}$ Rho kinase pathway. The delay in the modification of $G\alpha_{12}$ in rPMT-treated Vero cells explains the slow development of stress fibres. Such delay appears to be linked to its protein sequence and possibly molecular structure. The $G\alpha_{12}$ in Vero cells lacks 20% of the N-terminus found in the $G\alpha_{12}$ isoform of other species. The missing 20% N-terminal amino acid sequence in G_{12} of Vero cells may have a role in protein recognition, protein-protein interaction or other function. Amino acid analysis also revealed that the N-terminus of $G\alpha_{12}$ lacks the cysteine residue (Cys^{11}) that is required for acylation and palmitoylation, both of which are essential for cell transformation, protein interaction, membrane localisation or stress fibre formation (Ponimaskin et al., 2000; Jones and Gutkind, 1998; Suzuki et al., 2009; Waheed and Jones, 2002).

I also have shown that PMT is not apoptotic to either Swiss 3T3 or Vero cells. PMT at concentration of 1 and 10 ng/ml exerted anti-apoptotic property in Swiss 3T3 cells up to day 2 while a concentration of 0.1 ng/ml partially protected Swiss 3T3 cells from cell death. The anti-apoptotic effect of PMT in Swiss 3T3 cells was abolished by day 4. This PMT-mediated anti-apoptotic effect, on the other hand, was not observed in Vero cells. Cell death in Vero cells appears to be linked to the absence of serum. The

appearance of multiple bands in both the 1- and 3-week experiments was a sign of protein degradation of Gα subunits in Swiss 3T3 cells on days 5 - 7 which coincides with the loss of the anti-apoptotic property of PMT. All the Gα subunits are involved in resisting or stimulating apoptosis which appear to be cell-type specific and the proteins involved in the signalling pathway (Yanamadala et al., 2009). The Gα subunits that were being degraded may possibly be involved in the survival and mitogenic pathways in Swiss 3T3 cells.

The development of the above effects appears to be PMT dose-dependent. The rate of cellular response is directly proportional to concentration of PMT, meaning the higher the concentration of PMT used, the faster the appearance of the above effects. The activation of the downstream signalling via different G-proteins appears to be required for the synergistic effects of PMT in cell proliferation and immediate cytoskeletal reorganisation.

In summary, the differences in G-protein profile and their downstream signalling in Swiss 3T3 and Vero cells reflect the differential cell response to PMT.

7.2 FUTURE WORK

The heterotrimeric G-proteins are important intracellular signalling molecules. They are targets of various bacterial toxins which lead to the deregulation of the host's signalling system. The alteration in their normal signalling behaviour leads to various effects which affect their phenotype and normal function in maintaining cellular homoestasis.

In this research, I explored the different effects of PMT in greater detail and determined the cause of differential response of Swiss 3T3 and Vero cells to PMT. Activation of 3 of the 4 families of G-proteins by PMT lead to cell proliferation, cytoskeletal reorganisation, survival, and loss of adherence. However, the work reported in this thesis opens up several lines of further investigation.

The PMT-stimulated mitogenesis in Swiss 3T3 cells, delay in stress fibre formation and loss of adherence in Swiss 3T3 and Vero cells are possibly mediated by two G-protein families, G_q and G_{12}. The calcium signalling and the cysteine residue (Cys^{11}) in $G\alpha_{12}$ which is essential in acylation and palmitoylation for its transforming activity are both absent in Vero cells but are present in Swiss 3T3 cells. The missing 20% N-terminal amino acid sequences and the absence of cysteine residue (Cys^{11}) in $G\alpha_{12}$ may possibly have a role in membrane localisation, protein-protein interaction

and/or protein recognition and modification of the $G\alpha_{12}$ subunit by PMT. To determine the role of the missing amino acid sequences and cysteine residue in cell proliferation and stress fibre formation, expression of the long G_{12} isoform (similar to the 44 kDa G_{12} isoform in Swiss 3T3 cells) which contains the important cysteine residue in Vero cells will determine whether this missing sequence has a role in cell proliferation and early modification by PMT which may lead to the early development of full stress fibres.

The absence of calcium signalling may possibly have affected the cell-cell adhesion in Vero cells as cadherin, an adhesive protein, is dependent on calcium for its adhesive activity. RhoA, Rac1 and Cdc42 are required in the association of α-/β-catenin, cadherin, and actin filaments in cadherin-mediated cell-cell adhesion. I have shown the diminishing level of RhoA and Rac1 in Vero cells, which may explain the prominent loss of adhesion in Vero cells. The low but increasing amount of RhoA, Rac1 and Cdc42 in Swiss 3T3 cells over a period of 3 days may have played a role in keeping cell-cell adhesion thereby leading to slight detachment of cells. However, it is unknown whether RhoA, Rac1 and Cdc42 and calcium signalling are present after 3 days post PMT treatment in Swiss 3T3 cells. Both cell lines showed detachment after this period. A further analysis of the presence of RhoA, Rac1 and Cdc42 in both cell lines needs to be carried out in both cell lines. The continuous activation of calcium signalling in Swiss 3T3 cells after 3 days also needs to be determined. It would also be interesting to know if the absence of calcium would lead to prominent loss of adhesion in Swiss

3T3 cells. Thapsigargin, a non-competitive inhibitor of endoplasmic reticulum (ER) Ca^{2+} ATPase, which inhibits calcium release from the ER store may be used to explore the effect of the absence of calcium in cell adhesion and stress fibre formation in Swiss 3T3 cells. Ionomycin, an ionophore, which stimulate calcium flux from the ER may help determine if the presence of intracellular calcium will inhibit or attenuate the loss of adhesion, stimulate stress fibres assembly via G_q-Ca^{2+}-dependent phosphorylation of MLC and cell proliferation in PMT-treated Vero cells. The source of inhibition of calcium signalling pathway is unknown and should be explored. As discussed previously, proteins such as RGS2, RGS4, RACK1 and the suppressor domain in IP_3 receptors are possible inhibitors of the calcium signalling. Inhibition of these proteins and suppressor domain of IP_3 receptors by knocking them down may shed light if they mediate suppression of calcium signalling.

The loss of PMT-mediated anti-cell death effect, loss of adhesion and cessation of cell proliferation in Swiss 3T3 cells on day 4 appears to coincide with the degradation of G-protein observed on days 5 - 7. Although it appears that cessation of cell proliferation appears to be partially linked to the loss of nutrients and/or serum, I have not determined whether each specific PMT-modified $G\alpha$ subunit and the downstream signalling involved in all PMT effects are still present or active after 3 days. I have shown that the PMT-modified $G\alpha$ subunits in cell lysates are present up to a period of 3 weeks. It will also be interesting to know if PMT actively modifies $G\alpha$

subunits up to a period of 3 weeks. A monoclonal antibody with great avidity to PMT is needed to detect PMT molecules. Mass spectrophotometry may also be used as this technique can detect even the tiniest amount of specific molecule in the sample.

Since G-protein degradation was detected on day 5, it is possible to determine which specific PMT-modified Gα subunit disappeared after day 3 using the approach carried out in this research (immunoprecipitation). An anti-ubiquitin antibody can also be used to determine if the Gα subunits are targeted for degradation via the ubiquitin-proteasome degradation system. The PMT-induced G-protein signalling events also need to be determined if they are still active up to a period in which the modified Gα subunits are still present in both cell lines. It will also be interesting to see if changing of fresh media with nutrients and minimal amount of serum in PMT-treated cells will help PMT to promote cell proliferation for a longer period of time. Wilson et al. (2000) showed an increasing number of cells in confluent PMT-treated Swiss 3T3 cells maintained in fresh media with nutrients and serum up to 7 days.

Different Gα subunits were modified by PMT at different time in the two cell lines, with a delay in the modification of most Gα subunits in Vero cells. Due to this, a hyphothesis about a difference in trafficking the PMT to the cytosol in different cell types was proposed. As discussed in section 5.2 of chapter 5, actin, microtubules and Arf6 recruitment are important in trafficking and

translocation of PMT via endosomes inside the cells. Vero cells may have higher endosomal pH than Swiss 3T3 cells. A precise assessment of late endosomal pH in both cell lines, in particular Vero cells is needed to better understand the mechanism of PMT translocation and the early activity of the toxin.

Lastly, the specific role of each G-protein has not been fully explored in Vero cells. These G-proteins could be knocked down or inhibited to understand their role in stress fibre formation, adhesion, survival, cell death and cell proliferation in the two cell lines.

The above further studies suggested in this research will further explain how PMT-induced G-protein activation results in specific biochemical response in the two cell types. They will also further our understanding of G-protein signalling in different systems and the mechanisms by which many bacterial toxins deregulate signalling pathways and cause diseases.

8 APPENDIX

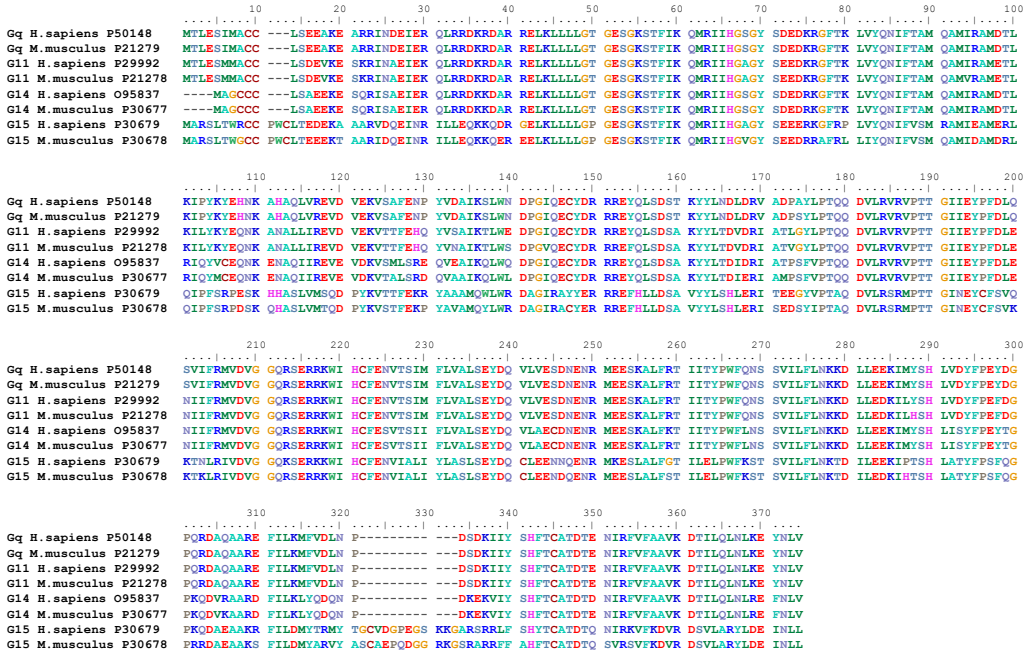

Fig A1 The Complete Aligned Protein Sequences of $G\alpha_{q/11}$ Family Members of *H. sapiens*, and *M. musculus*. Each Gα subtype bears the protein identifier after the name of species.

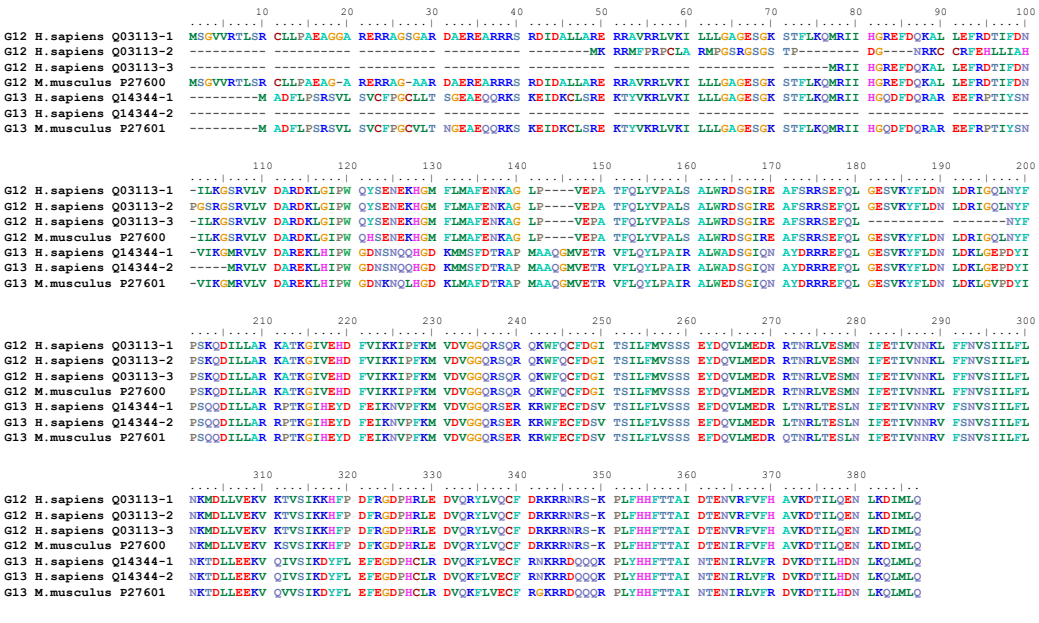

Fig A2 The Complete Aligned Protein Sequences of $G\alpha_{12/13}$ Family Members of *H. sapiens*, and *M. musculus*. Each Gα subtype bears the protein identifier after the name of species.

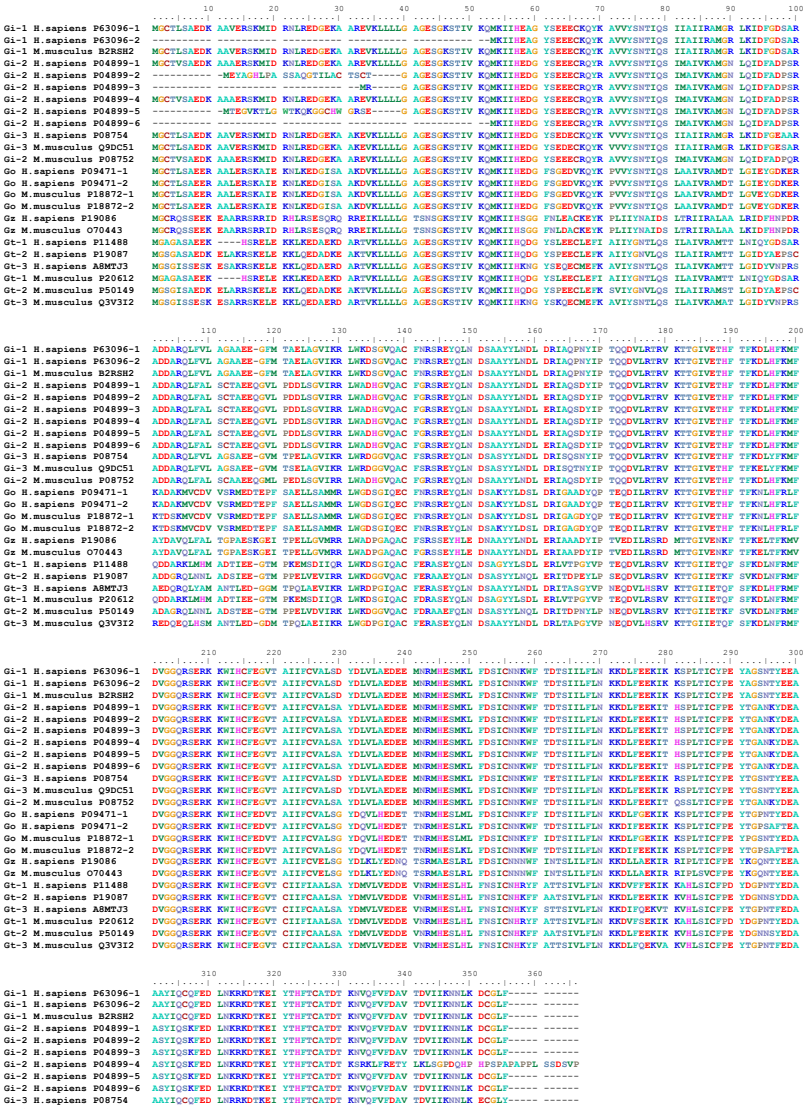

Fig A3 The Complete Aligned Protein Sequences of G$\alpha_{i/o}$ Family Members of *H. sapiens*, and *M. musculus*. Each Gα subtype bears the protein identifier after the name of species.

Fig A4 The Complete Aligned Protein Sequences of G$\alpha_{s/olf}$ Family Members of *H. sapiens*, and *M. musculus*. Each Gα subtype bears the protein identifier after the name of species.

Fig A4 (con'd)

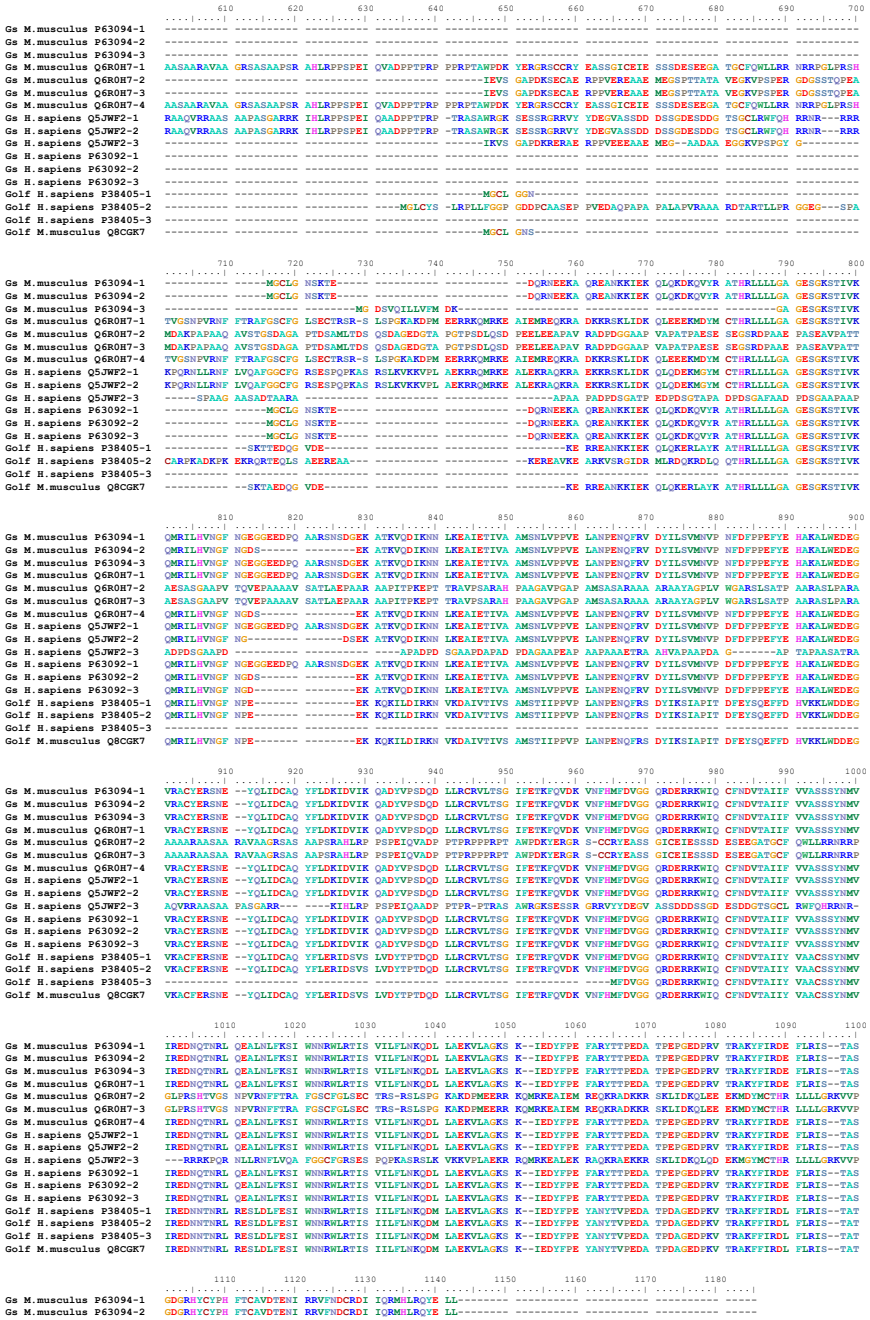
Gs M.musculus P63094-1
Gs M.musculus P63094-2
Gs M.musculus P63094-3
Gs M.musculus Q6RHT7-1
Gs M.musculus Q6RHT7-2
Gs M.musculus Q6RHT7-3
Gs M.musculus Q6RHT7-4
Gs H.sapiens Q5JWF2-1
Gs H.sapiens Q5JWF2-2
Gs H.sapiens Q5JWF2-3
Gs H.sapiens P63092-1
Gs H.sapiens P63092-2
Gs H.sapiens P63092-3
Golf H.sapiens P38405-1
Golf H.sapiens P38405-2
Golf H.sapiens P38405-3
Golf M.musculus Q8CGK7

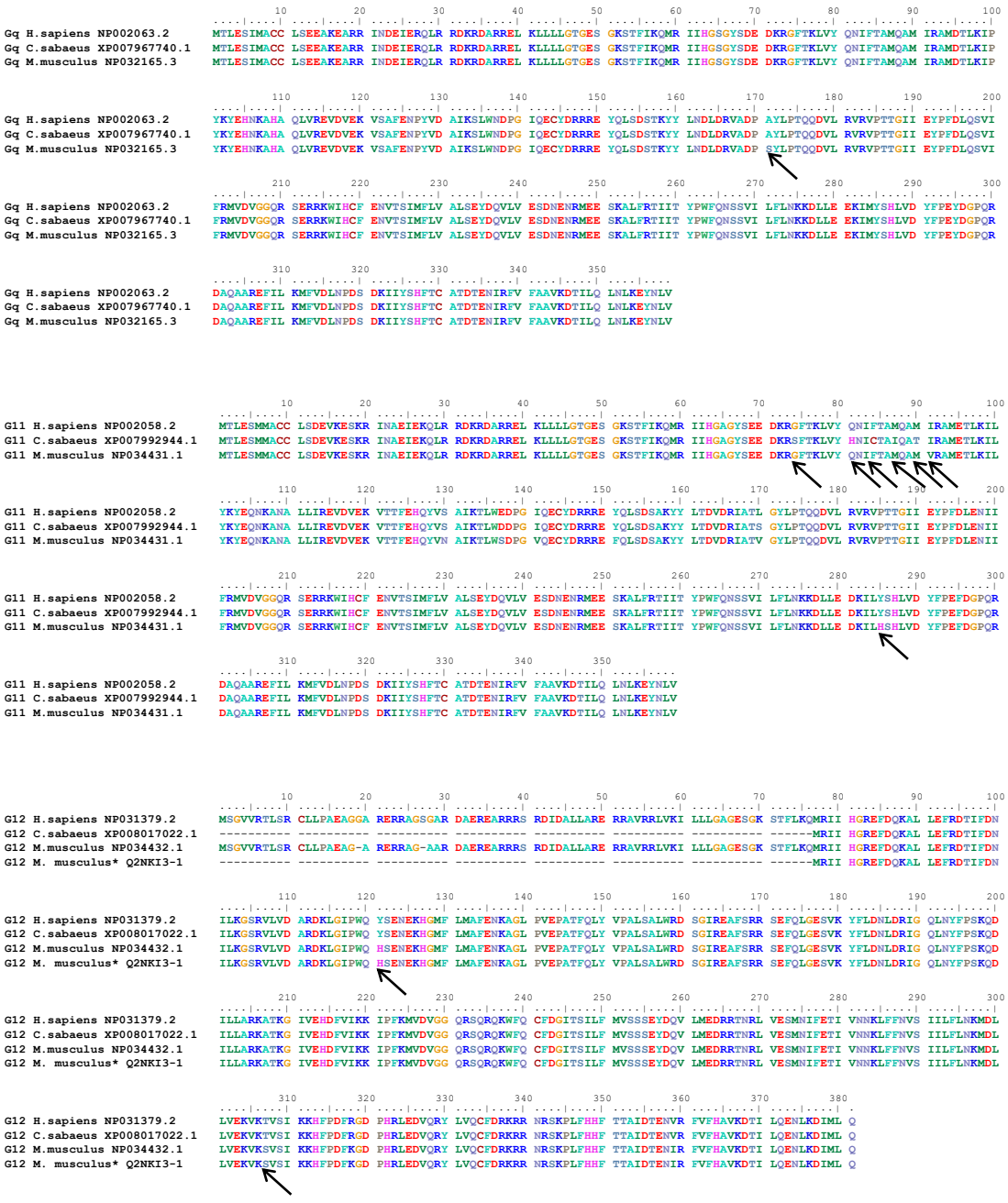

Fig A5 The Aligned Complete Amino Acid Sequences of Different Gα subunits of *H. sapiens*, *C. sabaeus*, and *M. musculus*. Differences in amino acid sequence were highlighted with an arrow. Each Gα subtype bears the protein identifier after the name of species. The amino acid sequences of $G\alpha_{12}$ of *M. musculus* obtained from Uniprot is designated with an asterisk (*).

Fig A5 (con'd)

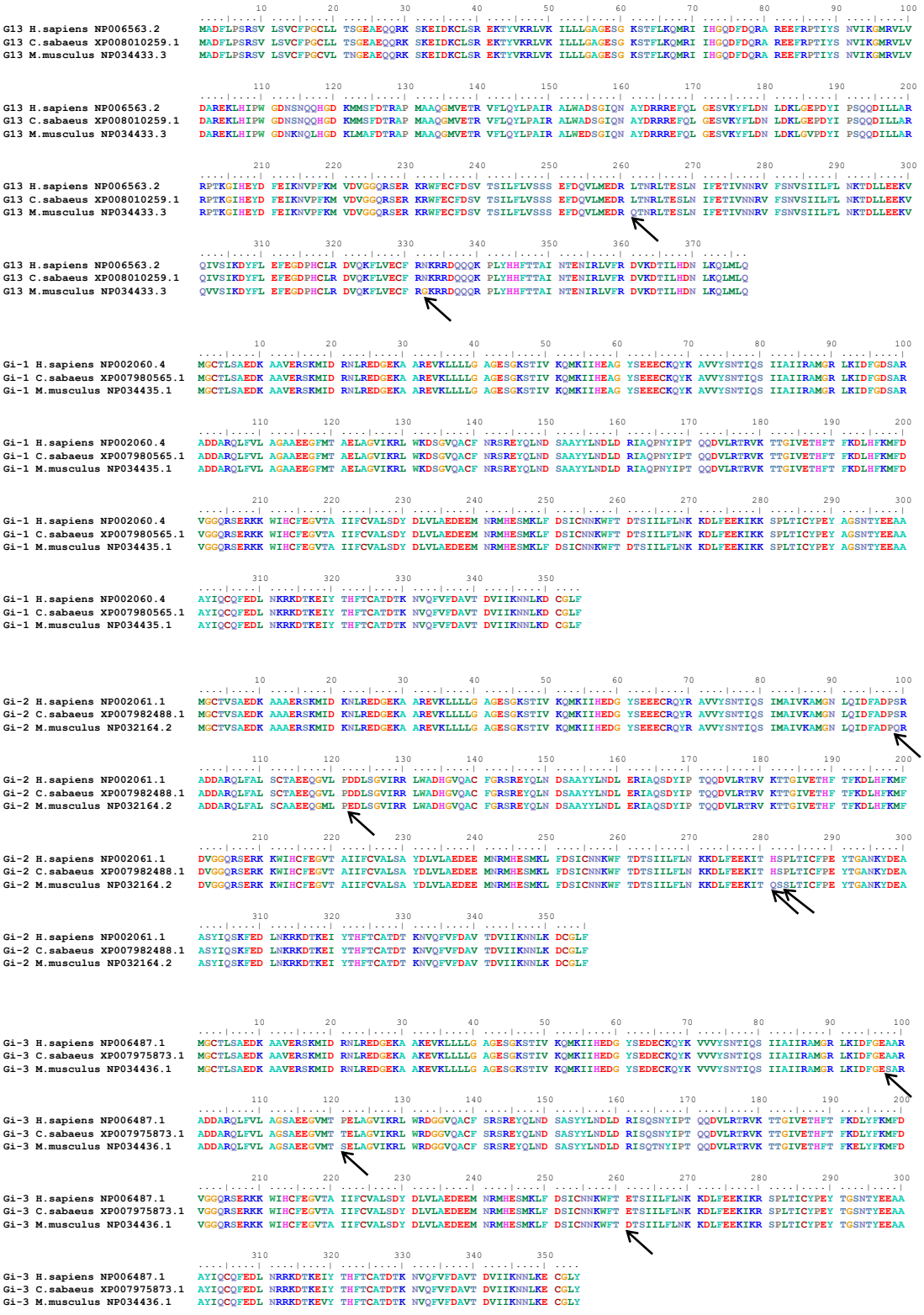
G13 H.sapiens NP006563.2
G13 C.sabaeus XP008010259.1
G13 M.musculus NP034433.3
Gi-1 H.sapiens NP002060.4
Gi-1 C.sabaeus XP007980565.1
Gi-1 M.musculus NP034435.1
Gi-2 H.sapiens NP002061.1
Gi-2 C.sabaeus XP007982488.1
Gi-2 M.musculus NP032164.2
Gi-3 H.sapiens NP006487.1
Gi-3 C.sabaeus XP007975873.1
Gi-3 M.musculus NP034436.1

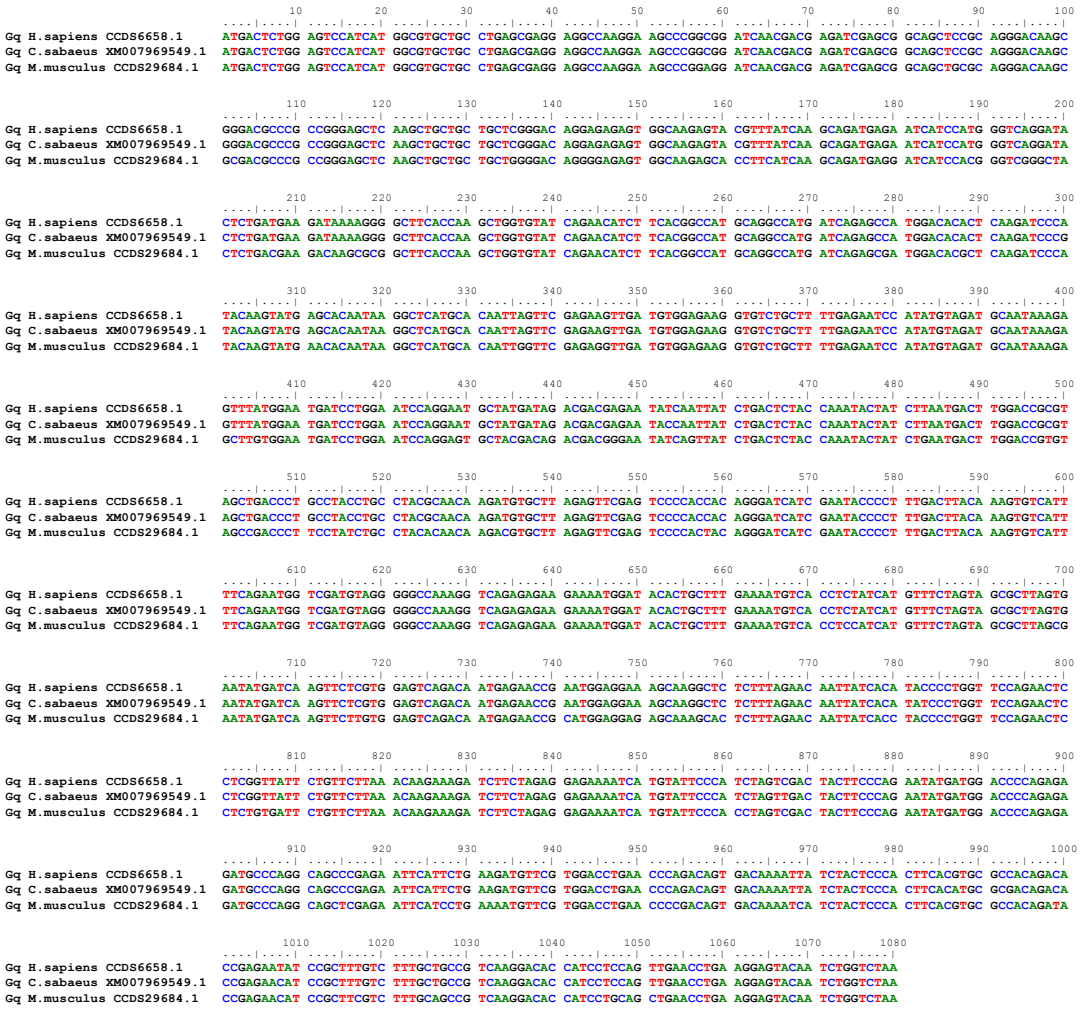

Fig A6 The Aligned CCDS of Different Gα subunits of *H. sapiens*, *C. sabaeus*, and *M. musculus*. Each Gα subtype bears the protein identifier after the name of species. The nucleotide sequences of $G\alpha_{12}$ of *M. musculus* obtained from Uniprot is designated with an asterisk (*).

Fig A6 (con'd)

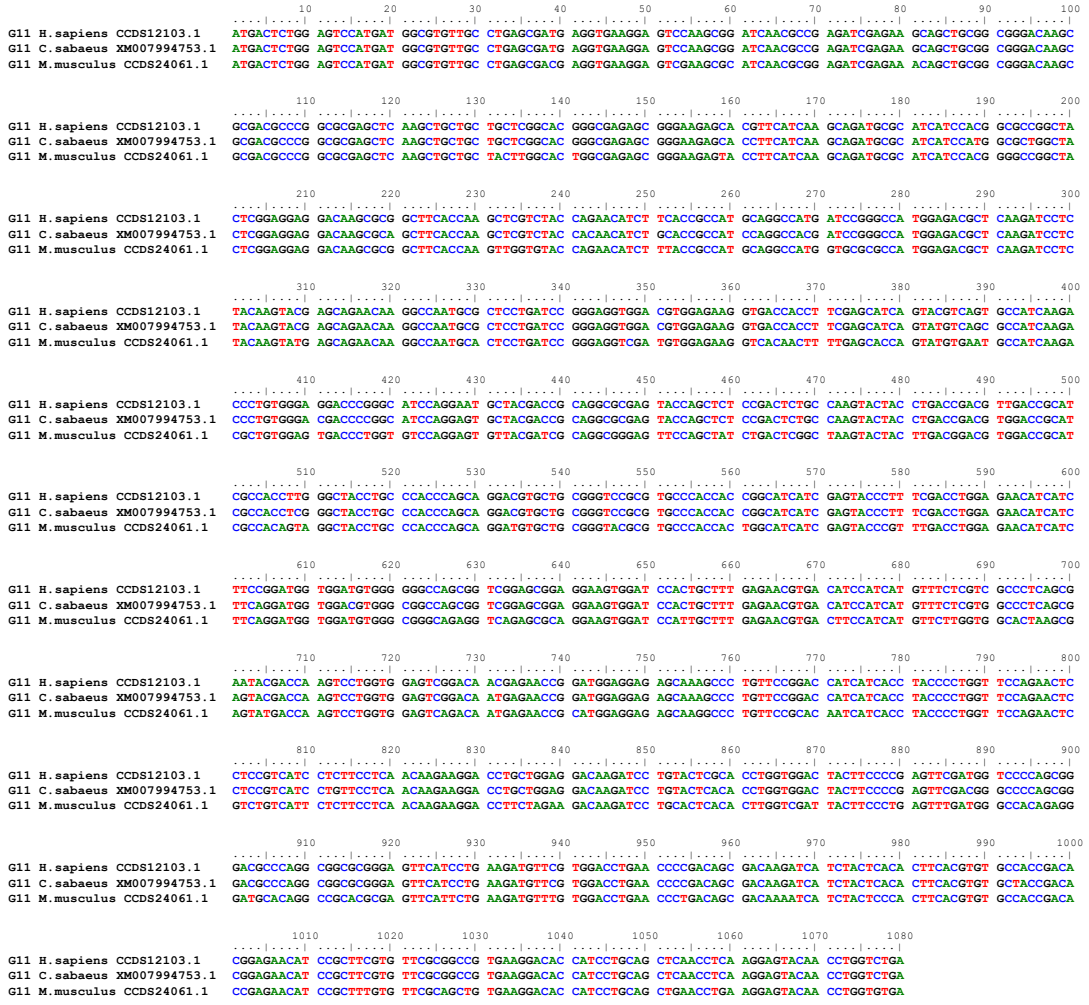
10 20 30 40 50 60 70 80 90 100
G11 H.sapiens CCDS12103.1 ATGACTCTGG AGTCCATGAT GGCGTGTTGC CTGAGCGATG AGGTGAAGGA GTCCAAGCGG ATCAACGCCG AGATCGAGAA GCAGCTGCGG CGGGACAAGC
G11 C.sabaeus XM007994753.1 ATGACTCTGG AGTCCATGAT GGCGTGTTGC CTGAGCGATG AGGTGAAGGA GTCCAAGCGG ATCAACGCCG AGATCGAGAA GCAGCTGCGG CGGGACAAGC
G11 M.musculus CCDS24061.1 ATGACTCTGG AGTCCATGAT GGCGTGTTGC CTGAGCGACG AGGTGAAGGA GTCGAAGCGC ATCAACGCGG AGATCGAGAA ACAGCTGCGG CGGGACAAGC
110 120 130 140 150 160 170 180 190 200
G11 H.sapiens CCDS12103.1 GCGACGCCCG GCGCGAGCTC AAGCTGCTGC TGCTCGGCAC GGGCGAGAGC GGGAAGAGCA CGTTCATCAA GCAGATGCGC ATCATCCACG GCGCCGGCTA
G11 C.sabaeus XM007994753.1 GCGACGCCCG GCGCGAGCTC AAGCTGCTGC TGCTCGGCAC GGGCGAGAGC GGGAAGAGCA CCTTCATCAA GCAGATGCGC ATCATCCATG GCGCTGGCTA
G11 M.musculus CCDS24061.1 GCGACGCCCG GCGCGAGCTC AAGCTGCTGC TACTTGGCAC TGGCGAGAGC GGGAAGAGTA CCTTCATCAA GCAGATGCGC ATCATCCACG GGGCCGGCTA
210 220 230 240 250 260 270 280 290 300
G11 H.sapiens CCDS12103.1 CTCGGAGGAG GACAAGCGCG GCTTCACCAA GCTCGTCTAC CAGAACATCT TCACCGCCAT GCAGGCCATG ATCCGGGCCA TGGAGACGCT CAAGATCCTC
G11 C.sabaeus XM007994753.1 CTCGGAGGAG GACAAGCGCA GCTTCACCAA GCTCGTCTAC CACAACATCT GCACCGCCAT CCAGGCCACG ATCCGGGCCA TGGAGACGCT CAAGATCCTC
G11 M.musculus CCDS24061.1 CTCGGAGGAG GACAAGCGCG GCTTCACCAA GTTGGTGTAC CAGAACATCT TTACCGCCAT GCAGGCCATG GTGCGCGCCA TGGAGACGCT CAAGATCCTC
310 320 330 340 350 360 370 380 390 400
G11 H.sapiens CCDS12103.1 TACAAGTACG AGCAGAACAA GGCCAATGCG CTCCTGATCC GGGAGGTGGA CGTGGAGAAG GTGACCACCT TCGAGCATCA GTACGTCAGT GCCATCAAGA
G11 C.sabaeus XM007994753.1 TACAAGTACG AGCAGAACAA GGCCAATGCG CTCCTGATCC GGGAGGTGGA CGTGGAGAAG GTGACCACCT TCGAGCATCA GTATGTCAGC GCCATCAAGA
G11 M.musculus CCDS24061.1 TACAAGTATG AGCAGAACAA GGCCAATGCA CTCCTGATCC GGGAGGTCGA TGTGGAGAAG GTCACAACTT TTGAGCACCA GTATGTGAAT GCCATCAAGA
410 420 430 440 450 460 470 480 490 500
G11 H.sapiens CCDS12103.1 CCCTGTGGGA GGACCCGGGC ATCCAGGAAT GCTACGACCG CAGGCGCGAG TACCAGCTCT CCGACTCTGC CAAGTACTAC CTGACCGACG TTGACCGCAT
G11 C.sabaeus XM007994753.1 CCCTGTGGGA CGACCCCGGC ATCCAGGAGT GCTACGACCG CAGGCGCGAG TACCAGCTCT CCGACTCTGC CAAGTACTAC CTGACCGACG TGGACCGCAT
G11 M.musculus CCDS24061.1 CGCTGTGGAG TGACCCTGGT GTCCAGGAGT GTTACGATCG CAGGCGGGAG TTCCAGCTAT CTGACTCGGC TAAGTACTAC TTGACGGACG TGGACCGCAT
510 520 530 540 550 560 570 580 590 600
G11 H.sapiens CCDS12103.1 CGCCACCTTG GGCTACCTGC CCACCCAGCA GGACGTGCTG CGGGTCCGCG TGCCCACCAC CGGCATCATC GAGTACCCTT TCGACCTGGA GAACATCATC
G11 C.sabaeus XM007994753.1 CGCCACCTCG GGCTACCTGC CCACCCAGCA GGACGTGCTG CGGGTCCGCG TGCCCACCAC CGGCATCATC GAGTACCCTT TCGACCTGGA GAACATCATC
G11 M.musculus CCDS24061.1 CGCCACAGTA GGCTACCTGC CCACCCAGCA GGATGTGCTG CGGGTACGCG TGCCCACCAC TGGCATCATC GAGTACCCGT TTGACCTGGA GAACATCATC
610 620 630 640 650 660 670 680 690 700
G11 H.sapiens CCDS12103.1 TTCCGGATGG TGGATGTGGG GGGCCAGCGG TCGGAGCGGA GGAAGTGGAT CCACTGCTTT GAGAACGTGA CATCCATCAT GTTTCTCGTC GCCCTCAGCG
G11 C.sabaeus XM007994753.1 TTCAGGATGG TGGACGTGGG CGGCCAGCGG TCGGAGCGGA GGAAGTGGAT CCACTGCTTT GAGAACGTGA CATCCATCAT GTTTCTCGTG GCCCTCAGCG
G11 M.musculus CCDS24061.1 TTCAGGATGG TGGATGTGGG CGGGCAGAGG TCAGAGCGCA GGAAGTGGAT CCATTGCTTT GAGAACGTGA CTTCCATCAT GTTCTTGGTG GCACTAAGCG
710 720 730 740 750 760 770 780 790 800
G11 H.sapiens CCDS12103.1 AATACGACCA AGTCCTGGTG GAGTCGGACA ACGAGAACCG GATGGAGGAG AGCAAAGCCC TGTTCCGGAC CATCATCACC TACCCCTGGT TCCAGAACTC
G11 C.sabaeus XM007994753.1 AGTACGACCA AGTCCTGGTG GAGTCGGACA ATGAGAACCG GATGGAGGAG AGCAAAGCCC TGTTCCGGAC CATCATCACC TACCCCTGGT TCCAGAACTC
G11 M.musculus CCDS24061.1 AGTATGACCA AGTCCTGGTG GAGTCAGACA ATGAGAACCG CATGGAGGAG AGCAAGGCCC TGTTCCGCAC AATCATCACC TACCCCTGGT TCCAGAACTC
810 820 830 840 850 860 870 880 890 900
G11 H.sapiens CCDS12103.1 CTCCGTCATC CTCTTCCTCA ACAAGAAGGA CCTGCTGGAG GACAAGATCC TGTACTCGCA CCTGGTGGAC TACTTCCCCG AGTTCGATGG TCCCCAGCGG
G11 C.sabaeus XM007994753.1 CTCCGTCATC CTGTTCCTCA ACAAGAAGGA CCTGCTGGAG GACAAGATCC TGTACTCACA CCTGGTGGAC TACTTCCCCG AGTTCGACGG GCCCCAGCGG
G11 M.musculus CCDS24061.1 GTCTGTCATT CTCTTCCTCA ACAAGAAGGA CCTTCTAGAA GACAAGATCC TGCACTCACA CTTGGTCGAT TACTTCCCTG AGTTTGATGG GCCACAGAGG
910 920 930 940 950 960 970 980 990 1000
G11 H.sapiens CCDS12103.1 GACGCCCAGG CGGCGCGGGA GTTCATCCTG AAGATGTTCG TGGACCTGAA CCCCGACAGC GACAAGATCA TCTACTCACA CTTCACGTGT GCCACCGACA
G11 C.sabaeus XM007994753.1 GACGCCCAGG CGGCGCGGGA GTTCATCCTG AAGATGTTCG TGGACCTGAA CCCCGACAGC GACAAGATCA TCTACTCACA CTTCACGTGT GCTACCGACA
G11 M.musculus CCDS24061.1 GATGCACAGG CCGCACGCGA GTTCATTCTG AAGATGTTTG TGGACCTGAA CCCTGACAGC GACAAAATCA TCTACTCCCA CTTCACGTGT GCCACCGACA
1010 1020 1030 1040 1050 1060 1070 1080
G11 H.sapiens CCDS12103.1 CGGAGAACAT CCGCTTCGTG TTCGCGGCCG TGAAGGACAC CATCCTGCAG CTCAACCTCA AGGAGTACAA CCTGGTCTGA
G11 C.sabaeus XM007994753.1 CGGAGAACAT CCGCTTCGTG TTCGCGGCCG TGAAGGACAC CATCCTGCAG CTCAACCTCA AGGAGTACAA CCTGGTCTGA
G11 M.musculus CCDS24061.1 CCGAGAACAT CCGCTTTGTG TTCGCAGCTG TGAAGGACAC CATCCTGCAG CTGAACCTGA AGGAGTACAA CCTGGTGTGA

Fig A6 (con'd)

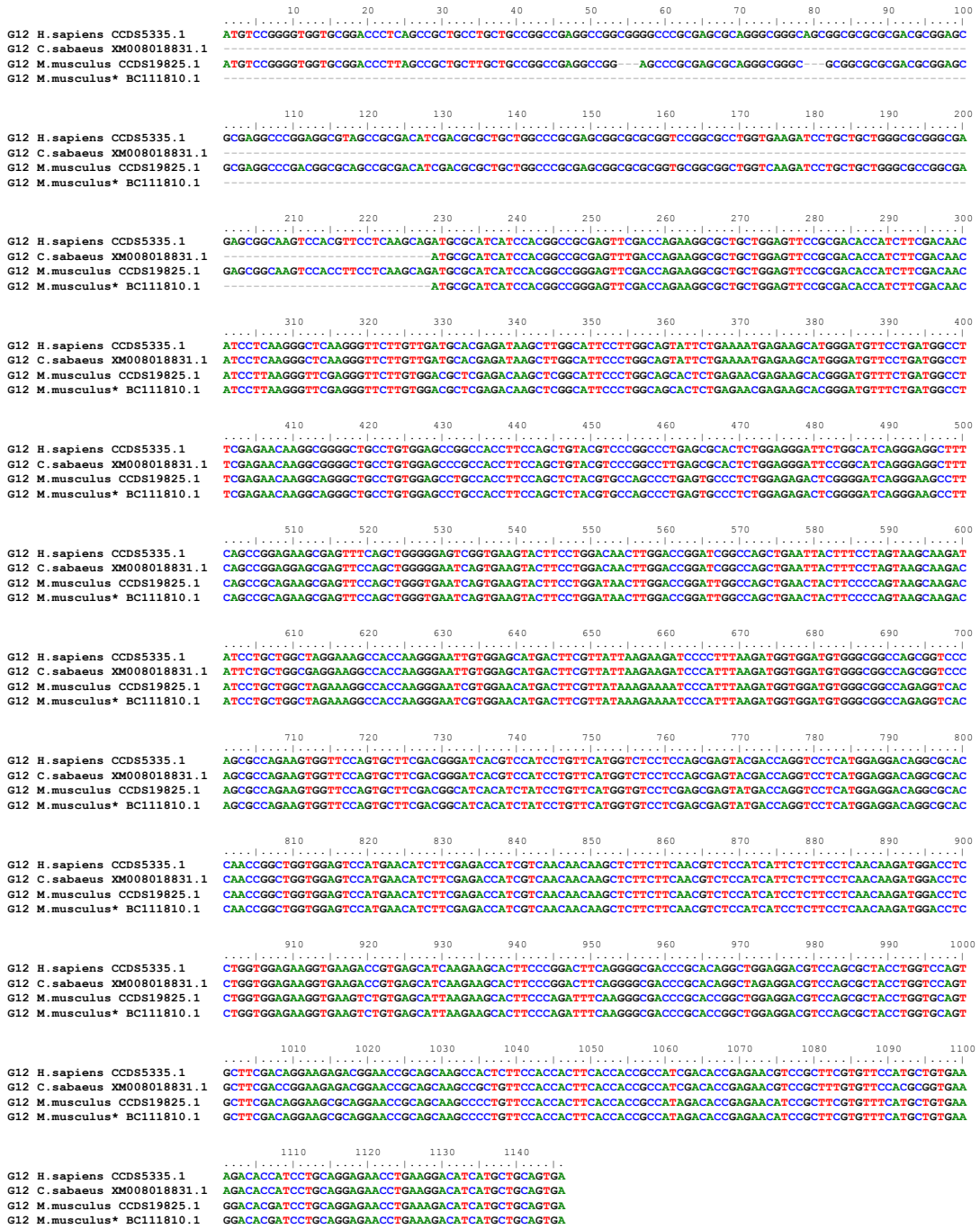
G12 H.sapiens CCDS5335.1
G12 C.sabaeus XM008018831.1
G12 M.musculus CCDS19825.1
G12 M.musculus* BC111810.1

Fig A6 (con'd)

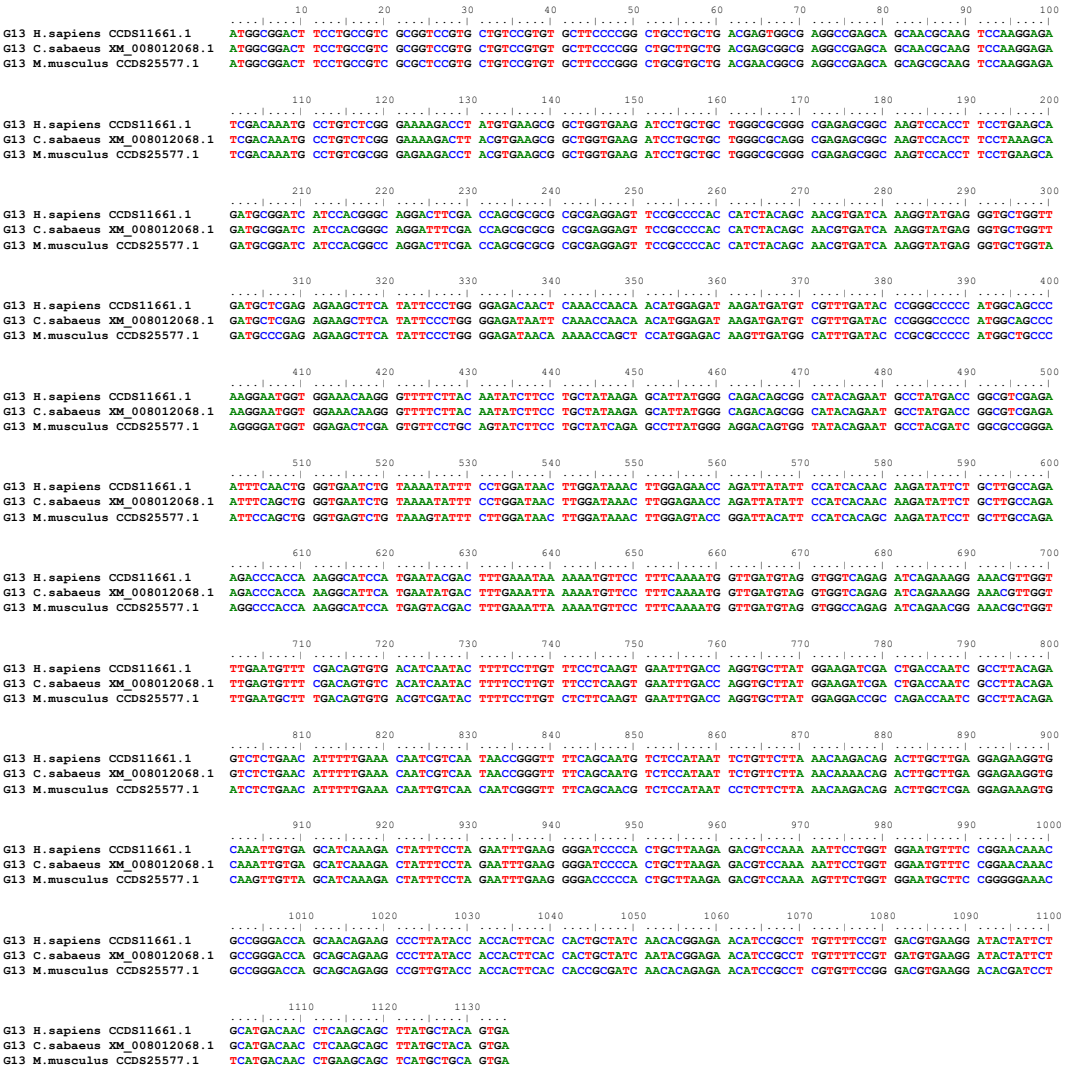
G13 H.sapiens CCDS11661.1
G13 C.sabaeus XM_008012068.1
G13 M.musculus CCDS25577.1

Fig A6 (con'd)

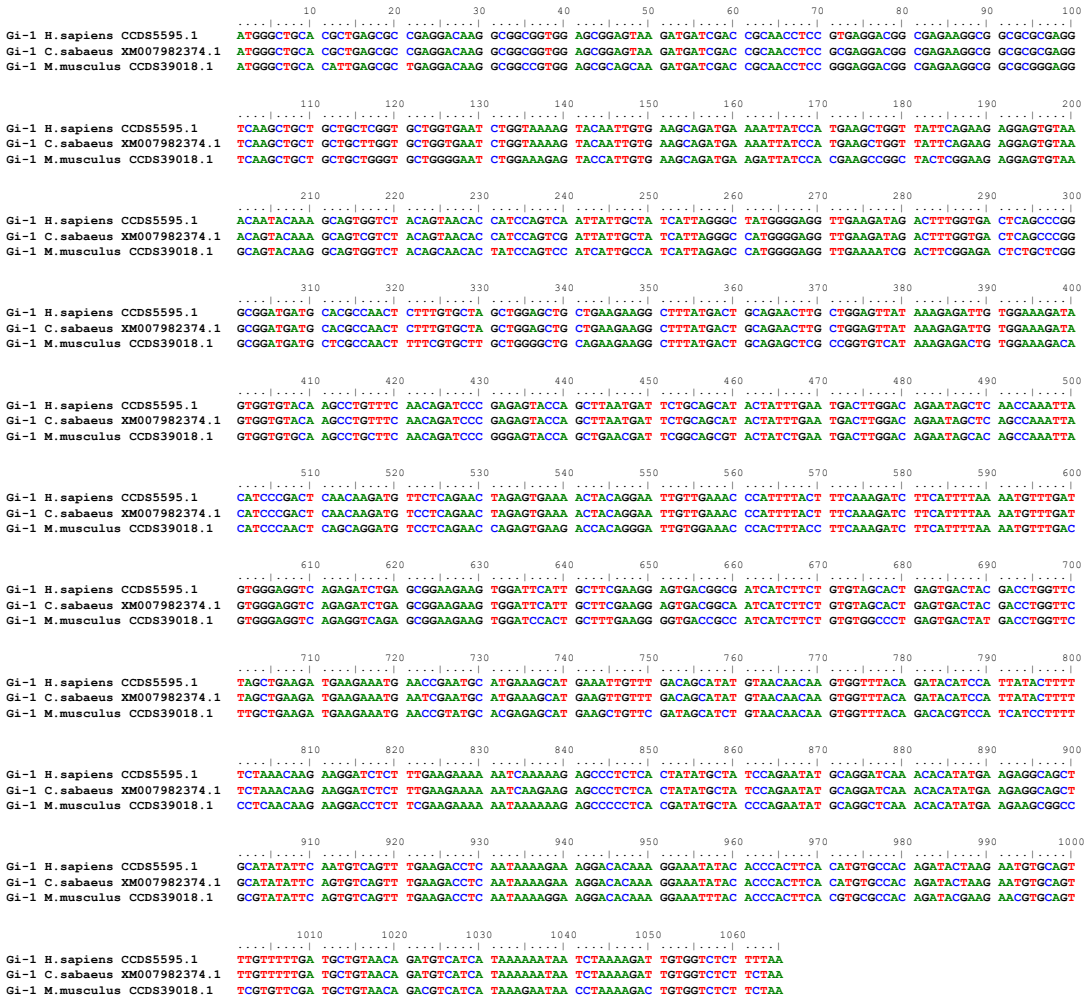
Gi-1 H.sapiens CCDS5595.1
Gi-1 C.sabaeus XM007982374.1
Gi-1 M.musculus CCDS39018.1

Fig A6 (con'd)

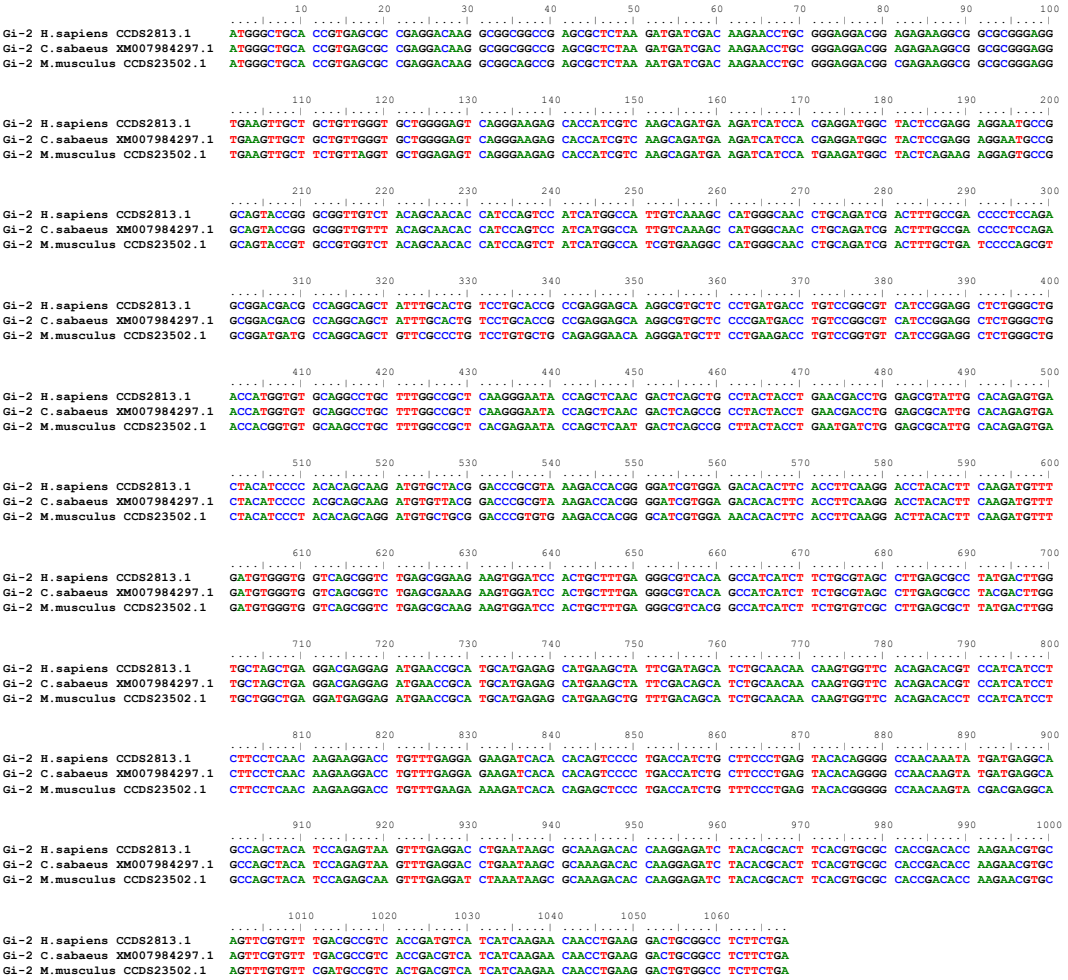
Gi-2 H.sapiens CCDS2813.1
Gi-2 C.sabaeus XM007984297.1
Gi-2 M.musculus CCDS23502.1

Fig A6 (con'd)

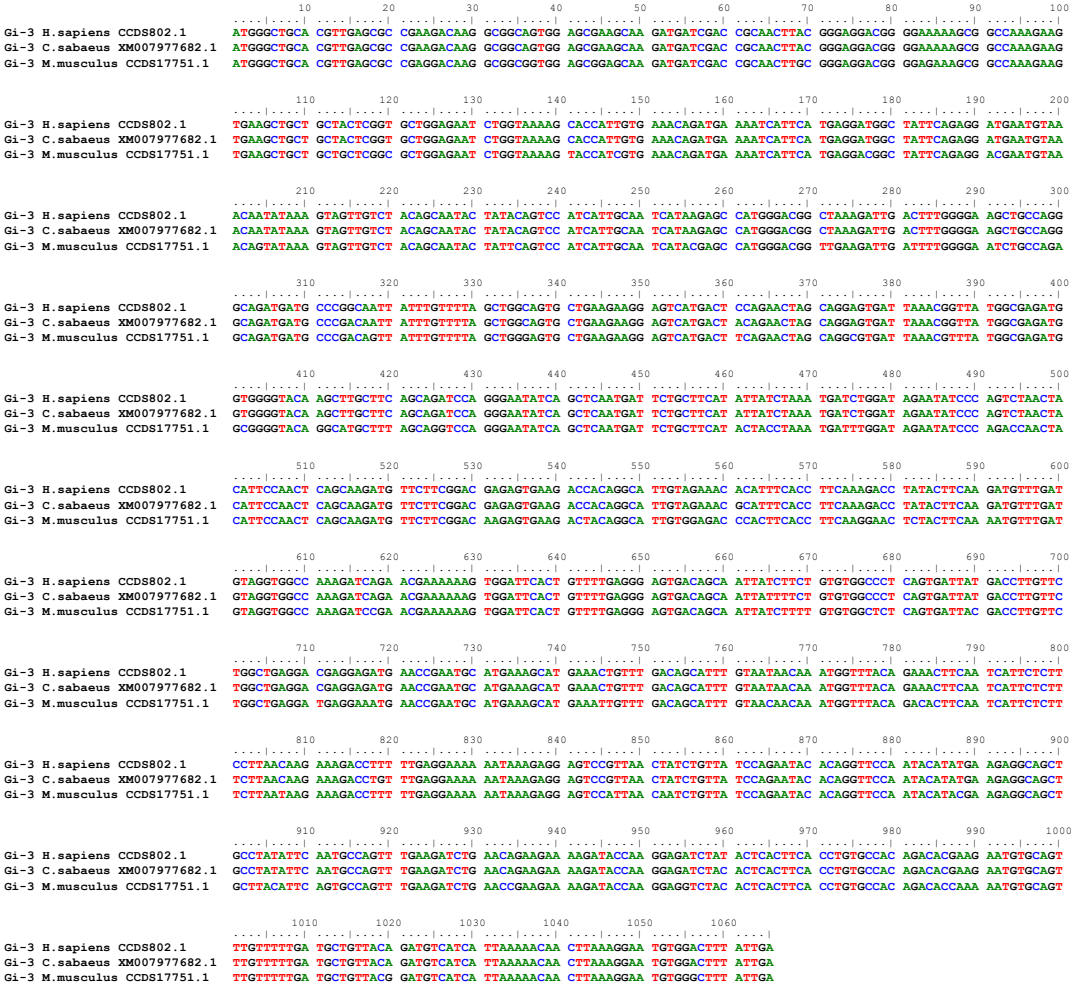
Gi-3 H.sapiens CCDS802.1
Gi-3 C.sabaeus XM007977682.1
Gi-3 M.musculus CCDS17751.1

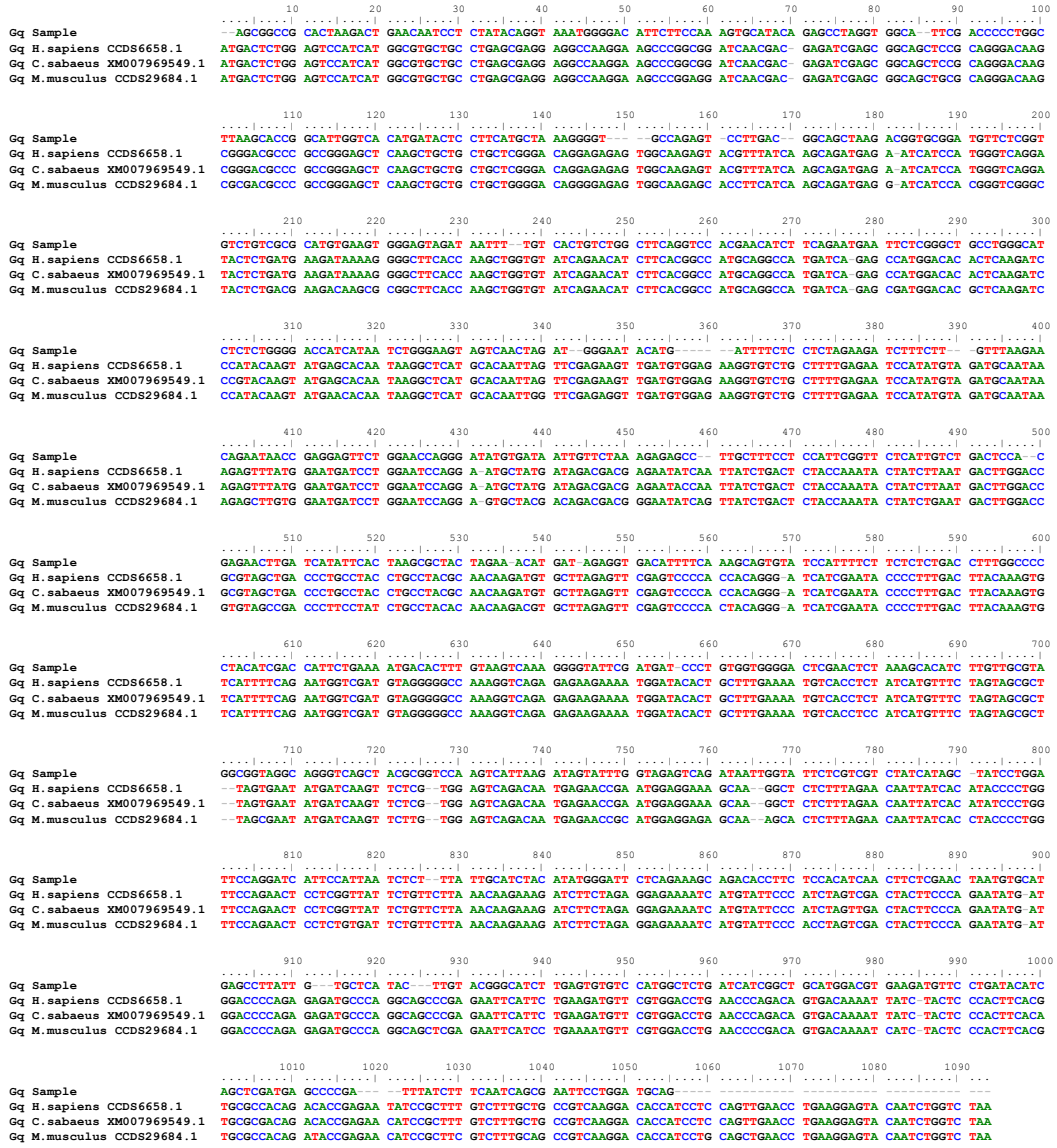

Fig A7 The Aligned Nucleotide Sequences of Gα subunits of *H. sapiens*, *C. sabaeus*, *M. musculus* and the Sample. A long segment of sequences with the fewest ambiguities was selected. Each Gα subtype bears the protein identifier after the name of species.

Fig A7 (con'd)

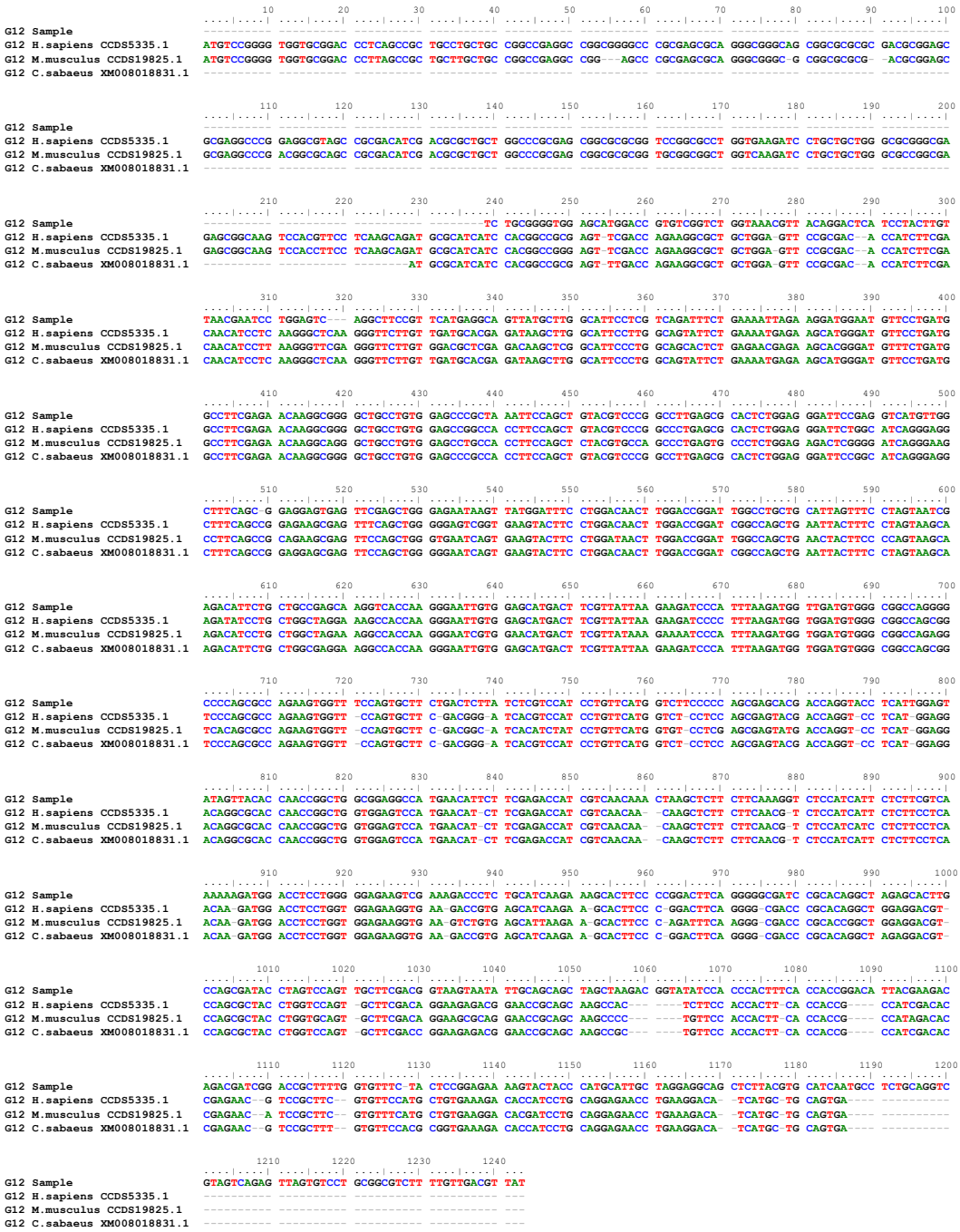
G12 Sample
G12 H.sapiens CCDS5335.1
G12 M.musculus CCDS19825.1
G12 C.sabaeus XM008018831.1

Fig A7 (con'd)

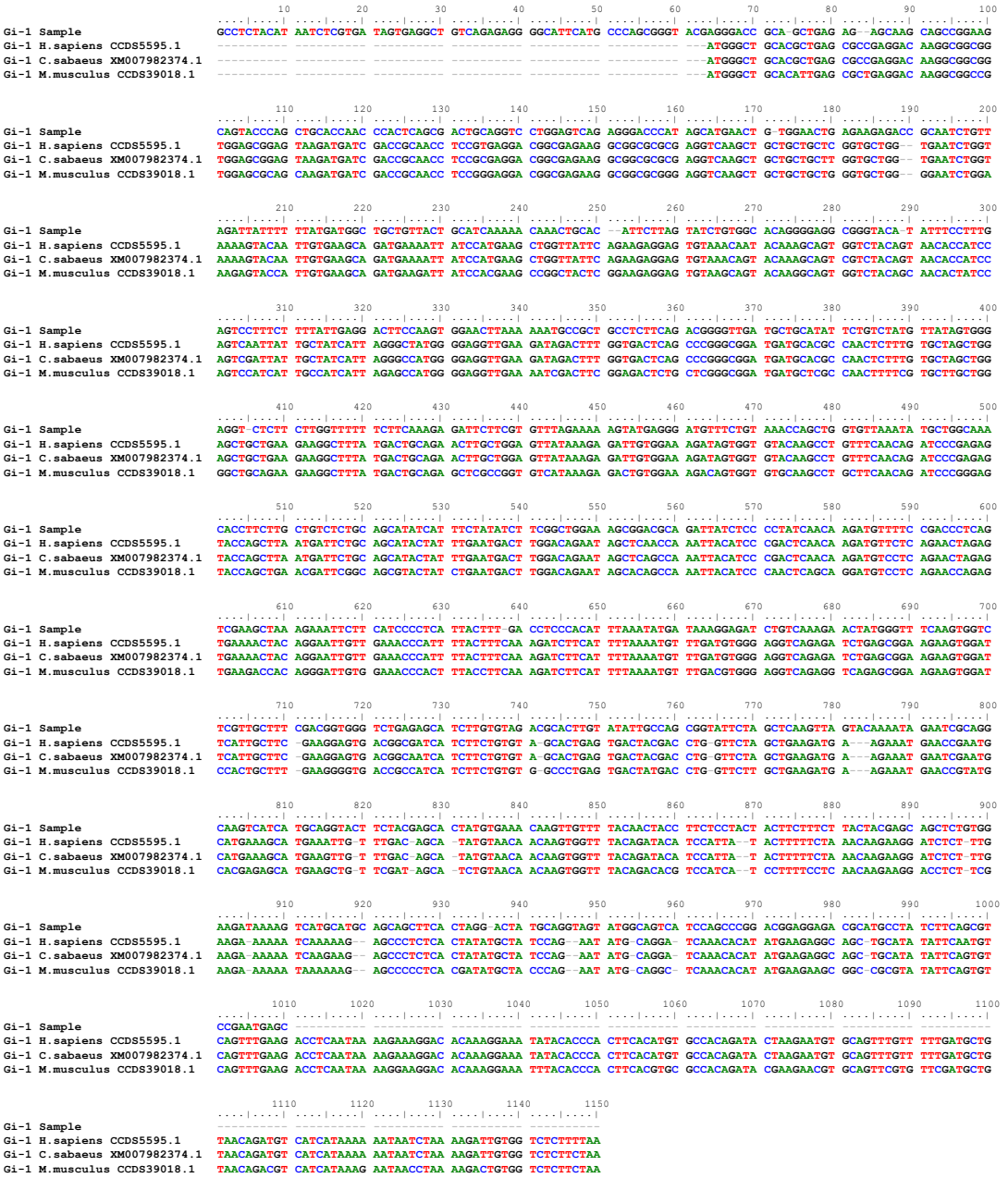
Gi-1 Sample
Gi-1 H.sapiens CCDS5595.1
Gi-1 C.sabaeus XM007982374.1
Gi-1 M.musculus CCDS39018.1

Fig A7 (con'd)


Gi-3 Sample
Gi-3 H.sapiens CCDS802.1
Gi-3 C.sabaeus XM007977682.1
Gi-3 M.musculus CCDS17751.1

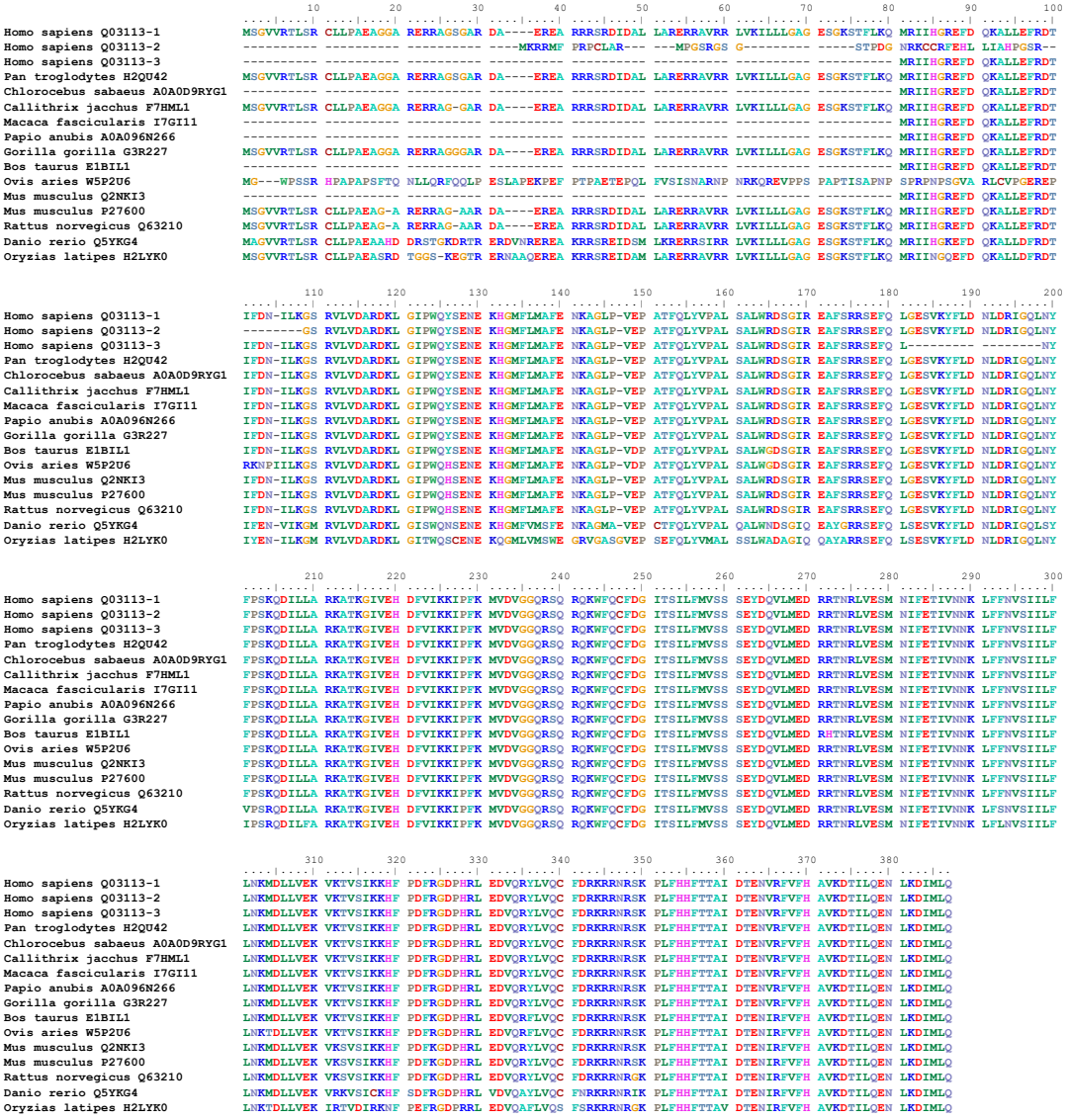

Fig A8 The Aligned Amino Acid Sequences of Gα_{12} subunit of different species. Each species bear the Gα_{12} protein identifier after the name of species. *H. sapiens* has three Gα_{12} isoforms: 1 unspliced form (44 kDa) and 2 spliced variants (34 kDa and 38 kDa) (NCBI).

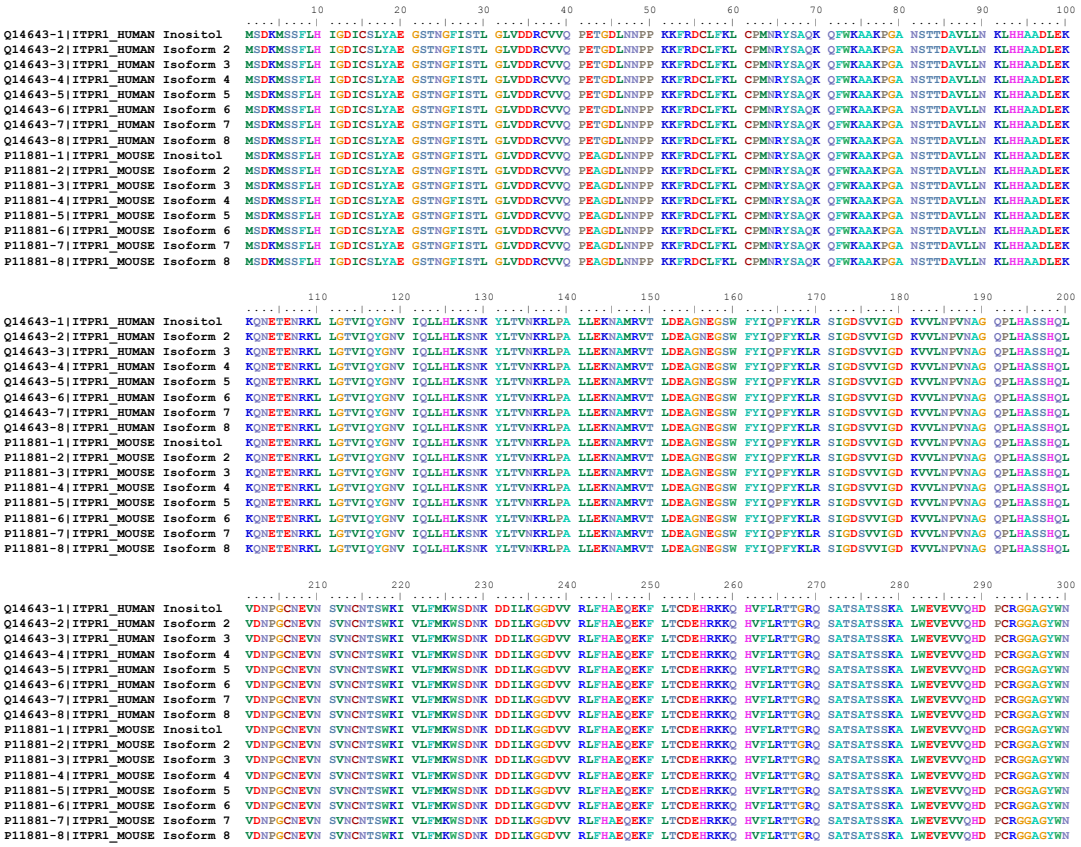

Fig A9 The Aligned Amino Acid Sequences of IP_3R1 of different species: human, mouse and rat. Each IP_3R1 isoform bears the protein identifier.

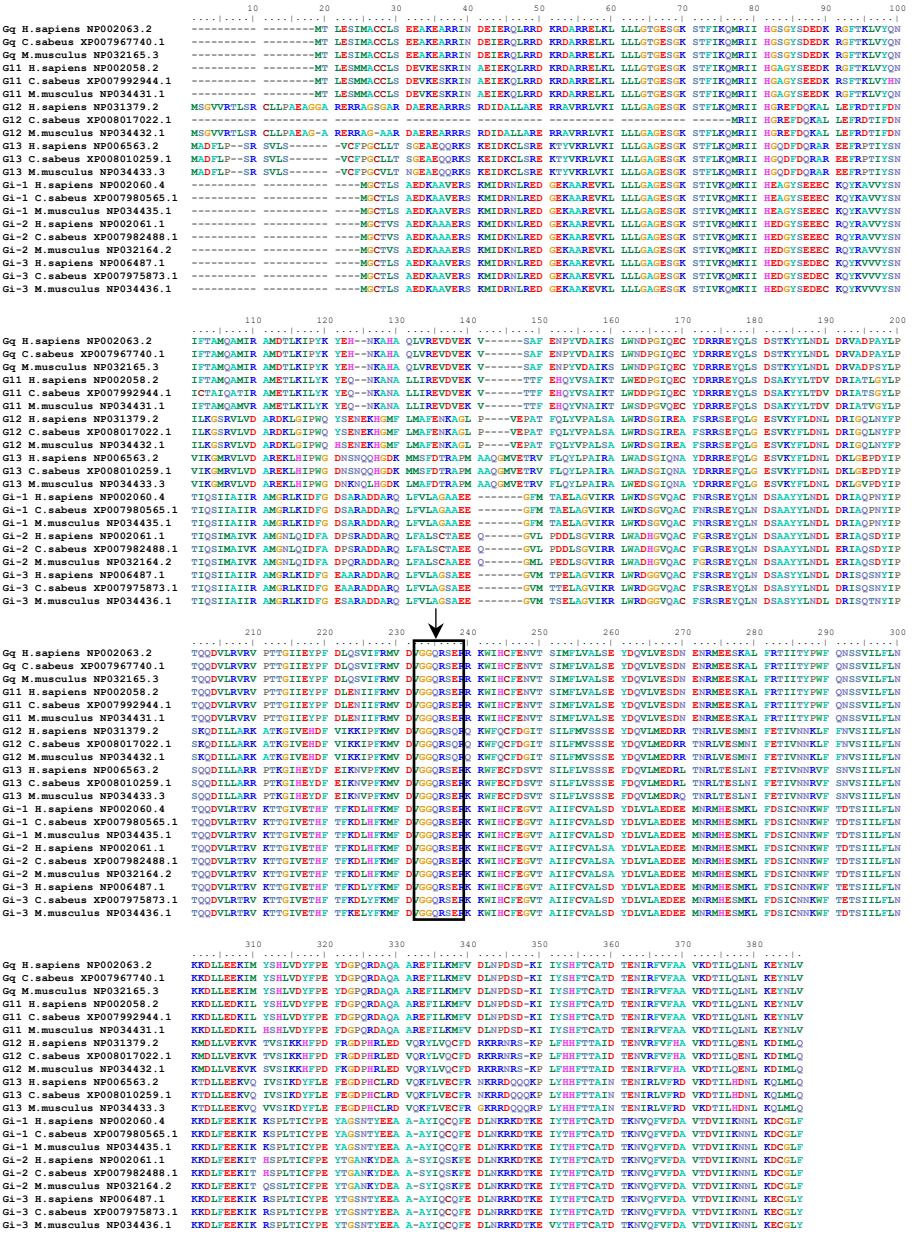

Fig A10 The Complete Amino Acid Sequences of Different Gα subunits of *H. sapiens*, *C. sabaeus*, and *M. musculus*. A segment of the conserved sequences containing the target amino acid of PMT, glutamine (Q) is highlighted with an arrow inside a black box. Each Gα subtype bears the protein identifier after the name of species.

Table A1. The Position of Glutamine (Q), the Target Amino Acid of PMT, in Different Gα Subunits of *H. sapiens*, *C. sabaeus*, and *M. musculus.*

Gα	*H. sapiens*	*M. musculus*	*C. sabaeus*
$G\alpha_q$	209	209	209
$G\alpha_{11}$	209	209	209
$G\alpha_{12}$	231	231	155
$G\alpha_{13}$	226	226	226
$G\alpha_{i-1}$	204	204	204
$G\alpha_{i-2}$	205	205	205
$G\alpha_{i-3}$	204	204	204

Table A2. The Size of CCDS and Protein of Different Gα subunits of *H. sapiens*, *C. sabaeus*, and *M. musculus*

	H. sapiens		*C. sabaeus*		*M. musculus*	
Gα	**Nucleotide**	**Protein**	**Nucleotide**	**Protein**	**Nucleotide**	**Protein**
	CCDS (bp)	AA	CCDS (bp)	AA	CCDS (bp)	AA
$G\alpha_q$	1080 CCDS6658.1	359 NP002063.2	1080 XM007969549.1	359 XP007967740.1	1080 CCDS29684.1	359 NP032165.3
$G\alpha_{11}$	1080 CCDS12103.1	359 NP002058.2	1080 XM007994753.1	359 XP007992944.1	1080 CCDS24061.1	359 NP034431.1
$G\alpha_{12}$	1146 CCDS5335.1	381 NP031379.2	918 XM008018831.1	305 XP008017022.1	1140 CCDS19825.1	379 NP034432.1
$G\alpha_{13}$	1134 CCDS11661.1	377 NP006563.2	1134 XM008012068.1	377 XP008010259.1	1134 CCDS25577.1	377 NP034433.3
$G\alpha_{i-1}$	1065 CCDS5595.1	354 NP002060.4	1065 XM007982374.1	354 XP007980565.1	1065 CCDS39018.1	354 NP034435.1
$G\alpha_{i-2}$	1068 CCDS2813.1	355 NP002061.1	1068 XM007984297.1	355 XP007982488.1	1068 CCDS23502.1	355 NP032164.2
$G\alpha_{i-3}$	1065 CCDS802.1	354 NP006487.1	1065 XM007977682.1	354 XP007975873.1	1065 CCDS17751.1	354 NP034436.1

* Gα subtypes with their unique CCDS and protein sequence identifier were obtained from the NCBI database.

Table A3. The Molecular Weight of Different Gα Subtypes of *H. sapiens*, *C. sabeus*, and *M. musculus*

H. Sapiens				*C. sabeus*			*M. musculus*		
Gα	**Identifier**	**Protein**	**Mol. Weight**	**Identifier**	**Protein**	**Mol. Weight**	**Identifier**	**Protein**	**Mol. Weight**
		AA	Da		AA	Da		AA	Da
$G\alpha_q$	P50148-1	359	42,142	A0A0D9R5U9-1	301	35,422	P21279-1	359	42,158
				XP007967740.1	359	42,011			
$G\alpha_{11}$	P29992-1	359	42,123	A0A0D9RFQ6-1	394	45,922	P21278-1	359	42,024
$G\alpha_{12}$	Q03113-1	381	44,279	A0A0D9RYG1-1	305	35,952	P27600-1	379	44,095
	Q03113-2	322	37,601				Q2NKI3-1	305	35,898
	Q03113-3	288	34,002						
$G\alpha_{13}$	Q14344-1	377	44,050	A0A0D9QVL0-1	377	44.050	P27601-1	377	44,055
	Q14344-2	282	33,287						
$G\alpha_{i-1}$	P63096-1	354	40,361	A0A0D9RHH6-1	354	40,361	B2RSH2-1	354	40,361
	P63096-2	302	34,775						
$G\alpha_{i-2}$	P04899-1	355	40,451	A0A0D9RPC3-1	355	40,451	P08752-1	355	40,489
	P04899-2	339	38,473						
	P04899-3	318	36,465						
	P04899-4	366	41,548						
	P04899-5	339	38,737						
	P04899-6	303	34,935						
$G\alpha_{i-3}$	P08754-1	354	40,532	A0A0D9S6I8-1	354	40,536	Q9DC51-1	354	40,538

Note: Gα proteins with their unique identifier were obtained from Uniprot with the exception of $G\alpha_q$ (XP007967740.1), which was obtained from NCBI database.

9 REFERENCES

Aktories K., Weller U. and Chhatwal G. S. (1987). Clostridium botulinum type C produces a novel ADP-ribosyltransferase distinct from botulinum C2 toxin. *FEBS Lett.*, 212, 109-113.

Aktories K. (1997). Rho proteins: targets for bacterial toxins. 44. *Trends Microbiol.*, 5, 282-8.

Aktories K. (2011). Bacterial protein toxins that modify host regulatory GTPases. *Nat Rev Microbiol.*, 9(7), 487-498.

Albert P. R. and Robillard L. (2002). G protein specificity: traffic direction required. *Cell Signal.*, 14(5), 407-418.

Alderton F., Rakhit S., Kong K. C., Palmer T., Sambi B., Pyne S. and Pyne N. J. (2001). Tethering of the platelet-derived growth factor beta receptor to G-protein-coupled receptors. A novel platform for integrative signaling by these receptor classes in mammalian cells. *J Biol Chem.*, 276(30), 28578-85.

Althoefer H., Eversole-Cire P. and Simon M. I. (1997). Constitutively active Galphaq and Galpha13 trigger apoptosis through different pathways. *J. Biol. Chem.*, 272**,** 24380-24386**.**

Amano M., Ito M., Kimura K., Fukata Y., Chihara K., Nakano T., Matsuura Y. and Kaibuchii K. (1996). Phosphorylation and Activation of Myosin by Rho-associated Kinase (Rho-kinase). *The Journal of Biological Chemistry*, 271(34), 20246 –20249.

Amatruda T.T., 3rd, Steele D.A., Slepak V.Z. and Simon M.I. (1991). G alpha 16, a G protein alpha subunit specifically expressed in hematopoietic cells. *Proc Natl Acad Sci USA*, 88(13), 5587-5591.

Aminova L. R. and Wilson B. A. (2007). Calcineurin-independent inhibition of 3T3-L1 adipogenesis by Pasteurella multocida toxin: suppression of Notch1, stabilization of beta-catenin and pre-adipocyte factor 1. *Cell Microbiol.*, 9(10), 2485-96.

Aranda P.S., LaJoie D.M. and Jorcyk C.L. (2012). Bleach gel: a simple agarose gel for analyzing RNA quality. *Electrophoresis*, 33(2), 366-369.

Astesano A., Regnauld K., Ferrand N. et al. (1999). Cellular and subcellular expression of Golf/Gs and Gq/G11 alpha-subunits in rat pancreatic endocrine cells. *J. Histochem. Cytochem*., 47(3), 289–302.

Azzi M., Charest P. G., Angers S., Rousseau G., Kohout T., Bouvier M. and Piñeyro G. (2003). Beta-arrestin-mediated activation of MAPK by inverse

agonists reveals distinct active conformations for G protein-coupled receptors. *Proc Natl Acad Sci USA*, 100(20), 11406-11.

Babb R. C., Homer K. A., Robbins J. and Lax A. J. (2012). Modification of heterotrimeric G-proteins in Swiss 3T3 cells stimulated with Pasteurella multocida toxin. *PLoS One*, 7(11), 471-88.

Balcueva E. A., Wang Q., Hughes H., Kunsch C., Yu Z. and Robishaw J. D. (2000). Human G protein gamma(11) and gamma(14) subtypes define a new functional subclass. *Exp Cell Res*., 257(2), 310-319.

Baldwin M. R., Lakey J. H. and Lax A. J. (2004). Identification and characterization of the Pasteurella multocida toxin translocation domain. *Mol Microbiol*., 54(1), 239-250.

Baldwin M. R., Pullinger G. D. and Lax A. J. (2003). Pasteurella multocida toxin facilitates inositol phosphate formation by bombesin through tyrosine phosphorylation of G alpha q. *J Biol Chem*., 278(35), 32719-32725.

Baltoumas F. A., Theodoropoulou M. C. and Hamodrakas S. J. (2013). Interactions of the alpha-subunits of heterotrimeric G-proteins with GPCRs, effectors and RGS proteins: A critical review and analysis of interacting surfaces, conformational shifts, structural diversity and electrostatic potentials. *J Struct Biol*., 182(3), 209-18.

Barltrop J. and Owen T. (1991). 5-(3-carboxymethoxyphenyl)-2-(4,5-dimethylthiazoly)-3-(4-sulfophenyl)tetrazolium, inner salt (MTS) and related analogs of 3-(4,5-dimethylthiazolyl)-2,5-diphenyltetrazolium bromide (MTT) reducing to purple water-soluble formazans as cell-viability indicators. *Bioorg Med Chem Lett*., 1, 611–614.

Bascands J. L., Pecher C. and Girolami J. (1993). Indirect inhibition by bradykinin of cyclic AMP generation in isolated rat glomeruli and mesangial cells. *Mol Pharmacol*., 44(4), 818-26.

Bhatnagar A., Sheffler D. J., Kroeze W. K., Compton-Toth B. and Roth B. L. (2004). Caveolin-1 interacts with 5-HT2A serotonin receptors and profoundly modulates the signaling of selected $G\alpha_q$-coupled protein receptors. *J Biol Chem*., 279, 34614–34623.

Bayewitch M.L., Avidor-Reiss T., Levy R., Pfeuffer T., Nevo I., Simonds W.F., and Vogel Z. (1998a). Differential modulation of adenylyl cyclases I and II by various G b subunits. *J Biol Chem*., 273, 2273–2276.

Bayewitch M. L., Avidor-Reiss T., Levy R., Pfeuffer T., Nevo I., Simonds W. F., and Vogel Z. (1998b). Inhibition of adenylyl cyclase isoforms V and VI by various Gbetagamma subunits. *FASEB J*., 12, 1019–1025.

Beas A. O., Taupin V., Teodorof C., Nguyen L. T., Garcia-Marcos M. and Farquhar M. G. (2012). Gαs promotes EEA1 endosome maturation and shuts down proliferative signaling through interaction with GIV (Girdin). *Molecular Biology of the Cell*, 23(23), 4623–4634.

Berenjeno I., Núñez, F. and Bustelo X. (2007). Transcriptomal profiling of the cellular transformation induced by Rho subfamily GTPases. *Oncogene*, 26(29), 4295–4305.

Berridge S.M. (n.d.) Cell Signalling Biology. [Online] Available from: http://www.biochemj.org/csb/ [Accessed: 5 May 2012]

Bharati K. and Ganguly N.K. (2011). Cholera toxin: A paradigm of a multifunctional protein. *Indian J Med Res*., 133(2), 179–187.

Bhattacharyya R. and Wedegaertner P.B. (2000). $G\alpha_{13}$ Requires Palmitoylation for Plasma Membrane Localization, Rho-dependent Signaling, and Promotion of p115-RhoGEF Membrane Binding. *J. Biol. Chem*., 275, 14992-14999.

Birikh K.R., Sklan E.H., Shoham S. and Soreq H. (2003). Interaction of “readthrough” acetylcholinesterase with RACK1 and PKCbeta II correlates with intensified fear-induced conflict behavior. *Proc Natl Acad Sci USA*, 100, 283–288.

Blagosklonny M.V. (2011). Cell cycle arrest is not senescence. *Aging*, 3(2), 94–101.

Bohm A., Gaudet R. and Sigler P.B. (1997). Structural aspects of heterotrimeric G-protein signaling. *Curr Opin Biotechnol*., 8(4), 480-487.

Bommakanti R.K., Vinayak S., Simonds W.F. (2000). Dual regulation of Akt/protein kinase B by heterotrimeric G protein subunits. *J Biol Chem.*, 275(49), 38870-6.

Bosanac I., Yamazaki H., Matsu-Ura, T., Michikawa T., Mikoshiba K. and Ikura M. (2005). Crystal structure of the ligand binding suppressor domain of type 1 inositol 1,4,5-trisphosphate receptor. *Mol. Cell*., 17, 193–203.

Braga V.M.M., Machesky L.M., Hall A., and Hotchin N.A. (1997). The Small GTPases Rho and Rac Are Required for the Establishment of Cadherin-dependent Cell–Cell Contacts. *The Journal of Cell Bio*., 137(6), 1421-1431.

Brogi S., Tafi A., Désaubry L. and Nebigil C. G. (2014). Discovery of GPCR ligands for probing signal transduction pathways. *Front. Pharmacol*., 5, 255.

Brockmeier S.L., Register K.B., Magyar T., Lax A.J., Pullinger G.D., & Kunkle R.A. (2002). Role of the Dermonecrotic Toxin of *Bordetella*

bronchiseptica in the Pathogenesis of Respiratory Disease in Swine. *Infection and Immunity*, 70(2), 481–490.

Brothers, M.C. et al. (2011). Membrane interaction of Pasteurella multocida toxin involves sphingomyelin. *FEBS J.*, 278(23), 4633-4648.

Brust T.F., Conley J.M., Watts V.J. (2015). Gα(i/o)-coupled receptor-mediated sensitization of adenylyl cyclase: 40 years later. *Eur J Pharmacol*., 763(Pt B), 223-32.

Bunel V., Ouedraogo M., Nguyen A. T., Stevigny C. and Duez P. (2014). Methods Applied to the In Vitro Primary Toxicology Testing of Natural Products: State of the Art, Strengths, and Limits. *Planta Medica*, 80(14), 1210-1226.

Burd J.F. and Usategui-Gomez M. (1971). A colorimetric assay for serum lactate dehydrogenase. *Clin Chim Acta*, 46(3), 223-227.

Burridge K. and Wennerberg K. (2004). Rho and Rac Take Center Stage. *Cell*, 116, 167–179.

Busch C., Orth J., Djouder N. and Aktories K. (2001). Biological Activity of a C-Terminal Fragment of Pasteurella multocida Toxin. Infection and *Immunity*, 69(6), 3628–3634.

Carbonetti, N. H. (2010). Pertussis toxin and adenylate cyclase toxin: key virulence factors of Bordetella pertussis and cell biology tools. Future *Microbiology*, 5, 455–469.

Casey P.J., Fong H.K., Simon M.I. and Gilman A.G. (1990). Gz, a guanine nucleotide-binding protein with unique biochemical properties. *J Biol Chem*., 265(4), 2383-2390.

Cassel D. and Pfeuffer T. (1978). Mechanism of cholera toxin action: covalent modification of the guanyl nucleotide-binding protein of the adenylate cyclase system. *Proc Natl Acad Sci USA*, 75(6), 2669-2673.

Cell Biolabs Product Manual (2015). RhoA/Rac1/Cdc42 Activation Assay Combo Kit. Cell Biolabs, Inc. Available from: http://www.cellbiolabs.com/sites/default/files/STA-405-rhoA-rac1-cdc42-activation-assay.pdf [Accessed: 10 Jan 2015]

Chan A.M., Fleming T.P., McGovern E.S., Chedid M., Miki, T. and Aaronson S. A. (1993). Expression cDNA cloning of a transforming gene encoding the wild-type G alpha 12 gene product. *Mol Cell Biol*., 13(2), 762-768.

Chan P., Thomas C.J., Sprang, S.R. and Tall G.G. (2013). Molecular chaperoning function of Ric-8 is to fold nascent heterotrimeric G protein α

subunits. *Proceedings of the National Academy of Sciences of the United States of America*, 110(10), 3794–3799.

Chang B.Y., Harte R.A. and Cartwright C.A. (2002). RACK1, a Receptor for Activated C Kinase and a Homolog of the β Subunit of G Proteins, Inhibits Activity of Src Tyrosine Kinases and Growth of NIH 3T3 Cells. *Oncogene*, 21, 7619–7629.

Chen Z., Sun J., Pradines A., Favre G., Adnane J. and Sebti S.M. (2000). Both farnesylated and geranylgeranylated RhoB inhibit malignant transformation and suppress human tumor growth in nude mice. *J. Biol. Chem*., 275, 17974–17978.

Chen C.A. and Manning D.R. (2001). Regulation of G proteins by covalent modification. *Oncogene*, 20(13), 1643-52.

Chen-Goodspeed M., Lukan A.N. and Dessauer C.W. (2005). Modeling of Galpha(s) and Galpha(i) regulation of human type V and VI adenylyl cyclase. *J Biol Chem*., 280(3), 1808-16.

Chidiac P. and Ross E.M. (1999). Phospholipase C-beta1 directly accelerates GTP hydrolysis by Galphaq and acceleration is inhibited by Gbeta gamma subunits. *J Biol Chem*., 274(28), 19639-43.

Chikumi H., Vázquez-Prado J., Servitja J. M., Miyazaki H. and Gutkind J. S. (2002). Potent activation of RhoA by Gαq and Gq-coupled receptors. *J Biol Chem.*, 277, 27130-27134.

Clapham D. E. and Neer E. J. (1997). G protein beta gamma subunits. Annu *Rev Pharmacol Toxicol*., 37, 167-203.

Conklin B.R., Farfel Z., Lustig K.D., Julius D. and Bourne H.R. (1993). Substitution of three amino acids switches receptor specificity of Gq alpha to that of Gi alpha. *Nature*, 363(6426), 274-276.

Conley J.M. and Watts V.J. (2013). Differential effects of AGS3 expression on D(2L) do- pamine receptor-mediated adenylyl cyclase signaling. *Cell. Mol. Neurobiol*., 33, 551–558.

Cooper G.M. The Cell: A Molecular Approach. 2nd edition. Sunderland (MA): Sinauer Associates; 2000. Transport of Small Molecules. Available from: http://www.ncbi.nlm.nih.gov/books/NBK9847/

Cory A.H., Owen T.C., Barltrop J.A. and Cory J.G. (1991). Use of an aqueous soluble tetrazolium formazan assay for cell growth assays in culture. *Cancer Communications*, 3, 207-212.

Daaka Y., Pitcher J.A., Richardson M., Stoffel R.H., Robishaw J. D., Lefkowitz R. J. (1997). Receptor and G betagamma isoform-specific interactions with G protein-coupled receptor kinases. *Proceedings of the National Academy Sciences USA*, 94, 2180–2185.

Daub H., Weiss F.U., Wallasch C. and Ullrich A. (1996). Role of transactivation of the EGF receptor in signalling by G-protein-coupled receptors. *Nature*, 379(6565), 557-60.

Davignon I., Barnard M., Gavrilova O., Sweet K. and Wilkie T.M. (1996). Gene structure of murine Gna11 and Gna15: tandemly duplicated Gq class G-protein α subunit genes. *Genomics*, 31, 359–366.

DeFlorio R., Brett M.E., Waszczak N., Apollinari E., Metodiev M.V., Dubrovskyi O., Eddington D., Arkowitz R.A., Stone D.E. (2013). Phosphorylation of Gβ is crucial for efficient chemotropism in yeast. *J Cell Sci.*, 126(Pt 14), 2997-3009.

Deguchi S. and Sato M. (2009). Biomechanical properties of actin stress fibers of non-motile cells. *Biorheology*. 46(2), 93-105.

De Lean, A., Stadel, J.M., and Lefkowitz, R.J. (1980). A ternary complex model explains the agonist-specific binding properties of the adenylate cyclase-coupled beta-adrenergic receptor. *J. Biol. Chem*., 255, 7108–7117.

Della Rocca G.J., Maudsley S., Daaka Y., Lefkowitz R.J., and Luttrell L.M. (1999). Pleiotropic coupling of G protein-coupled receptors to the mitogen-activated protein kinase cascade. Role of focal adhesions and receptor tyrosine kinases. *J Biol Chem*., 274, 13978–13984.

Denis C., Saulière A., Galandrin S., Sénard J-M. and Galés C. (2012). Probing heterotrimeric G protein activation: applications to biased ligands. *Current Pharmaceutical Design*, 18(2), 128–144.

Deupi X. and Kobilka B. (2007). Activation of G protein-coupled receptors. *Adv Protein Chem*., 74, 137-66.

Devivo M. and Iyengar R. (1994). G-Protein Pathways - Signal-Processing by Effectors. Molecular and Cellular Endocrinology. 100(1-2):65-70.

Dhanasekaran N., Tsim S. T., Dermott J. M. and Onesime D. (1998). Regulation of cell proliferation by G proteins. *Oncogene*, 17(11), 1383-1394.

Diel S., Klass K., Wittig B. and Kleuss C. (2006). G beta gamma activation site in adenylyl cyclase type II Adenylyl cyclase type III is inhibited by G beta gamma. *Journal of Biological Chemistry*, 281(1), 288-294.

Drin G., Douguet D. and Scarlata S. (2006). The Pleckstrin Homology Domain of Phospholipase Cβ Transmits Enzymatic Activation through

Modulation of Membrane - Domain Orientation. *Biochemistry*, 45(18), 5712–5724.

Drin G. and Scarlata, S. (2007). Stimulation of Phospholipase Cβ by Membrane Interactions, Interdomain Movmement, and G protein Binding - How Many Ways Can You Activate an Enzyme? *Cellular Signalling*, 19(7), 1383–1392.

Du W., Lebowitz, P.F., and Prendergast, G.C. (1999). Cell growth inhibition by farnesyltransferase inhibitors is mediated by gain of geranylgeranylated RhoB. *Mol. Cell. Biol*., 19,1831–1840.

Dudet L.I., Chailler P., Dubreuil J.D. and Martineau-Doize B. (1996). Pasteurella multocida toxin stimulates mitogenesis and cytoskeleton reorganization in Swiss 3T3 fibroblasts. *J Cell Physiol*., 168(1):173-82.

Dupre D.J., Robitaille M., Richer M., Ethier N., Mamarbachi A. M., Hébert T. E. (2007). Dopamine receptor-interacting protein 78 acts as a molecular chaperone for Ggamma subunits before assembly with Gbeta. *J Biol Chem*., 282(18), 13703–13715

Dupre D.J., Robitaille M., Rebois R.V. and Hebert T.E. (2009). The Role of G beta gamma Subunits in the Organization, Assembly, and Function of

GPCR Signaling Complexes. *Annual Review of Pharmacology and Toxicology*, 49, 31-56.

Eason M.G., Kurose H., Holt B.D., Raymond J.R., Liggett S. B. (1992). Simultaneous coupling of α_2-adrenergic receptors to two G-proteins with opposing effects. *J. Biol. Chem*., 267, 15795–15801.

Egerer M., Giesemann T., Jank T., Satchell K. J., Aktories K. (2007). Auto-catalytic cleavage of Clostridium difficile toxins A and B depends on cysteine protease activity. *J. Biol. Chem*., 282, 25314–25321.

Erhardt J.A. and Pittman R.N. (1998). Ectopic p21(WAF1) expression induces differentiation-specific cell cycle changes in PC12 cells characteristic of nerve growth factor treatment. *J. Biol. Chem*., 273, 23517–23523.

Fields T.A. and Casey P.J. (1995). Phosphorylation of Gz alpha by protein kinase C blocks interaction with the beta gamma complex. *J Biol Chem*., 270(39), 23119-25.

Fishburn C.S., Herzmark P., Morales J., Bourne H.R. (1999). Gβγ and Palmitate Target Newly Synthesized $G\alpha_z$ to the Plasma Membrane. *J. Biol. Chem*., 274, 18793-18800.

Fleige S. and Pfaffl M.W. (2006). RNA integrity and the effect on the real-time qRT-PCR performance. *Mol Aspects Med*., 27(2-3), 126-39.

Flatau G., Lemichez E., Gauthier M., Chardin P., Paris S., Fiorentini C. and Boquet P. (1997). Toxin-induced activation of the G protein p21 Rho by deamidation of glutamine. *Nature*, 387, 729-733.

Foley J.F., Singh S.P., Cantu M., Chen L., Zhang H.H. and Farber J.M. (2010). Differentiation of Human T Cells Alters Their Repertoire of G Protein α-Subunits. *The Journal of Biological Chemistry*, 285(46), 35537–35550.

Fong H.K., Yoshimoto K.K., Eversole-Cire P. and Simon M.I. (1988). Identification of a GTP-binding protein alpha subunit that lacks an apparent ADP-ribosylation site for pertussis toxin. *Proc Natl Acad Sci USA*, 85(9), 3066-3070.

Fotakis G. and Timbrell J.A. (2006). In vitro cytotoxicity assays: comparison of LDH, neutral red, MTT and protein assay in hepatoma cell lines following exposure to cadmium chloride. *Toxicol Lett*., 160(2), 171-177.

Fredriksson R., Lagerström M.C., Lundin L.G. and Schiöth H.B. (2003). The G-protein-coupled receptors in the human genome form five main families. Phylogenetic analysis, paralogon groups, and fingerprints. *Mol Pharmacol*., 63(6), 1256-72.

Friedman J., Babu B. and Clark R.B. (2002). β2-adrenergic receptor lacking the cyclic AMP-dependent protein kinase consensus sites fully activates extracellular signal-regulated kinase 1/2 in human embryonic kidney 293 cells: lack of evidence for GS/Gi switching. *Mol. Pharmacol*., 62, 1094–1102.

Fukuhara S., Chikumi H., Gutkind J.S. (2001). RGS-containing RhoGEFs: the missing link between transforming G proteins and Rho? *Oncogene*, 20(13), 1661-8.

Fukui A. and Horiguchi Y. (2004). Bordetella Dermonecrotic Toxin Exerting Toxicity through Activation of the Small GTPase Rho. *J. Biochem*., 136, 415–419.

Gabay M., Pinter M. E., Wright F.A., Chan P., Murphy A.J., Valenzuela D.M.… Tall G.G. (2011). Ric-8 Proteins Are Molecular Chaperones That Direct Nascent G Protein α Subunit Membrane Association. *Science Signaling*, 4(200), 10.1126/scisignal.2002223.

Gallego C., Gupta S.K., Winitz S., Eisfelder B.J., Johnson G.L. (1992). Myristoylation of the G alpha i2 polypeptide, a G protein alpha subunit, is required for its signaling and transformation functions. *Proc. Natl. Acad. Sci. USA*, 89, 9695-9699.

Galbiati F., Guzzi F., Magee A.I., Milligan G. and Parenti M. (1996). Chemical inhibition of myristoylation of the G-protein Gi1 alpha by 2-hydroxymyristate does not interfere with its palmitoylation or membrane association. Evidence that palmitoylation, but not myristoylation, regulates membrane attachment. *Biochemical Journal*, 313(Pt 3), 717–720.

Getz T.M., Dangelmaier C.A., Jin J., Daniel J.L. and Kunapuli S.P. (2010). Differential Phosphorylation of Myosin Light Chain (Thr)18 and (Ser)19 and Functional Implications in Platelets. *Journal of Thrombosis and Haemostasis : JTH*, 8(10), 2283–2293.

Gill D.M. and Meren R. (1978). ADP-ribosylation of membrane proteins catalyzed by cholera toxin: basis of the activation of adenylate cyclase. *Proc Natl Acad Sci USA*, 75(7), 3050-3054.

Glick J.L., Meigs T.E., Miron A., and Casey P.J. (1998). RGSZ1, a G_z-selective regulator of G protein signaling whose action is sensitive to the phosphorylation state of $G_z\alpha$. *J Biol Chem*., 273, 26008-26013.

Goldsmith Z.G. and Dhanasekaran D.N. (2007). G Protein regulation of MAPK networks. *Oncogene*, 26, 3122–3142.

Gonzalez E., Nagiel A., Lin A.J., Golan D.E. and Michel T. (2004). Small interfering RNA-mediated down-regulation of caveolin-1 differentially

modulates signaling pathways in endothelial cells. *J. Biol. Chem*., 279, 40659–40669.

Gonzalez E., Kou R. and Michel T. (2006) Rac1 modulates sphingosine 1-phosphate-mediated activation of phosphoinositide 3-kinase/Akt signaling pathways in vascular endothelial cells. *J Biol Chem*., 281, 3210–3216.

Gratacap M-P., Payrastre B., Nieswandt B. and Offermanns S. (2001). Differential regulation of Rho and Rac through heterotrimeric G-proteins and cyclic nucleotides. *J Biol Chem*., 276, 47906–47913.

Groves C.P. (2005). Wilson, D.E.; Reeder, D.M., eds. Mammal Species of the World: A Taxonomic and Geographic Reference (3rd ed.). Baltimore: Johns Hopkins University Press. pp. 158–159.

Greenbaum D., Colangelo C., Williams K. and Gerstein M. (2003). Comparing protein abundance and mRNA expression levels on a genomic scale. *Genome Biol*., 4(9), 117.

Gry M., Rimini R., Strömberg S., Asplund A., Pontén F., Uhlén M. and Nilsson P. (2009). Correlations between RNA and protein expression profiles in 23 human cell lines. *BMC Genomics*, 10(365), 1-14.

Guo F., Debidda M., Yang L., Williams D.A., and Zheng Y. (2006). Genetic Deletion of Rac1 GTPase Reveals Its Critical Role in Actin Stress Fiber Formation and Focal Adhesion Complex Assembly. *The Journal of Biological Chem*., 281(27),18652–18659.

Hall T.A. (1999). BioEdit: a user-friendly biological sequence alignment editor and analysis program for Windows 95/98/NT. *Nucl. Acids. Symp. Ser*., 41, 95-98.

Hallak H., Muszbek L., Laposata M., Belmonte E., Brass L.F., Manning D.R. (1994). Covalent binding of arachidonate to G protein alpha subunits of human platelets. *J Biol Chem*., 269(7), 4713-6.

Hamm, H.E. (2001). How activated receptors couple to G proteins. *Proceedings of the National Academy of Sciences of the United States of America*, 98(9), 4819–4821.

Hammerman P.S., Fox C.J., Birnbaum M.J. and Thompson C.B. (2005). Pim and Akt oncogenes are independent regulators of hematopoietic cell growth and survival. *Blood*, 105(11), 4477–4483.

Harmey D., Stenbeck G., Nobes C.D., Lax A.J. and Grigoriadis, A.E. (2004). Regulation of osteoblast differentiation by Pasteurella multocida toxin (PMT):

a role for Rho GTPase in bone formation. *J Bone Miner Res*., 19(4), 661-670.

Hart M.J., Sharma S., elMasry N., Qiu R-G., McCabe P., Polakis P. and Bollag G. (1996). Identification of a Novel Guanine Nucleotide Exchange Factor for the Rho GTPase. *The Journal of Bio. Chem*., 271(41), 25452–25458.

Haus T., Akom E., Agwanda B., Hofreiter M., Roos C., & Zinner D. (2013). Mitochondrial Diversity and Distribution of African Green Monkeys (*Chlorocebus* Gray, 1870). *American Journal of Primatology*, 75(4), 350–360.

Hausdorff W.P., Pitcher J.A., Luttrell D.K., Linder M.E., Kurose H., Parsons S.J., Caron M.G. and Lefkowitz R.J. (1992). Tyrosine phosphorylation of G protein alpha subunits by pp60c-src. *Proceedings of the National Academy of Sciences USA*, 89(13), 5720–5724.

Henkel J.S., Baldwin M.R. and Barbieri J.T. (2010). Toxins from Bacteria. *EXS*, 100, 1–29.

Hepler J.R., Biddlecome G.H., Kleuss C., Camp L.A., Hofmann S.L., Ross E.M. and Gilman A.G. (1996). Functional Importance of the Amino Terminus of $G_q\alpha$. *J. Biol. Chem.*, 271, 496-504.

Hermans E. (2003). Biochemical and pharmacological control of the multiplicity of coupling at G-protein-coupled receptors. *Pharmacol Ther*., 99, 25–44.

Heximer S.P., Srinivasa S.P., Bernstein L.S., Bernard J.L., Linder, M.E., Hepler, J.R. and Blumer, K.J. (1999). G protein selectivity is a determinant of RGS2 function. *J Biol Chem*., 274(48), 34253-9.

Heydorn A., Ward R.J., Jorgensen R., Rosenkilde M.M., Frimurer T.M., Milligan G. and Kostenis E. (2004). Identification of a novel site within G protein alpha subunits important for specificity of receptor-G protein interaction. *Mol Pharmacol*., 66(2), 250-9.

Higgins T.E., Murphy A.C., Staddon J.M., Lax A.J. and Rozengurt E. (1992). Pasteurella multocida toxin is a potent inducer of anchorage-independent cell growth. *Proceedings of the National Academy of Sciences USA*, 89(10), 4240-4244.

Higgins J.B. and Casey P.J. (1996). The role of prenylation in G-protein assembly and function. *Cell. Signal*., 8, 433–437.

Hildebrand D., Walker P., Dalpke A., Heeg K. and Kubatzky K.F. (2010) Pasteurella multocida Toxin-induced Pim-1 expression disrupts suppressor of cytokine signalling (SOCS)-1 activity. *Cell. Microbiol*., 12, 1732–1745.

Hildebrand D., Heeg K. and Kubatzky K.F. (2015). Pasteurella multocidaToxin Manipulates T Cell Differentiation. *Frontiers in Microbiology*, 6, 1273.

Hill C.S., Wynne J. and Treisman R. (1995). The Rho-Family Gtpases Rhoa, Rac1, and Cdc42hs Regulate Transcriptional Activation by Srf. *Cell*, 81(7), 1159-1170.

Hill S.J. and Baker J.G. (2003). The ups and downs of Gs- to Gi-protein switching. *British Journal of Pharmacology*, 138(7), 1188–1189.

Hill, S.J. (2006). G-protein-coupled receptors: past, present and future. *British Journal of Pharmacology*, 147(Suppl 1), S27–S37.

Hofmann F., Busch C., Prepens U., Just I. and Aktories K. (1997). Localization of the glucosyltransferase activity of Clostridium difficile toxin B to the N-terminal part of the holotoxin. *J. Biol. Chem*., 272, 11074–11078.

Hoffman B.B., Dukes D.F. and Lefkowitz R.J. (1981). Alpha-adrenergic receptors in liver membranes: delineation with subtype selective radioligands. *Life Sci*., 28(3), 265-72.

Holmes W.R., Lin B., Levchenko A. and Edelstein-Keshet L. (2012). Modelling Cell Polarization Driven by Synthetic Spatially Graded Rac Activation. *PLOS*, 8(6), 1-13.

Holtzman, Eric. (1976). Lysosomes : a survey. Wien; New York:Springer-Verlag, pp 102 - 103.

Horstman A.L. and Kuehn M.J. (2002). Bacterial surface association of heat-labile enterotoxin through lipopolysaccharide after secretion via the general secretory pathway. *J. Biol. Chem*., 277, 32538-32545.

Hotulainen P. and Lappalainen P. (2006). Stress fibers are generated by two distinct actin assembly mechanisms in motile cells. *J. Cell Bio*., 173(3), 383-394.

Hoskins I.C., Thomas L.H. and Lax A.J. (1997). Nasal infection with Pasteurella multocida causes proliferation of bladder epithelium in gnotobiotic pigs. *Veterinary Record*, 140(1), 22-22.

Howe G.A. and Addison C.L. (2012). RhoB controls endothelial cell morphogenesis in part via negative regulation of RhoA. *Vascular Cell*, 4, 1-11.

Hsiao E.C., Boudignon B.M., Halloran B.P., Nissenson R.A. and Conklin B.R. (2010). G(s) G Protein-Coupled Receptor Signaling in Osteoblasts Elicits Age-Dependent Effects on Bone Formation. *Journal of Bone and Mineral Research*, 25(3), 584-593.

Huang C., Duncan J.A., Gilman A.G. and Mumby S.M. (1999). Persistent membrane association of activated and depalmitoylated G protein α subunits. *Proc. Natl. Acad. Sci. USA*, 96, 412-417.

Huang J.C., Wun W.S., Goldsby J.S., Matijevic-Aleksic N., Wu K.K. (2004). Cyclooxygenase-2-derived endogenous prostacyclin enhances mouse embryo hatching. *Hum. Reprod*., 19, 2900–2906.

Hubbard K.B. and Hepler J.R. (2006). Cell signalling diversity of the Gqa family of heterotrimeric G proteins. *Cellular Signalling*, 18, 135–150.

Iacovache I, Bischofberger M, van der Goot FG. 2010. Structure and assembly of pore-forming proteins.Curr. Opin. Struct. Biol. 20:241–246

Iniguez-Lluhi J.A., Simon M.I., Robishaw J.D. and Gilman A.G. (1992). G protein beta gamma subunits synthesized in Sf9 cells. Functional characterization and the significance of prenylation of gamma. *J Biol Chem*., 267(32), 23409-23417.

Jernigan, K. K., Cselenyi, C. S., Thorne, C. A., Hanson, A. J., Tahinci, E., Hajicek, N., … Lee, E. (2010). Gβγ Activates GSK3 to Promote LRP6-Mediated β-Catenin Transcriptional Activity. *Science Signaling*, *3*(121), ra37. http://doi.org/10.1126/scisignal.2000647

Jiang Y., Ma W., Wan Y., Kozasa T., Hattori S. and Huang X.Y. (1998). The G protein G alpha 12 stimulates Bruton's tyrosine kinase and a rasGAP through a conserved PH/BM domain. *Nature*, 395(6704), 808-813.

Jin T., Peng L., Mirshahi T., Rohacs T., Chan K.W., Sanchez R., Logothetis D.E. (2002). The βγ Subunits of G Proteins Gate a K^+ Channel by Pivoted Bending of a Transmembrane Segment. *Mol. Cell*., 10, 469–481.

Johanson J.F., Carney J.A., Go V.L. and Koch T.R. (1991). Segmental distribution of colonic neuropeptides in Hirschsprung's disease. *Regul Pept*., 36(1), 59-69.

Johnson M.A., Kaushik R.S., Francis D.H., Fleckenstein J.M. and Hardwidge P.R. (2009). Heat-Labile Enterotoxin Promotes Escherichia coli Adherence to Intestinal Epithelial Cells. *J. Bacteriol*., 191(1), 178-186.

Jones D.T. and Reed R.R. (1989) Golf: an olfactory neuron specific G-protein involved in odorant signal transduction. Science. 244:790–795.

Jones T. L. and Gutkind J. S. (1998). Galpha12 requires acylation for its transforming activity. *Biochemistry*, 37, 3196–3202.

Jones T.L., Simonds W.F., Merendino J.J., Brann M.R. and Spiegel A.M. (1990). Myristoylation of an inhibitory GTP-binding protein alpha subunit is essential for its membrane attachment. *Proceedings of the National Academy of Sciences USA*, 87(2), 568–572.

Juneja J., Cushman I. and Casey P.J. (2011). G12 signaling through c-Jun NH2-terminal kinase promotes breast cancer cell invasion. *PLoS One*, 6(11), e26085.

Just I., Mohr C., Schallehn G., Menard L., Didsbury J.R., Vandekerckhove J. et al. (1992). Purification and characterization of an ADP-ribosyltransferase produced by Clostridium limosum. *J Biol Chem*., 267, 10274–80.

Just I. et al. (1995). Glucosylation of Rho proteins by Clostridium difficile toxin B. *Nature*, 375, 500–503.

Just I. and Gerhard R. 2004. Large clostridial cytotoxins. Rev. Physiol. Biochem. *Pharmacol*., 152, 23-47.

Kadhum H.J., Finlay D., Rowe M.T., Wilson I.G. and Ball H.J. (2008). Occurrence and characteristics of cytotoxic necrotizing factors, cytolethal

distending toxins and other virulence factors in Escherichia coli from human blood and faecal samples. *Epidemiology and Infection*, 136(6), 752–760.

Kalinec G., Nazarali A.J., Hermouet S., Xu, N. and Gutkind J.S. (1992). Mutated alpha subunit of the Gq protein induces malignant transformation in NIH 3T3 cells. *Mol Cell Biol*., 12(10), 4687-4693.

Kamitani S. et al. (2011). Enzymatic actions of Pasteurella multocida toxin detected by monoclonal antibodies recognizing the deamidated alpha subunit of the heterotrimeric GTPase Gq. *FEBS J*., 278(15), 2702-2712.

Kamp T.J. and Hell, J.W. (2000). Regulation of Cardiac L-Type Calcium Channels by Protein Kinase A and Protein Kinase C. *Circ Res*., 87, 1095-1102.

Karnoub A.E. and Der C.J. Rho Family GTPases and Cellular Transformation. In: Madame Curie Bioscience Database [Internet]. Austin (TX): Landes Bioscience; 2000-2013. Available from: http://www.ncbi.nlm.nih.gov/books/NBK6594/

Katoh K., Kano Y., Amano M., Onishi H., Kaibuchi K. and Fujiwara K. (2001a). Rho-kinase-mediated contraction of isolated stress fibers. *J. Cell Biol*., 153, 569-584.

Katoh K., Kano Y., Amano M., Kaibuchi K. and Fujiwara K. (2001b). Stress fiber organization regulated by MLCK and Rho-kinase in cultured human fibroblasts. *Am J. Physiol Cell Physiol*., 280, C1669-C1679.

Katoh, K., Kano, Y., and Noda, Y. (2011). Rho-associated kinase-dependent contraction of stress fibres and the organization of focal adhesions. *Journal of the Royal Society Interface*, 8(56), 305–311.

Kaziro Y., Itoh H., Kozasa T., Nakafuku M. and Satoh T. (1991). Structure and function of signal-transducing GTP-binding proteins. *Annu. Rev. Biochem*., 60, 349-400.

Kenakin T. (1995a). Agonist-receptor efficacy. I: Mechanisms of efficacy and receptor promiscuity. *Trends Pharmacol Sci*., 16(6), 188-92.

Kenakin T. (1995b). Agonist-receptor efficacy. II. Agonist trafficking of receptor signals. *Trends Pharmacol Sci*., 16(7), 232-8.

Khan S.M., Sleno R., Gora S., Zylbergold P., Laverdure J., Labbé J., Miller G.J. and Hébert T.E. (2013). The Expanding Roles of Gbg Subunits in G Protein–Coupled Receptor Signaling and Drug Action. *Pharmacol Rev*., 65, 545–577.

Kitadokoro K., Kamitani S., Miyazawa M., Hanajima-Ozawa M., Fukui A., Miyake M. and Horiguchi Y. (2007). Crystal structures reveal a thiol protease-like catalytic triad in the C-terminal region of Pasteurella multocida toxin. *Proc Natl Acad Sci U S A*, 104(12), 5139-5144.

Klages B., Brandt U., Simon M.I., Schultz G. and Offermanns S. (1999). Activation of G_{12}/G_{13} Results in Shape Change and Rho/Rho-Kinase–mediated Myosin Light Chain Phosphorylation in Mouse Platelets. *The Journal of Cell Biology*, 144(4), 745–754.

Klein S., Reuveni H. and Levitzki A. (2000). Signal transduction by a nondissociable heterotrimeric yeast G protein. *Proc Natl Acad Sci USA*, 97(7), 3219-3223.

Kleuss C., Hescheler J., Ewel C., Rosenthal W., Schultz G. and Wittig B. (1991). Assignment of G-protein subtypes to specific receptors inducing inhibition of calcium currents. *Nature*, 353(6339), 43-48.

Kleuss C., Scherubl H., Hescheler J., Schultz G. and Wittig B. (1992). Different beta-subunits determine G-protein interaction with transmembrane receptors. *Nature*, 358(6385), 424-426.

Kleuss C., Scherubl H., Hescheler J., Schultz G. and Wittig B. (1993). Selectivity in signal transduction determined by gamma subunits of

heterotrimeric G proteins. *Science,* 259(5096), 832-834.

Kleuss C., Raw A.S., Lee E., Sprang S.R., Gilman A.G. (1994). Mechanism of GTP hydrolysis by G-protein alpha subunits. *Proc Natl Acad Sci USA*, 91, 9828–31.

Klinge C., Rao C., Glob. libr. women's med., (ISSN: 1756-2228) 2008; DOI 10.3843/GLOWM.10282

Kochs E., Werner C., Hoffman W.E., Mollenberg O. and Schulte am Esch J. (1991). Concurrent increases in brain electrical activity and intracranial blood flow velocity during low-dose ketamine anaesthesia. *Can J Anaesth*., 38(7), 826-830.

Kozasa T., Hepler J.R., Smrcka A.V., Simon M.I., Rhee S.G., Sternweis P.C. and Gilman A.G. (1993). Purification and characterization of recombinant G16 from Sf9 cells: activation of purified phospholipase C isozymes by G-protein subunits. *Proc Natl Acad Sci USA*, 90, 9176–9180.

Kozasa T. and Gilman A.G. (1996). Protein kinase C phosphorylates G12 alpha and inhibits its interaction with G beta gamma. *J Biol Chem*., 271(21), 12562-7.

Kozasa T., Jiang X., Hart M. J., Sternweis P.M., Singer W.D., Gilman A.G., Bollag G., Sternweis P.C. (1998). p115 RhoGEF, a GTPase activating protein for Galpha12 and Galpha13. *Science*, 280(5372), 2109-11.

Krumins A.M. and Gilman A.G. (2006). Targeted knockdown of G protein subunits selectively prevents receptor-mediated modulation of effectors and reveals complex changes in non-targeted signaling proteins. *J Biol Chem.*, 281(15), 10250-62.

Kubota S., Kubota H. and Nagata K. (2006). Cytosolic chaperonin protects folding intermediates of Gβ from aggregation by recognizing hydrophobic β-strands. *Proc. Natl. Acad. Sci. USA,* 103, 8360–8365.

Kuehne S.A., et al. 2010. The role of toxin A and toxin B in Clostridium difficile infection. *Nature*, 467, 711–713.

Krupinski J., Rajaram R., Lakonishok M., Benovic J.L., Cerione R.A. (1988). Insulin-dependent phosphorylation of GTP-binding proteins in phospholipid vesicles. *J Biol Chem*. 263(25), 12333-41.

Kuroda S., Fukata M., Fujii K., Nakamura T., Izawa I. and Kaibuchi K. (1997). Regulation of Cell–Cell Adhesion of MDCK Cells by Cdc42 and Rac1 Small GTPases. *Biochemical and Biophysical Research Communications*, 240(2), 430–435.

Lacerda H.M., Lax A.J. and Rozengurt E. (1996). Pasteurella multocida toxin, a potent intracellularly acting mitogen, induces p125FAK and paxillin tyrosine phosphorylation, actin stress fiber formation, and focal contact assembly in Swiss 3T3 cells. *J Biol Chem*., 271(1), 439-445.

LaMorte V.J., Goldsmith P.K., Spiegel A.M., Meinkoth J.L. and Feramisco J.R. (1999). Inhibition of DNA synthesis in living cells by microinjection of Gi2 antibodies. *J Biol Chem*., 267(2), 691-4.

Lax A.J. and Chanter N. (1990). Cloning of the Toxin Gene from Pasteurella-Multocida and Its Role in Atrophic Rhinitis. *Journal of General Microbiology*, 136, 81-87.

Lax A.J., Pullinger G.D., Baldwin M.R., Harmey D., Grigoriadis A.E. and Lakey J.H. (2004). The pasteurella multocida toxin interacts with signalling pathways to perturb cell growth and differentiation. *Int J Med Microbiol*., 293(7-8), 505-512.

Lax A.J. and Grigoriadis A.E. (2001). Pasteurella multocida toxin: the mitogenic toxin that stimulates signalling cascades to regulate growth and differentiation. *Int J Med Microbiol*., 291, 261–268.

Lecker S.H., Goldberg A.L., Mitch W.E. (2006). Protein degradation by the ubiquitin-proteasome pathway in normal and disease states. *J Am Soc Nephrol.*, 17(7), 1807-19.

Lee S.B., Shin S.H., Hepler J.R., Gilman A.G. and Rhee S.G. (1993). Activation of phospholipase C-β2 mutants by G protein α_q and βγ subunits. *J Biol. Chem*., 268, 25952-25957.

Lee C.M., Chang P.P., Tsai S.C., Adamik R., Price S.R., Kunz B.C., Moss J., Twiddy E.M., Holmes, R.K. (1991). Activation of Escherichia coli heat-labile enterotoxins by native and recombinant adenosine diphosphate-ribosylation factors, 20-kD guanine nucleotide-binding proteins. *Journal of Clinical Investigation*, 87(5), 1780–1786.

Leff P. (1995). The two-state model of receptor activation. *Trends Pharmacol Sci*., 16(3), 89-97.

Lefkowitz R.J., Mukherjee C., Coverstone M. and Caron M.G. (1974). Stereospecific ^{3}H (-)-alprenolol binding sites, beta-adrenergic receptor and adenylate cyclase. Biochem. Biophys. *Res. Commun*., 60, 703–709.

Lefkowitz R.J., Cotecchia S., Samama P., Costa T. (1993). Constitutive activity of receptors coupled to guanine nucleotide regulatory proteins. *Trends Pharmacol Sci*., 14(8),303-7.

Lefkowitz R.J., Pierce K.L., and Lutrell L.M. (2002). Dancing with different partners: protein kinase A phosphorylation of seven membrane-spanning receptors regulates their G-protein coupling specificity. *Mol. Pharmacol*., 62, 971–974.

Lefkowitz R.J. (2004) Historical review: A brief history and personal retrospective of seven-transmembrane receptors. *TRENDS in Pharmacological Sciences*, 25(8), 413-422.

Lefkowitz R. and Shenoy S. (2005). Transduction of receptor signals by beta-arrestins. *Science*, 308, 512–517.

Lefkowitz R.J. (2013). A Brief History of G-Protein Coupled Receptors (Nobel Lecture). *Angew Chem. Int. Ed*., 52, 6366–6378.

Lemichez E., Flatau G., Bruzzone M., Boquet P. and Gauthier M. (1997). Molecular localization of the Escherichia coli cytotoxic necrotizing factor CNF1 cell-binding and catalytic domains. *Mol Microbiol*., 24(10), 61-70.

Lemichez E. and Barbieri J.T. (2013). General Aspects and Recent Advances on Bacterial Protein Toxins. *Cold Spring Harbor Perspectives in Medicine*, 3(2), a013573.

Leninger, A.L. Biochemistry, 2nd ed., Worth Publishers, New York, 1975.

Lerm M., Schmidt G., Goehring U.M., Schirmer J. and Aktories K. (1999). Identification of the region of rho involved in substrate recognition by Escherichia coli cytotoxic necrotizing factor 1 (CNF1). *J. Biol. Chem*., 274, 28999-29004.

Leung T., Chen X. Q., Manser E. and Lim L. (1996). The p160 RhoA-binding kinase ROKα is a member of a kinase family and is involved in the reorganization of the cytoskeleton. *Mol. Cell. Biol*., 16, 5313–5327.

Levitzki A. and Klein S. (2002). G-protein subunit dissociation is not an integral part of G-protein action. *Chembiochem*., 3(9), 815-8.

Li B., Zhong H., Scheuer T. and Catterall W.A. (2004). Functional role of a C-terminal Gbetagamma-binding domain of Ca(v)2.2 channels. *Mol Pharmacol*., 66(3),761-769.

Li G. and Iyengar R. (2002). Calpain as an effector of the Gq signaling pathway for inhibition of Wnt/beta -catenin-regulated cell proliferation. *Proc Natl Acad Sci USA*, 99(20), 13254-13259.

Liebmann C., Graneß A., Boehmer A., Kovalenko M., Adomeit A., Steinmetzer T., Nurnbergi B., Wetzker R., and Boehmer F. (1996). Tyrosine Phosphorylation of G_s^{α} and Inhibition of Bradykinin-induced Activation of the

Cyclic AMP Pathway in A431 Cells by Epidermal Growth Factor Receptor. *The Journal of Biological Chemistry*, 271, 31098-31105.

Lin Y. and Smrcka A. V. (2011). Understanding molecular recognition by G protein betagamma subunits on the path to pharmacological targeting. *Mol Pharmacol*., 80(4), 551-557.

Little P.J., Burch M.L. and Osman N. (2012). The Growing Promiscuity of G Protein Coupled Receptors. *Clin Exp Pharmacol*., 2:3, 1-2.

Lloret A., Egberink H., Addie D., Belák S., Boucraut-Baralon C., Frymus T., Gruffydd-Jones T., Hartmann K., Hosie M.J., Lutz H., Marsilio F., Möstl K., Pennisi M.G., Radford A.D., Thiry E., Truyen U. and Horzinek M.C. (2013). PASTEURELLA MULTOCIDA INFECTION IN CATS ABCD guidelines on prevention and management. *Journal of Feline Medicine and Surgery*, 15, 570–572.

Locht C. (1999). Molecular aspects of Bordetella pertussis pathogenesis. *Int Microbiol*., 2(3), 137-44.

Locht C., Coutte L. and Mielcarek N. (2011). The ins and outs of pertussis toxin. *FEBS J*., 278(23), 4668-82.

Lodish H., Berk A., Zipursky S.L., et al. Molecular Cell Biology. 4th edition. New York: W. H. Freeman; 2000. Section 20.3, G Protein –Coupled Receptors and Their Effectors. Available from: http://www.ncbi.nlm.nih.gov/books/NBK21718/

Logothetis D.E., Kurachi Y., Galper J., Neer E.J. and Clapham D.E. (1987). The beta gamma subunits of GTP-binding proteins activate the muscarinic K+ channel in heart. *Nature*, 325(6102), 321-326.

Los, F. C. O., Randis, T. M., Aroian, R. V., & Ratner, A. J. (2013). Role of Pore-Forming Toxins in Bacterial Infectious Diseases. *Microbiology and Molecular Biology Reviews : MMBR*, *77*(2), 173–207.

Luttrell L.M., Ferguson S.S.G., Daaka Y., Miller W.E., Maudsley S., Della Rocca G.J., Lin F.T., Kawakatsu H., Owada K., Luttrell D.K. et al. (1999) b-arrestin-dependent formation of b2 adrenergic receptor-Src protein kinase complexes. *Science*, 283, 655-661.

Luttrell L.M. and Lefkowitz R.J. (2002). The role of β-arrestins in the termination and transduction of G-protein-coupled receptor signals. *Journal of Cell Science*, 115, 455-465.

Lutz S., Shankaranarayanan A., Coco C., Ridilla M., Nance M.R., Vettel C., Baltus D., Evelyn C.R., Neubig R.R., Wieland T. and Tesmer J.J. (2007).

Structure of Galphaq-p63RhoGEF-RhoA complex reveals a pathway for the activation of RhoA by GPCRs. *Science*, 318(5858), 1923-7.

Lyon A.M. and Tesmer J.J.G. (2013). Structural Insights into Phospholipase C-β Function. *Molecular Pharmacology*, 84(4), 488–500.

Maehle A.H. (2009). A binding question: the evolution of the receptor concept. *Endeavour*, 33:4, 135 – 140.

Maier U., Babich A. and Nürnberg B. (1999). Roles of non-catalytic subunits in gbetagamma-induced activation of class I phosphoinositide 3-kinase isoforms b and g. *J Biol Chem*., 274, 29311–29317.

Malbon C.C. (2005). G proteins in development. *Nat Rev Mol Cell Biol*., 6(9), 689-701.

Mamidipudi V., Chang B.Y., Harte R.A., Lee K.C. and Cartwright C.A. (2004). RACK1 inhibits the serum- and anchorage-independent growth of v-Src transformed cells. *FEBS Lett*., 567(2-3), 321-6.

Manganello J.M., Huang J. S., Kozasa T., Voyno-Yasenetskaya T.A., Le Breton G.C. (2003). Protein kinase A-mediated phosphorylation of the Galpha13 switch I region alters the Galphabetagamma13-G protein-coupled receptor complex and inhibits Rho activation. *J Biol Chem*., 278(1), 124-30.

Marrari Y., Crouthamel M., Irannejad R. and Wedegaertner P.B. (2007). Assembly and trafficking of heterotrimeric G proteins. *Biochemistry*, 46, 7665–7677.

Marx C., Held J.M., et al. (2010). ErbB2 Trafficking and Degradation Associated with K48 and K63 Polyubiquitination. *Cancer Res*., 70, 3709–3717.

Maudsley S., Martin B. and Luttrell L.M. (2005). The Origins of Diversity and Specificity in G Protein-Coupled Receptor Signaling. *The Journal of Pharmacology and Experimental Therapeutics*, 314(2), 485–494.

Marinissen M.J., Servitja J.M., Offermanns S., Simon M.I. and Gutkind J.S. (2003). Thrombin protease-activated receptor-1 signals through Gq- and G13-initiated MAPK cascades regulating c-Jun expression to induce cell transformation. *J Biol Chem*., 278(47), 46814-25.

Matsuzawa T., Fukui A., Kashimoto T., Nagao K., Oka K., Miyake M., and Horiguchi Y. (2004). Bordetella Dermonecrotic Toxin Undergoes Proteolytic Processing to Be Translocated from a Dynamin-related Endosome into the Cytoplasm in an Acidification-independent Manner. *Journal of Biological Chemistry*, 279(4), 2866–2872.

Mberu E. K., Wansor T., Sato H., Nishikawa Y. and Watkins W. M. (1995). Japanese poor metabolizers of proguanil do not have an increased risk of malaria chemoprophylaxis breakthrough. *Trans R Soc Trop Med Hyg*., 89(6), 658-659.

McCudden C.R., Hains M.D., Kimple R.J. Siderovski D.P. and Willard F.S. (2005). G-protein signaling: back to the future. *Cellular and Molecular Life Sciences*, 62(5), 551–577.

Meigs T.E., Fields T.A., Mckee, D.D. (2001). Interaction of Ga12 and Ga13 with the cytoplasmic domain of cadherin provides a mechanism for b-catenin release. *Proceedings of the National Academy of Sciences USA*, 98(2), 9-24.

Meoli, L. (2010). Comprehensive phenotyping of two mouse mutants reveals a potential novel role of G protein-coupled receptor 30. (Doctoral Thesis Max-Planck Institute, Berlin, Germany). Retrieved from http://edoc.hu-berlin.de/dissertationen/meoli-luca-2010-08-03/PDF/meoli.pdf.

Mignone F., Gissi C., Liuni S. and Pesole G. (2002). Untranslated regions of mRNAs. *Genome Biology*, 3(3), reviews0004.1–reviews0004.10.

Milligan G. and Kostenis E. (2006). Heterotrimeric G-proteins: a short history. *British Journal of Pharmacology*, 147(Suppl 1), S46–S55.

Mills M., Meysick K.C. and O'Brien A.D. (2000). Cytotoxic Necrotizing Factor Type 1 of Uropathogenic Escherichia coli Kills Cultured Human Uroepithelial 5637 Cells by an Apoptotic Mechanism. *Infection and Immunity*, 68(10), 5869–5880.

Mirshahi T., Mittal V., Zhang H., Linder M.E. and Logothetis D.E. (2002). Distinct sites on G protein beta gamma subunits regulate different effector functions. *J Biol Chem*., 277(39), 36345-36350.

Mirshahi T., Jin T., and Logothetis D.E. (2003). Gβγ and K_{ACh}: old story, new insights. *Sci STKE*, (194), PE32.

Miyata M., Kogure A., Sato H., Kodama E., Watanabe H., Ohira H., Kuroda M., Takagi T., Sato Y. and Kasukawa R. (1995). Detection of antibodies to 65 KD heat shock protein and to human superoxide dismutase in autoimmune hepatitis-molecular mimicry between 65 KD heat shock protein and superoxide dismutase. *Clin Rheumatol*., 14(6), 673-677.

Mizuno N. and Itoh H. (2009). Functions and Regulatory Mechanisms of Gq-Signaling Pathways. *Neurosignals*,17, 42-54.

Modiano J.F., Ritt M.G., Wojcieszyn J. and Smith R. (1999). Growth arrest of melanoma cells is differentially regulated by contact inhibition and serum deprivation. *DNA Cell Biol*., 18, 357-67.

Mohamed A.J., et al. (2009). Bruton's tyrosine kinase (Btk): function, regulation, and transformation with special emphasis on the PH domain. *Immunological reviews*, 228, 58–73.

Morales J., Fishburn C.S., Wilson P.T. and Bourne H.R. (1998). Plasma Membrane Localization of $G\alpha_z$ Requires Two Signals. *Molecular Biology of the Cell*, 9(1), 1–14.

Moreira I.S. (2014). Structural features of the G-protein/GPCR interactions. *Biochim Biophys Acta*., (1), 16-33.

Moss J. and Vaughan M. (1991). Activation of cholera toxin and Escherichia coli heat-labile enterotoxins by ADP-ribosylation factors, a family of 20 kDa guanine nucleotide-binding proteins. *Mol Microbiol*., 5(11), 2621-7.

Mullan P.B. and Lax A.J. (1996). Pasteurella multocida toxin is a mitogen for bone cells in primary culture. *Infect Immun*., 64(3), 959-965.

Mumby S.M., Kleuss C. and Gilman A.G. (1994). Receptor regulation of G-protein palmitoylation. *Proceedings of the National Academy of Sciences USA*, 91(7), 2800–2804.

Murakami S., Horimoto T., Ito M., Takano R., Katsura H., Shimojima M.and Kawaoka Y. (2012). Enhanced Growth of Influenza Vaccine Seed Viruses in

Vero Cells Mediated by Broadening the Optimal pH Range for Virus Membrane Fusion. *Journal of Virology*, 86(3), 1405–1410.

Murga C., Laguinge L., Wetzker R., Cuadrado A. and Gutkind J. (1998). Activation of Akt/protein kinase B by G protein-coupled receptors. *J. Biol. Chem.*, 273,19080–19085.

Murphy A.C. and Rozengurt E. (1992). Pasteurella multocida toxin selectively facilitates phosphatidylinositol 4,5-bisphosphate hydrolysis by bombesin, vasopressin, and endothelin. Requirement for a functional G protein. *The Journal of Biological Chemistry*, 267(35), 25296-303.

Nagahama M. et al. (2011). Clostridium perfringens TpeL glycosylates the Rac and Ras subfamily proteins. *Infect Immun*., 79, 905–910.

Nagao M., Yamauchi J., Kaziro Y., and Itoh H. (1998). Involvement of Protein Kinase C and Src Family Tyrosine Kinase in Gaq/11-induced Activation of c-Jun N-terminal Kinase and p38 Mitogen-activated Protein Kinase. *The Journal of Bio. Chem*., 273(36), 22892–22898.

Nakashima A., Takeuchi H., Imai T., Saito H., Kiyonari H., Abe T., Chen M., Weinstein L.S., Yu C.R., Storm D.R. and Nishizumi H., Sakano H. (2013). Agonist-independent GPCR activity regulates anterior-posterior targeting of olfactory sensory neurons. *Cell*, 154(6), 1314-25.

Narumiya S., Tanji M. and Ishizaki T. (2009). Rho signaling, ROCK and mDia1, in transformation, metastasis and invasion. Cancer and Metastasis *Reviews*, 28(1), 65-76.

Nataro J.P. and Kaper J.B. (1998). Diarrheagenic Escherichia coli. *Clin. Microbiol. Rev*., 11, 142-201.

Naumanen P., Lappalainen P. and Hotulainen P. (2008). Mechanisms of actin stress fibre assembly. *J Microsc*., 231(3), 446-54.

Neer E. J., Schmidt C. J., Nambudripad R. and Smith T. F. (1994). The ancient regulatory-protein family of WD-repeat proteins. *Nature*, 371(6495), 297-300.

Neer, E.J. (1995). Heterotrimeric G proteins: organization of transmembrane signals. *Cell*, 80, 249–251.

Nelson P.J. and Daniel T.O. (2002). Emerging targets: molecular mechanisms of cell contact-mediated growth control. *Kidney Int*., 61(1), S99-105.

Nelson, J. (2008). Structure and Function in Cell Signalling. West Sussex: John Wiley & Sons. p. 216.

Nielsen M.D., Chan G.C.K., Poser S.W. and Storm D.R. (1996). Differential regulation of type I and type VIII Ca2+-stimulated adenylyl cyclases by Gi-coupled receptors in vivo. *J Biol Chem*., 271(52), 33308–33316.

Niebur E., Schuster H. G., Kammen D. M. and Koch C. (1991). Oscillator-phase coupling for different two-dimensional network connectivities. *Phys Rev A*., 44(10), 6895-6904.

Nishimura A., Okamoto M., Sugawara Y., Mizuno N., Yamauchi J., Itoh H. (2006). Ric-8A potentiates Gq-mediated signal transduction by acting downstream of G protein-coupled receptor in intact cells. *Genes Cells*, 11(5), 487-98.

Niu J., Profirovic J., Pan H., Vaiskunaite R. and Voyno-Yasenetskaya T. (2003). G Protein βγ Subunits Stimulate p114RhoGEF, a Guanine Nucleotide Exchange Factor for RhoA and Rac1 Regulation of Cell Shape and Reactive Oxygen Species Production. *Circ Res*., 93, 848-856.

Nobes C.D. and Hall A. (1995). Rho, rac and cdc42 GTPases: regulators of actin structures, cell adhesion and motility. *Biochem Soc Trans*., 23(3), 456-9.

Offermanns S., Mancino V., Revel J.P. and Simon, M.I. (1997). Vascular system defects and impaired cell chemokinesis as a result of Galpha13 deficiency. *Science*, 275, 533–536.

Oh P. and Schnitzer J.E. (2001). Segregation of Heterotrimeric G Proteins in Cell Surface Microdomains: G_q Binds Caveolin to Concentrate in Caveolae, whereas G_i and G_s Target Lipid Rafts by Default. *Molecular Biology of the Cell*, 12(3), 685–698.

O'Neill M.D. (2012) Bringing GPCR Research to the Fore. [Online] 32 (8). Available from: http://www.genengnews.com/keywordsandtools/print/1/26745/ [Accessed: 3 February 2013] (Dupre, Robitaille, Rebois, and Hebert, 2009).

Ong O.C., Yamane H.K., Phan K.B., Fong H.K., Bok D., Lee R.H. and Fung B.K. (1995). Molecular cloning and characterization of the G protein gamma subunit of cone photoreceptors. *J Biol Chem*., 270(15), 8495-8500.

Orth J.H. and Aktories K. (2010). Pasteurella multocida toxin activates various heterotrimeric G proteins by deamidation. *Toxins (Basel),* 2(2), 205-214.

Orth J.H., Aktories K. and Kubatzky K.F. (2007). Modulation of host cell gene expression through activation of STAT transcription factors by Pasteurella multocida toxin. *J Biol Chem*., 282(5),3050-3057.

Orth J. H., Fester I., Siegert P., Weise M., Lanner U., Kamitani, S., Tachibana T., Wilson B. A., Schlosser A., Horiguchi Y. and Aktories, K. (2013). Substrate specificity of Pasteurella multocida toxin for alpha subunits of heterotrimeric G proteins. *FASEB J*., 27(2), 832-842.

Orth J.H., Lang S., Taniguchi M. and Aktories K. (2005). Pasteurella multocida toxin-induced activation of RhoA is mediated via two families of G{alpha} proteins, G{alpha}q and G{alpha}12/13. *J Biol Chem*., 280(44), 36701-36707.

Orth J.H.C., Fester I., Siegert P., Weise M., Lanner U., Kamitani S., … Aktories K. (2013). Substrate specificity of Pasteurella multocida toxin for α subunits of heterotrimeric G proteins. *The FASEB Journal*, 27(2), 832–842.

Osada N., Kohara A., Yamaji T., Hirayama N., Kasai F., Sekizuka T., … Hanada K. (2014). The Genome Landscape of the African Green Monkey Kidney-Derived Vero Cell Line. *DNA Research: An International Journal for Rapid Publication of Reports on Genes and Genomes*, 21(6), 673–683.

Oswald E., Sugai M., Labigne A., Wu H. C., Fiorentini C., Boquet P., et al. (1994). Cytotoxic necrotizing factor type 2 produced by virulent Escherichia coli modifies the small GTP-binding proteins Rho involved in assembly of actin stress fibers. *Proc Natl Acad Sci*., 91, 3814-8.

Oubrahim H., Wong A., Wilson B. A. and Chock P. B. (2013). Mammalian Target of Rapamycin Complex 1 (mTORC1) Plays a Role in Pasteurella multocida Toxin (PMT)-induced Protein Synthesis and Proliferation in Swiss 3T3 Cells. *The Journal of Biological Chemistry*, 288(4), 2805–2815.

Parekh H.K., Adikari M. and Vennapusa B. (2006). Differential partitioning of Gαi1 with the cellular microtubules: a possible mechanism of development of Taxol resistance in human ovarian carcinoma cells. Journal of Molecular Signaling. 1(3):1-12.

Pascal L.E., True L.D., Campbell D.S., Deutsch E.W., Risk M., Coleman I. M. Eichner L.J., Nelson P.S. and Liu A.Y. (2008). Correlation of mRNA and protein levels: Cell type-specific gene expression of cluster designation antigens in the prostate. *BMC Genomics*, 9(246), 1-13.

Patterson R.L., van Rossum D.B., Barrow R.K. and Snyder S.H. (2004). RACK1 binds to inositol 1,4,5-trisphosphate receptors and mediates Ca^{2+}release. *Proceedings of the National Academy of Sciences USA*, 101(8), 2328–2332.

Park P.S., Lodowski D.T. and Palczewski K. (2008). Activation of G protein-coupled receptors: beyond two-state models and tertiary conformational changes. *Annu Rev Pharmacol Toxicol*., 48, 107-41.

Park D., O'Doherty I., Somvanshi R.K., Bethke A., Schroeder, Kumar U. and Riddle D.L. (2012). Interaction of structure-specific and promiscuous G-protein–coupled receptors mediates small-molecule signaling in Caenorhabditis elegans. *PNAS*, 109, 25 9917–9922.

Paulssen R.H., Woodson J., Liu Z. and Ross E.M. (1996). Carboxyl-terminal fragments of phospholipase C-beta1 with intrinsic Gq GTPase-activating protein (GAP) activity. *J Biol Chem*., 271(43), 26622-9.

Pellegrin S. and Mellor H. (2007). Actin Stress Fibres. *Journal of Cell Science*, 120, 3491-3499.

Peng L.Y., Mirshahi T., Zhang H.L., Hirsch J.P. and Logothetis D.E. (2003). Critical determinants of the G protein gamma subunits in the G beta gamma stimulation of G protein-activated inwardly rectifying potassium (GIRK) channel activity. *Journal of Biological Chemistry*, 278(50), 50203-50211.

Pennings A.M. and Storm P.K. (1984). A test in vero cell monolayers for toxin production by strains of Pasteurella multocida isolated from pigs suspected of having atrophic rhinitis. *Vet Microbiol*., 9(5), 503-508.

Pfeifer G., Schirmer J., Leemhuis J., Busch C., Meyer D. K., Aktories K. and Barth H. (2003). Cellular uptake of *Clostridium difficile* toxin B. Translocation of the N-terminal catalytic domain into the cytosol of eukaryotic cells. *J. Biol. Chem*., 278,44535–44541.

Pitcher J.A., Fredericks Z.L., Stone W.C., Premont R.T., Stoffel R.H., Koch W.J., Lefkowitz R.J. (1996). Phosphatidylinositol 4,5-bisphosphate (PIP2)-enhanced G protein-coupled receptor kinase (GRK) activity. Location, structure, and regulation of the PIP2 binding site distinguishes the GRK subfamilies. *J Biol Chem*., 271(40), 24907-13.

Plummer N.W. et al. (2012). Development of the Mammalian Axial Skeleton Requires Signaling through the Gαi Subfamily of Heterotrimeric G Proteins. *Proceedings of the National Academy of Sciences USA*, 109(52), 21366–21371.

Pollard T.D. and Cooper J.A. (2009). Actin, a Central Player in Cell Shape and Movement. *Science*, 326(5957), 1208–1212.

Ponimaskin E., Behn H., Adarichev V., Voyno-Yasenetskaya T.A., Offermanns S. and Schmidt M.F. (2000). Acylation of Galpha(13) is important for its interaction with thrombin receptor, transforming activity and actin stress fiber formation. *FEBS Lett*., 478(1-2), 173-7.

Prasad M.V.V. S.V., Shore S.K. and Dhanasekaran N. (1994). Activated Mutant of G-Alpha(13) Induces Egr-1, C-Fos, and Transformation in Nih 3t3 Cells. *Oncogene*, 9(8), 2425-2429.

Prather P.L., Loh H.H. and Law P.Y. (1994). Interaction of delta-opioid receptors with multiple G proteins: a non-relationship between agonist potency to inhibit adenylyl cyclase and to activate G proteins. *Mol Pharmacol*., 45(5), 997-1003.

Preuss I., Kurig B., Nurnberg B., Orth J.H. and Aktories K. (2009). Pasteurella multocida toxin activates Gbetagamma dimers of heterotrimeric G proteins. *Cell Signal*., 21(4), 551-558.

Preuss H.D., Orth J.H., Aktories K. and Kubatzky K.F. (2010) Pasteurella multocida toxin is a potent activator of anti-apoptotic signalling pathways. *Cell Microbiol*., 12(8), 1174-85.

Pronin A.N. and Gautam N. (1992). Interaction between G-protein beta and gamma subunit types is selective. *Proc Natl Acad Sci USA*, 89(13), 6220-6224.

Pruitt K.D., Harrow J., Harte R. A., Wallin C., Diekhans M., Maglott, D.R., … Lipman D. (2009). The consensus coding sequence (CCDS) project:

Identifying a common protein-coding gene set for the human and mouse genomes. *Genome Research*, 19(7), 1316–1323.

Pullinger G.D., Bevir T. and Lax, A.J. (2004). The Pasteurella multocida toxin is encoded within a lysogenic bacteriophage. *Mol Microbiol*., 51(1), 255-269.

Pullinger G.D. and Lax A.J. (2007). Histidine Residues at the Active Site of the Pasteurella multocida Toxin. *Open Biochem J*., 1, 7-11.

Pullinger G.D., Sowdhamini R. and Lax A.J. (2001). Localization of functional domains of the mitogenic toxin of Pasteurella multocida. *Infect Immun*., 69(12), 7839-7850.

Purves D., Augustine G.J., Fitzpatrick D., et al., editors. Neuroscience. 2nd edition. Sunderland (MA): Sinauer Associates; 2001. G-Proteins and Their Molecular Targets. Available from: http://www.ncbi.nlm.nih.gov/books/NBK10832/

Pyne N.J. and Pyne S. (2011). Receptor tyrosine kinase-G-protein-coupled receptor signalling platforms: out of the shadow? *Trends Pharmacol Sci*., 32(8), 443-50.

Radhika V. and Dhanasekaran N. (2001). Transforming G proteins. *Oncogene*, 20(13), 1607-1614.

Rajakylä E.K. and Vartiainen M.K. (2014). Rho, nuclear actin, and actin-binding proteins in the regulation of transcription and gene expression. *Small GTPases*, 5(1), e27539.

Ramachandran G. (2014). Gram-positive and gram-negative bacterial toxins in sepsis: A brief review. *Virulence*, 5(1), 213–218.

Rebois R.V., Warner D.R. and Basi N.S. (1997). Does subunit dissociation necessarily accompany the activation of all heterotrimeric G proteins! *Cellular Signalling*, 9(2), 141-151.

Rebres R.A., Roach T.I., Fraser I.D., Philip F., Moon C., Lin, K.M., Liu J. Santat L., Cheadle L., Ross E.M., Simon M.I., and Seaman W.E. (2011). Synergistic Ca2+ responses by G{alpha}i- and G{alpha}q-coupled G-protein-coupled receptors require a single PLC{beta} isoform that is sensitive to both G{beta}{gamma} and G{alpha}q. *J Biol Chem*., 286(2), 942-951.

Rehm A. and Ploegh H.L. (1997). Assembly and Intracellular Targeting of the βγ Subunits of Heterotrimeric G Proteins. *The Journal of Cell Biology*, 137(2), 305–317.

Rajendram R., Preedy, V.R. and Hunter R.J., “Cellular Effects of Bacterial Toxins: Implications for Foodborned Illness,” in Preedy, V.R. and Watson, R.R, ed., Reviews in Food and Nutrition Toxicity 2 (MA: CRC Press, 2003) 189-212.

Reineke J., Tenzer S., Rupnik M., Koschinski A., Hasselmayer O., Schrattenholz A., Schild H., Von Eichel-Streiber C. (2007). Autocatalytic cleavage of Clostridium difficile toxin B. *Nature*, 446, 415–419.

Repella T.L., Ho, M., Chong T.P.M., Bannai Y. and Wilson B.A. (2011). Arf6-Dependent Intracellular Trafficking of Pasteurella multocida Toxin and pH-Dependent Translocation from Late Endosomes. *Toxins*, 3(3), 218–241.

Ridley A.J. and Hall A. (1992). The small GTP-binding protein rho regulates the assembly of focal adhesions and actin stress fibers in response to growth factors. *Cell*, 70(3), 389-99.

Riento K., Guasch R.M., Garg R., Jin B., and Ridley A.J. (2003). RhoE Binds to ROCK I and Inhibits Downstream Signaling. *Molecular and Cellular Biology*, 23(12), 4219–4229.

Riobo N.A. and Manning D.R. (2005). Receptors coupled to heterotrimeric G proteins of the G12 family. *Trends Pharmacol Sci*., 26, 146–154.

Robillard L., Ethier N., Lachance M. and Hebert T.E. (2000). Gbetagamma subunit combinations differentially modulate receptor and effector coupling in vivo. *Cell Signal*., 12(9-10), 673-682.

Robishaw J.D. and Berlot C.H. (2004). Translating G protein subunit diversity into functional specificity. *Curr Opin Cell Biol*., 16(2), 206-209.

Rodbell M., Birnbaumer L., and Pohl S.L. (1971). Characteristics of glucagon action on the hepatic adenylate cyclase system. *Biochemical Journal*, 125(3), 58–59.

Rohrbeck A., Kolbe T., Hagemann S., Genth H. and Just I. (2012). Distinct biological activities of C3 and ADP-ribosyltransferase-deficient C3-E174Q. *FEBS Journal*, 279, 2657–2671.

Rohrbeck A., Schröder A., Hagemann S., Pich A., Höltje M., Ahnert-Hilger G. and Just, I. (2014). Vimentin Mediates Uptake of C3 Exoenzyme. *PLoS ONE*, 9(6), e101071.

Rojas R.J., Yohe M.E., Gershburg S., Kawano T., Kozasa T. and Sondek J. (2007). $G\alpha_q$ Directly Activates p63RhoGEF and Trio via a Conserved Extension of the Dbl Homology-associated Pleckstrin Homology Domain. *The Journal of Biological Chemistry*, 282(40), 29201–29210.

Roychowdhury S., Panda D., Wilson L. and Rasenick M.M. (1999). G protein alpha subunits activate tubulin GTPase and modulate microtubule polymerization dynamics. *J Biol Chem*., 274, 13485–13490.

Rozengurt E., Higgins T., Chanter N., Lax A.J. and Staddon J.M. (1990). Pasteurella multocida toxin: potent mitogen for cultured fibroblasts. *Proc Natl Acad Sci USA*, 87(1), 123-127.

Rybak S.L. AND Murphy R.F. (1998). Primary Cell Cultures From Murine Kidney and Heart Differ in Endosomal pH. *J Cell Physiology*, 176, 216–222.

Sabri A., Wilson B.A. and Steinberg S.F. (2002). Dual actions of the Galpha(q) agonist Pasteurella multocida toxin to promote cardiomyocyte hypertrophy and enhance apoptosis susceptibility. *Circ Res*., 90(8), 850-857.

Sabbatini M.E., Bi Y., Ji B., Ernst S.A. and Williams J.A. (2010). CCK activates RhoA and Rac1 differentially through Galpha13 and Galphaq in mouse pancreatic acini. *Am J Physiol Cell Physiol*., 298(3), C592-601.

Sadana R. and Dessauer C.W. (2009). Physiological Roles for G Protein-Regulated Adenylyl Cyclase Isoforms: Insights from Knockout and Overexpression Studies. *Neuro-Signals*, 17(1), 5–22.

Sandhya K. and Vemuri M.C. (1997). Regulation of cellular signals by G-proteins. *Journal of Biosciences*, 22(3), 375-397.

Sankaran B., Osterhout J., Wu D. and Smrcka A.V. (1998). Identification of a Structural Element in Phospholipase C β2 That Interacts with G Protein βγ Subunits. *J. Biol. Chem*., 273, 7148–7154.

Schafer W.R. and Rine J. (1992). Protein prenylation: genes, enzymes, targets, and functions. *Annu Rev Genet*., 26, 209-37.

Schallmach E., Steiner D. and Vogel Z. (2006). Adenylyl cyclase type II activity is regulated by two different mechanisms: implications for acute and chronic opioid exposure. *Neuropharmacology*, 50, 998–1005.

Schedel M., Carr D., Klopp N., Woitsch B., Illig T., Stachel D et al. (2004). A signal transducer and activator of transcription 6 haplotype influences the regulation of serum IgE levels. *J Allergy Clin Immunol*., 114, 1100–1105.

Schmidt C J., Thomas T.C., Levine M.A. and Neer E.J. (1992). Specificity of G protein beta and gamma subunit interactions. *J Biol Chem*., 267(20), 13807-13810.

Schmidt G. et al. (1997). Gln63 of Rho is deamidated by Escherichia coli cytotoxic necrotizing factor 1. *Nature*, 387, 725–729.

Schmidt G., Selzer J., Lerm M. and Aktories K. (1998). The Rho-deamidating cytotoxic-necrotizing factor CNF1 from Escherichia coli possesses transglutaminase activity. Cysteine-866 and histidine-881 are essential for enzyme activity. *J. Biol. Chem*., 273, 13669–13674.

Schmidt G., Goehring U.-M., Schirmer J., Lerm M. and Aktories K. (1999). Identification of the C-terminal part of Bordetella dermonecrotic toxin as a transglutaminase for Rho GTPases. *J. Biol. Chem*., 274, 31875–31881.

Schmitt C.K., Meysick K.C. and O'Brien O.D. (1999). Bacterial Toxins: Friends or Foes? *Emerging Infectious Diseases*, 5(2), 224-234.

Schmitt J.M. and Stork P.J. (2000). Beta 2-adrenergic receptor activates extracellular signal-regulated kinases (ERKs) via the small G protein rap1 and the serine/threonine kinase B-Raf. *J Biol Chem*., 275(33), 25342-50.

Schubert B., VanDongen A.M.J., Kirsch G.E and Brown A.M. (1989). β-adrenergic inhibition of cardiac sodium channels by dual G-protein pathways. *Science*, 245, 516–519.

Schwab S., Spranger M., Schwarz S. and Hacke W. (1997). Barbiturate coma in severe hemispheric stroke: useful or obsolete? *Neurology*, 48(6), 1608-1613.

Schwindinger W.F. and Robishaw J.D. (2001). Heterotrimeric G-protein beta gamma-dimers in growth and differentiation. *Oncogene*, 20(13), 1653-1660.

Schwindinger W.F., Betz K.S., Giger K.E., Sabol A., Bronson S.K. and Robishaw J.D. (2003). Loss of G protein gamma 7 alters behavior and reduces striatal alpha(olf) level and cAMP production. *J Biol Chem*., 278(8), 6575-6579.

Sehr P. et al. (1998). Glucosylation and ADP-ribosylation of Rho proteins; effects on nucleotide binding, GTPase activity, and effector-coupling. *Biochemistry*, 37, 5296–5304.

Sekine A., Fujiwara M. and Narumiya S. (1989). Asparagine residue in the rho gene product is the modification site for botulinum ADP-ribosyltrans-ferase. *J. Biol. Chem*., 264, 8602-8605.

Seo B., Choy E.W., Maudsley S., Miller W.E., Wilson B.A. and Luttrell L.M. (2000). Pasteurella multocida toxin stimulates mitogen-activated protein kinase via G(q/11)-dependent transactivation of the epidermal growth factor receptor. *J Biol Chem*., 275(3), 2239-2245.

Shao F. et al. (2003). Biochemical characterization of the Yersinia YopT protease: cleavage site and recognition elements in Rho GTPases. *Proc. Natl Acad. Sci. USA*, 100, 904–909.

Shenoy S.K., Drake M. T., Nelson C.D., Houtz D.A., Xiao K., Madabushi S., Reiter E., Premont R.T., Lichtarge O. and Lefkowitz R.J. (2005). beta-arrestin-dependent, G protein-independent ERK1/2 activation by the beta2 adrenergic receptor. *J Biol Chem*., 281(2), 1261-73.

Siegert P., Schmidt G., Papatheodorou P., Wieland T., Aktories K. and Orth J.H. (2013). Pasteurella Multocida Toxin Prevents Osteoblast Differentiation by Transactivation of the MAP-Kinase Cascade via the Galphaq/11 - p63RhoGEF - RhoA Axis. *PLoS Pathog*., 9(5), e1003385.

Simon M.I., Strathmann M.P. and Gautam N. (1991). Diversity of G-Proteins in Signal Transduction. *Science*, 252(5007), 802-808.

Slomiany B.L. and Slomiany A. (2005). Gastric mucin secretion in response to beta-adrenergic G protein-coupled receptor activation is mediated by SRC kinase-dependent epidermal growth factor receptor transactivation. *J Physiol Pharmacol*., 56(2), 247-58.

Smith M.R., Ryu S.H., Suh P.G., Rhee S.G. and Kung H.F. (1989). S-phase induction and transformation of quiescent NIH 3T3 cells by microinjection of phospholipase C. *Proc Natl Acad Sci USA*, 86(10), 3659-3663.

Smyth M.G., Pickersgill R.W. and Lax A.J. (1995). The potent mitogen Pasteurella multocida toxin is highly resistant to proteolysis but becomes susceptible at lysosomal pH. *FEBS Lett*., 360(1), 62-66.

Smrcka A.V. (2008). G protein βγ subunits: Central mediators of G protein-coupled receptor signaling. *Cellular and Molecular Life Sciences : CMLS*, 65(14), 2191–2214.

Somlyo, A.P., & Somlyo, A.V. (2000). Signal transduction by G-proteins, Rho-kinase and protein phosphatase to smooth muscle and non-muscle myosin II. *The Journal of Physiology*, 522(Pt 2), 177–185.

Spangler B.D. (1992). Structure and function of cholera toxin and the related Escherichia coli heat-labile enterotoxin. *Microbiol. Rev*., 56, 622-647.

Spengler D., Waeber C., Pantaloni C., Holsboer F., Bockaert J., Seeburg P. H. and Journot L. (1993). Differential signal transduction by five splice variants of the PACAP receptor. *Nature*, 365(6442), 170-5.

Sprang S.R. (1997a). G protein mechanisms: insights from structural analysis. *Annu Rev Biochem*., 66, 639-678.

Sprang S.R. (1997b). G proteins, effectors and GAPs: structure and mechanism. *Curr Opin Struct Biol*., 7(6), 849-856.

Spranger M., Krempien S., Schwab S., Donneberg S. and Hacke W. (1997). Superoxide dismutase activity in serum of patients with acute cerebral ischemic injury. Correlation with clinical course and infarct size. *Stroke*, 28(12), 2425-2428.

Spring D.J. and Neer E.J. (1994). A 14-amino acid region of the G protein gamma subunit is sufficient to confer selectivity of gamma binding to the beta subunit. *J Biol Chem*., 269(36), 22882-22886.

Staddon, J.M., Chanter, N., Lax, A.J., Higgins, T.E. and Rozengurt, E. (1990). Pasteurella multocida toxin, a potent mitogen, stimulates protein kinase C-dependent and -independent protein phosphorylation in Swiss 3T3 cells. *J Biol Chem*., 265(20), 11841-11848.

Steelman, L.S. et al. (2011). Roles of the Raf/MEK/ERK and PI3K/PTEN/Akt/mTOR pathways in controlling growth and sensitivity to therapy-implications for cancer and aging. *Aging*, 3(3), 192-222.

Steiner D., Saya D., Schallmach E., Simonds W.F., and Vogel Z. (2006). Adenylyl cyclase type-VIII activity is regulated by G(betagamma) subunits. *Cell Signal*., 18(1), 62-8.

Stephens L.R., Eguinoa A., Erdjument-Bromage H., Lui M., Cooke F., Coadwell J., Smrcka A.S., Thelen M., Cadwallader K., and Tempst P., et al.

(1997). The G b g sensitivity of a PI3K is dependent upon a tightly associated adaptor. *Cell*, 89, 105–114.

Strathmann M.P. and Simon M.I. (1991) G alpha 12 and G alpha 13 subunits define a fourth class of G protein alpha subunits. *Proc. Natl. Acad. Sci. USA*, 88, 5582–5586.

Sugawara Y., Nishii H., Takahashi T., Yamauchi J., Mizuno N., Tago K., Itoh H. (2007). The lipid raft proteins flotillins/reggies interact with Galphaq and are involved in Gq-mediated p38 mitogen-activated protein kinase activation through tyrosine kinase. *Cell Signal*., 19(6), 1301-8.

Sun S. (2008). Deubiquitylation and regulation of the immune response. *Nature Reviews Immunology*, 8, 501-511.

Sunder, J. and Kumar A.A. (2000). Effect of Pasteurella multocida toxin on Vero cell culture. *The Indian Journal of Animal Science*, 70(3), 240-242.

Supino, R. (1995). MTT Assays. *Methods in Molecular Biology*, 43, 137-149.

Suzuki A., Kawano H., Hayashida M., Hayasaki Y., Tsutomi Y. and Akahane K. (2000). Procaspase 3/p21 complex formation to resist fas-mediated cell death is initiated as a result of the phosphorylation of p21 by protein kinase

A. *Cell Death Differ*., 7, 721–728.

Suzuki N., Nakamura S., Mano H., Kozasa T. (2003). $G\alpha_{12}$ activates Rho GTPase through tyrosine-phosphorylated leukemia-associated RhoGEF. *Proc Natl Acad Sci USA*, 100, 733–738

Suzuki N., Hajicek N. and Kozasa T. (2009) Regulation and physiological functions of G12/13-mediated signaling pathways. *Neurosignals*, 17, 55–70.

Takai Y., Sasaki T. and Matozaki T. (2001). Small GTP-Binding Proteins. *Physiological Reviews*, 81(1), 153-208.

Takaishi K., Sasaki T., Kotani H., Nishioka H., and Takai Y. (1997). Regulation of Cell–Cell Adhesion by Rac and Rho Small G Proteins in MDCK Cells. *The Journal of Cell Bio*., 139(4), 1047-1059.

Tall G. G., Krumins A. M. and Gilman A. G. (2003). Mammalian Ric-8A (synembryn) is a heterotrimeric Galpha protein guanine nucleotide exchange factor. *J Biol Chem*. 278, 8356–8362.

Tamura K., Stecher G., Peterson D., Filipski A. and Kumar S. (2013). MEGA6: Molecular Evolutionary Genetics Analysis Version 6.0. *Molecular Biology and Evolution*, 30(12), 2725–2729.

Tanaka H., Yamashita T., Asada M., Mizutani S., Yoshikawa H., Tang W.J. and Gilman A.G. (1991). Type-specific regulation of adenylyl cyclase by G protein beta gamma subunits. *Science*, 254(5037), 1500-3.

Tang W.J. and Gilman A.G. (1991). Type-specific regulation of adenylyl cyclase by G protein beta gamma subunits. *Science*, 254, 1500–1503.

Tojkander S., Gateva G. and Lappalainen P. Actin stress fibers--assembly, dynamics and biological roles. *J. Cell. Sci.*, 125, 1855-1864.

Taussig R., Tang W.J., Hepler J. R., Gilman A.G. (1994). Distinct patterns of bidirectional regulation of mammalian adenylyl cyclases. J Biol Chem. 269(8):6093-100.

Tohyama M. (2002). Cytoplasmic p21Cip1/WAF1 regulates neurite remodeling by inhibiting Rho-kinase activity. *The Journal of Cell Biology*, 158(2), 321–329.

Tojkander S., Gateva G. and Lappalainen P. (2012). Actin stress fibers – assembly, dynamics and biological roles. *J Cell Sci.*, 125, 1855-1864.

Tolkacheva T., Feuer B., Lorenzi M.V., Saez R. and Chan A.M.L. (1997). Cooperative transformation of NIH3T3 cells by Ga12 and Rac1. *Oncogene*, 15, 727–735.

Totsukawa G., Yamakita Y., Yamashiro S., Hartshorne D. J., Sasaki Y. and Matsumura F. (2000). Distinct Roles of Rock (Rho-Kinase) and Mlck in Spatial Regulation of Mlc Phosphorylation for Assembly of Stress Fibers and Focal Adhesions in 3t3 Fibroblasts. *The Journal of Cell Biology*, 150(4), 797–806.

Touhara K., Hawes B.E., van Biesen T. and Lefkowitz, R.J. (1995). G protein beta gamma subunits stimulate phosphorylation of Shc adapter protein. *Proceedings of the National Academy of Sciences USA*, 92(20), 9284–9287.

Tseliou M., Al-Qahtani A., Alarifi S., Alkahtani S.H., Stournaras C., Sourvinos G. (2016). The Role of RhoA, RhoB and RhoC GTPases in Cell Morphology, Proliferation and Migration in Human Cytomegalovirus (HCMV) Infected Glioblastoma Cells. *Cell Physiol Biochem*., 38, 94-109.

Tu Y., Wang J. and Ross E.M. (1997). Inhibition of brain G_z GAP and other RGS proteins by palmitoylation of G protein α subunits. *Science*, 278, 1132–1135.

Turcu, F. E. R., Ventii, K. H., & Wilkinson, K. D. (2009). Regulation and Cellular Roles of Ubiquitin-specific Deubiquitinating Enzymes. *Annual Review of Biochemistry*, 78, 363–397.

Ueda H., Morishita R., Yamauchi J., Itoh H., Kato K., and Asano T. (2000). Regulation of Rac and Cdc42 Pathways by Gi during Lysophosphatidic Acid-induced Cell Spreading. *The Journal of Bio. Chem.,* 276(9), 6846–6852.

Ueda H., Itoh H., Yamauchi J., Morishita R., Kaziro Y., Kato K., and Asano T. (2000). G Protein betagamma Subunits Induce Stress Fiber Formation and Focal Adhesion Assembly in a Rho-dependent Manner in HeLa Cells. *The Journal of Bio. Chem*., 275(3), 2098–2102.

Ueda H., Morishita R., Itoh H., Narumiya S., Mikoshiba K., Kato K. and Asano T. (2001). Galpha11 induces caspase-mediated proteolytic activation of Rho-associated kinase, ROCK-I, in HeLa cells. *J Biol Chem*., 276(45), 42527-33.

Ueda H., Morishita R., Narumiya S., Kato K. and Asano T. (2004). Galphaq/11 signaling induces apoptosis through two pathways involving reduction of Akt phosphorylation and activation of RhoA in HeLa cells. *Exp Cell Res*., 298(1), 207-17.

Uings I.J., and Farrow S.N. (2000). Cell receptors and cell signalling. *Molecular Pathology*, 53(6), 295–299.

Umemori H., Inoue T., Kume S., Sekiyama N., Nagao M., Itoh H., Nakanishi S., Mikoshiba K., Yamamoto T. (1997). Activation of the G protein Gq/11

through tyrosine phosphorylation of the alpha subunit. *Science*, 276(5320), 1878-81.

Van Corven E.J., Groenink A., Jalink K., Eichholtz T., Moolenaar W. (1989). Lysophosphatidate-induced cell proliferation: Identification and dissection of signaling pathways mediated by G proteins. *Cell*, 59(1), 45–54.

Vaque J.P. et al. (2013). A genome-wide RNAi screen reveals a Trio-regulated Rho GTPase circuitry transducing mitogenic signals initiated by G protein-coupled receptors. *Mol Cell*., 49(1), 94-108.

Verstraeten, N., Fauvart, M., Versées, W., & Michiels, J. (2011). The Universally Conserved Prokaryotic GTPases. *Microbiology and Molecular Biology Reviews : MMBR*, *75*(3), 507–542.

Vicente-Manzanares M., Ma X., Adelstein R.S. and Horwitz A.R. (2009). Non-muscle myosin II takes centre stage in cell adhesion and migration. *Nature Reviews*: *Molecular Cell Biology*, 10(11), 778–790.

Vogler O., Barcelo J.M., Ribas C. and Escriba P.V. (2008). Membrane interactions of G-proteins and other related proteins. *Biochim Biophys Acta,* 1778, 1640–1652.

Von Dannecker L.E.C., Mercadante A.F. and Malnic B. (2005). Ric-8B, an

Olfactory Putative GTP Exchange Factor, Amplifies Signal Transduction through the OlfactorySpecific G-Protein Gαolf. *The Journal of Neuroscience*, 25(15), 3793–3800.

Wagner P.L. and Waldor M.K. (2002). Bacteriophage Control of Bacterial Virulence. *Infection and Immunity*, 70(8), 3985–3993.

Waheed A.A. and Jones T.L.Z. (2002). Hsp90 Interactions and Acylation Target the G Protein $G\alpha_{12}$ but Not $G\alpha_{13}$ to Lipid Rafts. *The Journal of Biological Chem*., 277(36), 32409–32412.

Walsh M.P., Thornbury K., Cole W.C., Sergeant G., Hollywood M. and McHale N. (2011). Rho-associated kinase plays a role in rabbit urethral smooth muscle contraction, but not via enhanced myosin light chain phosphorylation. *American Journal of Physiology*, 300(1), F73-F85.

Wang J., Tu Y.P., Woodson J., Song X.L. and Ross E.M. (1997a). A GTPase-activating protein for the G protein G alpha(z) - Identification, purification, and mechanism of action. *Journal of Biological Chemistry*, 272(9), 5732-5740.

Wang Q., Mullah B., Hansen C., Asundi J. and Robishaw J.D. (1997b). Ribozyme-mediated suppression of the G protein gamma(7) subunit

suggests a role in hormone regulation of adenylylcyclase activity. *Journal of Biological Chemistry*, 272(41), 26040-26048.

Wang J., Ducret A., Tu Y, Kozasa T., Aebersold R., Ross E.M. (1998). RGSZ1, a G_z-selective RGS Protein in Brain Structure, Membrane Association, Regulation by $G\alpha_z$ Phosphorylation, and Relationship to a G_z GTPase-activating Protein Subfamily. *J. Biol. Chem*., 273, 26014-26025.

Wang J., Frost J.A., Cobb M.H., Ross E.M. (1999a). Reciprocal signaling between heterotrimeric G proteins and the p21-stimulated protein kinase. *J. Biol. Chem*., 274, 31641-31647.

Wang Q., Mullah B.K. and Robishaw J.D. (1999b). Ribozyme approach identifies a functional association between the G protein beta1gamma7 subunits in the beta-adrenergic receptor signaling pathway. *J Biol Chem*., 274(24), 17365-17371.

Wang Q., Jolly J.P., Surmeier J.D., Mullah B.M., Lidow M.S., Bergson C.M. and Robishaw J.D. (2001a). Differential dependence of the D-1 and D-5 dopamine receptors on the G protein gamma(7) subunit for activation of adenylylcyclase. *Journal of Biological Chemistry*, 276(42), 39386-39393.

Wang C., Wilson W.A. and Moore S.D. (2001b). Role of NMDA, non-NMDA, and GABA receptors in signal propagation in the amygdala formation. *J Neurophysiol*., 86(3), 1422-1429.

Wang X., Gao X., and Hardwidge P.R. (2012). Heat-labile enterotoxin-induced activation of NF-κB and MAPK pathways in intestinal epithelial cells impacts enterotoxigenic Escherichia coli (ETEC) adherence. *Cell Microbiol*., 14(8), 1231-41.

Ward P.N., Miles A.J., Sumner I. G., Thomas L.H. and Lax A.J. (1998). Activity of the mitogenic Pasteurella multocida toxin requires an essential C-terminal residue. *Infect Immun*., 66(12), 5636-5642.

Watanabe N., Madaule P., Reid T., Ishizaki T., Watanabe G., Kakizuka A., Saito Y., Nakao K., Jockusch B.M. and Narumiya S. (1997). p140mDia, a mammalian homolog of *Drosophila* diaphanous, is a target protein for Rho small GTPase and is a ligand for profilin. *EMBO (Eur. Mol. Biol. Organ.) J*., 16, 3044–3056.

Weber D.J., Wolfson J.S., Swartz M.N., and Hooper D.C. (1984). Pasteurella multocida infections. Report of 34 cases and review of the literature. *Medicine (Baltimore)*, 63(3), 133-54.

Wedegaertner P.B., Chu D.H., Wilson P.T., Levis M.J. and Bourne H.R. (1993). Palmitoylation is required for signaling functions and membrane attachment of Gq alpha and Gs alpha. *J Biol Chem*., 268, 25001-25008.

Wedegaertner P.B. and Bourne H.R. (1994). Activation and depalmitoylation of Gs alpha. *Cell*, 77(7),1063-70.

Wedegaertner P.B., Wilson P.T., and Bourne H.R. (1995). Lipid modifications of trimeric G proteins. *J Biol Chem*., 270(2), 503-506.

Weise M., Vettel C., Spiger K., Gilsbach R., Hein L., Lorenz K., Wieland T., Aktories K. and Orth, J.H.C. (2015). A systemic Pasteurella multocida toxin aggravates cardiac hypertrophy and fibrosis in mice. *Cellular Microbiology*, 17(9), 1320–1331.

Wettschureck N. and Offermanns S. (2005). Mammalian G proteins and their cell type specific functions. *Physiol Rev*., 85(4), 1159-204.

Wickman K. and Clapham D.E. (1995a). Ion-Channel Regulation by G-Proteins. *Physiological Reviews*, 75(4), 865-885.

Wickman K.D. and Clapham D.E. (1995b). G-Protein Regulation of Ion Channels. *Current Opinion in Neurobiology*, 5(3), 278-285.

Wieczorek D., Delauriere L. and Schagat T. Methods of RNA Quality Assessment. Promega Corporation Web site. http://www.promega.com/resources/pubhub/methods-of-rna-quality-assessment/ Updated October 2012. Accessed October 1, 2015.

Wilde C., Vogelsgesang M., and Aktories K. (2003). Rho-specific Bacillus cereus ADP- ribosyltransferase C3cer cloning and characterization. *Biochemistry*, 42, 9694–702.

Wilde C., Chhatwal G.S., Schmalzing G., Aktories K., Just I. (2001). A novel C3-like ADP- ribosyltransferase from Staphylococcus aureus modifying RhoE and Rnd3. *J Biol Chem*., 276, 9537–42.

Wilkie T.M., Scherle P.A., Strathmann M.P., Slepak V.Z., and Simon, M.I. (1991). Characterization of G-protein alpha subunits in the Gq class: expression in murine tissues and in stromal and hematopoietic cell lines. *Proc Natl Acad Sci USA*, 88(22), 10049-10053.

Williams L.T., Snyderman R. and Lefkowitz R J. (1976). Identification of β-adrenergic receptors in human leukocytes by (-) [^{3}H]-alprenolol binding.J. clin. *Invest*., 56, 149–155.

Williams S.L., Lutz S., Charlie N.K., Vettel C., Ailion M., Coco C., Tesmer J.J., Jorgensen E.M., Wieland T. and Miller, K.G. (2007). Trio's Rho-specific

GEF domain is the missing $G\alpha_q$effector in C. elegans. *Genes and Development*, 21(21), 2731–2746.

Wilson B.A., Zhu X., Ho M. and Lu L. (1997). Pasteurella multocida toxin activates the inositol triphosphate signaling pathway in Xenopus oocytes via G(q)alpha-coupled phospholipase C-beta1. *J Biol Chem*., 272, 1268–1275.

Wilson B.A., Aminova L.R., Ponferrada V.G. and Ho M. (2000). Differential modulation and subsequent blockade of mitogenic signaling and cell cycle progression by Pasteurella multocida toxin. *Infect Immun*., 68(8), 4531-4538.

Wilson B.A. and Ho M. (2011). Cellular and molecular action of the mitogenic protein-deamidating toxin from Pasteurella multocida. *FEBS J*., 278(23), 4616-4632.

Wilson B.A. and Ho M. (2004). Pasteurella multocida toxin as a tool for studying G_q signal transduction. *Reviews of Physiology, Biochemistry and Pharmacology*, 152, 93–109.

Wilson B.A. and Ho M. (2012). Pasteurella multocida Toxin Interaction with Host Cells: Entry and Cellular Effects. Current Topics in Microbiology and *Immunology*, 361, 93–111.

Woodford N. and Livermore D.M. (2009). Infections caused by Gram-positive bacteria: a review of the global challenge. *J Infect*., 59, S4-16.

Worby, C.A. et al. (2009). The Fic domain: regulation of cell signaling by adenylylation. *Mol. Cell*., 34, 93–103.

Wojciak-Stothard B. and Ridley A.J. (2003). Shear stress–induced endothelial cell polarization is mediated by Rho and Rac but not Cdc42 or PI 3-kinases. *J Cell Biol*., 161(2), 429–439.

Wu E.H.T., Tam B.H.L. and Wong Y.H. (2006). Constitutively active α subunits of Gq/11 and G12/13 families inhibit activation of the pro-survival Akt signaling cascade. *FEBS Journal*, 273, 2388–2398.

Yanamadala V., Negoro H., and Denker B.M. (2009). Heterotrimeric G Proteins and Apoptosis: Intersecting Signaling Pathways Leading to Context Dependent Phenotypes. *Current Molecular Medicine*, 9(5), 527.

Yoshikawa F., Morita M., Monkawa T., Michikawa T., Furuichi T. and Mikoshiba K. (1996). Mutational analysis of the ligand binding site of the inositol 1,4,5-trisphosphate receptor. *J. Biol. Chem*., 271, 18277–18284.

Yoshikawa F., Iwasaki H., Michikawa T., Furuichi T. and Mikoshiba K. (1999). Cooperative formation of the ligand-binding site of the inositol 1,4, 5-

trisphosphate receptor by two separable domains. *J. Biol. Chem*., 274, 328–334.

Zeng H., Zhao D., Mukhopadhyay D. (2002a). Flt-1-mediated Down-regulation of Endothelial Cell Proliferation through Pertussis Toxin-sensitive G Proteins, βγ Subunits, Small GTPase CDC42, and Partly by Rac-1. *J. Biol. Chem*., 277, 4003–4009.

Zeng H., Zhao D. and Mukhopadhyay D. (2002b). KDR Stimulates Endothelial Cell Migration through Heterotrimeric G Protein Gq/11-mediated Activation of a Small GTPase RhoA. *The Journal of Biological Chemistry*, 277, 46791-46798.

Zha Z., Han X., Smith M. D., Liu Y., Giguere P. M., Kopanja D., et al. (2015). A Non-Canonical Function of Gβ as a Subunit of E3 Ligase in Targeting GRK2 Ubiquitylation. *Mol. Cell*, 58, 794–803.

Zhang L., DiLizio C., Kim D., Smyth E. M. and Manning D. R. (2006). The G_{12} family of G proteins as a reporter of thromboxane A 2 receptor activity. *Mol Pharmacol*., 69, 1433–1440.

Zheng H., Loh H. H. and Law P. Y. (2010). Agonist-selective signaling of G protein-coupled receptor: mechanisms and implications. *IUBMB Life*, 62(2), 112-9.